

K. Binnemans, *Coordination Chemistry Reviews* **295**, 1–45 (2015).

Interpretation of europium(III) spectra

Koen Binnemans*

KU Leuven, Department of Chemistry, Celestijnenlaan 200F, P.O. Box 2404, B-3001

Heverlee (Belgium)

* Corresponding author:

E-mail: Koen.Binnemans@chem.kuleuven.be

Phone: +32 16 32 7446

Contents

Abbreviations	4
Abstract	7
1. Introduction.....	8
2. Energy level structure of the [Xe]4f ⁶ configuration	11
3. Luminescence spectra	24
3.1 General features and selection rules	24
3.2 Transition ⁵ D ₀ → ⁷ F ₀	30
3.3 Transition ⁵ D ₀ → ⁷ F ₁	40
3.4 Transition ⁵ D ₀ → ⁷ F ₂	45
3.5 Transition ⁵ D ₀ → ⁷ F ₃	49
3.6 Transition ⁵ D ₀ → ⁷ F ₄	51
3.7 Transitions ⁵ D ₀ → ⁷ F ₅ and ⁵ D ₀ → ⁷ F ₆	53
3.8 Emission from higher excited states	54
3.9 Polarized emission spectra	58
3.10 Sensitized luminescence.....	59
4. Absorption spectra	67
4.1 General features and “hot” bands	67
4.2 Transitions within the ⁷ F ground term	73
4.3 Transition to the ⁵ D ₀ level.....	74
4.4 Transitions to the ⁵ D ₁ level	77
4.5 Transitions to the ⁵ D ₂ level.....	79
4.6 Transitions to higher energy levels	80
4.7 Charge-transfer bands.....	81
5. Excitation spectra	85
6. Other spectroscopic techniques.....	89
6.1 Two-photon absorption (TPA).....	89
6.2 Zeeman spectroscopy.....	90
6.3 Magnetic circular dichroism (MCD).....	92
7. Eu ³⁺ as a spectroscopic probe	96
8. Nephelauxetic effect	110
9. Judd-Ofelt parametrization of europium(III) spectra	115
9.1. Determination of Judd-Ofelt intensity parameters.....	115
9.2. Use of Judd-Ofelt parameters for calculation of photophysical quantities	119

9.3. Hypersensitivity	121
10. Dynamics of excited states	126
10.1 Decay processes and lifetimes	126
10.2 Determination of hydration numbers	139
11. Concluding remarks.....	145
Acknowledgments	147
References.....	148

Abbreviations

A	probability for radiative decay (= Einstein coefficient A)
acac	acetylacetonate
bipy	2,2'-bipyridine
bmpyr	<i>N</i> -butyl- <i>N</i> -methylpyrrolidinium
CD	circular dichroism
C ₄ mim	1-butyl-3-methylimidazolium
C ₆ mim	1-hexyl-3-methylimidazolium
CN_L	maximum ligand coordination number
CT	charge transfer
D	dipole strength
D_{ED}	dipole strength of an electric dipole transition
D_{MD}	dipole strength of a magnetic dipole transition
dbm	dibenzoylmethanate
dmbipy	4,4'-dimethyl-2,2'-bipyridine
DOTA	1,4,7,10-tetraazacyclododecane-1,4,7,10-tetraacetate
DPA	2,6-pyridinedicarboxylate (= dipicolinate)
E_{eff}	effective field
ED	(induced) electric dipole
EDTA	ethylenediaminetetraacetate
EPR	electron paramagnetic resonance
EXAFS	Extended X-ray Absorption Fine Structure
f	oscillator strength
H	Hamiltonian

<i>I</i>	intensity
I	nuclear spin
<i>J</i>	total angular momentum quantum number
<i>L</i>	total orbital angular momentum quantum number
LCP	left circularly polarized light
LMCT	ligand-to-metal charge transfer
MCD	magnetic circular dichroism
MCPE	magnetic circularly polarized emission
MD	magnetic dipole
MRI	magnetic resonance imaging
<i>n</i>	refractive index
NTA	nitrilotriacetate
ODA	oxydiacetate
<i>p</i>	formal charge
PCEM	point charge electrostatic model
<i>q</i>	hydration number
RCP	right circularly polarized light
<i>S</i>	total spin quantum number
S	singlet
T	triplet
terpy	2,2';6',2"-terpyridine (= terpyridine)
Tf ₂ N ⁻	bis(trifluoromethylsulfonyl)imide (= bistriflimide)
TMU	tetramethylurea
Tp	hydrotris(1-pyrazolyl)borate
TPA	two-photon absorption

TPP	tricapped trigonal prism
TTHA	triethylenetetraaminehexaacetate
W	probability for non-radiative decay
$X_A(T)$	fractional thermal population at temperature T
β_R	branching ratio
$\chi_{\text{opt}}(X)$	optical electronegativity of the ligand
$\chi_{\text{uncorr}}(M)$	uncorrected optical electronegativity of the metal
η_{sens}	sensitization efficiency
λ	wavelength
$\tilde{\nu}$	wavenumber
τ	lifetime
τ_{obs}	observed luminescence lifetime
τ_{rad}	radiative lifetime
Φ	quantum yield
Φ_{Ln}^L	overall quantum yield
Φ_{Ln}^{Ln}	intrinsic quantum yield
Ω_λ	Judd-Ofelt intensity parameter

Abstract

The trivalent europium ion (Eu^{3+}) is well known for its strong luminescence in the red spectral region, but this ion is also interesting from a theoretical point of view. Due to the even number of electrons in the 4f shell ($4f^6$ configuration), the crystal-field perturbation by the crystalline host matrix lifts partly or completely the degeneracies of the $^{2S+1}L_J$ levels. The Eu^{3+} ion has the great advantage over other lanthanide ions with an even number of 4f electrons that the starting levels of the transitions in both the absorption and the luminescence spectrum are non-degenerate ($J = 0$). Moreover, the interpretation of the spectra is facilitated by the small total angular momentum J of the end levels in the transitions. The number of lines observed for the $^5D_0 \rightarrow ^7F_J$ transitions in the luminescence spectrum or the $^5D_J \leftarrow ^7F_0$ transitions in the absorption spectrum allows determining the site symmetry of the Eu^{3+} ion. This review describes the spectroscopic properties of the trivalent europium ion, with emphasis on the energy level structure, the intensities of the f-f transitions (including the Judd-Ofelt theory), the decay times of the excited states and the use of the Eu^{3+} ion as a spectroscopic probe for site symmetry determination. It is illustrated how the maximum amount of information can be extracted from optical absorption and luminescence spectra of europium(III) compounds, and how pitfalls in the interpretation of these spectra can be avoided.

Keywords: europium; lanthanides; luminescence; luminescent materials; rare earths; spectroscopy.

1. Introduction

The trivalent europium ion (Eu^{3+}) exhibits an intense red photoluminescence upon irradiation with UV radiation. This photoluminescence is observed not only for Eu^{3+} ions doped into crystalline host matrices or glasses, but also for europium(III) complexes with organic ligands. These ligands can act as an antenna to absorb the excitation light and to transfer the excitation energy to the higher energy levels of the Eu^{3+} ion, from which the emitting excited levels can be populated. The photoluminescence of europium(III) complexes has been studied in solutions [1,2], polymer matrices [3,4], sol-gel glasses [5,6], functionalized sol-gel glasses [7-11], ionogels [12,13], liquid crystals [14-16], encapsulated into inorganic hosts such as zeolites [17-20] and in metal-organic frameworks (MOFs) [21,22]. The design of europium(III)-containing inorganic-organic hybrid materials is a popular research field [23-26]. Europium(III) complexes can be excellent luminescent probes for biochemical or biomedical applications [27-33]. The most important application of europium is the red phosphor $\text{Y}_2\text{O}_3:\text{Eu}^{3+}$ (YOX) in fluorescent lamps [34-36]. The red emission of Eu^{3+} can be achieved not only by excitation with UV light, but also by irradiation with an electron beam (cathodoluminescence) [37,38], X-rays, γ -rays, α - or β -particles (radioluminescence) [39-42], strong electric fields (electroluminescence) [43,44], mechanical agitation (triboluminescence or mechanoluminescence) [45-47] or by chemical reactions (chemiluminescence) [48]. A well-known cathodoluminescent phosphor is $\text{Y}_2\text{O}_2\text{S}:\text{Eu}^{3+}$, which is the red phosphor used in the old-fashioned cathode-ray tubes of color television screens or computer monitors [37,38,49]. This compound replaced the older cathodoluminescent europium(III) phosphor $\text{YVO}_4:\text{Eu}^{3+}$ [50,51]. It is worth mentioning that europium is present in the anti-counterfeiting ink of EURO banknotes [52].

Not only its red luminescence, but also the narrow transitions in the absorption and luminescence spectra are typical features of the Eu^{3+} ion, and these spectroscopic properties

have been known from the earliest history of the chemical element europium. The sharp lines in the absorption spectra of Eu^{3+} in solution were first described in 1900 by Demarçay, the discoverer of europium [53], and his observations were confirmed by Prandtl in 1920 [54]. Prandtl was the first to publish a picture of an absorption spectrum of Eu^{3+} [55]. In 1906, Urbain reported on the red luminescence of Eu_2O_3 diluted in lime [56,57]. However, two years earlier in 1904, Urbain had already noticed that crystals of europium(III) sulfate octahydrate, $\text{Eu}_2(\text{SO}_4)_3 \cdot 8\text{H}_2\text{O}$, had a faint pink color [58], but he did not realize that this color was caused by the photoluminescence of Eu^{3+} ions excited by the UV part of sunlight [59]. In the absence of this luminescence, europium(III) compounds are colorless. In 1909, Urbain described the cathodoluminescence of $\text{Gd}_2\text{O}_3:\text{Eu}^{3+}$ [60].

The fine structure and the relative intensities of the transitions in the absorption and luminescence spectra of Eu^{3+} can be used to probe the local environment of the Eu^{3+} ion. The spectroscopic data give information on the point group symmetry of the Eu^{3+} site and sometimes also information on the coordination polyhedron. However, a rigorous interpretation of europium(III) spectra can be a daunting task for newcomers in the field of lanthanide coordination chemistry. Chemists who have been trained in the synthesis and characterization of luminescent lanthanide complexes are often lacking a sound theoretical background in lanthanide spectroscopy. The classical books or reviews on spectroscopy of rare earths are often too theoretical or put little emphasis on the relationship between features observed in spectra and structural properties [61-70]. There exist several reviews on the luminescence of lanthanide-based molecular materials or photophysics of lanthanides, but only few of them focus on the Eu^{3+} ion in detail [23,24,27,28,33,64,71-100]. In general, these works do not give a detailed description of the transitions in europium(III) spectra. As a consequence, many authors who describe luminescent europium(III) complexes do not go beyond reporting general statements with little information content, such as mentioning that

the transitions observed in the luminescence spectra are the $^5D_0 \rightarrow ^7F_J$ ($J = 0-6$) transitions or that a very intense hypersensitive transition $^5D_0 \rightarrow ^7F_2$ indicates that the Eu^{3+} is not at a site with a center of symmetry.

The aim of this review is to give a sound introduction to the spectroscopic properties of the trivalent europium ion, with emphasis on the energy level structure, the intensities of the f-f transitions, the decay times of the excited states and the use of the Eu^{3+} ion as a spectroscopic probe for site symmetry determination. It is shown how the maximum amount of information can be extracted from optical absorption and luminescence spectra of europium(III) compounds, and how pitfalls in the interpretation of these spectra can be avoided. In this review, europium(III) is represented as Eu^{3+} rather than Eu(III) . In principle Eu^{3+} is the trivalent europium ion in the gas phase. However, it is common practice among spectroscopists to use the symbol Eu^{3+} for europium(III)-doped solid materials and even for europium(III) in solutions. In Figure 1 shows a selection of ligands that are found in the europium(III) complexes mentioned in this review paper.

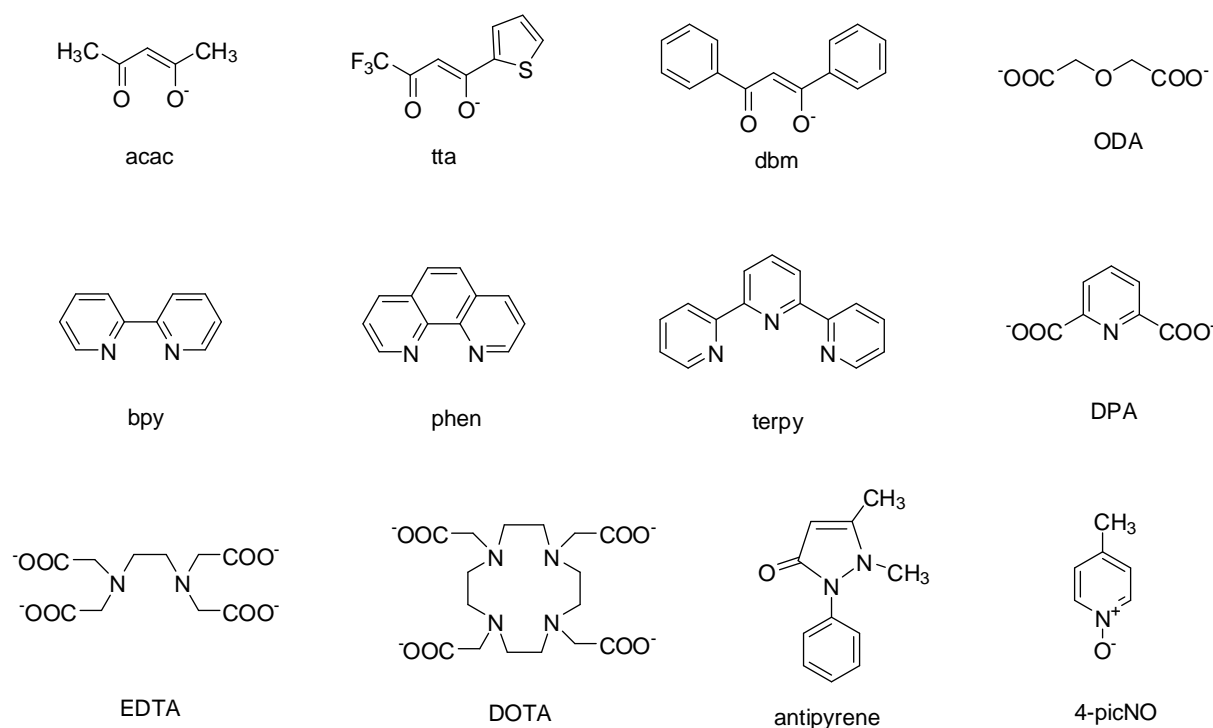


Figure 1. Selection of ligands of luminescent europium(III) complexes. Abbreviations: *acac* = acetylacetonate, *tta* = 2-thenoyltrifluoroacetylacetonate, *dbm* = dibenzoylmethanate, *ODA* = oxydiacetate, *bpy* = 2,2'-bipyridine, *phen* = 1,10-phenanthroline, *terpy* = 2,2';6',2''-terpyridine, *DPA* = 2-pyridinedicarboxylate (= dipicolinate), *EDTA* = ethylenediaminetetraacetate, *DOTA* = 1,4,7,10-tetraazacyclododecane-1,4,7,10-tetraacetate, *antipyrene* = 2,3-dimethyl-1-phenyl-3-pyrazolin-5-one, *4-PicNO* = 4-picoline-N-oxide.

2. Energy level structure of the [Xe]4f⁶ configuration

Eu³⁺ has 60 electrons: 54 electrons in the same closed shells as the xenon atom and 6 electrons in the 4f shell. This electronic configuration can be written as [Xe]4f⁶, or 4f⁶ for short. The 4f shell is well shielded from its environment by the closed 5s² and 5p⁶ outer shells [101]. The six electrons in the 4f shell can be arranged in 3003 different ways into the seven 4f orbitals, so that the total degeneracy of the [Xe]4f⁶ electronic configuration of the trivalent Eu³⁺ ion is 3003. The degeneracy of a 4f^{*n*} electronic configuration is given by the binomial coefficient:

$$\binom{14}{n} = \frac{14!}{n!(14-n)!} \quad (1)$$

Here, *n* is the number of 4f electrons (*n* = 6 for Eu³⁺). Each different electronic arrangement is called a *microstate*. The degeneracy of the 4f⁶ configuration is partly or totally lifted by several perturbations acting on the Eu³⁺ ion: electron repulsion, spin-orbit coupling, the crystal-field perturbation and eventually the Zeeman effect (Figure 2). The electron repulsion is the electrostatic interaction between the different electrons in the 4f shell. The spin-orbit coupling results from the interaction between the spin magnetic moment of the electron and

the magnetic field created by the movement of the electron around the nucleus. The crystal-field effect is caused by the interactions between the 4f electrons and the electrons of the ligands. The Zeeman effect is the splitting of the energy levels by an external magnetic field. After introduction of electron repulsion, the $[\text{Xe}]4f^6$ configuration is characterized by $119^{2S+1}L(\tau)$ terms (Table 1) [102]. The degeneracy of each term is $(2S+1)(2L+1)$. S is the *total spin quantum number* and L is the *total orbital angular momentum quantum number*. τ is an additional quantum number to differentiate between terms with identical S and L quantum numbers [103]. Terms are denoted by capital letters of the Latin alphabet: S ($L = 0$), P ($L = 1$), D ($L = 2$), F ($L = 3$), G ($L = 4$), H ($L = 5$), I ($L = 6$), K ($L = 7$), L ($L = 8$), M ($L = 9$), ... Notice that the letter J is not used as a term label. The term with the highest L value of the $4f^6$ configuration has $L = 12$, giving a 1Q term. $2S+1$ is the *spin multiplicity* of the term. The nomenclature for spin multiplicity is *singlet, doublet, triplet, quartet, quintet, sextet, septet* for $2S+1 = 1, 2, 3, 4, 5, 6, 7$, respectively. The term with the highest spin multiplicity for the $4f^6$ configuration is a septet, which corresponds to six unpaired electrons: $S = [\frac{1}{2} + \frac{1}{2} + \frac{1}{2} + \frac{1}{2} + \frac{1}{2} + \frac{1}{2}] = 3$ or $2S+1 = 7$. The L value of this septet is 3 (or an F term), which corresponds to the sum of the m_l values: $L = [(+3) + (+2) + (+1) + 0 + (-1) + (-2)] = 3$. For configurations with an even number of electrons, all terms have odd multiplicity. Only singlets, triplets, quintets and septets occur in the $4f^6$ configuration with six electrons, such as in the case of Eu^{3+} . The $^{2S+1}L(\tau)$ terms can be rigorously classified by the group theoretical labels introduced by Racah [104], but in practice the $^{2S+1}L(\tau)$ labels are preferred. The separation between the different $^{2S+1}L(\tau)$ terms is of the order of 10000 cm^{-1} for the lower terms of the $4f^6$ configuration.

Table 1. The 119 $^{2S+1}L(\tau)$ terms of the $4f^6$ configuration of Eu^{3+} [102].

${}^7\text{F}$	${}^3\text{K}(6)$	${}^3\text{F}(8)$	${}^1\text{I}(6)$
${}^5\text{L}$	${}^3\text{I}(1)$	${}^3\text{F}(9)$	${}^1\text{I}(7)$
${}^5\text{K}$	${}^3\text{I}(2)$	${}^3\text{D}(1)$	${}^1\text{H}(1)$
${}^5\text{I}(1)$	${}^3\text{I}(3)$	${}^3\text{D}(2)$	${}^1\text{H}(2)$
${}^5\text{I}(2)$	${}^3\text{I}(4)$	${}^3\text{D}(3)$	${}^1\text{H}(3)$
${}^5\text{H}(1)$	${}^3\text{I}(5)$	${}^3\text{D}(4)$	${}^1\text{H}(4)$
${}^5\text{H}(2)$	${}^3\text{I}(6)$	${}^3\text{D}(5)$	${}^1\text{G}(1)$
${}^5\text{G}(1)$	${}^3\text{H}(1)$	${}^3\text{P}(1)$	${}^1\text{G}(2)$
${}^5\text{G}(2)$	${}^3\text{H}(2)$	${}^3\text{P}(2)$	${}^1\text{G}(3)$
${}^5\text{G}(3)$	${}^3\text{H}(3)$	${}^3\text{P}(3)$	${}^1\text{G}(4)$
${}^5\text{F}(1)$	${}^3\text{H}(4)$	${}^3\text{P}(4)$	${}^1\text{G}(5)$
${}^5\text{F}(2)$	${}^3\text{H}(5)$	${}^3\text{P}(5)$	${}^1\text{G}(6)$
${}^5\text{D}(1)$	${}^3\text{H}(6)$	${}^3\text{P}(6)$	${}^1\text{G}(7)$
${}^5\text{D}(2)$	${}^3\text{H}(7)$	${}^1\text{Q}$	${}^1\text{G}(8)$
${}^5\text{D}(3)$	${}^3\text{H}(8)$	${}^1\text{N}(1)$	${}^1\text{F}(1)$
${}^5\text{P}$	${}^3\text{H}(9)$	${}^1\text{N}(2)$	${}^1\text{F}(2)$
${}^5\text{S}$	${}^3\text{G}(1)$	${}^1\text{M}(1)$	${}^1\text{F}(3)$
${}^3\text{O}$	${}^3\text{G}(2)$	${}^1\text{M}(2)$	${}^1\text{F}(4)$
${}^3\text{N}$	${}^3\text{G}(3)$	${}^1\text{L}(1)$	${}^1\text{D}(1)$
${}^3\text{M}(1)$	${}^3\text{G}(4)$	${}^1\text{L}(2)$	${}^1\text{D}(2)$
${}^3\text{M}(2)$	${}^3\text{G}(5)$	${}^1\text{L}(3)$	${}^1\text{D}(3)$
${}^3\text{M}(3)$	${}^3\text{G}(6)$	${}^1\text{L}(4)$	${}^1\text{D}(4)$
${}^3\text{L}(1)$	${}^3\text{G}(7)$	${}^1\text{K}(1)$	${}^1\text{D}(5)$
${}^3\text{L}(2)$	${}^3\text{F}(1)$	${}^1\text{K}(2)$	${}^1\text{D}(6)$
${}^3\text{L}(3)$	${}^3\text{F}(2)$	${}^1\text{K}(3)$	${}^1\text{P}$
${}^3\text{K}(1)$	${}^3\text{F}(3)$	${}^1\text{I}(1)$	${}^1\text{S}(1)$
${}^3\text{K}(2)$	${}^3\text{F}(4)$	${}^1\text{I}(2)$	${}^1\text{S}(2)$
${}^3\text{K}(3)$	${}^3\text{F}(5)$	${}^1\text{I}(3)$	${}^1\text{S}(3)$
${}^3\text{K}(4)$	${}^3\text{F}(6)$	${}^1\text{I}(4)$	${}^1\text{S}(4)$
${}^3\text{K}(5)$	${}^3\text{F}(7)$	${}^1\text{I}(5)$	

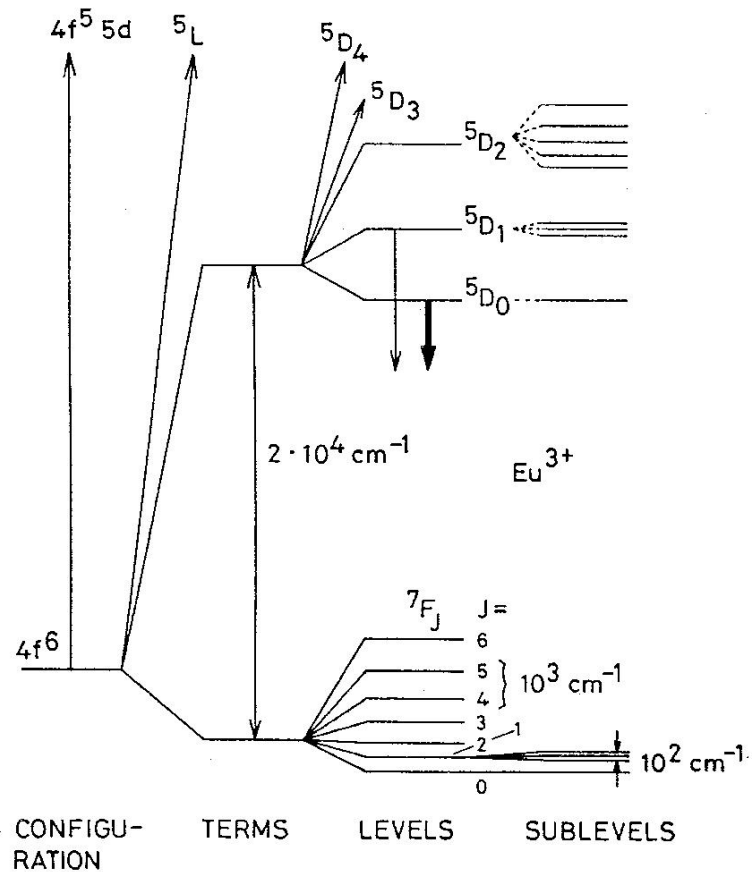


Figure 2. Partial energy diagram of $\text{Eu}^{3+} (4f^6)$ showing the relative magnitude of the interelectronic repulsion (terms), spin-orbit coupling (levels) and crystal-field effects (sublevels). The downward arrows indicate the excited states 5D_0 and 5D_1 from which luminescence occurs. Reprinted with permission from reference [105]. Copyright 1987 Elsevier.

The ${}^{2S+1}L(\tau)$ terms of the $[\text{Xe}]4f^6$ configuration are split by the spin-orbit interaction in $295 {}^{2S+1}L(\tau)_J$ levels. J is the total angular quantum number and it indicates the relative orientation of the spin and the orbital momenta. The possible values for J are $L+S, L+S-1, L+S-2, \dots, |L-S|$. For the 7F term, $L = 3$ and $S = 3$, so that the possible J values are: 6, 5, 4, 3, 2, 1, 0. The degeneracy of each spin-orbit level is $2J+1$. The quantum number τ is often omitted, so that the free-ion levels are labeled as ${}^{2S+1}L_J$. In the Russell-Saunders coupling

scheme (also called *LS* coupling scheme), each free-ion level is characterized by a $^{2S+1}L_J$ label. For Eu^{3+} , only the J levels of the 7F and 5D terms are adequately described by the Russell-Saunders coupling scheme. A better description of the free-ion levels can be done by applying the *intermediate coupling scheme*, in which each level is a linear combination of different $^{2S+1}L_J$ states, but with the same J quantum level. For example, the wave functions of the 7F_0 level in the intermediate coupling scheme is: $0.9680 ^7F_0 + 0.0016 ^5D(2)_0 + 0.1659 ^5D(3)_0 - 0.1815 ^5D(1)_0$ [106]. The splitting of the terms into J states by the spin-orbit coupling interaction is of the order of 1000 cm^{-1} . The $2J+1$ degeneracy of the energy levels in the free ion is further lifted by the crystal-field effect, after which the energy levels are characterized by the *irreducible representation (irreps)* of the point group of the Eu^{3+} site [95]. These levels are called *crystal-field levels* (or *Stark levels*). The splitting of the energy levels by the crystal-field effect is of the order of a few hundred cm^{-1} or less. In systems with an orthorhombic or lower symmetry, all degeneracy is lifted by the crystal field. In systems with a higher symmetry, all degeneracy can be lifted by an external magnetic field, via the so-called *Zeeman effect*. Even in strong magnetic fields, the splitting of the energy levels by the Zeeman effect is only a few cm^{-1} . The J quantum numbers are well defined in the free Eu^{3+} ion, but J -mixing occurs when the Eu^{3+} is located in a non-spherically symmetric ligand environment (*vide infra*) [107,108]. J -mixing is induced by the even-parity components of the crystal-field potential.

Hund's rules explain why 7F_0 is the ground state of the $4f^6$ electronic configuration: Rule 1: the spin multiplicity has to be as large as possible; Rule 2: in case there is more than one term with the same spin multiplicity, the term with the highest total orbital angular momentum (or L value) is the ground state; Rule 3: For electronic shells that are less than half-filled, the ground state has the lowest possible J value. For electronic shells that are more than half-filled, the ground state has the highest possible J value. Since the highest

multiplicity of the terms of the $4f^6$ electronic configuration is a septet and since there is only one septet, 7F is the ground term. The $4f^6$ shell is less than half filled and, as explained above, the possible J values for the 7F term are 0, 1, 2, 3, 4, 5, 6, so that the ground state of Eu^{3+} is 7F_0 . The order of energies of the levels within the 7F term is therefore: ${}^7F_0 < {}^7F_1 < \dots < {}^7F_6$. However, the relative positions of the energy levels of the excited states can be determined only by calculations.

The energy levels and wave functions of the Eu^{3+} ion can be obtained by diagonalization of the energy matrix [95]. The matrix elements are of the type $\langle \Psi_{l^n \tau SLJM} | H | \Psi_{l'^n \tau' S' L' J' M'} \rangle$, where H is the effective-operator Hamiltonian, and $\Psi_{l^n \tau SLJM}$ and $\Psi_{l'^n \tau' S' L' J' M'}$ are basis functions of the $4f^n$ configuration ($n = 6$ for Eu^{3+}). The angular parts of the matrix elements can be calculated exactly, whereas the radial parts are treated as adjustable parameters. A parameter set is obtained by optimizing a start set of parameters by a general least-squares fitting process in which the energy differences between the calculated and experimental energy levels are minimized. The best known fitting programs are those written by Crosswhite [109], and by Reid [110]. The total Hamiltonian can be written as the sum of a free-ion and a crystal-field part:

$$H = H_{free\ ion} + H_{crystal\ field} \quad (2)$$

The free-ion Hamiltonian is characterized by a set of three electron repulsion parameters (F^2 , F^4 , F^6), by the spin-orbit coupling constant ζ_{4f} , the Trees configuration interaction parameters (α , β , γ), the three-body configuration interaction parameters (T^2 , T^3 , T^4 , T^6 , T^7 , T^8) and parameters which describe magnetic interactions (M^0 , M^2 , M^4 , P^2 , P^4 , P^6). An additional parameter E_{ave} (*ave* stands for ‘‘average’’) takes into account the kinetic energy

of the electrons and their interaction with the nucleus. It only shifts the barycenter of the whole $4f^6$ configuration. The free-ion Hamiltonian can be written as [109,111]:

$$\begin{aligned}
H_{free\ ion} = E_{ave} + \sum_{k=2,4,6} F^k f_k + \zeta_{4f} A_{SO} + \alpha L(L+1) + \beta G(G_2) + \gamma G(R_7) \\
+ \sum_{i=2,3,4,6,7,8} T^i t_i + \sum_{l=0,2,4} M^l m_l + \sum_{k=2,4,6} P^k p_k
\end{aligned} \tag{3}$$

Here f_k and A_{SO} represent the angular part of the electrostatic and spin-orbit interaction, respectively. L is the total orbital angular momentum. $G(G_2)$ and $G(R_7)$ are the so-called Casimir operators for the groups G_2 and R_7 , respectively. The t_i are the three-particle operators. The m_l and p_k represent the operators for the magnetic corrections. The F^k parameters decrease if k increases. The F^4 and F^6 parameters can be expressed approximately in function of F^2 : $F^4/F^2 = 0.668$ and $F^6/F^2 = 0.495$ [112]. These ratios are those of the hydrogenic wave functions and are applied if the number of experimental data is insufficient to vary the three electrostatic parameters independently. For instance, if data are restricted to the energy levels of the 7F and 5D terms are available for Eu^{3+} , only one parameter can be varied. This doesn't imply that the f orbitals are hydrogenic, but that the ratios F^4/F^2 and F^6/F^2 are rather insensitive to the exact composition of the wave functions [61]. Although electron repulsion and spin-orbit coupling can explain the free-ion level structure in a qualitative way, other minor interactions have to be taken into account for detailed calculations of the free-ion energy levels. These weak interactions include configuration interactions, electrostatic correlated spin-orbit interaction, spin-spin, spin-other-orbit and

relativistic interactions. Diagonalization of the energy matrix which incorporates only the electrostatic and spin-orbit interaction, often results in discrepancies between experimental and calculated levels of several hundred cm^{-1} [61]. Additional parameters and operators are required to describe the configuration interaction. Configuration interaction is the spin-independent interaction between configurations of equal parity. The new operators are two-particle and three-particle operators working within the $4f^n$ configuration. The two-particle correction term in the free-ion Hamiltonian is $\alpha L(L + 1) + \beta G(G_2) + \gamma G(R_7)$ [113]. The values of the parameters α , β and γ are rather constant across the lanthanide series, because processes such as excitation of one or two particles to the high energy continuum states have large contributions to the parameters and the energies of these continuum states relative to the $4f^n$ configurations do not change significantly with the atomic number Z [111]. For $4f^n$ configurations with three or more f electrons, the free-ion Hamiltonian is expanded with the term $\sum_{i=2,3,4,6,7,8} T^i t_i$ to take the three-particle configuration interaction into account [114]. Notice that t_5 and the corresponding parameter T^5 do not exist. Variation of the T^i parameters in a fitting procedure has to be done carefully, since these parameters are only sensitive to particular $^{2S+1}L_J$ levels. If the level for which a T^i parameter shows a great sensitivity is not observed in the spectra, a variation of that T^i parameter will result in a meaningless parameter value [115]. The parameter has to be constrained in that case. Magnetically correlated corrections such as spin-spin and spin-other-orbit interactions are represented by the term $\sum_{l=0,2,4} M^l m_l$ in the Hamiltonian. In the calculations, these parameters are mostly maintained by the pseudo-relativistic Hartree-Fock ratios $M^2/M^0 = 0.56$ and $M^4/M^0 = 0.38$, allowing only M^0 to vary freely [109]. The electrostatic correlated spin-orbit interactions are described by the term $\sum_{k=2,4,6} P^k p_k$. The parameters P^k can be varied in the ratios $P^4/P^2 = 0.75$, $P^6/P^2 = 0.5$ [109]. Since the introduction of new parameters may alter the values of the parameters already fitted, Judd and Crosswhite have introduced orthogonalized operators [116]. These

operators yield parameters that more precisely defined and more stable than the conventional ones. Görrler-Walrand and Binnemans reported a set of free-ion parameters for Eu^{3+} , by averaging different parameter sets that are available in the literature for Eu^{3+} ions doped into single crystals (Table 2) [95], and this set of parameters has been used to calculate the free-ion levels of the $4f^6$ configuration between 0 and 40000 cm^{-1} (Table 3) [117].

Table 2. Average free-ion parameters for Eu^{3+} [95].

Parameter	Value (cm^{-1})
E_{AVE}	63736
F^2	82786
F^4	59401
F^6	42644
α	19.80
β	-617
γ	1460
T^2	370
T^3	40
T^4	40
T^6	-330
T^7	380
T^8	370
ζ_{4f}	1332
M^0	2.38
M^2	1.33
M^4	0.90
P^2	303
P^4	227
P^6	152

Table 3. Calculated energies of free-ion levels for Eu^{3+} between 0 and 40000 cm^{-1} , calculated with the parameters listed in Table 2 [117].

$^{2S+1}L_J$	E_{calc} (cm^{-1})
7F_0	0
7F_1	379
7F_2	1043
7F_3	1896
7F_4	2869
7F_5	3912
7F_6	4992
5D_0	17227
5D_1	18973
5D_2	21445
5D_3	24335
5L_6	25125
5L_7	26177
5G_2	26269
5G_3	26493
5G_4	26611
$^5G_5, ^5G_6$	26642
5L_8	27095
5D_4	27583
5L_9	27844
$^5L_{10}$	28341
5H_3	30870
5H_7	31070
5H_4	31292
$^5H_6, ^5H_5$	31511
3P_0	32790
5F_2	33055
5F_3	33092
5F_1	33366
5F_4	33513
5F_5	34040
5I_4	34057
5I_5	34388
5I_6	34966
5I_7	35429
5I_8	35453
5K_5	36168
5K_6	37320
3P_1	38132

${}^5\text{K}_7$	38247
${}^5\text{G}_2$	38616
${}^5\text{K}_8$	38667
${}^3\text{K}_6, {}^3\text{I}_6$	38780
${}^5\text{G}_3$	39143
${}^5\text{K}_9$	39518
${}^5\text{G}_4$	39726

The terms in the Hamiltonian that represent the non-spherical part of the interactions with the host matrix are described by using the crystal-field Hamiltonian. According to Wybourne, the *crystal-field Hamiltonian* can be written as [61,95]:

$$H_{crystal\ field} = \sum_{i=0}^n \sum_{k=0}^{\infty} \sum_{q=-k}^k B_q^k C_q^k(i) \quad (4)$$

Here $C_q^k(i)$ are tensor operators of rank k , with components q . These tensor operators transform like the spherical harmonics. The B_q^k are the crystal-field parameters, n is the number of electrons (6 in the case of Eu^{3+}) and i represents the i -th electron. For f electrons, $k = 2, 4, 6$. The number of non-zero parameters is determined by the point-group site symmetry of the lanthanide ion. The number of parameters increases if the site symmetry is lowered. Whereas only 2 parameters are required to describe the crystal- field splitting in O_h symmetry, 27 parameters are required in C_1 symmetry. In general, the B_q^k parameters are complex numbers, but in some symmetry the imaginary part of the parameters is zero. The increase in number of crystal-field parameters upon a lowering of symmetry can be illustrated by the crystal-field Hamiltonians for D_{2d} and S_4 symmetry [118]:

$$H_{D_{2d}} = B_0^2 C_0^2 + B_0^2 C_0^4 + B_4^4 (C_{-4}^4 + C_4^4) + B_0^6 C_0^6 + B_4^6 (C_{-4}^6 + C_4^6) \quad (5)$$

$$H_{S_4} = H_{D_{2d}} + iB_4^4 (C_{-4}^4 - C_4^4) + iB_4^6 (C_{-4}^6 - C_4^6) \quad (6)$$

D_{2d} is the symmetry of an undistorted dodecahedron, which should be more correctly be called triangular dodecahedron, to distinguish it from the conventional dodecahedron with pentagonal faces. A small distortion lowers the symmetry from D_{2d} to S_4 . The determination of a reliable set of crystal-field parameters for sites with a low symmetry is very challenging [119-122]. A problem with sites of a low symmetry is that a large number of parameters is required to describe the crystal-field perturbation and that some of these parameters can take unrealistic values, since they will compensate for wrong values of other parameters [123].

The crystal-field perturbation destroys the spherical symmetry of the free-ion and the $^{2S+1}L_J$ terms split up in a number of crystal-field levels. The extent to which the $2J+1$ degeneracy of a $^{2S+1}L_J$ term is removed depends on the symmetry class (icosahedral, cubic, octagonal, hexagonal, pentagonal, tetragonal, trigonal, orthorhombic, monoclinic, triclinic) and not on the point itself (Table 4). The splitting pattern of the J levels can be derived from full-rotational group compatibility tables. For all point groups within a symmetry class, the splitting of a J term is identical. For instance, the splitting of the $^{2S+1}L_J$ terms is the same for all tetrahedral groups (D_{4h} , D_4 , C_{4v} , C_{4h} , C_4 , D_{2d} , S_4). All the $2J+1$ degeneracy is lifted in orthorhombic symmetry, so that a further symmetry lowering will not result in an additional splitting of the $^{2S+1}L_J$ terms in more crystal-field levels. The differences between the different point groups are reflected in different selection rules or in different numbers of transitions that are allowed between two $^{2S+1}L_J$ terms. A lowering in symmetry results in a relaxation of the selection rules and to an increase in the number of allowed transitions. For the point group C_1 , no transitions are forbidden by the selection rules and transitions are allowed between all the

crystal-field sublevels of two $^{2S+1}L_J$ terms. It should be noticed that in spectroscopy, not only the 32 crystallographic point groups are considered, but also molecular point groups such as I_h or D_{4d} .

Table 4. Number of sublevels of a $^{2S+1}L_J$ term for the different symmetry classes.

Symmetry class	Point groups	$J = 0$	$J = 1$	$J = 2$	$J = 3$	$J = 4$	$J = 5$	$J = 6$
Icosahedral	I_h, I	1	1	1	2	2	3	4
Cubic	O_h, O, T_d, T_h, T	1	1	2	3	4	4	6
Octagonal	D_8, C_{8v}, S_8, D_{4d}	1	2	3	4	6	7	8
Hexagonal	$D_{6h}, D_6, C_{6v}, C_{6h},$ C_6, D_{3h}, C_{3h}	1	2	3	5	6	7	9
Pentagonal	$D_{5h}, D_5, C_{5v}, C_{5h}, C_5$	1	2	3	4	5	7	8
Tetragonal	$D_{4h}, D_4, C_{4v}, C_{4h},$ C_4, S_4, D_{2d}	1	2	4	5	7	8	10
Trigonal	$D_{3d}, D_3, C_{3v},$ $C_{3i} (= S_6), C_3$	1	2	3	5	6	7	9
Orthorhombic	D_{2h}, D_2, C_{2v}	1	3	5	7	9	11	13
Monoclinic	C_{2h}, C_2, C_s	1	3	5	7	9	11	13
Triclinic	C_1, C_i	1	3	5	7	9	11	13

The convention to describe a transition between two $^{2S+1}L_J$ levels is to write the high energy state at the left hand side and the low energy state at the right hand side. The arrow points from the initial to the final state. For instance, the transition from the 5D_0 excited state to the 7F_1 state in the luminescence spectrum is written as $^5D_0 \rightarrow ^7F_1$. The same convention is used

for the absorption spectra. The transition from the 7F_1 state to the 5D_0 state is written as ${}^5D_0 \leftarrow {}^7F_1$ (not ${}^7F_1 \rightarrow {}^5D_0$).

3. Luminescence spectra

3.1 General features and selection rules

A luminescence spectrum (or emission spectrum) is recorded by fixing the excitation wavelength, while the detection wavelength of the spectrofluorimeter is scanned. The luminescence spectra of europium(III) compounds are more informative than the corresponding absorption spectra. Many europium(III) compounds show an intense photoluminescence, due to the ${}^5D_0 \rightarrow {}^7F_J$ transitions ($J = 0 - 6$) from the 5D_0 excited state to the J levels of the ground term 7F . An overview of the transitions is given in Table 5. Very often the transitions to the 7F_5 and 7F_6 levels are not observed, because they are outside the wavelength range of the detectors of spectrofluorimeters (*vide infra*). In Figure 3, the luminescence spectrum of the europium β -diketonate complex $[\text{Eu}(\text{tta})_3(\text{phen})]$ is shown (tta = 2-thenoyltrifluoroacetylacetonate, phen = 1,10-phenanthroline). Transitions from higher excited states (5D_1 , 5D_2 , 5D_3) are much less common (see section 3.8).

Table 5. Overview of the transitions observed in luminescence spectra of europium(III) compounds.

Transition ^a	Dipole character ^b	Wavelength range (nm)	Relative intensity ^c	Remarks
$^5D_0 \rightarrow ^7F_0$	ED	570–585	vw to s	only observed in C_n , C_{nv} and C_s symmetry
$^5D_0 \rightarrow ^7F_1$	MD	585–600	s	intensity largely independent of environment
$^5D_0 \rightarrow ^7F_2$	ED	610–630	s to vs	hypersensitive transition; intensity very strongly dependent on environment
$^5D_0 \rightarrow ^7F_3$	ED	640–660	vw to w	forbidden transition
$^5D_0 \rightarrow ^7F_4$	ED	680–710	m to s	intensity dependent on environment, but no hypersensitivity
$^5D_0 \rightarrow ^7F_5$	ED	740–770	vw	forbidden transition
$^5D_0 \rightarrow ^7F_6$	ED	810–840	vw to m	rarely measured and observed

^a Only transitions starting from the 5D_0 level are shown. ^b ED = induced magnetic dipole transition, MD = magnetic dipole transition; ^c vw = very weak, w = weak, m = medium, s = strong, vs = very strong.

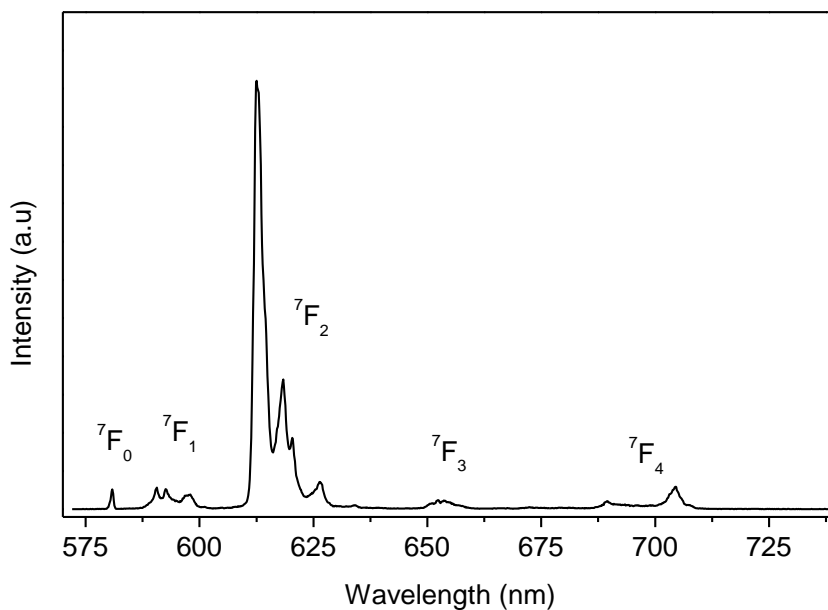


Figure 3. Luminescence spectrum $[Eu(tta)_3(phen)]$ at 77 K. The excitation wavelength is 396 nm. All the transitions start from the 5D_0 state. Adapted by permission of The Royal Society of Chemistry from reference [15]. Copyright 2002 The Royal Society of Chemistry.

Table 6. Selection rules for intraconfigurational $f-f$ transitions.

Induced electric dipole transitions (ED)	Magnetic dipole transitions (MD)
$ \Delta S = 0$	$\Delta S = 0$
$ \Delta L \leq 6$	$\Delta L = 0$
$ \Delta J \leq 6$ and $ \Delta J = 2, 4, 6$ if $J = 0$ or $J' = 0$	$\Delta J = 0, \pm 1$, but $0 \leftrightarrow 0$ is forbidden
(as in the case of Eu^{3+})	

An observation that can be made from the inspection of the positions of the different $^5D_0 \rightarrow ^7F_J$ transitions is that the distance between a J and the $J+1$ line increases with increasing J value, i.e. the $^5D_0 \rightarrow ^7F_1$ transition is very close to the $^5D_0 \rightarrow ^7F_0$ transition, but the $^5D_0 \rightarrow ^7F_6$ transition is lying more than 50 nm further to the infrared than the $^5D_0 \rightarrow ^7F_5$ transition [124]. This behavior can be explained by the fact that the splitting of the 7F_J multiplet corresponds quite well to the *Landé interval rule*: the interval between successive energy levels is proportional to the larger of their total angular momentum values J (i.e. the splitting increases with increasing J values). The majority of the transitions observed in the luminescence spectrum are *induced electric dipole transitions* (ED transitions). An electric dipole transition is the consequence of the interaction of the lanthanide ion with the electric field vector through an electric dipole. The creation of an electric dipole supposes a linear movement of charge. Such a transition has odd parity. Therefore, the electric dipole operator has odd transformation properties under inversion with respect to an inversion center. Intraconfigurational electric dipole transitions (e.g. s-s, p-p, d-d, or f-f transitions) are forbidden by the *Laporte selection rule*. The Laporte selection rule strictly applies to a lanthanide ion in the gas phase (i.e., a centrosymmetric environment); however, it is relaxed for lanthanide ions embedded in a medium, since the transitions can be partly allowed by vibronic coupling or via mixing of higher configurations into the 4f wavefunctions by the crystal-field effect. The observed transitions are much weaker than ordinary electric dipole transitions. Therefore, they are often called “*induced*” *electric dipole transitions* (or “*forced*” *electric dipole transitions*), rather than just electric dipole transitions. The intensities of the ED transitions can be described by the Judd-Ofelt theory (JO-theory; see section 9) [94,125-129]. Some transitions such as the $^5D_0 \rightarrow ^7F_1$ transition have magnetic dipole character. *Magnetic dipole transitions* (MD transitions) are allowed by the Laporte selection rule, but their intensities are weak and comparable to those of the induced electric dipole transitions

[94]. The intensity of a magnetic dipole transition is largely independent of the environment and can be considered in a first approximation to be constant [130]. For the calculation of the intensities of MD transitions, only the free-ion wave functions are needed, not the crystal-field wave functions. A MD transition is caused by interaction of the lanthanide ion with the magnetic field component of the light via a magnetic dipole. If charge is displaced over a curved path during the transition, the transition will possess magnetic dipole character. The curvature of the displacement will only be weakly apparent in a volume as small as the extent of a lanthanide ion, so that magnetic dipole transitions have a weak intensity. Magnetic dipole radiation can also be considered as a rotational displacement of charge. Since the sense of a rotation is not reversed under inversion through an inversion center, a magnetic dipole transition has even parity. Therefore, a magnetic dipole operator possesses even transformation properties under inversion and allows transitions between states with even parity (i.e. intraconfigurational transitions such as 4f-4f transitions). The selection rules for ED and MD transitions are summarized in Table 6. In principle, also *electric quadrupole transitions* could occur. An electric quadrupole transition arises from a displacement of charge that has quadrupolar character. An electric quadrupole consists of four point charges with overall zero charge and zero dipole moment. It can be considered as two dipoles arranged in such a way that their dipole moments cancel out. An electric quadrupole has even parity. Electric quadrupole transitions are much weaker than magnetic dipole and induced electric dipole transitions. There is no convincing evidence for electric quadrupole transitions in lanthanide spectra, although hypersensitive induced electric dipole transitions obey the selection rules for electric quadrupole transitions (see section 9.3).

The selection rules on ΔS and ΔL are only strictly valid in the Russell-Saunders coupling scheme. They are relaxed in the intermediate coupling scheme, so S and L are not good quantum numbers in that scheme. Since J remains a good quantum number in the

intermediate coupling scheme, the selection rule for ΔJ is more rigorous. It can be relaxed only by J -mixing. For these reasons, the ${}^5D_0 \rightarrow {}^7F_J$ ($J = 0, 3, 5$) transitions have very weak intensities. J -mixing involves the mixing of the wave functions of sublevels of different J levels, when their irreducible representations are the same. Thus, wave functions with the same symmetry can mix under the influence of the crystal field. The degree of J -mixing between two multiplets J and J' is inversely proportional to the energy difference between the J and J' states.

In general, luminescence spectra are recorded in a wavelength scale (expressed in nanometers, nm). To facilitate the comparison between different spectra, it is recommended to plot the spectra with the shortest wavelength at the left hand side and the longest wavelength at the right hand side. In the older literature, the opposite convention is often used. The frequency of light is physically more significant than its wavelength, since the frequency remains unchanged when the light wave propagates through various media. Moreover, the frequency ν is directly proportional to the energy E of the transition, via the formula $E = h\nu$, where h is Planck's constant. Most spectroscopists prefer to deal with wavenumbers (number of waves per cm) rather than frequencies. The wavenumber $\tilde{\nu}$ is defined as:

$$\tilde{\nu} = \frac{\nu}{c} = \frac{1}{\lambda_{vac}} = \frac{1}{n_{air}\lambda_{air}} \quad (7)$$

To find the wavenumber for a transition measured in air, one has to correct in principle for the refractive index of air, which is wavelength dependent. Except for high accuracy spectroscopic work, one can assume that $n_{air} = 1$. In other cases, n_{air} has to be calculated, for instance via the empirical Edlén formula [131]. Wavenumbers are expressed in units of reciprocal centimeters (cm^{-1}). A spectrum recorded in wavelength scale (in nanometers) can be converted to wavenumber scale (in cm^{-1}) by applying the following formula:

$$\tilde{\nu} (/cm^{-1}) = \frac{10^7}{\lambda (/nm)} \quad (8)$$

It is recommended to plot spectra in wavenumber scale with the highest wavenumber at the left hand side and the lowest wavenumber at the right hand side of the spectrum.

3.2 Transition ${}^5D_0 \rightarrow {}^7F_0$

The ${}^5D_0 \rightarrow {}^7F_0$ transition is strictly forbidden according to the standard Judd-Ofelt theory. The occurrence of this transition is a well-known example of the breakdown of the selection rules of the Judd-Ofelt theory (a 0–0 transition is forbidden by the ΔJ selection rule of the Judd-Ofelt theory). Several authors have tried to theoretically explain why this transition is observed [132-142]. Theoretical models include the breakdown of the closure approximation in the Judd-Ofelt theory and third order perturbation theory. However, the most obvious explanation is to assume that this transition is due to J -mixing [143-147] or to mixing of low-lying charge-transfer states into the wavefunctions of the $4f^6$ configuration [148]. As explained in section 3.1, J -mixing is due to the crystal-field perturbation and causes mixing of the wavefunctions of terms with different J values. The wavefunction of the 7F_0 state contains after J -mixing also contributions from the $J = 2, 4, 6$ states. The mixing of the charge-transfer states is described in section 4.6. The two mechanisms are not independent, since it has been noticed that an inverse relationship exists between the energy of the transfer state and the crystal-field strength: low energies for the charge-transfer states result in strong crystal-field effects [149,150]. Strong crystal-field effects enhance J -mixing.

The ${}^5D_0 \rightarrow {}^7F_0$ transition belongs to the 4f-4f transitions with the smallest linewidth ever observed. The half width at half maximum of the ${}^5D_0 \rightarrow {}^7F_0$ transition in $\text{EuCl}_3 \cdot 6\text{H}_2\text{O}$ is

about 0.12 cm^{-1} at 4.2 K and about 1 cm^{-1} at 250 K [151]. For $\text{Eu}(\text{NO}_3)_3 \cdot 6\text{H}_2\text{O}$, the values are 0.18 cm^{-1} and 2 cm^{-1} , respectively [151]. For $\text{Eu}(\text{BrO}_3)_3 \cdot 9\text{H}_2\text{O}$, the values are 1.1 cm^{-1} at 77 K and 2.3 cm^{-1} at 295 K [152]. In glasses, the ${}^5\text{D}_0 \rightarrow {}^7\text{F}_0$ transition is much broader due to inhomogeneous line broadening. For example, the line width is 105 cm^{-1} in calcium diborate glass [153], 119 cm^{-1} in phosphate glasses and 149 cm^{-1} in silicate and germanate glasses [154]. It was concluded that about 50 slightly different sites of C_s symmetry are present in phosphate, silicate and germanate glasses, by comparison of the half width at half maximum in glasses with the value of 2 cm^{-1} in Eu_2O_3 . The slight differences in the environment are the result of small differences in metal-ligand angles and distances.

The observation of the ${}^5\text{D}_0 \rightarrow {}^7\text{F}_0$ transition is an indication that the Eu^{3+} ion occupies a site with C_{nv} , C_n or C_s symmetry [155]. The occurrence of the ${}^5\text{D}_0 \rightarrow {}^7\text{F}_0$ transition in these symmetries can be understood by considering the selection rules. A $J = 0$ state must transform as the identity representation of the point symmetry group and this requires that some of the components of the electric dipole operator also transform as the identity representation. This is the case for point groups for which the crystal-field potential contains C_{1q} spherical harmonics, i.e. the symmetry groups C_{nv} , C_n or C_s . Nieuwpoort and Blasse noticed that the ${}^5\text{D}_0 \rightarrow {}^7\text{F}_0$ transition always appears whenever it is allowed by the observed site symmetry [139]. The fact that this transition is observed only for certain symmetries is nicely illustrated by the consecutive formation of dipicolinate (DPA) complexes. The ${}^5\text{D}_0 \rightarrow {}^7\text{F}_0$ transition occurs for the intermediate low symmetry complexes $[\text{Eu}(\text{DPA})]^+$ and $[\text{Eu}(\text{DPA})_2]^-$, but not for the high symmetry complexes $[\text{Eu}(\text{H}_2\text{O})_9]^{3+}$ (D_{3h}) and $[\text{Eu}(\text{DPA})_3]^{3-}$ (D_3). This was first observed in the absorption spectra of these complexes [156], and later in the luminescence spectra (Figure 4) [157].

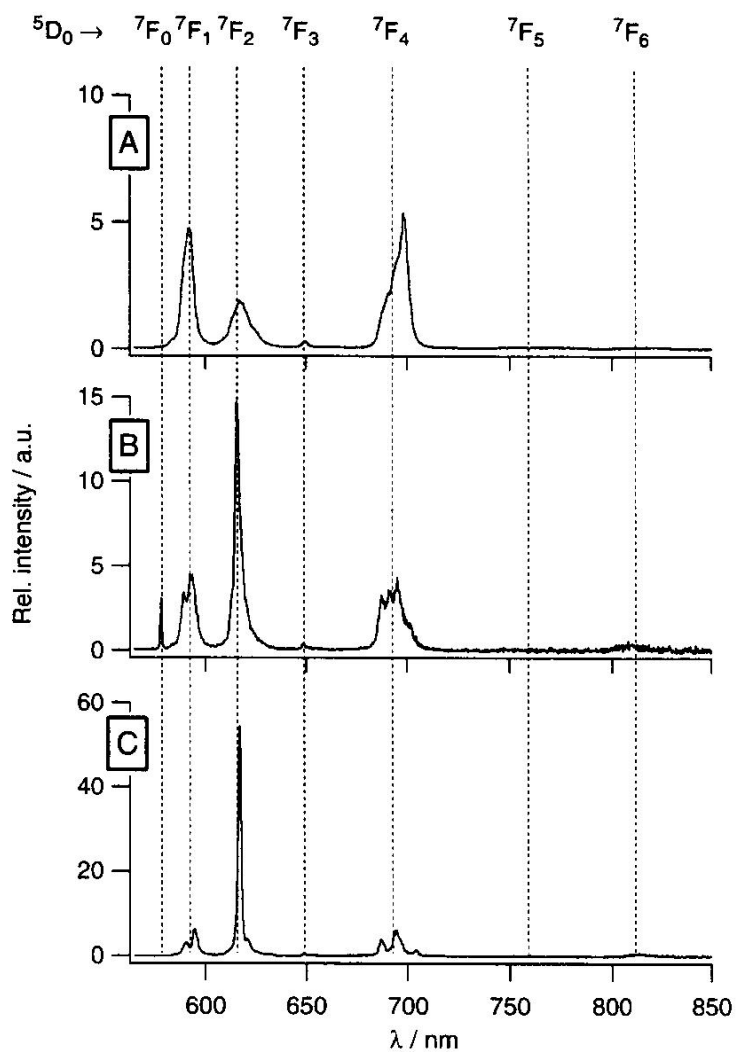


Figure 4. Corrected luminescence spectra of Eu^{3+} in different ligand environments: (A) Eu^{3+} in water; (B) $[\text{Eu}(\text{DPA})]^+$ in water; (C) $[\text{Eu}(\text{DPA})_3]^{3-}$ in water. The spectra have been scaled so that the respective ${}^5\text{D}_0 \rightarrow {}^7\text{F}_1$ bands have identical areas. Note the different scales of the Y-axes. Reprinted with permission of The Royal Society of Chemistry from reference [157].

Copyright 2002 The Royal Society of Chemistry.

In most europium(III) spectra, the $^5D_0 \rightarrow ^7F_0$ transition is very weak, even for complexes with C_{nv} , C_n or C_s symmetry. However, the $^5D_0 \rightarrow ^7F_0$ transition is unusually intense in the β -diketonate complex $[\text{Eu}(\text{dbm})_3(\text{H}_2\text{O})]$, (dbm = dibenzoylmethanate), with the Eu^{3+} ion at a site with C_3 symmetry [158]. In the luminescence spectrum of this complex, the $^5D_0 \rightarrow ^7F_0$ transition has a higher peak height than the $^5D_0 \rightarrow ^7F_1$ transition, although the latter transition has the largest integrated peak area, due to the extreme narrowness of the $^5D_0 \rightarrow ^7F_0$ transition. Other examples of europium(III) complexes with intense $^5D_0 \rightarrow ^7F_0$ transitions are the complexes of nitrilotriacetate (NTA) and of the macrocyclic ligand DOTA [159]. In $\text{Sr}_2\text{TiO}_4:\text{Eu}^{3+}$, the transition $^5D_0 \rightarrow ^7F_0$ is 1.65 times more intense than the $^5D_0 \rightarrow ^7F_1$ transition [160]. The high intensity was ascribed to the ordered crystal structure of Sr_2TiO_4 , which leads to large linear terms in the crystal-field potential. Unusually high intensities for the $^5D_0 \rightarrow ^7F_0$ transition are also observed for Eu^{3+} in fluorapatite $\text{Ca}_5(\text{PO}_4)_3\text{F}:\text{Eu}^{3+}$ [161], hydroxyapatite [162], oxysulfates $\text{Ln}_2\text{O}_2\text{SO}_4:\text{Eu}^{3+}$ (Ln = La, Gd, Y) [163], $\text{LaOCl}:\text{Eu}^{3+}$ [164], α -cordierite [165,166], mullite [167], $\text{La}_2\text{Si}_2\text{O}_7$ [167], $\text{La}_2\text{O}_3:\text{Eu}^{3+}$ [168], C-type oxides (Gd_2O_3 , Lu_2O_3 , Lu_2O_3 , Y_2O_3 , In_2O_3 , Sc_2O_3) [169] and $\text{Ba}_4\text{Ln}_2\text{ZrWO}_{12}:\text{Eu}^{3+}$ (Ln = La, Gd, Y) [170]. In $\text{Sr}_5(\text{PO}_4)_3\text{F}:\text{Eu}^{3+}$, with the Eu^{3+} ion in the Sr^{2+} site with a charge-compensating oxide ion substituting a nearest-neighbor fluoride ion in the lattice, the $^5D_0 \rightarrow ^7F_0$ transition dominates the spectrum: the intensity ratio $I(^5D_0 \rightarrow ^7F_0)/I(^5D_0 \rightarrow ^7F_1)$ is larger than 20 [171]. This intensity ratio shows the following trend for Eu^{3+} doped in oxybromides: YOBBr (<0.01), GdOBBr (0.2), LaOBBr (2.5) (Figure 5) [149]. The $^5D_0 \rightarrow ^7F_0$ transition is the most intense transition in the luminescence spectrum of $\text{LaOBBr}:\text{Eu}^{3+}$. In layered crystal structures, the intensity of the transition strongly depends on the details of the layer packing and the interionic distances [172]. The most intense $^5D_0 \rightarrow ^7F_0$ transition ever reported is that of the $C_s(\text{O}^{2-})$ site of $\text{BaFCl}:\text{Eu}^{3+}$, with a charge-compensating oxide ion substituting a nearest-neighbor fluoride

ion in the lattice [148]. This transition is 25 times more intense than the ${}^5D_0 \rightarrow {}^7F_1$ magnetic dipole transition! Such an extreme intensity cannot be explained by J -mixing. A possible explanation is mixing of charge-transfer states into the $4f^6$ levels of Eu^{3+} . As will be explained in section 4.6, the charge-transfer states are lying at a much lower energy in Eu^{3+} than in the other lanthanide ions. As a consequence, a much stronger interaction between the charge-transfer states and the lower levels of the $4f^n$ configuration is expected. This mixing also gives rise to other anomalies in the crystal-field spectra, as described by Chen and Liu [148]. There is a correlation between the solvent basicity and the intensity of the ${}^5D_0 \rightarrow {}^7F_0$ transition in a tetrakis β -diketonate complex with a tetraalkylphosphonium counter ion [173]. The higher intensity in the more basic solvents was attributed to a higher nucleophilicity of the solvent and a resulting change in the coordination sphere by interaction between the solvent and the Eu^{3+} ion.

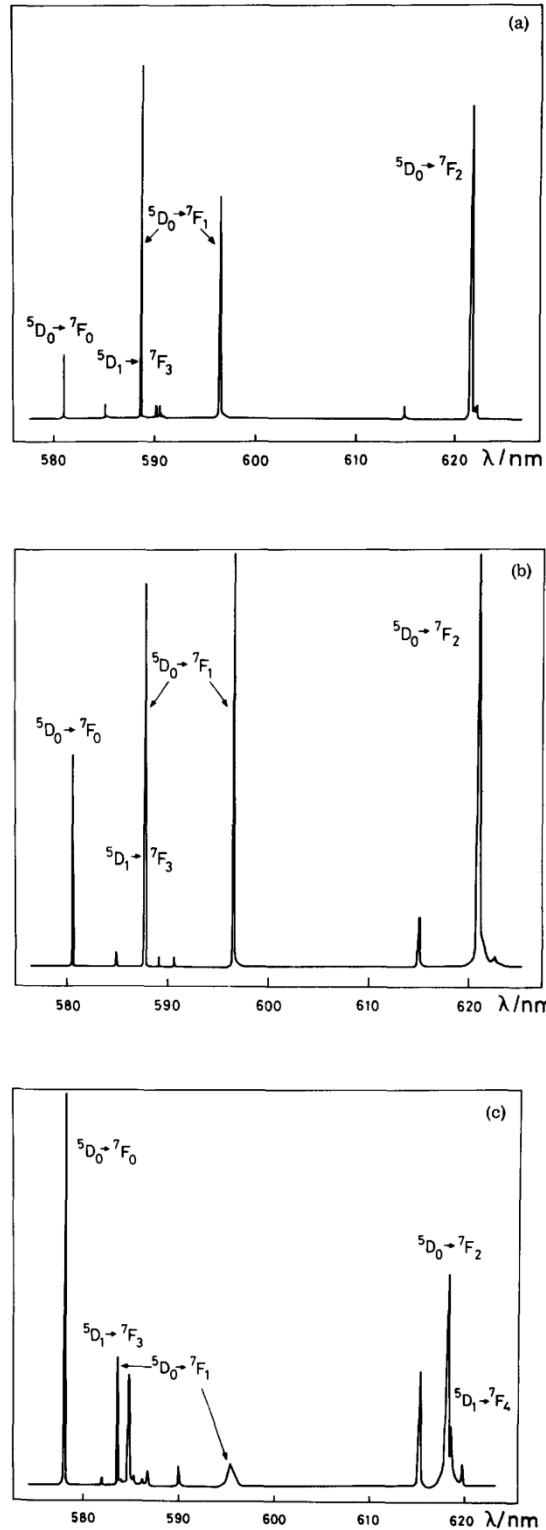


Figure 5. Part of the luminescence spectra of Eu^{3+} doped in oxybromides at 77 K: (a) YOBr; (b) GdOBr and (c) LaOBr. The increase in the intensity of the ${}^5\text{D}_0 \rightarrow {}^7\text{F}_0$ transition in the order YOBr < GdOBr < LaOBr is clearly visible. Reprinted with permission from reference [149] Copyright 1982 AIP Publishing LLC.

The ${}^5D_0 \rightarrow {}^7F_0$ transition is also useful for the determination of the presence of non-equivalent sites in a host crystal or for determination of the number of different europium(III) species in solution, because maximum one peak is expected for a single site or species, due to the non-degeneracy of the 7F_0 and 5D_0 levels [80,98,174,175]. The observation of more than one peak in the spectral region where the ${}^5D_0 \rightarrow {}^7F_0$ transition is expected, shows that more than one site or species is present, but it does not allow the determination of the exact number of sites or species, because sites or species with a symmetry other than C_{nv} , C_n or C_s do not give an observable ${}^5D_0 \rightarrow {}^7F_0$ transition. The luminescence spectra of the individual sites of emitting species can be observed separately by site-selective excitation via a tunable laser source. This was nicely illustrated by Bünzli and coworkers for europium(III) crown ether complexes (Figure 6) [176,177]. Four luminescence centers could be detected in the garnet $Y_3Al_5O_{12}:Eu^{3+}$ by site-selective excitation [178]. Site selective excitation has often been used to probe the local structure in Eu^{3+} -doped glasses and glass ceramics (Figure 7) [179-186].

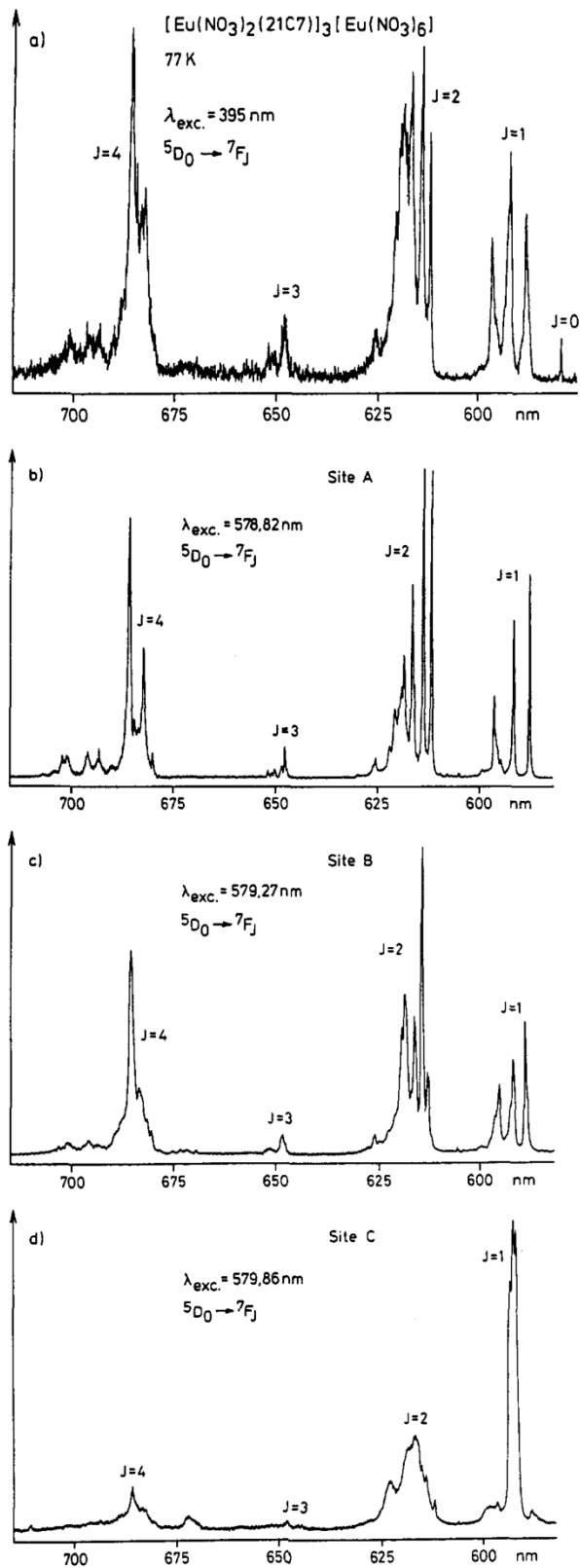


Figure 6. Luminescence spectra of the europium(III) 21-crown-7 complex $[Eu(NO_3)_2(21C7)]_3[Eu(NO_3)_6]$ at 77 K: (a) excitation at 395 nm, (b-d): site-selective

excitation of the $^5D_0 \rightarrow ^7F_0$ transitions of the different sites. Reprinted with permission from reference [177]. Copyright 1989 American Chemical Society.

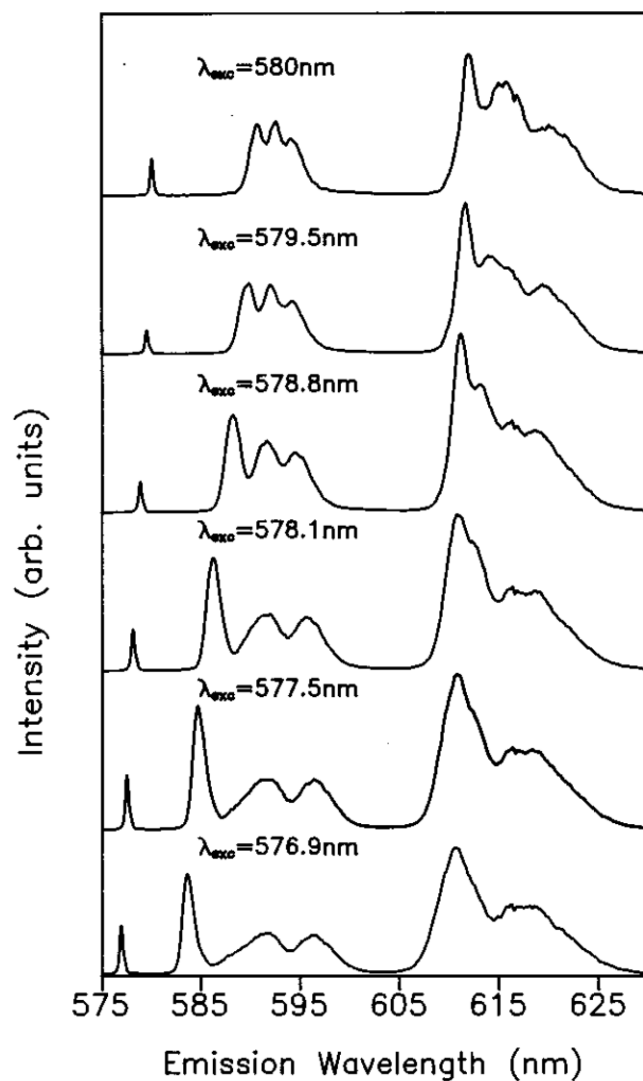


Figure 7. Time-resolved line-narrowed emission spectra of $^5D_0 \rightarrow ^7F_{0,1,2}$ transitions of Eu^{3+} ions in $60\text{NaPO}_3\text{-}15\text{BaF}_2\text{-}24.5\text{YF}_3\text{-}0.5\text{EuF}_3$ fluorophosphate glass. The luminescence was measured at 4.2 K at a time delay of 1 ms after the laser pulse and at different excitation wavelengths. Different sites can be recognized. Reprinted with permission from reference [186]. Copyright 1996 The American Physical Society.

If the structural difference between two sites is small, the energy differences between the different peaks in the ${}^5D_0 \rightarrow {}^7F_0$ region are small as well and the presence of more than one site is only revealed by an asymmetric shape of the ${}^5D_0 \rightarrow {}^7F_0$ line or as a shoulder. However, the presence of two distinct geometrical isomers in a crystal structure can result in quite a large energy difference between the transitions in the ${}^5D_0 \rightarrow {}^7F_0$ region. This is illustrated by the splitting of 35 cm^{-1} in the luminescence spectrum of tris(dipivaloylmethanato)(2,9-dimethyl-1,10-phenanthroline)europium(III) [187]. It is evident that when mixtures of different complexes are present in solution the energy differences between the different transitions in the ${}^5D_0 \rightarrow {}^7F_0$ region can be large as well. Monitoring the intensity of the ${}^5D_0 \rightarrow {}^7F_0$ transition as a function of the ligand concentration has been used to determine stability constants of complexes [188-191]. It must be mentioned that often luminescence excitation spectra rather than emission spectra are being used for measurement of stability constants (see section 5). The quadratic shift of the ${}^5D_0 \rightarrow {}^7F_0$ transition energy of Eu^{3+} with temperature has been used to determine the operating temperature of phosphor screens in cathode-ray tubes. The method is reliable than measurement of the relative intensities of the transitions in the luminescence spectrum [192].

If the ${}^5D_0 \rightarrow {}^7F_0$ transition is strictly forbidden by the selection rules, the determination of the energy of the 5D_0 state becomes less straightforward. However, an accurate location of the 5D_0 state is required for a precise determination of the 7F_J levels, because the 5D_0 state is the initial level for the ${}^5D_0 \rightarrow {}^7F_J$ transitions. In the absence of the ${}^5D_0 \rightarrow {}^7F_0$ transition, the position of the 7F_1 level can be determined from the wavenumber of the ${}^5D_1 \rightarrow {}^7F_1$ transition, and the wavenumber of the ${}^5D_0 \rightarrow {}^7F_1$ transition can then be used to determine the position of the 5D_0 level. In case the ${}^5D_1 \rightarrow {}^7F_1$ transition is not observed in the luminescence spectrum,

the corresponding absorption spectrum can be measured to determine the position of the ${}^5D_1 \leftarrow {}^7F_1$ transition.

At low temperatures and by using a spectroscopic setup with an extremely high resolution, it is possible to observe fine structure for the ${}^5D_0 \rightarrow {}^7F_0$ transition due to the hyperfine interactions with the nuclear momenta I of the nuclei of the ${}^{151}\text{Eu}$ and ${}^{153}\text{Eu}$ isotopes. By this interaction, the 7F_0 and 5D_0 levels split each into three sublevels. Hyperfine splitting has been observed in the high resolution spectra of $\text{EuCl}_3 \cdot 6\text{H}_2\text{O}$ [193,194]. Further hyperfine structure was observed due to interactions with the nuclear momenta of H, Cl and O isotopes in the sample [193].

3.3 Transition ${}^5D_0 \rightarrow {}^7F_1$

The ${}^5D_0 \rightarrow {}^7F_1$ transition is a magnetic dipole (MD) transition. Although the intensity of a magnetic dipole transition is largely independent of the environment of the Eu^{3+} ion, it must be noticed that the invariability of the intensity of the ${}^5D_0 \rightarrow {}^7F_1$ transition only applies to the total integrated intensity of this transition and not to the individual intensities of the crystal-field components [130]. The total intensity of the ${}^5D_0 \rightarrow {}^7F_1$ transition can be influenced by J -mixing. Nevertheless, the intensity of this transition is often considered to be constant and this transition is used to calibrate the intensity of europium(III) luminescence spectra. For comparison of two luminescence spectra, the intensities are scaled in such a way that the ${}^5D_0 \rightarrow {}^7F_1$ transition has the same (integrated) intensity in the two spectra. The ${}^5D_0 \rightarrow {}^7F_1$ transition directly reflects the crystal-field splitting of the 7F_1 level. In cubic or icosahedral crystal fields, the 7F_1 level is not split. In hexagonal, tetragonal and trigonal crystal fields, the 7F_1 level is split into a non-degenerate and a twofold degenerate crystal-field level. In orthorhombic or lower symmetries, the total removal of crystal field degeneracies will result

in three sublevels for 7F_1 . The total splitting of the 7F_1 level in highly symmetric compounds ranges between 0 cm^{-1} for the cubic elpasolites (e.g. $\text{Cs}_2\text{NaEuCl}_6$) [195,196] to 346 cm^{-1} for LaOBr:Eu^{3+} [149]. For Eu^{3+} compounds with a low site symmetry, examples of an even larger total splitting of the 7F_1 level have been reported: 392 cm^{-1} for $\text{LaMgB}_5\text{O}_{10}:\text{Eu}^{3+}$ [197], 456 cm^{-1} for the A site in $\text{Gd}_2(\text{SiO}_4)\text{O}:\text{Eu}^{3+}$ [198], 476 cm^{-1} for $\text{LaBGeO}_5:\text{Eu}^{3+}$ [199], 553 cm^{-1} for $\text{Y}_6\text{WO}_{16}:\text{Eu}^{3+}$ [200], 653 cm^{-1} for the A site in $\text{Ca}_{10-x}\text{Eu}_x(\text{PO}_4)_6\text{O}_{1+x/2}$ [201], 724 cm^{-1} for cordierite [166], and 887 cm^{-1} for hydroxyapatite [167]. If the crystal-field splitting of the 7F_1 level is very large, there will be an overlap with the crystal-field sublevels of the 7F_2 state. As a consequence, the crystal-field lines of the ${}^5D_0 \rightarrow {}^7F_1$ transition overlap with those of the ${}^5D_0 \rightarrow {}^7F_2$ transition. This is a very exceptional situation. The crystal-field sublevels of the 7F_1 level can be discriminated from those of the 7F_2 level, by relying on the empirical correlations between the barycenter of the 7F_1 state and the position of the 5D_0 level, as well as between the barycenters of the 7F_1 and 7F_2 levels [202]. A spectrum with very large splitting of the 7F_1 level into three components and a missing ${}^5D_0 \rightarrow {}^7F_0$ transition can be mistaken for a spectrum consisting of a splitting of the 7F_1 level in two components and the ${}^5D_0 \rightarrow {}^7F_0$ transition present. Here too, the empirical correlation between the barycenter of the 7F_1 state and the 5D_0 level is helpful, as illustrated for the luminescence spectrum of an ionic europium(III) complex with Schiff base ligands [203]. On the other hand, a small splitting of the 7F_1 level is observed not only for systems with a cubic or approximately cubic symmetry, such as the elpasolites [196,204,205] and oxyfluorides ($\text{LaOF}:\text{Eu}^{3+}$, $\text{GdOF}:\text{Eu}^{3+}$, $\text{YOF}:\text{Eu}^{3+}$) [206,207], but also for the double nitrates $\text{Eu}_2\text{M}_3(\text{NO}_3)_{12}\cdot 24\text{H}_2\text{O}$ ($\text{M} = \text{Mg}, \text{Zn}$) [208,209], which have a symmetry close to that of an icosahedron [210]. A small splitting of the 7F_1 level is also present in many systems with a tricapped trigonal prism as the coordination polyhedron around the Eu^{3+} ion, such as $\text{Na}_3[\text{Eu}(\text{ODA})_3]\cdot 2\text{NaClO}_4\cdot 6\text{H}_2\text{O}$ (also called EuODA) [112,211,212], $\text{Eu}(\text{BrO}_3)_3\cdot 9\text{H}_2\text{O}$ [152,213,214], $\text{Eu}(\text{C}_2\text{H}_5\text{SO}_4)_3\cdot 9\text{H}_2\text{O}$ [215,216], and

LaCl₃:Eu³⁺ [217]. It is not totally unexpected that small splittings of the ⁷F₁ level are found for systems with a tricapped trigonal prism or an icosahedron as coordination polyhedron. In these polyhedra with a high coordination number, the atoms in the first coordination sphere have a fairly equal spatial distribution and this distribution is mimicking a spherical distribution for which no splitting of the ⁷F₁ level occurs [218]. This small crystal-field splitting can also be explained by simple calculations based on a point charge electrostatic model (PCEM) [219]. The PCEM model has been used to study the splitting of the ⁷F₁ level in a series of oxide host matrices [220]. Due to the presence of many different sites with different crystal-field strengths, a large range of ⁷F₁ splitting sizes can be observed in one glass host. For instance, by the laser-induced fluorescence line narrowing technique, a variation for the ⁷F₁ splitting between 150 and 550 cm⁻¹ was observed for Eu³⁺ in a silicate glass [221]. Similar results were observed for Eu³⁺-doped 40Bi₂O₃-40PbO-10Ga₂O₃-10GeO₂ and 60GeO₂-25PbO-15Nb₂O₅ glasses [222], as well as TeO₂-TiO₂-Nb₂O₅ glass [223].

The ⁵D₀ → ⁷F₁ transition is the most intense transition in the spectra of solids with a centrosymmetric crystal structure. This is nicely illustrated by the luminescence spectra of Ba₂GdNbO₆:Eu³⁺ (perovskite structure, O_h symmetry) and Gd₂Ti₂O₇:Eu³⁺ (pyrochlore structure, approximate symmetry D_{3d}) [224]. This ⁷F₁ level is not split for Ba₂GdNbO₆:Eu³⁺ (O_h), whereas it is split for Gd₂Ti₂O₇:Eu³⁺ (D_{3d}), as predicted by theory. For these two centrosymmetric host crystals, the transition ⁵D₀ → ⁷F₄ was not observed. Besides Gd₂Ti₂O₇:Eu³⁺, other compounds with a pyrochlore structure such as Gd₂Sn₂O₇:Eu³⁺ and Gd₂TiSnO₇:Eu³⁺ have a luminescence spectrum that is dominated by the ⁵D₀ → ⁷F₁ transition [225]. Also in perovskites other than Ba₂GdNbO₆:Eu³⁺, such as Ba₂GdTaNbO₆:Eu³⁺ and Ba₂GdNbO₆:Eu³⁺, the ⁵D₀ → ⁷F₁ transition is dominant [225]. The influence of the cation size on the structure of the host matrix and hence on the luminescence spectra of Eu³⁺ in these host matrices is nicely illustrated for a series of borate compounds [226]. The low-temperature

luminescence spectra of $\text{Ba}_2\text{LnNbO}_6:\text{Eu}^{3+}$ ($\text{Ln} = \text{Gd}, \text{Y}$) are dominated by the ${}^5\text{D}_0 \rightarrow {}^7\text{F}_1$ transition [227]. The coordination polyhedron can be described as a distorted octahedron. The analysis of the splitting pattern reveals that the actual symmetry is C_{2h} or C_i . The fact that the coordination polyhedron is close to an ideal octahedron is evident from the very small splitting of the ${}^7\text{F}_1$ level (13 cm^{-1}). Interestingly, the low-temperature luminescence spectrum of the related compound $\text{Ba}_2\text{LaNbO}_6:\text{Eu}^{3+}$ is dominated by the ${}^5\text{D}_0 \rightarrow {}^7\text{F}_2$ transition [228]. The symmetry of this compound is low: C_2 or C_{2v} . In SrTiO_3 with the cubic perovskite structure, the Eu^{3+} enters the centrosymmetric Sr^{2+} site and is twelve-coordinate [229]. This results in the typical spectrum of a centrosymmetric europium(III) compound with an intense ${}^5\text{D}_0 \rightarrow {}^7\text{F}_1$ transition. A similar situation is found for $\text{SrSnO}_3:\text{Eu}^{3+}$, where up to 2 at.% of Eu^{3+} can enter the Sr^{2+} sites [230,231]. The ${}^5\text{D}_0 \rightarrow {}^7\text{F}_1$ transition is the most intense transition in the cathodoluminescence spectra of $\text{InBO}_3:\text{Eu}^{3+}$ and $\text{ScBO}_3:\text{Eu}^{3+}$ with the centrosymmetric rhombohedral calcite structure (C_{3i} symmetry). $\text{LuBO}_3:\text{Eu}^{3+}$ occurs as two polymorphs, one with the calcite structure and one with the pseudovaterite structure (D_3 symmetry, no center of symmetry). The ${}^5\text{D}_0 \rightarrow {}^7\text{F}_1$ transition is the most intense transition for the two structures, but the ${}^5\text{D}_0 \rightarrow {}^7\text{F}_2$ transition is more intense in the pseudo-vaterite polymorph than in the calcite polymorph. $\text{YBO}_3:\text{Eu}^{3+}$ and $\text{GdBO}_3:\text{Eu}^{3+}$ have a pseudo-vaterite structure (D_3 symmetry). In these compounds, the ${}^5\text{D}_0 \rightarrow {}^7\text{F}_1$ transition still dominates the luminescence spectrum, but the intensity of the ${}^5\text{D}_0 \rightarrow {}^7\text{F}_2$ transition cannot be neglected. $\text{LaBO}_3:\text{Eu}^{3+}$ with the largest host cation has the orthorhombic aragonite structure (with Eu^{3+} in an asymmetric site with C_s symmetry), and in this case the ${}^5\text{D}_0 \rightarrow {}^7\text{F}_1$ transition is no longer the most intense transition. The ${}^5\text{D}_0 \rightarrow {}^7\text{F}_2$ transition is the most intense, but the ${}^5\text{D}_0 \rightarrow {}^7\text{F}_4$ transition has a remarkably high intensity. The ${}^5\text{D}_0 \rightarrow {}^7\text{F}_1$ transition dominates the luminescence spectrum of $[\text{Eu}(\text{TMU})_6(\text{AsF}_6)_3]$ (TMU = tetramethylurea), where the Eu^{3+} is at an octahedral site with O_h symmetry [232]. Dominance of the ${}^5\text{D}_0 \rightarrow {}^7\text{F}_1$ transition is also seen in the room-temperature

luminescence spectra of the cubic site of $\text{ThO}_2:\text{Eu}^{3+}$ [233,234]. In many fluoride-containing compounds, the $^5\text{D}_0 \rightarrow ^7\text{F}_1$ transition is the most intense transition, for instance $\text{LaF}_3:\text{Eu}^{3+}$ [235-241], EuF_3 [242,243], $\text{GdF}_3:\text{Eu}^{3+}$ [236,244,245] and $\text{KGdF}_4:\text{Eu}^{3+}$ [246,247], but not $\text{LiGdF}_4:\text{Eu}^{3+}$ [248,249], in hexagonal or cubic $\text{NaGdF}_4:\text{Eu}^{3+}$ [250-253]. In compounds with the delafossite structure, e.g. $\text{CuLa}_{1-x}\text{Eu}_x\text{O}_2$, Eu^{3+} is at a centrosymmetric site and the luminescence has an orange color due to the strong $^5\text{D}_0 \rightarrow ^7\text{F}_1$ and $^5\text{D}_0 \rightarrow ^7\text{F}_0$ transitions [254-256]. The luminescence spectrum of $\text{Eu}(\text{ClO}_4)_3$ in water shows the $^5\text{D}_0 \rightarrow ^7\text{F}_1$ transition as the most intense transition in the spectrum, indicating that the Eu^{3+} aquo ion probably possesses an inversion centre [257]. Another observation is that the relative intensities of the transitions and the shapes of the luminescence bands do not depend on the concentration of the perchlorate ion. These data show that the perchlorate ion does not coordinate to the Eu^{3+} ion, even not at high salt concentrations.

The presence of more than three lines for the $^5\text{D}_0 \rightarrow ^7\text{F}_1$ transition is an indication for the presence of more than one non-equivalent site for the Eu^{3+} ion. This transition can be used to detect multiple sites if the $^5\text{D}_0 \rightarrow ^7\text{F}_0$ transition is forbidden. However, one has to be cautious not to confuse vibronic transitions with purely electronic transitions. The splitting of the $^7\text{F}_1$ level observed by the $^5\text{D}_0 \rightarrow ^7\text{F}_1$ transition in the luminescence spectrum of a europium(III) can be used as a direct measure of the value of the second rank crystal-field parameter B_0^2 [258]. This parameter is directly proportional to the magnetic anisotropy $\Delta\chi$ of the lanthanide complex. Therefore, the splitting of the $^7\text{F}_1$ level in the luminescence spectrum can be used as a probe for the magnetic anisotropy of lanthanide complexes. The magnetic anisotropy is of importance to explain the lanthanide-induced shift in NMR spectra and the alignment of lanthanide-containing liquid crystals in an external magnetic field [259-262].

3.4 Transition ${}^5D_0 \rightarrow {}^7F_2$

The ${}^5D_0 \rightarrow {}^7F_2$ transition is a so-called “*hypersensitive transition*”, which means that its intensity is much more influenced by the local symmetry of the Eu^{3+} ion and the nature of the ligands than the intensities of the other ED transitions. Hypersensitive transitions obey the selection rules $|\Delta S| = 0$, $|\Delta L| \leq 2$ and $|\Delta J| \leq 2$ [94]. These selection rules are the same as the selection rules for a quadrupole transition, but calculations have shown that the intensities of hypersensitive transitions are several orders of magnitude larger than the values expected for quadrupole transitions. Therefore, hypersensitive transitions have been labeled also *pseudo-quadrupole transitions* [263]. Hypersensitivity is discussed in more detail in section 9.3. The intensity of the hypersensitive transition ${}^5D_0 \rightarrow {}^7F_2$ is often used as a measure for the asymmetry of the Eu^{3+} site (see section 7). Large variations are observed for the intensity of this transition, depending on the type of europium(III) compound. The ${}^5D_0 \rightarrow {}^7F_2$ transition is responsible for the typical red luminescence observed in europium(III) phosphors such as $\text{Y}_2\text{O}_3:\text{Eu}^{3+}$ or $\text{Y}_2\text{O}_2\text{S}:\text{Eu}^{3+}$ [49,264]. The intensity of the ${}^5D_0 \rightarrow {}^7F_2$ transition is directly proportional to the value of the Judd-Ofelt intensity parameter Ω_2 (see section 9.1). Instead of the absolute intensity of the ${}^5D_0 \rightarrow {}^7F_2$ transition, the ratio R of the intensities of the transitions ${}^5D_0 \rightarrow {}^7F_2$ and ${}^5D_0 \rightarrow {}^7F_1$, $I({}^5D_0 \rightarrow {}^7F_2)/I({}^5D_0 \rightarrow {}^7F_1)$ is also often used to compare the intensities of the hypersensitive transition in different europium(III) compounds.

Europium(III) β -diketonate complexes, either Lewis base adducts of tris complexes or tetrakis complexes, have typically a very intense hypersensitive ${}^5D_0 \rightarrow {}^7F_2$ transition. It is not uncommon that the ${}^5D_0 \rightarrow {}^7F_2$ transition is 10 times more intense than the ${}^5D_0 \rightarrow {}^7F_1$ transition in this type of complexes [12,13,15,265,266]. In Figure 8, the luminescence spectrum of the europium(III) tetrakis β -diketonate complex $[\text{C}_6\text{mim}][\text{Eu}(\text{tta})_4]$ (where $\text{C}_6\text{mim} = 1\text{-hexyl-3-methylimidazolium}$ and $\text{tta} = 2\text{-thenoyltrifluoroacetylacetonate}$) doped into an ionogel is shown [13]. The ${}^5D_0 \rightarrow {}^7F_2$ transition dominates the spectrum. The high intensity is often attributed

to the low symmetry of the Eu^{3+} , but it is more realistic to consider the high polarizability of the chelating β -diketonate ligands as the intensity enhancing mechanism [158]. A dramatic increase in intensity of the hypersensitive transition ${}^5\text{D}_0 \rightarrow {}^7\text{F}_2$ is observed for the luminescence spectrum of Eu^{3+} in an aqueous solution of K_2CO_3 in comparison with the spectrum of the europium(III) aquo ion [267,268]. This intensity enhancement is due to the formation of the anionic carbonato complex $[\text{Eu}(\text{CO}_3)_4]^{5-}$ in solution. The intensification finds applications in analytical chemistry: Sinha developed a spectrofluorimetric method to detect Eu^{3+} concentrations as low as 10^{-7} M using a 3M aqueous solution of K_2CO_3 [269]. A sharp decrease in the intensity of the ${}^5\text{D}_0 \rightarrow {}^7\text{F}_2$ transition was observed when water was added to $\text{Eu}(\text{Tf}_2\text{N})_3$ dissolved in the hydrophobic ionic liquids *N,N*-diethyl-*N*-methyl-*N*-(2-methoxyethyl)ammonium bis(trifluoromethylsulfonyl)imide or 1-butyl-3-methylimidazolium bis(trifluoromethylsulfonyl)imide [270]. Addition of dipicolinate ions to an aqueous solution of Eu^{3+} led to a very strong increase in the intensity of the ${}^5\text{D}_0 \rightarrow {}^7\text{F}_2$ transition, reaching a maximum when the $[\text{Eu}(\text{DPA})_3]^{3-}$ complex was formed [157].

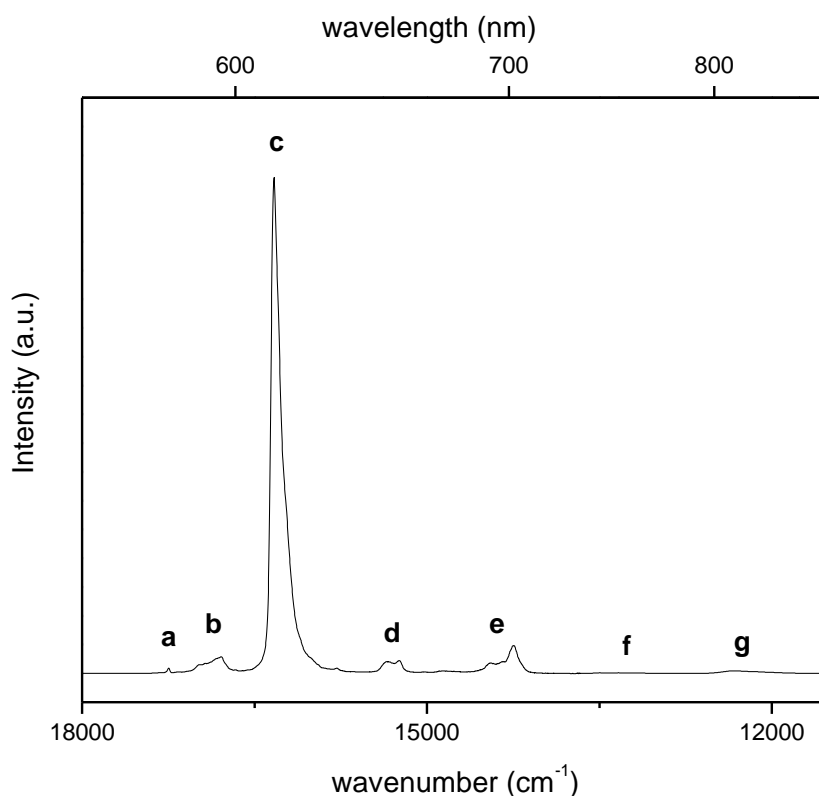


Figure 8. Luminescence spectrum of the tetakis β -diketonate complex $[C_6mim][Eu(tta)_4]$, $C_6mim = 1$ -hexyl-3-methylimidazolium, $tta = 2$ -thenoyltrifluoroacetylacetonate (room temperature, $\lambda_{exc} = 340$ nm). The assignment of the lines is: (a) $^5D_0 \rightarrow ^7F_0$; (b) $^5D_0 \rightarrow ^7F_1$; (c) $^5D_0 \rightarrow ^7F_2$; (d) $^5D_0 \rightarrow ^7F_3$; (e) $^5D_0 \rightarrow ^7F_4$; (f) $^5D_0 \rightarrow ^7F_5$ and (g) $^5D_0 \rightarrow ^7F_6$. The dominance of the spectrum by the hypersensitive transition $^5D_0 \rightarrow ^7F_2$ is evident. Reprinted with permission from reference [13]. Copyright 2009 American Chemical Society.

If the $^5D_0 \rightarrow ^7F_2$ transition is very weak, the luminescence spectrum is dominated by the $^5D_0 \rightarrow ^7F_1$ transition and an orange luminescence color is observed [271]. Examples of europium(III) compounds with an orange photoluminescence are $Na_9EuW_{10}O_{36} \cdot 18H_2O$ (D_{4d} symmetry) [272], $YF_3:Eu^{3+}$ (D_{4d}) [273], $GdB_3O_6:Eu^{3+}$ (D_{4d}), $CeO_2:Eu^{3+}$ (O_h) [274], $[Eu(4\text{-picoline-}N\text{-oxide})_8](PF_6)_3$ (D_{4d}) [275], $[Eu(\text{pyridine-}N\text{-oxide})_8](ClO_4)_3$ (D_{4d}) [276],

Eu(antipyrene)₆I₃ (S₆) (antipyrene = 1-phenyl-2,3-dimethyl-5-pyrazolone) [277,278], compounds with the hexakis(nitrito)europate(III) ion [Eu(NO₂)₆]³⁻ (T_h) [279-282], SnO₂:Eu³⁺ (D_{2h}) [283], Gd₂Sn₂O₇:Eu³⁺ (D_{3d}) [284], Na₃[Eu(oxydiacetato)₃]·2NaClO₄·6H₂O (D₃) [271,285], [Eu(terpy)₃](ClO₄)₃ (D₃) [286], [Eu(H₂O)₉](BrO₃)₃ (D_{3h}) [152,287], and [Eu(H₂O)₉](EtSO₄)₃ (C_{3h}) [215]. A pink luminescence is observed for Cs₂NaEuCl₆ (O_h) at room temperature, but an orange luminescence at 77 K, due to a decrease of the vibronic intensity of the ⁵D₀ → ⁷F₂ transition [271]. These examples show that correlating the luminescence color with a particular symmetry point group is difficult. The list contains compounds with different symmetries, and both centrosymmetric and non-centrosymmetric point groups occur. One could conclude from an orange luminescence that the ⁵D₀ → ⁷F₂ transition must be weak and much less intense than the ⁵D₀ → ⁷F₁ transition, but one has to be cautious for compounds that also show emission from higher excited states (⁵D₁, ⁵D₂, ⁵D₃). Emission from higher excited states can shift the luminescence towards orange and yellow emission colors [288]. The relative contribution of emission from the higher excited states can be tuned by variation of the Eu³⁺ concentration in the host matrix, because higher doping concentrations favor emission from the ⁵D₀ level at the expense of emission from the higher excited states. Not all phosphors show a strong color shift as a function of Eu³⁺ concentrations. Only phosphors with a large contribution of ⁵D₁ and ⁵D₂ emission at low Eu³⁺ concentrations exhibit strong color shifts. Examples are the white to orange to red emission with (Y_{1-x}Eu_x)₂OS₂ and the yellow to red emission with (Y_{1-x}Eu_x)₂O₃ [288]. On the other hand, (Y_{1-x}Eu_x)VO₄ shows very little color change upon variation of the Eu³⁺ concentration. Also compounds with an intense ⁵D₀ → ⁷F₂ transition shifted to higher energies (shorter wavelengths) can show an orange photoluminescence is expected.

A typical feature of europium(III) complexes with a D_{3h} symmetry is the narrowness of the ⁵D₀ → ⁷F₂ transition, because only one crystal-field line is allowed in this symmetry.

This can be seen in the luminescence spectra of tris(hydrotris(1-pyrazolyl)borato)europium(III) (Figure 9) [289]. For D_3 symmetry, two components are expected for the ${}^5D_0 \rightarrow {}^7F_2$ transition. This splitting is sometimes not resolved, as in the case of the europium(III) tris dipicolinate complex $[\text{Eu}(\text{DPA})_3]^{3-}$ [157].

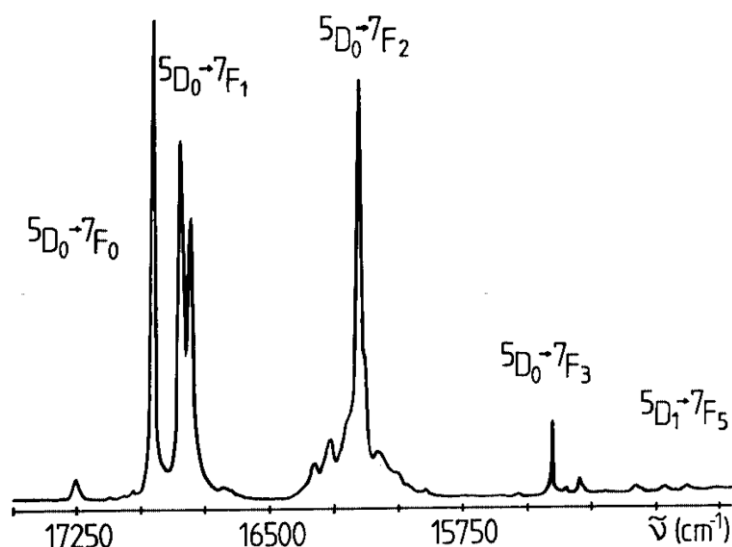


Figure 9. Luminescence spectrum of tris(hydrotris(1-pyrazolyl)borato)europium(III), a complex with D_{3h} symmetry. Reprinted with permission from reference [289]. Copyright 2002 Wiley-VCH.

3.5 Transition ${}^5D_0 \rightarrow {}^7F_3$

The ${}^5D_0 \rightarrow {}^7F_3$ transition is in general very weak, because it is forbidden according to the Judd-Ofelt theory, and this transition can only gain intensity via J -mixing [290]. An intense ${}^5D_0 \rightarrow {}^7F_3$ transition is a sign of strong J -mixing and a strong crystal-field perturbation. This transition is not considered when the Eu^{3+} ion is used as a spectroscopic probe. The β -diketonate complex $[\text{Eu}(\text{dbm})_3(\text{H}_2\text{O})]$ is one of the rare examples of an intense ${}^5D_0 \rightarrow {}^7F_3$ transition [158]. In fact, the ${}^5D_0 \rightarrow {}^7F_3$ transition of this compound is more intense

than its ${}^5D_0 \rightarrow {}^7F_4$ transition. It should be noted that also the ${}^5D_0 \rightarrow {}^7F_0$ transition and the ${}^5D_0 \rightarrow {}^7F_2$ hypersensitive transition are very intense in this compound. This observation can be explained by strong crystal-field effects and hence strong J -mixing. On the other hand, the ${}^5D_0 \rightarrow {}^7F_3$ transition is totally absent in $\text{BaEu}(\text{CO}_3)_2\text{F}$ and $\text{Na}_3\text{La}_2(\text{CO}_3)_4\text{F}:\text{Eu}^{3+}$, although these compound give fairly intense luminescence spectra [291]. The absence of this transition was attributed to weak J -mixing, which was also evident from the small values of the second and fourth rank crystal-field parameters (B_q^2 and B_q^4). Another remarkable feature in the luminescence spectra of these compounds is the absence of luminescence from excited states higher than 5D_0 . This is attributed to the high phonon energies of the carbonate groups which efficiently depopulate the excited states. The ${}^5D_0 \rightarrow {}^7F_3$ transition of the C_{2v} site in $\text{BaFCl}:\text{Eu}^{3+}$ is more intense than the strongest line of the ${}^5D_0 \rightarrow {}^7F_4$ transition [148]. This anomalous behavior was explained by J -mixing induced by the large fourth rank crystal field parameters ($B_0^4 = -1489 \text{ cm}^{-1}$ and $B_4^4 = 1266 \text{ cm}^{-1}$). The extent of J -mixing was estimated to be about 6.5 % (which means that the “ 7F_3 ” state has 93.5 % 7F_3 character and 6.5 % 7F_2 character). Interestingly, the extent of J -mixing of 7F_2 into 7F_0 was in this compound only about 2 %, due to the small second rank crystal field parameters ($B_0^2 = -72 \text{ cm}^{-1}$ and $B_2^2 = -290 \text{ cm}^{-1}$). As a result, the ${}^5D_0 \rightarrow {}^7F_0$ transition has a weak intensity.

In the luminescence spectrum of $\text{Mg}_3\text{F}_3\text{BO}_3:\text{Eu}^{3+}$, a very intense transition is observed in the ${}^5D_0 \rightarrow {}^7F_3$ transition region at 658.3 nm [292]. This transition is much more intense than the ${}^5D_0 \rightarrow {}^7F_4$ transition. The compound has also other remarkable properties, such as a very intense ${}^5D_0 \rightarrow {}^7F_0$ transition situated at a very high energy (17615 cm^{-1} or 567.7 nm) and a very large splitting of the 7F_1 level (700 cm^{-1}). This very large splitting causes an overlap between the energy levels of the 7F_1 and 7F_2 levels. The fact that a very strong crystal-field effect is present inspired the authors to give an alternative explanation for the transition at 658.3 nm instead of attributing this line to the ${}^5D_0 \rightarrow {}^7F_3$ transition. The authors suggest that

the line could also be a crystal-field component of the ${}^5D_0 \rightarrow {}^7F_2$ transition. In that case, a very large crystal-field splitting of the 7F_2 level would occur (1750 cm^{-1}). Further research on this interesting compound is recommended.

3.6 Transition ${}^5D_0 \rightarrow {}^7F_4$

One must be careful with the interpretation of the intensity of the ${}^5D_0 \rightarrow {}^7F_4$ ED transition. The transition lies in a spectral region in which most photomultiplier tubes have a low sensitivity. Correction of the luminescence spectra is required, because otherwise erroneous conclusions could be drawn. In an uncorrected luminescence spectrum, the intensity of the ${}^5D_0 \rightarrow {}^7F_4$ transition is too low compared to the other transitions, whereas the intensity of this transition is exaggerated in an over-corrected spectrum. The intensity of the ${}^5D_0 \rightarrow {}^7F_4$ transition should not be considered in terms of absolute values, but rather compared to the intensity of the ${}^5D_0 \rightarrow {}^7F_1$ magnetic dipole transition. In many europium luminescence spectra, the ${}^5D_0 \rightarrow {}^7F_4$ transition is weaker than the ${}^5D_0 \rightarrow {}^7F_2$ transition, but several exceptions are known. The luminescence spectra of compounds with D_{4d} symmetry are often dominated by the ${}^5D_0 \rightarrow {}^7F_4$ transition. In D_{4d} symmetry, the ${}^5D_0 \rightarrow {}^7F_2$ transition is forbidden, but the ${}^5D_0 \rightarrow {}^7F_4$ transition is intense because a center of symmetry is absent [271,293]. Examples of such compounds are: $\text{Na}_9[\text{EuW}_{10}\text{O}_{36}] \cdot 14\text{H}_2\text{O}$ (Eu^{3+} decatungstate) [272,294], $\text{YF}_3:\text{Eu}^{3+}$, $\text{GdB}_3\text{O}_6:\text{Eu}^{3+}$ [293], $[\text{Eu}(4\text{-picoline-}N\text{-oxide})_8](\text{PF}_6)_3$ [295] and $[\text{Eu}(4\text{-picoline-}N\text{-oxide})_8](\text{ClO}_4)_3$ [296]. An undistorted square antiprism has D_{4d} symmetry, so that for compounds with a lower symmetry than D_{4d} , but with a coordination polyhedron close to a square antiprism, have an intense ${}^5D_0 \rightarrow {}^7F_4$ transition (and a weak ${}^5D_0 \rightarrow {}^7F_2$ transition). In the macrocyclic complex $[\text{Eu}(\text{DOTA})(\text{H}_2\text{O})]^-$, the Eu^{3+} is nine-coordinate, with a coordination polyhedron that can be described as a monocapped square antiprism [159,297]. A very intense ${}^5D_0 \rightarrow {}^7F_4$ transition has been observed for the alkali metal-europium dinitrosalicylates

(especially for the sodium complex), but the crystal structure of these compounds is not known yet [298]. In these compounds, the ${}^5D_0 \rightarrow {}^7F_4$ transition is less intense than the ${}^5D_0 \rightarrow {}^7F_2$ transition, but much more intense than the ${}^5D_0 \rightarrow {}^7F_1$ magnetic dipole transition. The same remark can be made for $\text{LaBO}_3:\text{Eu}^{3+}$ with an orthorhombic aragonite structure (with Eu^{3+} in an asymmetric site with C_s symmetry) [226]. The very high intensity of the ${}^5D_0 \rightarrow {}^7F_4$ transition in $\text{Ca}_3\text{Sc}_2\text{Si}_3\text{O}_{12}:\text{Eu}^{3+}$ was attributed to a distortion of the cubic geometry of the Eu^{3+} site in this garnet host towards the actual D_2 symmetry (Figure 10) [299]. However, an alternative explanation is a distortion of the cube to a square antiprism. The ${}^5D_0 \rightarrow {}^7F_4$ transition dominates the spectrum of $\text{GdOBr}:\text{Eu}^{3+}$, whereas the ${}^5D_0 \rightarrow {}^7F_2$ transition is the most intense transition in the isostructural $\text{GdOCl}:\text{Eu}^{3+}$ compound [172]. This clearly shows that the intensity of the ${}^5D_0 \rightarrow {}^7F_4$ transition is determined not only by symmetry factors, but also by the chemical composition of the host matrix. Other examples of europium(III)-containing systems with an intense ${}^5D_0 \rightarrow {}^7F_4$ transition are: $\text{Eu}(\text{Tp})_3$ (Tp = hydrotris(pyrazol-1-yl)borate) [300], $\text{Eu}(\text{Tp})_3$ in PMMA polymer matrix [301] and the two-dimensional frameworks of the formula ${}^2_\infty[\text{Eu}_2\text{Cl}_6(4,4'\text{-bipy})_3] \cdot 2(4,4'\text{-bipy})$, where 4,4'-bipy = 4,4'-bipyridine [302]. In a recent paper, Skaudzius *et al.* have made a systematic study of the intensity of the ${}^5D_0 \rightarrow {}^7F_4$ transition of Eu^{3+} in different orthophosphate and garnet host matrices and investigated the influence of the host material, in particular of the electronegativity, the radius of the rare earth and of other trivalent cations [303]. An increase in the average electronegativity of the trivalent cations, i.e. a decrease of the optical basicity, in the octahedral and tetrahedral sites in the structure of the garnets and orthophosphates led to an increase of the relative intensity of the ${}^5D_0 \rightarrow {}^7F_4$ transition. In $\text{Y}_3\text{Al}_5\text{O}_{12}:\text{Eu}^{3+}$ (1%), the ${}^5D_0 \rightarrow {}^7F_4$ transition accounts for 39.5 % of the total intensity of the ${}^5D_0 \rightarrow {}^7F_J$ transitions, whereas this value increases to 49.8 % in $\text{LuPO}_4:\text{Eu}^{3+}$ (1 %). The ${}^5D_0 \rightarrow {}^7F_4$ transition is sometimes considered as a hypersensitive one, but this it is not correct, since it does not obey

the selection rules for quadrupole transitions ($\Delta J \neq 2$). The variations in the intensity ratios $I(^5D_0 \rightarrow ^7F_4)/I(^5D_0 \rightarrow ^7F_1)$ are much less pronounced than variations in the ratio $I(^5D_0 \rightarrow ^7F_2)/I(^5D_0 \rightarrow ^7F_1)$.

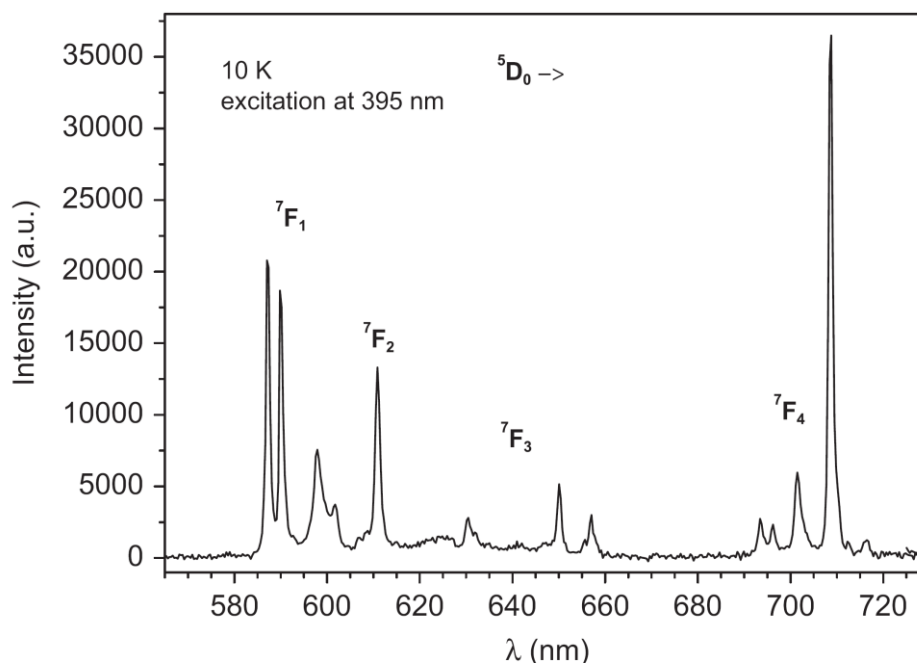


Figure 10. Luminescence spectrum of $Ca_3Sc_2Si_3O_{12}:Eu^{3+}$, with an intense $^5D_0 \rightarrow ^7F_4$ transition. Reprinted with permission from reference [299]. Copyright 2011 Elsevier.

3.7 Transitions $^5D_0 \rightarrow ^7F_5$ and $^5D_0 \rightarrow ^7F_6$

In many studies, the $^5D_0 \rightarrow ^7F_5$ transition (740–770 nm) and the $^5D_0 \rightarrow ^7F_6$ transition (810–840 nm) are not discussed because they cannot be observed by blue-sensitive PMTs of several commercial spectrofluorimeters. The classic red-sensitive Hamamatsu R928 PMT has a very low sensitivity in the spectral region where these transitions occur. Moreover, the intensities of these transitions are very low. For this reason, many reported europium(III) luminescence spectra show only the $^5D_0 \rightarrow ^7F_J$ ($J = 0 - 4$) transitions or even only the $^5D_0 \rightarrow$

7F_J ($J = 0 - 2$) transitions. For $\text{Eu}(\text{NO}_3)_3 \cdot 6\text{H}_2\text{O}$, it was reported that the relative intensities for the ${}^5D_0 \rightarrow {}^7F_J$ ($J = 0 - 6$) transitions upon selective excitation in the 5D_0 level at 77 K are 0.03, 1.0, 4.9, 0.01, 1.8, 0.05 and 0.4, respectively [304]. The relative luminescence intensities of the ${}^5D_0 \rightarrow {}^7F_J$ ($J = 0 - 6$) transitions in $\text{LaF}_3:\text{Eu}^{3+}$ at 77 K are: <0.4, 6.45, 5.25, 0.19, 2.80, 0.05 and 0.08 [305]. Whereas the transitions to 7F_5 and 7F_6 cannot be observed for Eu^{3+} in water, they become visible as weak bands after addition of dipicolinate (DPA) ligands [157]. On the other hand, in the luminescence spectra of hydrated Eu^{3+} in crystalline matrices such as $\text{Eu}(\text{BrO}_3)_3 \cdot 9\text{H}_2\text{O}$ [287] or $\text{Na}[\text{Yb}_{0.95}\text{Eu}_{0.05}(\text{dpa})_3] \cdot \text{NaClO}_4 \cdot 10\text{H}_2\text{O}$ [306] weak transitions to 7F_5 and 7F_6 are present if laser excitation is used. Also luminescence spectra of Eu^{3+} ions in glasses show that these transitions are weak [153,182,307]. On the other hand, the intensity of the ${}^5D_0 \rightarrow {}^7F_6$ transition is comparable to that of the ${}^5D_0 \rightarrow {}^7F_4$ transition for the C_s site of $\text{BaFCl}:\text{Eu}^{3+}$ [148]. This site has also another unusual spectroscopic property: the ${}^5D_0 \rightarrow {}^7F_0$ transition is the strongest transition in the spectrum (see section 3.2).

3.8 Emission from higher excited states

In some spectra, and especially in those of Eu^{3+} in inorganic host lattices, luminescence can also originate from the 5D_1 , 5D_2 and 5D_3 levels, even though examples of luminescence from the 5D_3 level are very scarce. Crystalline europium(III) compounds with emission from the higher excited states have complicated luminescence spectra with a large number of crystal-field transitions. For instance, more than 120 transitions are observed in the luminescence spectrum of $\text{La}_2\text{O}_3:\text{Eu}^{3+}$ recorded at 77 K [168], and more than 100 lines have been reported for the low-temperature luminescence spectra of the Eu^{3+} -doped oxychlorides LnOCl ($\text{Ln} = \text{La}, \text{Gd}, \text{Y}$) [308]. In molecular compounds, often only transitions from the 5D_0 excited state are observed because of stronger radiationless deactivation. This is especially the case for room-temperature luminescence spectra. In spectra with luminescence from the

higher excited states, there can be an overlap between the ${}^5D_0 \rightarrow {}^7F_J$ and the ${}^5D_{1,2} \rightarrow {}^7F_J$ lines. An overlap has been observed between the following pairs of transitions: ${}^5D_0 \rightarrow {}^7F_0$ and ${}^5D_2 \rightarrow {}^7F_5$, ${}^5D_0 \rightarrow {}^7F_2$ and ${}^5D_1 \rightarrow {}^7F_4$, ${}^5D_0 \rightarrow {}^7F_3$ and ${}^5D_1 \rightarrow {}^7F_5$, ${}^5D_1 \rightarrow {}^7F_0$ and ${}^5D_2 \rightarrow {}^7F_4$, ${}^5D_1 \rightarrow {}^7F_1$ and ${}^5D_2 \rightarrow {}^7F_4$, ${}^5D_1 \rightarrow {}^7F_2$ and ${}^5D_2 \rightarrow {}^7F_4$, ${}^5D_0 \rightarrow {}^7F_4$ and ${}^5D_1 \rightarrow {}^7F_6$. Discrimination between these is possible by means of time-gated luminescence spectra, because the decay times of the 5D_1 and 5D_2 states are much shorter than the decay time of the 5D_0 state. Time-gated spectra are recorded by a pulsed excitation source. Data collection is started after a given delay time. By a careful choice of the delay time, the measurement of the luminescence of the 5D_0 state is started after the 5D_1 and higher excited states have already been depopulated. It is possible to selectively excite the 5D_0 level by a tunable laser source, avoiding population of higher excited states. More information on time-gated spectroscopy is given in section 10.1. The overlap of the lines can also be avoided by working at higher temperatures or at higher Eu^{3+} concentrations, because these conditions favor quenching of the 5D_1 and 5D_2 excited states. At lower temperature, more transitions starting from the higher excited states are observed. A consequence of the quenching of emission from the 5D_1 , 5D_2 and 5D_3 excited states is that the emission color shifts from yellow to red with increasing Eu^{3+} concentrations or with an increase in temperature [309]. Contrary to what is intuitively expected, deuteration of hydrated europium(III) complexes leads to a decrease of the intensity of the transitions from the 5D_1 level compared to those of the 5D_0 levels, as shown in a luminescence study of $\text{Eu}(\text{NO}_3)_3 \cdot 6\text{H}_2\text{O}$ and $\text{Eu}(\text{NO}_3)_3 \cdot 6\text{D}_2\text{O}$ [304]. This is explained by the fact that deuteration strongly reduces the quenching of the luminescence from the long lived 5D_0 state. The deuterated compound has a similar formula. Emission from the 5D_2 level is common for Eu^{3+} in fluoride host matrices, such as LiYF_4 [310], KY_3F_{10} [311-313], LaF_3 [314] and NaYF_4 [315]. Other examples include $\text{LnOF}:\text{Eu}^{3+}$ ($\text{Ln} = \text{La}, \text{Gd}, \text{Y}$) [316], $\text{Cs}_2\text{NaEuCl}_6$ [317], $\text{Cs}_2\text{AgEuCl}_6$ [318] and $\text{LaCl}_3:\text{Eu}^{3+}$ [217]. Low temperatures induce

sharpening of the luminescence lines by reducing the lattice thermal agitation. However, lowering the temperature can also induce other changes in the luminescence spectra originating from the higher excited states. The relative populations of the different crystal-field levels of the 5D_1 and 5D_2 excited states are determined by the Boltzmann distribution. At 4.2 K, only the lower crystal-field levels of the 5D_1 and 5D_2 states are populated during the radiative decay (luminescence), so that the number of lines is reduced in the spectra at 4.2 K compared to the spectra at room temperature or even at 77 K [311]. This considerably simplifies the luminescence spectrum.

Emission from the 5D_3 level is observed only for host matrices with very low phonon energies, so that the radiationless decay to the 5D_2 , 5D_1 and 5D_0 states is very slow. Strong emission from the 5D_3 level was observed for the fluorozirconate glass $57ZrF_4-34BaF_2-4AlF_3-3LaF_3-2EuF_3$ [319]. The ${}^5D_3 \rightarrow {}^7F_0$ transition was not observed because it is strictly forbidden, but the ${}^5D_3 \rightarrow {}^7F_J$ ($J = 1-4$) transitions were observed in the intensity ratios 2:2:1:4, at 417, 430, 445 and 465 nm, respectively. The total emission ratios of the transitions from the 5D_3 , 5D_2 , 5D_1 and 5D_0 state are 1:1:2:6, respectively. The intense emission from the excited states 5D_3 and 5D_2 makes this glass unique in comparison to other europium(III)-doped host matrices. Even in similar fluorozirconate glasses, such as $64ZrF_4-32BaF_2-2LaF_3-2EuF_3$, the emission from the 5D_3 and 5D_2 states is much weaker than emission from 5D_1 and 5D_0 [320]. In Figure 11, the luminescence spectra of Eu^{3+} in two different fluoride glasses are given, showing very clearly the emission from higher excited states [321].

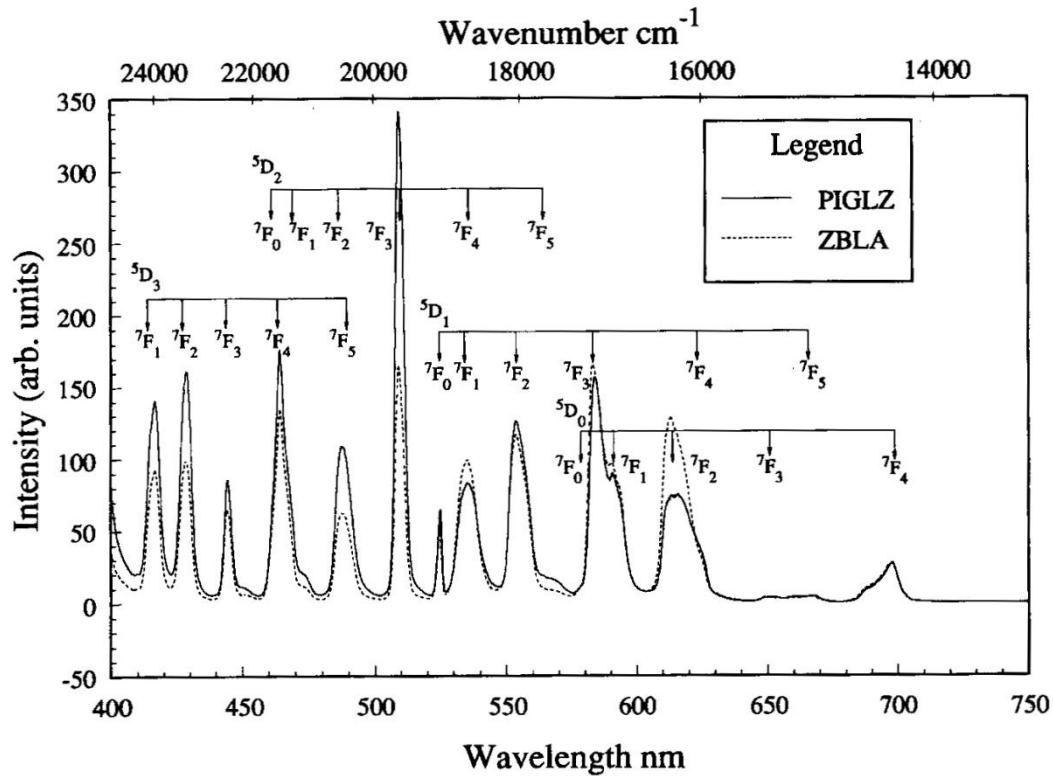


Figure 11. Luminescence spectra of Eu^{3+} doped in the fluoride glasses ZBLA ($57\text{ZrF}_4-36\text{BaF}_2-4\text{LaF}_3-3\text{AlF}_3$) and PIGLZ ($43\text{PbF}_2-17\text{InF}_3-17\text{GaF}_3-4\text{LaF}_3-19\text{ZnF}_2$), showing emission from higher excited states. Reproduced with permission from reference [321].

Copyright 1995 Elsevier.

Occurrence of ${}^5\text{D}_3$ emission in glasses is not restricted to fluoride glasses. It was also observed for Eu^{3+} in tellurite and germanate glasses [322]. In crystalline matrices, ${}^5\text{D}_3$ emission has been reported for $\text{LaF}_3:\text{Eu}^{3+}$ [305], $\text{GdF}_3:\text{Eu}^{3+}$ [323], $\text{LiGdF}_4:\text{Eu}^{3+}$ [249,323], $\text{NaYF}_4:\text{Eu}^{3+}$ [252,315], $\text{NaGdF}_4:\text{Eu}^{3+}$ [250,251,324], $\text{NaGdF}_4:(\text{Eu}^{3+},\text{Ce}^{3+})$ [325], $\text{CsGd}_2\text{F}_7:\text{Eu}^{3+}$ [326], $\text{GdOF}:\text{Eu}^{3+}$ [327], $\text{BaY}_2\text{ZnO}_5:\text{Eu}^{3+}$ [328], $\text{La}_2\text{O}_3:\text{Eu}^{3+}$ [168] and in several europium(III)-doped chloroelpasolites [329,330]. It should be noted that ${}^5\text{D}_3$ emission can be observed for Eu^{3+} diluted in $\text{Cs}_2\text{NaYCl}_6$, but not for neat $\text{Cs}_2\text{NaEuCl}_6$ due to concentration quenching [331].

Weak emission from the $^5\text{H}_3$ level of Eu^{3+} has been reported by Kiliaan and Blasse for $\text{NaGdF}_4:(\text{Eu}^{3+},\text{Ce}^{3+})$ after excitation into the f-d band of Ce^{3+} [325]. The transitions were assigned to the $^5\text{H}_3 \rightarrow ^7\text{F}_1$ ($\lambda_{\text{max}} = 329$ nm), $^5\text{H}_3 \rightarrow ^7\text{F}_2$ ($\lambda_{\text{max}} = 337$ nm) and $^5\text{H}_3 \rightarrow ^7\text{F}_4$ ($\lambda_{\text{max}} = 358$ nm) transitions. The authors assumed that $^5\text{H}_3$ emission is probably restricted to fluoride matrices, because the charge-transfer band of Eu^{3+} has to be at high enough energy to avoid non-radiative relaxation via the charge-transfer state. However, Tanner and coworkers observed emission from the $^5\text{H}_3$ level in $\text{Cs}_2\text{NaIn}_{0.995}\text{Eu}_{0.005}\text{Cl}_6$ upon excitation with synchrotron radiation [329]. Triply doped $\text{NaYF}_4:(\text{Yb}^{3+},\text{Er}^{3+},\text{Eu}^{3+})$ nanocrystals showed luminescence of the $^5\text{H}_{3-7} \rightarrow ^7\text{F}_{0-3}$ and $^5\text{L}_6 \rightarrow ^7\text{F}_0$ transitions, as well as emission from the $^5\text{D}_3$ and $^5\text{D}_2$ levels after infrared excitation at 980 nm [332]. After an upconversion process, the Er^{3+} ion transfers part of its excitation energy to the Eu^{3+} ion.

3.9 Polarized emission spectra

The emitted light originating from transitions between crystal-field levels of Eu^{3+} ions embedded in a non-cubic single crystal host matrix is linearly polarized and the polarization directions of the emission lines depend on the selection rules for the symmetry point group of the Eu^{3+} site. The polarization characteristics of the emission lines are useful for the assignment of symmetry labels to the different crystal-field levels [152,333-337]. Emission of linearly polarized light has also been observed for lanthanide complexes embedded in less ordered anisotropic media than non-cubic single crystals. For instance, polarized emission was obtained for europium(III) β -diketonate complexes embedded in stretched polyethylene films [338,339], for an aligned vitrified mesophase of a liquid-crystalline europium(III) complex [340], and for europium(III) complexes dissolved in aligned liquid crystal solvents [16]. Polarized luminescence was studied for $[\text{Eu}(\text{DPA})_3]^{3-}$ complexes in a glass obtained by freezing a water/ethylene glycol (1:2 by volume) [341]. Light polarization can be observed by

using linear polarizers. In π polarization, the polarizer is parallel to the main crystallographic axis of the host or the alignment/stretching direction. In σ polarization, the polarizer is perpendicular to these directions.

3.10 Sensitized luminescence

Even though light emission by Eu^{3+} can be an efficient process, the weak light absorption is an issue. The ${}^5\text{L}_6 \leftarrow {}^7\text{F}_0$ transition at about 395 nm is the most intense transition in the absorption spectra of europium(III) compounds and this transition is often used for direct excitation into the $4f^6$ levels of the Eu^{3+} ion. However, the molar absorptivity ϵ of this transition is less than $5 \text{ L mol}^{-1} \text{ cm}^{-1}$, so that only a small part of the excitation light is absorbed. Since the luminescence intensity is proportional to not only the luminescence quantum yield, but also to the amount of light absorbed, weak light absorption results in weak luminescence. Fortunately, the problem of weak light absorption can be overcome by the so-called “*antenna effect*” (or *sensitization*). Weissman discovered in 1942 that intense metal-centered luminescence is observed for europium(III) complexes of salicylaldehyde, benzoylacetone, dibenzoylmethane and *meta*-nitrobenzoylacetone upon excitation in an absorption band of the organic ligand [342]. The absorption bands of the organic chromophores are very strong, so that the ligands can absorb much more light than the Eu^{3+} ion itself. After light absorption, the excitation energy is transferred from the organic ligands to the Eu^{3+} ion via intramolecular energy transfer. It took about 20 years before the importance of the seminal work of Weissman was fully appreciated. After the mechanisms of the energy transfer from the organic ligand to the lanthanide ion were discovered in the early 1960s and after one realized that lanthanide β -diketonate complexes have potential as the active component in chelate lasers, an intense research activity has been going on in the field of luminescent materials based on molecular lanthanide complexes [23]. For a detailed

discussion of energy transfer processes in lanthanide complexes, the reader is referred to a recent review by Bünzli and Eliseeva [75].

The commonly accepted mechanism of energy transfer from the organic ligands to the lanthanide ion is that proposed by Crosby and Whan (Figure 12) [343-345]. Upon irradiation with ultraviolet radiation, the organic ligands of the lanthanide complex absorb the ultraviolet radiation and are excited to a vibrational level of the first excited singlet state ($S_1 \leftarrow S_0$). The molecule undergoes fast *internal conversion* to lower vibrational levels of the S_1 state, for instance through interactions with solvent molecules. The excited singlet state can be deactivated radiatively to the ground state (*molecular fluorescence*, $S_1 \rightarrow S_0$), or can undergo non-radiative *intersystem crossing* from the singlet state S_1 to the triplet state T_1 . The triplet state T_1 can be deactivated radiatively to the ground state S_0 , by the spin-forbidden transition $T_1 \rightarrow S_0$. This results in *molecular phosphorescence*. Alternatively, the complex may undergo an intramolecular energy transfer from the triplet state to a level of the lanthanide ion. The triplet level is the donor level (energy-transferring level) and the 4f level of the lanthanide ion is the acceptor level (resonance level). By transferring its energy from the triplet level to the lanthanide ion, the organic ligand goes back to its ground state. The energy takes place via an *electron-exchange mechanism (Dexter mechanism)*. This mechanism requires a physical overlap between the orbitals of the donor and the acceptor. Therefore, the energy transfer is strongly distance-dependent and decreases rapidly at distances larger than 0.5 nm. In order to get an efficient energy transfer from the triplet state to the lanthanide, the triplet state should be located at least 1500 cm^{-1} , but preferably 2000 to 3500 cm^{-1} above the emitting level of the lanthanide ion. If the energy difference between the triplet level and the emitting level of the lanthanide ion is too small, back transfer can occur and the energy transfer efficiency will drastically decrease. If the energy of the triplet level is below the lowest emitting level of the lanthanide ion, no energy transfer will take place and no lanthanide-centered emission will be

observed. The luminescence observed for a specific lanthanide complex is therefore a sensitive function of the lowest triplet level of the complex relative to a resonance level of the lanthanide ion. When speaking about the energy of the triplet state, the energy of the zero-phonon energy of the triplet state is meant. In the case of Eu^{3+} , the $^5\text{D}_0$ level (at about 17250 cm^{-1}) is the preferred emitting level, but it is not the best acceptor level. In a systematic study of europium(III) tetrakis β -diketonate complexes, the highest quantum yields are observed for energy transfer via the $^5\text{D}_1$ level, which is about 19000 cm^{-1} above the ground state $^7\text{F}_0$. The triplet energy for optimal energy transfer is 20200 cm^{-1} [346]. The preferential energy transfer via the $^5\text{D}_1$ level is in accordance with the selection rules for energy transfer via the Dexter mechanism. When the energy of the triplet level is higher than 20200 cm^{-1} , the quantum yield first decreases, but then increases again when triplet levels becomes resonant with the $^5\text{D}_2$ level of Eu^{3+} (located at about 21500 cm^{-1}). However, energy transfer via the $^5\text{D}_1$ level is less efficient than via the $^5\text{D}_1$ level. Similar results have been observed for europium(III) polyaminocarboxylate complexes in aqueous solution [347]. As a rule of thumb, the energy gap in between the triplet state and the emitting level $^5\text{D}_0$ should be between 1500 and 5000 cm^{-1} in order to observe efficient luminescence of the europium(III) complex. Since the position of the triplet level depends on the type of ligand, it is therefore possible to control the luminescence intensity of Eu^{3+} by variation of the ligand. The position of the triplet level is temperature dependent, so that the luminescence caused by indirect excitation through the organic ligands is much more temperature sensitive than luminescence caused by direct excitation of the 4f levels. High pressures have a significant influence on the singlet and triplet levels of the ligands, whereas the 4f levels are much less sensitive to changes in pressure. Therefore, the energy transfer from the triplet state to the 4f levels can be tuned by applying an external pressure on the lanthanide complex [348]. Although Kleinerman proposed a mechanism of direct transfer of energy from the excited singlet state S_1 to the

energy levels of the lanthanide ion [349], it is not easy to unambiguously prove this mechanism as the main sensitization route due to the very short lifetime of the singlet excited state [75]. When the energy transfer is not very efficient, it is possible to observe some remaining ligand emission together with the lanthanide-centered emission. Molecular oxygen is an external triplet quencher. Quenching of the triplet state by dissolved oxygen in a solution is a competitive process with energy transfer from the triplet state to the lanthanide ion [97]. Therefore, it is recommended to degas solutions of lanthanide complexes prior to measurement of the luminescence spectra. The position of the lowest triplet state of a lanthanide complex can be determined experimentally by recording the luminescence spectrum (phosphorescence spectrum) of the corresponding gadolinium(III) complex [346,350,351]. The energy levels of the Gd^{3+} ion are well above those of the triplet level so that no gadolinium(III)-centered emission is observed. Moreover, the heavy paramagnetic Gd^{3+} ion enhances the intersystem crossing from the singlet to the triplet state, because of mixing of the triplet and singlet states (“*heavy atom effect*” and “*paramagnetic effect*”) [352-356]. The triplet state acquires partially a singlet character by the spin-orbit coupling interaction, and the selection rules are relaxed. The paramagnetic Gd^{3+} ions lowers the lifetimes of the triplet states of the organic ligands much more than the diamagnetic La^{3+} and Lu^{3+} ions. Cryogenic temperatures are often necessary to observe phosphorescence, since the triplet state can be deactivated by non-radiative processes. There is also a competition between fluorescence and phosphorescence. At 77 K, the solvent quenching of the triplet state is negligible. The triplet levels are always located at a lower energy than the singlet levels. Different theoretical approaches have been developed for a prediction of the position of the singlet and triplet levels of a lanthanide(III) complex. First the geometry of the ground state of the complex is optimized by a Sparkle Model, and then the energies of the singlet and triplet

levels are calculated by time-dependent DFT calculations or by a semiempirical INDO/S method [87,357-365].

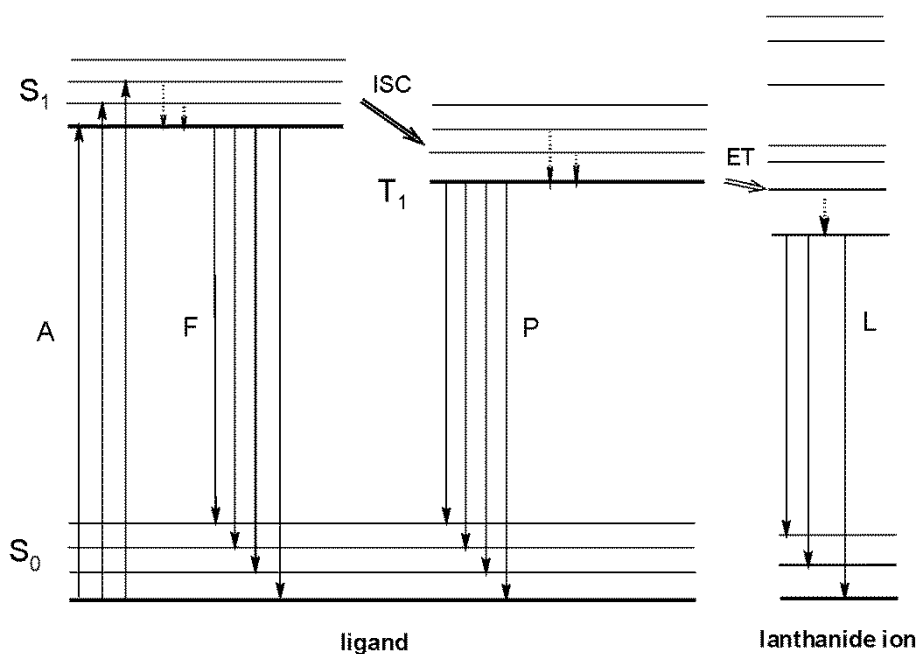


Figure 12. Schematic representation of photophysical processes in lanthanide(III) complexes (antenna effect). Abbreviations: A = absorption, F = fluorescence, P = phosphorescence, L = lanthanide-centered luminescence, ISC = intersystem crossing, ET = energy transfer; S = singlet, T = triplet. Full vertical lines: radiative transitions, dotted vertical lines: non-radiative transitions. Reprinted with permission from reference [23]. Copyright 2009 American Chemical Society.

The sensitization of europium(III) luminescence by the antenna effect is not restricted to organic chromophores. Inorganic chromophores can do the job as well. The chromophores can be a constituent of the host matrix or the chromophore can be a co-dopant. Examples of luminescent compounds with chromophores as part of the host matrix are europium(III)-doped vanadates, molybdates and tungstates such as $\text{YVO}_4:\text{Eu}^{3+}$, $\text{GdVO}_4:\text{Eu}^{3+}$, $\text{CaMoO}_4:\text{Eu}^{3+}$ and $\text{CaWO}_4:\text{Eu}^{3+}$ [50,366-371]. This mechanism is also responsible for the sensitization of

the luminescence in europium(III)-doped polyoxometalate complexes [272,372-375]. In all these chromophores the intense absorption bands are oxygen-to-metal charge-transfer bands. Notice that the Eu^{3+} ion is not involved in these charge-transfer transitions, in contrast to the ligand-to-metal charge transitions discussed further in this section. Although sensitization of lanthanide luminescence via d-block transitions in f-d complexes is an active research field, this approach is mainly used for sensitization of near-infrared-emitting lanthanide ions and not for Eu^{3+} ions [75,376]. Many d-block transition metals quench luminescence of Eu^{3+} since the tails of the d-d absorption bands often have a lower energy than the $^5\text{D}_0$ excited state of Eu^{3+} . However, one must realize that the energy of the d-d transitions is very strongly influenced by the ligand field and thus by the ligands, so that one given transition metal ion can act either as a sensitizer or quencher of Eu^{3+} luminescence, depending on the ligand environment. An example of a d-block transition metal ion that can act both as a sensitizer or quencher is Cr^{3+} . The transition metals Fe^{3+} , Co^{3+} , Ni^{2+} and Cu^{2+} are known to be efficient quenchers for Eu^{3+} luminescence [75]. The quenching of Eu^{3+} luminescence by even small concentration of these elements has been used to develop sensitive analytical methods for the determination of trace elements of heavy metal ions in water, mainly for Cu^{2+} [377-379]. The luminescence of Eu^{3+} is completely quenched in the trinuclear trichloroacetate complex $\text{CuEu}_2(\text{CCl}_3\text{COO})_8 \cdot 6\text{H}_2\text{O}$ [380].

The best known example of sensitization of Eu^{3+} by *p*-block elements is via the Bi^{3+} ion. Bi^{3+} itself is an efficient activator in luminescent materials, such as $\text{LaPO}_4:\text{Bi}^{3+}$ [368]. Luminescence of Bi^{3+} originates from the $6s^2$ shell. Upon codoping of bismuth(III)-containing phosphors with Eu^{3+} , the Bi^{3+} luminescence is quenched by energy transfer from Bi^{3+} to Eu^{3+} and intense red Eu^{3+} photoluminescence is observed. This energy transfer has been intensively studied in glasses and in crystalline inorganic compounds [381-419]. Other ions of *p*-block elements that can sensitize Eu^{3+} luminescence are Pb^{2+} and Sb^{3+} [418,420,421].

The effect of codoping of europium(III)-containing compounds with other trivalent lanthanide ions depends on the nature of the lanthanide ion. A rule of thumb is that near-infrared emitting lanthanide ions will quench the Eu^{3+} luminescence, because the Eu^{3+} ions will efficiently transfer its excitation energy to the near-infrared emitting lanthanide ion, especially if the other lanthanide ion has energy levels that are resonant with the $^5\text{D}_0$ state of Eu^{3+} . This is nicely illustrated by a luminescence study of $\text{Y}_2\text{O}_3:\text{Eu}^{3+}$ (1 %) codoped with other trivalent lanthanide ions [422]. Nd^{3+} , Dy^{3+} , Er^{3+} , Tm^{3+} and Yb^{3+} partly quench the Eu^{3+} luminescence. Quenching by Nd^{3+} is very efficient, whereas quenching by Yb^{3+} is not very efficient due to the lack of resonant levels. The results for Sm^{3+} depended on the excitation wavelength; luminescence enhancement was observed after excitation in a Sm^{3+} level (at 407 nm), whereas weak quenching was observed for other excitation wavelengths. A lanthanide ion that quenches Eu^{3+} luminescence also leads to a decrease of the decay time of the $^5\text{D}_0$ state. Ce^{3+} , Pr^{3+} and Tb^{3+} were not included in this study, since it is difficult to keep these ions in the trivalent oxidation state. Reisfeld and Boehm described the energy transfer from Sm^{3+} to Eu^{3+} in phosphate glasses that contain both Eu^{3+} and Sm^{3+} [423]. The energy transfer is not only evident from an increase in the luminescence intensity of Eu^{3+} , but also from the appearance of extra peaks in the excitation spectrum which can be attributed to Sm^{3+} . Energy transfer from Sm^{3+} to Eu^{3+} has been described by several authors for co-doped glasses [424-430] and inorganic phosphors [412,431-443]. Probably the best documented energy transfer of another lanthanide ion to Eu^{3+} is the energy transfer from Tb^{3+} to Eu^{3+} . The emitting level $^5\text{D}_4$ of Tb^{3+} is well above the $^5\text{D}_0$ emitting level of Eu^{3+} , so that the energy transfer from Tb^{3+} to Eu^{3+} leads to an enhancement of the luminescence intensity of Eu^{3+} . The energy transfer has been studied in glasses [444,445], inorganic compounds [446-448], solid molecular compounds (including metal-organic frameworks) [449,450], and in solution [451-462]. Finally, the uranyl ion (UO_2^{2+}) can sensitize Eu^{3+} luminescence by energy transfer [463-474].

Another possibility to sensitize lanthanide luminescence is via *charge-transfer states*. This is especially the case for trivalent lanthanide ions which can easily be reduced to the divalent state (redox-sensitive lanthanide ions) like Sm^{3+} , Yb^{3+} and Eu^{3+} , where light can be absorbed by an intense ligand-to-metal charge transfer state (LMCT state) from which the excitation energy can be transferred to the 4f-levels of the lanthanide ion. This process only works well if the energy of the LMCT state is high enough. For instance, for Eu^{3+} sensitization through a LMCT state is efficient if the LMCT is lying above 40000 cm^{-1} . Low lying LMCT states will partially or totally quench the luminescence [475]. In the case of Eu^{3+} , metal-centered luminescence is totally quenched if the energy of the LMCT is less than 25000 cm^{-1} . Quenching by low lying charge-transfer states is the reason for the weak luminescence or the absence of luminescence in europium(III) dithiocarbamate complexes [476-479]. In hydrated europium(III) acetylacetonate, $\text{Eu}(\text{acac})_3 \cdot 3\text{H}_2\text{O}$, no luminescence is observed upon excitation in the ligand absorption band, but the compound does show luminescence after excitation in the $^5\text{D}_1$, $^5\text{D}_2$ or $^5\text{L}_6$ levels [480]. The low efficiency of the intramolecular energy transfer is attributed to the presence of low-lying charge-transfer excited states below the ligand singlet levels. Sensitization of Eu^{3+} luminescence via charge-transfer states is much less investigated for molecular europium(III) complexes than for Eu^{3+} in inorganic host matrices [477,481-488]. For inorganic compounds, sensitization of Eu^{3+} luminescence via charge-transfer states is a very important mechanism (see section 4.6).

4. Absorption spectra

4.1 General features and “hot” bands

An overview of the transitions that can be observed in the absorption spectra of europium(III) compounds is given in Table 7. Although these transitions in the optical absorption spectrum can be used in a similar way as the transitions in the luminescence spectrum to extract information on the coordination environment of the Eu^{3+} ion, the absorption spectra are much less often used and their interpretation is also much less convenient. The main reason is that the most relevant transitions for determination of the point group symmetry (${}^5\text{D}_0 \leftarrow {}^7\text{F}_0$, ${}^5\text{D}_1 \leftarrow {}^7\text{F}_1$, ${}^5\text{D}_1 \leftarrow {}^7\text{F}_0$, ${}^5\text{D}_2 \leftarrow {}^7\text{F}_1$ and ${}^5\text{D}_2 \leftarrow {}^7\text{F}_0$) are very weak, with molar absorptivity values ϵ less than $1 \text{ L mol}^{-1} \text{ cm}^{-1}$. This means that highly doped crystals or concentrated solutions (in combination with quartz cuvettes with a long optical path length, up to 10 cm) have to be used to obtain a good signal-to-noise ratio in this optical region. Moreover, these weak transitions often overlap with the tails of ligand absorption band or with intense absorption bands of low-lying charge transfer states. However, absorption spectra of europium(III) compounds allow the determination of the higher energy levels of the $4f^6$ electronic configuration of the Eu^{3+} ion. In the older literature, the transitions to the ${}^5\text{D}_0$, ${}^5\text{D}_1$ and ${}^5\text{D}_2$ levels were called the yellow, green and blue bands, respectively, on the basis of their positions in the visible spectrum [214,489]. With decreasing temperatures, these lines red-shift and the crystal-field splitting of the ${}^5\text{D}_1$ and ${}^5\text{D}_2$ levels slightly increase. The barycenters of the ${}^5\text{D}_0$, ${}^5\text{D}_1$ and ${}^5\text{D}_2$ levels show a similar temperature shift relative to the ${}^7\text{F}_0$ level. The size of the shift is about 10 cm^{-1} between 295 K and 59 K [214,489].

Table 7. Overview of the transitions observed in absorption spectra of europium(III) compounds.^a

Transition ^b	Dipole character ^c	Wavelength (nm)	Remarks
${}^7F_6 \leftarrow {}^7F_0$	ED	1850–2200	If observed, most intense transition
${}^5D_0 \leftarrow {}^7F_1$	MD	585–600	Observed also in luminescence spectrum
${}^5D_0 \leftarrow {}^7F_0$	ED	570–585	Observed also in luminescence spectrum
${}^5D_1 \leftarrow {}^7F_1$	ED	530–540	Hypersensitive transition
${}^5D_1 \leftarrow {}^7F_0$	MD	520–530	Intensity independent of environment
${}^5D_2 \leftarrow {}^7F_1$	ED	470–480	---
${}^5D_2 \leftarrow {}^7F_0$	ED	460–470	Hypersensitive transition
${}^5D_3 \leftarrow {}^7F_1$	ED	410–420	---
${}^5L_6 \leftarrow {}^7F_1$	ED	400–410	Often overlaps with ${}^5L_6 \leftarrow {}^7F_0$ transition
${}^5L_6 \leftarrow {}^7F_0$	ED	390–405	Most intense transition in UV-VIS absorption spectrum
${}^5D_4 \leftarrow {}^7F_1$	ED	365–370	---
${}^5D_4 \leftarrow {}^7F_0$	ED	355–365	---

^a *The transitions have been limited to these that are useful for determination of the site symmetry. Many more transitions can be observed in the absorption spectra of europium(III)*

compounds, corresponding to transitions from the 7F_0 ground state to the excited levels listed in Table 3.

^b Transitions starting from the 7F_1 level can be observed only in room-temperature spectra. They disappear in low-temperature spectra due to depopulation of the 7F_1 level. Transitions starting from the 7F_2 level are only observed in room-temperature spectra of samples with high concentrations of europium(III) and they are not shown in the table.

^c ED = induced magnetic dipole transition, MD = magnetic dipole transition.

In order to extract the maximum of information from absorption spectra of europium(III)-doped single crystals, it is recommended to record *polarized absorption spectra*. In a cubic symmetry, the directions x , y and z are equivalent in the sense that they are interchangeable by the symmetry operations of the point group. For symmetries lower than cubic, the x , y and z directions are no longer equivalent. In other words, x , y and z do not belong to the same irreducible representation. For uniaxial crystals (hexagonal, tetragonal and trigonal) x and y remain interchangeable. Only for orthorhombic, monoclinic and triclinic symmetries the three directions are independent. For uniaxial and lower symmetries, the phenomenon of polarization is encountered. A transition will be allowed only in certain directions and forbidden in other directions. For uniaxial crystals, three different polarized spectra can be recorded, depending on the vibration direction of the electric field vector \mathbf{E} and the magnetic field vector \mathbf{H} with respect to the crystallographic c -axis:

α -spectrum: $\mathbf{E} \perp \mathbf{c}, \mathbf{H} \perp \mathbf{c}$,

σ -spectrum: $\mathbf{E} \perp \mathbf{c}, \mathbf{H} // \mathbf{c}$,

π -spectrum: $\mathbf{E} // \mathbf{c}, \mathbf{H} \perp \mathbf{c}$.

In an α -spectrum or axial spectrum, the light propagates along the c -axis, which has the same direction as the optic axis. Both \mathbf{E} and \mathbf{H} are perpendicular to the c -axis. An α -spectrum is recorded with unpolarized light. In a σ - and π -spectrum, the light propagates perpendicular to the c -axis. These spectra are therefore also called orthoaxial spectra. In a σ -spectrum, the electric field vector \mathbf{E} is perpendicular to the c -axis, which incorporates that \mathbf{H} is parallel to the c -axis. In a π -spectrum, the electric field vector is parallel to the c -axis and the magnetic field vector is perpendicular to it. The nature of an intra-configurational 4f-4f transition can be determined by comparing the three polarized spectra: for an ED transition the α - and σ -spectra are identical, while for a MD transition the α - and π -spectra are the same. For orthorhombic, monoclinic and triclinic crystal fields, the labels α , σ and π cannot be used. More information on the use of polarized spectra for the assignment of crystal-field levels in lanthanide spectra can be found in reference [95]. Examples of polarized absorption studies of europium(III) compounds are: $\text{YPO}_4:\text{Eu}^{3+}$ [490], $\text{LiYF}_4:\text{Eu}^{3+}$ [118], $\text{GdAl}_3(\text{BO}_3)_4:\text{Eu}^{3+}$ [115], Eu^{3+} -doped hexakis antipyrene triiodide [491], $\text{Na}_3[\text{Eu}(\text{oxydiacetato})_3]\cdot 2\text{NaClO}_4\cdot 6\text{H}_2\text{O}$ [112] and $\text{Eu}(\text{BrO}_3)_3\cdot 9\text{H}_2\text{O}$ [213,214].

For study of the energy level structure of Eu^{3+} , it is advantageous to measure the absorption spectra of europium(III)-doped crystals both at room temperature and at 77 K. The reason is that spectra measured at room temperature allow observing transitions starting from the ${}^7\text{F}_1$ and even from the ${}^7\text{F}_2$ excited state. Some of these transitions are to energy levels that cannot be reached from the ground state ${}^7\text{F}_0$, since they are forbidden by the selection rules for the point symmetry group of the Eu^{3+} site. The transitions from the ${}^7\text{F}_1$ level are weaker than those of the ${}^7\text{F}_0$ level, because at room temperature about 35 % of the ions are populating the ${}^7\text{F}_1$ level compared to the 65 % that are populating the ${}^7\text{F}_0$ ground state. The actual population numbers depend on the temperature and on the relative energy position of the ${}^7\text{F}_1$ level with

respect to the 7F_0 ground state, and can be calculated by the formula of the Boltzmann distribution:

$$X_A(T) = \frac{g_A \exp(-\Delta E_A/kT)}{\sum_i g_i \exp(-\Delta E_i/kT)} \quad (9)$$

where $X_A(T)$ is the fractional thermal population of the initial level A (= level from which the absorption or luminescence process starts) at temperature T , g_A is the degeneracy of level A , g_i is the degeneracy of level i , ΔE_A is the energy difference between level A and the ground state, ΔE_i is the energy difference between level i and the ground state (in cm^{-1}), $k = 0.695 \text{ cm}^{-1} \text{ K}^{-1}$ (Boltzmann's constant) and T is the absolute temperature (in K). In principle, the summation runs over all levels of the $4f^n$ configuration. In practice, the summation can be truncated at 2000 cm^{-1} or even lower energy, since higher energy levels have only a very small contribution to the sum. Level A can be either a crystal-field level or a ${}^{2S+1}L_J$ free-ion level. In the latter case the degeneracy g_A is equal to $2J+1$.

Given the fact that the population of the 7F_2 level is very small at room temperature ($\ll 1$ %), the transitions from the 7F_2 level are very weak and only very few studies report such transitions. Examples of studies on crystals showing transitions starting from the 7F_2 level are: $\text{Y}_3\text{Al}_5\text{O}_{12}:\text{Eu}^{3+}$ [492], $\text{Y}_3\text{Ga}_5\text{O}_{12}:\text{Eu}^{3+}$ [493], $\text{GdAl}_3(\text{BO}_3)_4:\text{Eu}^{3+}$, and $\text{EuCl}_3 \cdot 6\text{H}_2\text{O}$ [489]. The transitions ${}^5D_0 \leftarrow {}^7F_1$ and ${}^5D_0 \leftarrow {}^7F_2$ are useful for location of the 5D_0 level if the ${}^5D_0 \leftarrow {}^7F_0$ transition is forbidden. A general observation is that the line widths of the transitions starting from the 7F_1 level (and from the 7F_2 level) are much broader than those of the transitions starting from the 7F_0 ground state [489]. Probably this is due to the shorter residence times of the ions in the excited states compared to the ground state. Shorter lifetimes lead to broader spectral lines. Upon cooling to liquid nitrogen temperature (77 K), the transitions from the 7F_2 and 7F_1 levels will disappear, because only the 7F_0 ground state is populated. Since the

transitions from the 7F_1 and 7F_2 level are observed only at elevated temperatures, they are called “hot” bands. A comparison of the spectra at room temperature and 77 K is useful to detect the hot transitions (i.e. the transitions from the 7F_1 and 7F_2 states), especially in the regions with a high density of energy levels. The line widths of the transitions from 7F_0 are smaller at 77 K than at room temperature, due to less vibrations of the host matrix. Unless the splitting of the energy levels is very small, all the crystal-field fine structure is already resolved in the room temperature spectra of europium(III) spectra at room temperature. For this reason, there is often no need to cool the samples below 77 K for high-resolutions spectra, unless for very special cases (e.g. if one wants to observe the hyperfine splitting). This makes the Eu^{3+} ion so attractive from a spectroscopic point of view. For the other lanthanides (with the exception of Gd^{3+}), it is required to cool the sample to liquid helium temperature (4.2 K) to fully resolve the crystal-field fine structure. The non-degenerate ground state and the very weak vibronic coupling are the main reasons why cooling is not required for recording well resolved absorption spectra of europium(III) compounds. The advantage of a non-degenerate ground state becomes evident when one compares Eu^{3+} (ground state 7F_0) with for instance Ho^{3+} (ground state 5I_8). At room temperature, the 17 crystal field levels of the 5I_8 ground state of Ho^{3+} are more or less equally populated and there is a considerable vibronic line broadening. As a consequence, the crystal-field fine structure is not resolved in the absorption spectra of holmium(III) compounds at room temperature or 77 K. However, Ho^{3+} shows very narrow line widths for the crystal-field transitions at 4.2 K or lower temperatures. Ho^{3+} can also show hyperfine structure in the absorption spectrum, due to the interaction of the 4f electrons with the nuclear angular momentum [494]. In contrast to the absorption spectra, it can be an advantage to measure luminescence spectra of Eu^{3+} at 4.2 K, if transitions from the higher excited states are observed. As mentioned in section 3.9, the luminescence spectra at 4.2 K contain fewer lines than the luminescence spectra at 77 K, because at 4.2 K only the

lowest crystal-field levels of the 5D_1 and 5D_2 levels are populated. Since the total splittings of the 5D_1 and 5D_2 levels are relatively small, the upper crystal-field levels have still a non-negligible population at 77 K. The occurrence of “hot bands” in the absorption spectra of europium(III) compounds in solution has confused earlier researchers working in the field of lanthanide spectroscopy. In a study of $\text{Eu}(\text{NO}_3)_3$ and EuCl_3 in different solvents [495], the hot bands were originally wrongly assigned to the presence of non-ionized $\text{Eu}(\text{NO}_3)_3$ and EuCl_3 species in equilibrium with the solvated species, before the correct assignment was made [496].

It is a general trend that the line broadening due to coupling of the electronic states of the lanthanide ion with the vibrations of the ligands and host matrix decreases towards the middle of the lanthanide series, with a minimum line broadening for Gd^{3+} [497-499]. Eu^{3+} and Tb^{3+} , standing in the lanthanide series left and right of Gd^{3+} , have also little line broadening due to vibronic coupling (electron-phonon coupling).

4.2 Transitions within the 7F ground term

Transitions within the 7F ground term are only observed for Eu^{3+} ions doped in inorganic matrices with low phonon energies, since these transitions are otherwise masked by the much stronger overtones and combination bands of the vibrations of the host matrix or ligands. However, if transitions within the 7F term are observed, these transitions are the most intense transitions in the absorption spectrum, because they are spin-allowed ($\Delta S = 0$). These transitions are the only spin-allowed transitions in the absorption spectrum, since the $4f^6$ configuration has only one septet (7F). With an UV-VIS-NIR spectrophotometer only the 7F_6 level can be observed, because the transitions to the other 7F_J levels are at too low energies and outside the operational range of the spectrophotometer. In principle, these low energy transitions can be observed with an FTIR spectrometer, but the 7F_J levels are in general

probed by luminescence spectroscopy. Examples of spectroscopic studies on single crystals in which transitions to the 7F_6 level are observed are: $Y_3Al_5O_{12}:Eu^{3+}$ [492,500], $Y_3Ga_5O_{12}:Eu^{3+}$ [493], $Eu_3Fe_5O_{12}$ [501], $LiYF_4:Eu^{3+}$ [118] and $LaCl_3:Eu^{3+}$ [217]. Several studies on glasses also report the 7F_7 levels in the absorption spectrum (Figure 13) [321,502-505]. One of the most complete studies of the 7F_J multiplet by absorption spectroscopy is the spectroscopic study of $Y_2O_3:Eu^{3+}$ by Chang and Gruber, who report transitions to the 7F_2 , 7F_3 , 7F_4 , 7F_5 and 7F_6 levels [264].

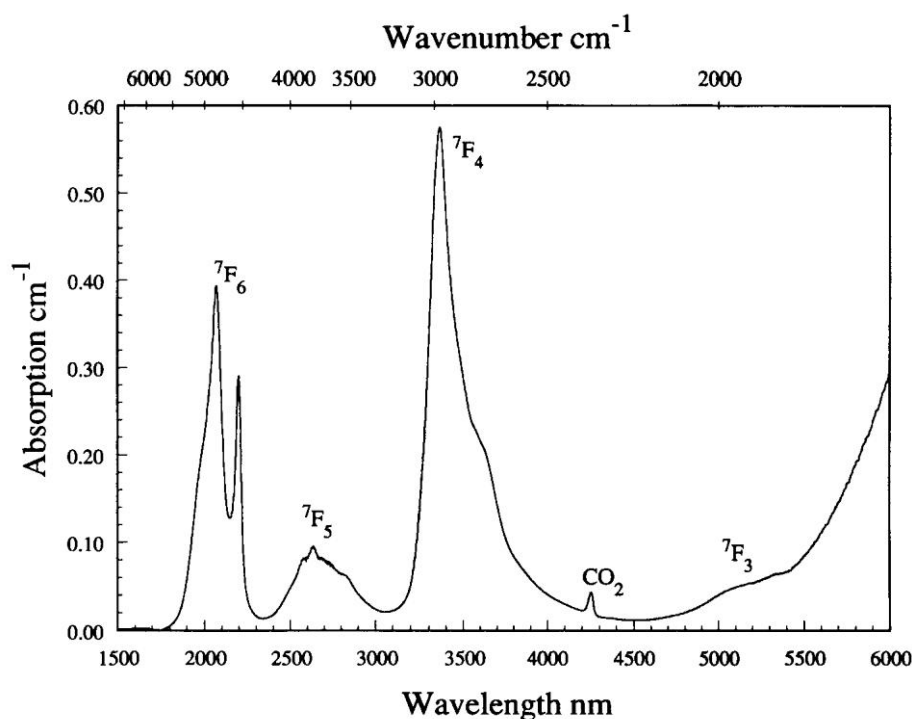


Figure 13. Infrared absorption spectrum of 1 mole% Eu^{3+} doped $ZrF_4-BaF_2-LaF_3-AlF_3$ (ZBLA) glass, showing the ${}^7F_J \leftarrow {}^7F_0$ transitions. Reproduced with permission from reference [321]. Copyright 1995 Elsevier.

4.3 Transition to the 5D_0 level

If a europium(III) compound does not luminesce, the ${}^5D_0 \leftarrow {}^7F_1$ and ${}^5D_0 \leftarrow {}^7F_2$ transitions in the absorption spectrum can be used to locate the 7F_1 and 7F_2 levels, As mentioned in

section 3.3, the ${}^5D_0 \leftarrow {}^7F_1$ transition is also useful to determine the position of the 5D_0 level, provided that the position of the 7F_1 level can be determined from other transitions, such as ${}^5D_1 \leftarrow {}^7F_1$ or ${}^5D_2 \leftarrow {}^7F_1$. The features of the ${}^5D_0 \leftarrow {}^7F_0$ transition are similar to those of the ${}^5D_0 \rightarrow {}^7F_0$ transition in the luminescence spectrum (see section 3.2).

The ${}^5D_0 \leftarrow {}^7F_0$ transition can be used to determine the number of non-equivalent sites in europium(III)-doped crystals or the number of complexes in solution. Geier and Jørgensen observed for the spectra of europium(III) complexes of ethylenediaminetetraacetate ($EDTA^{4-}$) dissolved in water two lines for the ${}^5D_0 \leftarrow {}^7F_0$ transition, with an energy difference of 14 cm^{-1} [506]. With an increase in temperature, the intensity of the band at lower energy increased in intensity at the expense of the band at higher energy, but the sum of the two ϵ values remained more or less constant at different temperatures. These two bands were assigned to two complexes with a different number of coordinated water molecules. At higher temperatures, the complex with the smaller number of coordinated water molecules is favored, so that the band with decreasing intensity as a function of temperature can be assigned to this complex. Merbach and coworkers used the evolution of the shape of the ${}^5D_0 \leftarrow {}^7F_0$ transition as a function of temperature and pressure to investigate the coordination equilibria and the water exchange kinetics of europium(III) complexes of hexadentate polyaminocarboxylate ligands, such as $EDTA^{4-}$ [507]. The results were explained in terms of equilibria between eight-coordinate and nine-coordinate species, where the eight-coordinate species has one water molecule less in the first coordination sphere than the nine-coordinate species. Whereas the energy differences for the ${}^5D_0 \leftarrow {}^7F_0$ transition of two hydrated forms of europium(III) complexes are relatively large (about 0.5 nm) and two distinct peaks can be observed in the absorption spectrum, the energy differences for two isomeric forms are in general much smaller (about 0.15 nm) and give only rise to an asymmetric ${}^5D_0 \leftarrow {}^7F_0$ transition. It is evident that these measurements require the use of a high-resolution spectrophotometer and

that the spectra have to be recorded with a small slit and the smallest possible step size of the monochromator. The contributions of the two isomers have to be determined by deconvolution of the absorption band. Isomers were observed for europium(III) complexes of DOTA-like ligands (DOTA = 1,4,7,10-tetraazacyclododecane-1,4,7,10-tetraacetic acid) [508]. The DOTA complexes occur in solution in two isomeric forms, M and m, which differ by the configuration of the acetate arms: the M isomer has an antiprismatic geometry, whereas the m isomer has a twisted antiprismatic geometry. The integration of the absorption bands after deconvolution allows determining the relative abundances of the two isomers. This method was used to investigate the contribution to the equilibrium mixture by the isomers of a DOTA-derivative in which one of the acetate pendant arms was replaced by a 2-methylpyridine-*N*-oxide group (Figure 14) [509]. Study of the $^5D_0 \rightarrow ^7F_0$ transition of $[\text{Eu}(\text{DO2A})(\text{H}_2\text{O})_n]^+$ (DO2A = 1,7-bis(carboxymethyl)1,4,7,10-tetraazacyclododecane) showed the existence of a temperature dependent equilibrium between eight-coordinate ($n = 2$) and nine-coordinate ($n = 3$) species [510]. At lower temperatures, the nine-coordinate species dominates the mixture, whereas the contribution of the eight-coordinate species increases with increasing temperatures.

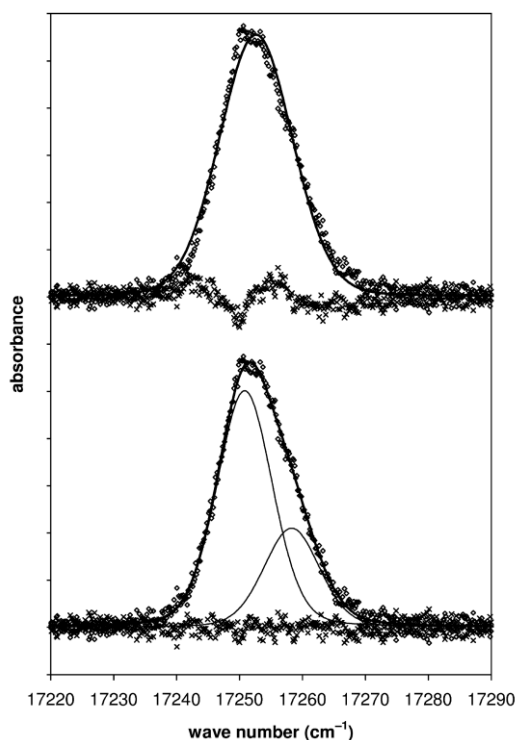


Figure 14. Absorption spectrum measured at 25.3 °C of the ${}^7F_0 \leftarrow {}^5D_0$ transition of the $[Eu(H_2O)(L)]$ complex, where L is a DOTA-derivative in which one of the acetate pendant arms was replaced by a 2-methylpyridine-N-oxide group. The complex occurs in solution in the form of two isomers. Comparison of the fitting with one band (upper figure) and two bands (lower figure). The measured data (diamonds) are shown with residual errors (crosses). Reproduced with permission from reference [509]. Copyright 2009 American Chemical Society.

4.4 Transitions to the 5D_1 level

The ${}^5D_1 \leftarrow {}^7F_1$ transition is a hypersensitive one ($\Delta J = 2$). The hypersensitivity is nicely illustrated by a study of the absorption spectra of the Eu^{3+} ion in the presence of different amounts of dipicolinate (DPA) ligand (Figure 15) [156]. From this figure, it is evident that the intensity of the magnetic dipole transition ${}^5D_1 \leftarrow {}^7F_0$ does not change, whereas drastic changes occur for the intensity of the ${}^5D_1 \leftarrow {}^7F_1$ transition. The magnetic dipole transition ${}^5D_1 \leftarrow {}^7F_0$ is

used to locate the 5D_1 level, but also to study the splitting of the $J = 1$ levels by the crystal-field perturbation. The crystal-field splitting pattern of the 5D_1 level is quantitatively identical to that of the 7F_1 level, but the total splitting is smaller [219]. It is predicted by theory that the ratio of the splitting $\Delta(^5D_1)/\Delta(^7F_1)$ equals 0.298 in the Russell-Saunders approximation [511]. The smaller splitting of the 5D_1 level is related to the fact that the 5D term has a smaller L value than the 7F term [489]. Experimentally, the splitting of the 5D_1 level is about 1/5 of the splitting of the 7F_1 level. These deviations from theory can be attributed to intermediate coupling or J -mixing.

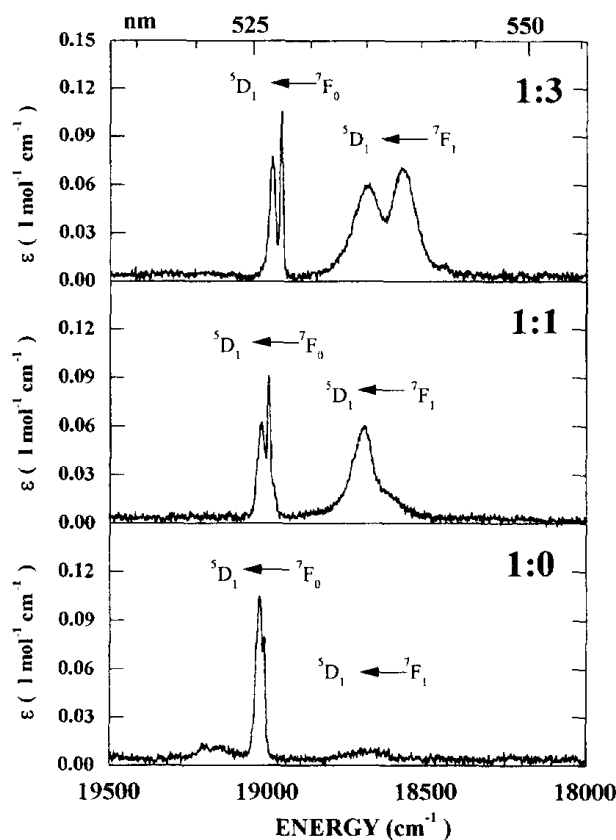


Figure 15. Room-temperature absorption spectra of the transitions to the 5D_1 level in $[Eu(DPA)_3]^{3-}$ (top), $[Eu(DPA)]^+$ (center) and Eu^{3+}_{aq} (bottom), where DPA = dipicolinate. Reproduced with permission from reference [156]. Copyright 1997 Elsevier.

4.5 Transitions to the 5D_2 level

Of the transitions to the 5D_2 level, the $^5D_2 \leftarrow ^7F_0$ transition is the most useful, because it allows determining the position of the 5D_2 level. This electric dipole transition is a hypersensitive transition ($\Delta J = 2$). The hypersensitivity of this transition is very well illustrated by considering the europium(III) dipicolinate system (Figure 16) [156]. The 5D_2 level is often used to directly excite the Eu^{3+} ion with one of the lines of an argon-ion laser (465.8 nm) [512] or with a diode laser.

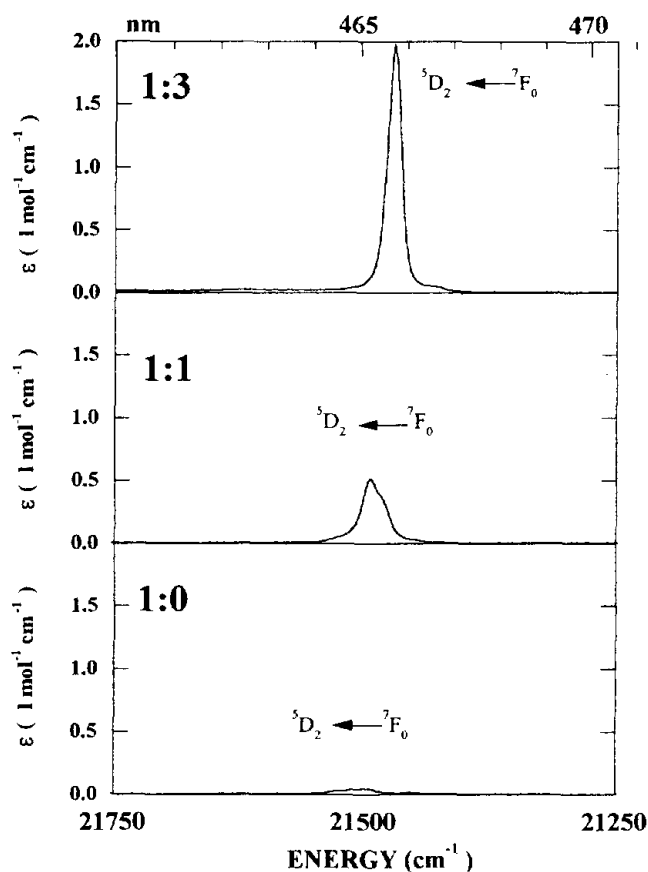


Figure 16. Hypersensitivity of the $^5D_2 \leftarrow ^7F_0$ transition in the room-temperature absorption spectra of $[\text{Eu}(\text{DPA})_3]^{3-}$ (top), $[\text{Eu}(\text{DPA})]^+$ (center) and $\text{Eu}^{3+}_{\text{aq}}$ (bottom), where DPA = dipicolinate. Reproduced with permission from reference [156]. Copyright 1997 Elsevier.

4.6 Transitions to higher energy levels

The ${}^5D_3 \leftarrow {}^7F_0$ transition is very weak and often not observed, because it is strictly forbidden by the Judd-Ofelt theory and can only gain intensity via J -mixing. The ${}^5D_3 \leftarrow {}^7F_1$ transition is commonly used to locate the 5D_3 level. This transition is also hypersensitive ($\Delta J = 2$), but its hypersensitivity has not been studied in detail yet.

The ${}^5L_6 \leftarrow {}^7F_0$ transition is the most intense transition in the absorption spectrum of europium(III) compounds, except when the ${}^7F_6 \leftarrow {}^7F_0$ transition is observed in the near-infrared region. This transition is commonly used to excite Eu^{3+} to induce photoluminescence, if excitation via the ligands is not possible due to the absence of efficient energy transfer. Excitation in the 5L_6 level allows direct population of the 4f levels. By radiationless deactivation, the 5D_3 , 5D_2 , 5D_1 and finally the 5D_0 level are populated. The ${}^5L_6 \leftarrow {}^7F_1$ transition is situated in the spectrum between the ${}^5L_6 \leftarrow {}^7F_0$ and the ${}^5D_3 \leftarrow {}^7F_{0,1}$ transitions. It is useful to observe crystal-field sublevels of the 5L_6 level that cannot be observed via the ${}^5L_6 \leftarrow {}^7F_0$ transition, due to the selection rules. Transitions to the 5L_7 , 5L_8 and the 5G_J ($J = 2, 3, 4, 5, 6$) levels are located in the region between 26000 and 27100 cm^{-1} in the absorption spectrum. The density of energy levels in this spectral region is very high and assignment of these levels is only possible by comparison of the experimentally observed energy levels with a list of calculated energy levels. As a consequence of the high density of energy levels, the wave functions of these energy levels contain contributions of many ${}^{2S+1}L$ levels and it is very difficult to unambiguously assign a ${}^{2S+1}L_J$ label to these levels. Only a small number of papers discuss these high-energy levels [112,115,118,213,264,306,492,493,513-516]. The ${}^5D_4 \leftarrow {}^7F_{0,1}$ transitions allow location of the crystal-field sublevels of the 5D_4 level. The 5D_4 level is located in a spectral region where there is no overlap with other ${}^{2S+1}L_J$ levels, so that

assignment of its crystal-field sublevels is relatively straightforward. In principle, transitions to the 5L_9 and ${}^5L_{10}$ are expected in this region, but their intensities are negligibly low and they are not observed. This is not unexpected because $\Delta J > 6$. Transitions to the following levels are located in the spectral region between 30000 and 40000 cm^{-1} : 5H_J ($J = 3, 4, 5, 6, 7$), 5F_J ($J = 1, 2, 3, 4, 5$), 5I_J ($J = 4, 5, 6, 7, 8$), 5K_J ($J = 5, 6, 7, 8$) and 3P_J ($J = 0, 1$). The density of energy levels in this region is very high, and assignment is only possible by comparison with a list of calculated energy levels.

Most of the transitions in europium(III) absorption spectra are transitions between two energy levels within the $[\text{Xe}]4f^6$ configuration (intra-configurational transitions). The first excited configuration $[\text{Xe}]4f^55d^1$ starts circa 70000 cm^{-1} above the ground state 7F_0 of the $[\text{Xe}]4f^6$ configuration and this excited configuration can be observed only by optical spectroscopy in the gas phase, not in the solid phase [102]. Data on the energy levels structure of Eu^{3+} in the gas phase (Eu IV spectra) are still very limited. It should be noted that our knowledge about the higher excited states of the $[\text{Xe}]4f^6$ configuration is largely based on calculations, because of difficulties to interpret the very complex gas-phase spectra with thousands of line transitions. The ionization energy of the Eu^{3+} ion is $344000 \pm 5000 \text{ cm}^{-1}$ ($42.7 \pm 0.6 \text{ eV}$) [102].

4.7 Charge-transfer bands

Europium(III) can also show broad absorption bands in the ultraviolet region of the electromagnetic spectrum. These bands are due to electron transfer: an electron is transferred from one or more neighbouring atoms to the Eu^{3+} ion and Eu^{3+} is formally reduced to Eu^{2+} . Eu^{3+} is the most oxidizing of the trivalent rare-earth ions, because Eu^{3+} is lacking only one electron to achieve a stable half-filled shell. The electron configuration of Eu^{2+} is $[\text{Xe}]4f^7$, so that this ion is iso-electronic with Gd^{3+} . These absorption bands in the ultraviolet region are

so-called *charge-transfer* (CT) bands, or, more precisely, *ligand-to-metal charge transfer* (LMCT) bands. They are very intense compared to the f-f transitions, since the transitions are allowed by the Laporte selection rule. The position of the charge-transfer bands strongly depends on the nature of the ligands. This relationship between the nature of the ligands and the energy position of the charge-transfer bands was first observed by Ryan and Jørgensen [517], but was studied in much more detail by Dorenbos [518,519]. The energies of the charge-transfer bands of common complexes are: Eu^{3+} aquo ion (53200 cm^{-1}), $\text{Eu}_2(\text{CO}_3)_3 \cdot 3\text{H}_2\text{O}$ (42400 cm^{-1}), EuPO_4 (43200 cm^{-1}), $\text{Eu}_2(\text{SO}_4)_3$ (42200 cm^{-1}), $\text{Eu}_2(\text{SO}_4)_3 \cdot 8\text{H}_2\text{O}$ (41700 cm^{-1}), $[\text{Eu}(\text{SO}_4)]^+$ in water (41700 cm^{-1}), $[\text{EuCl}_6]^{3-}$ in acetonitrile (33200 and 42600 cm^{-1}), $[\text{EuBr}]^{2+}$ in ethanol (31200 cm^{-1}), EuBr_3 (26000 cm^{-1}), $[\text{EuBr}_6]^{3-}$ in acetonitrile (24500 , 32400 and 37000 cm^{-1}), and $[\text{EuI}_6]^{3-}$ in acetonitrile (14800 , 22200 and 26700 cm^{-1}) [64]. Dorenbos gives an extensive compilation of the energies of the charge-transfer transitions of europium(III) compounds in the solid state [519]. The general trend of the energies of the charge-transfer transitions is: fluorides > oxides > nitrides > chlorides > bromides > iodides > sulfides > selenides > phosphides > arsenides > tellurides > antimonides. According to Jørgensen, the energy of the charge-transfer transition for a given metal ion depends mainly on the nearest neighbours of the metal ion and more particularly on the optical electronegativity of the ligand [64]:

$$E_{CT} = 30000[\chi_{opt}(X) - \chi_{uncorr}(M)] \quad (10)$$

E_{CT} is the energy of the lowest Laporte-allowed charge-transfer transition (in cm^{-1}), $\chi_{opt}(X)$ is the optical electronegativity of the ligand and $\chi_{uncorr}(M)$ is the uncorrected optical electronegativity of the metal. “Uncorrected” means that the contributions of spin-pairing energy and other interelectronic repulsion parameters, as well as relativistic effects are not

taken into account. For $\chi_{\text{opt}}(X)$, the values of the Pauling electronegativity can be used: F^- (3.9), Cl^- (3.0), Br^- (2.8) and I^- (2.5). $\chi_{\text{uncorr}}(M)$ is a value that must be determined empirically from the observed charge-transfer energies. For Eu^{3+} , a $\chi_{\text{uncorr}}(\text{Eu})$ value of 2.0 can be taken [517]. The application of Jørgensen's formula is largely restricted to halide compounds. It does not work to predict the charge-transfer energies of oxides. Dorenbos showed that the CT energies also depends on the size of the Eu^{3+} site and the binding strength of the valence band electrons [519]. He presented a theoretical model that allows estimation of the charge-transfer energy of any lanthanide ions from the knowledge of the position of the charge-transfer band of Eu^{3+} [520]. Europium(III) complexes with charge-transfer bands in the visible spectral region are strongly colored. For instance, $[\text{EuI}_6]^{3-}$ is dark green [521]. Blasse and coworkers made a detailed investigation of the influence of the position of the charge-states on the luminescence properties of Eu^{3+} compounds [522]. They considered the mixing of the $4f^6$ states with the charge-transfer states of opposite parity as an important mechanism to explain the intensity of induced electric dipole transitions. One of the arguments was that an inverse correlation exists between the energy of the lowest charge-transfer state and the intensity of the $^5\text{D}_0 \rightarrow ^7\text{F}_2$ transition: the lower the energy, the more intense the transition. Mixing of states is stronger if the energy difference between the states involved in mixing is small. Blasse also suggested that there is a tendency of shifting the charge-transfer band to lower energies for higher coordination numbers [523]. Li *et al.* developed a theoretical model based on the dielectric theory of chemical bond for complex crystals that allows the calculation of the charge-transfer energy of crystalline europium(III) compounds if the crystal structure and refractive index are known [524,525].

A marked difference between charge-transfer bands and broad f-d transitions is the absence of a distinct splitting of the charge-transfer bands [526]. They are in general broad without fine structure. $\text{CaF}_2:\text{Eu}^{3+}$ is a rare example of a europium(III) compound in which

both the f-d transitions and the charge-transfer band are observed [526]. The $4f^5 5d^1 \leftarrow 4f^6$ transitions appear at 68456, 69686 and 73551 cm^{-1} . The broad charge-transfer band is at about 66000 cm^{-1} . The half-width of the band is 5000 cm^{-1} . Charge-transfer states of Eu^{3+} at low energies have serious consequences for the spectroscopic properties of this ion, due to a non-negligible mixing of the $4f^6$ electronic states and the charge-transfer states. This mixing has been used to explain the unusually high intensity of the $^5D_0 \rightarrow ^7F_0$ transition in some europium(III) compounds (see section 3.3) [148]. Charge-transfer band at low energies also shorten the luminescence decay times. The luminescence decay times in the isostructural compounds $\text{LiGdF}_4:\text{Eu}^{3+}$ and $\text{GdNbO}_4:\text{Eu}^{3+}$ are 7.3 ms and 0.65 ms, respectively [526]. The charge-transfer state in $\text{LiGdF}_4:\text{Eu}^{3+}$ is at a much higher energy than in $\text{GdNbO}_4:\text{Eu}^{3+}$.

Charge-transfer bands can be useful for sensitization of europium(III) luminescence, because they can act as an antenna to absorb light and to transfer the excitation energy to the Eu^{3+} ion, in a way similar to sensitization of lanthanide luminescence by organic chromophores (see section 3.10). The best known example of a compound with sensitization via a charge-transfer band is probably the red phosphor $\text{Y}_2\text{O}_3:\text{Eu}^{3+}$, in which the 254 nm UV emission light of mercury is absorbed by the charge-transfer band of the phosphor and subsequently transferred to the Eu^{3+} ion. The excitation in the charge-transfer state rapidly thermalizes to the bottom of the charge-transfer state and then feeds the 4f states with resonance crossovers near the charge-transfer state minimum [475,527]. In $\text{Y}_2\text{O}_2\text{S}:\text{Eu}^{3+}$ and $\text{La}_2\text{O}_2\text{S}:\text{Eu}^{3+}$, the emitting 5D_J states are directly fed; while in $\text{Y}_2\text{O}_3:\text{Eu}^{3+}$ the higher 4f states are fed. The energy of the charge-transfer states should not be too low, because otherwise the 5D_0 excited state will be quenched and no europium emission will be observed [477,482,486,528,529]. The position of the charge-transfer bands is strongly temperature-dependent, so that the luminescence quenching by these charge-transfer states also strongly depends on the temperature. The emissions from the 5D_J levels in $\text{Y}_2\text{O}_2\text{S}:\text{Eu}^{3+}$, $\text{La}_2\text{O}_2\text{S}:\text{Eu}^{3+}$

and LaOCl are quenched sequentially with increasing temperature in the simple order 5D_3 , 5D_2 , 5D_1 and 5D_0 [475]. The quenching occurs at lower temperatures for the lanthanum(III) compound compared to the yttrium(III) compound. This quenching of the 5D_J states is attributed to thermally activated resonance crossovers from a 5D_J state to the charge-transfer states, followed by return crossovers to a lower 5D_J state. The charge-transfer states do not quench the luminescence in $Y_2O_3:Eu^{3+}$ [527]. The absence of the $Eu^{3+} - O^{2-}$ CT band in europium(III)-doped fluoride compounds can be used as an indication that no oxygen is built in the fluoride matrix and thus as a method for determination of the purity of fluoride compounds [251]. A strong charge-transfer band due to oxygen impurities was present in the reflection spectrum of $NaEuF_4$ [252]. Of course, such a charge-transfer band is also present in oxyfluorides, such as $YOF:Eu^{3+}$ [530,531]. The weakly luminescent *N,N*-dimethyldithiocarbamate complexes a example of luminescence europium(III) compounds that can be excited by a sulfur-to-europium charge-transfer band [476,479].

5. Excitation spectra

Excitation spectra are recorded by monitoring the luminescence intensity as a function of the excitation wavelength: the detection wavelength is fixed and the excitation wavelength is scanned over the spectral region of interest. An excitation spectrum looks similar to an absorption spectrum, but there is no one-to-one relationship. The relative intensities of the transitions can be different and there can be extra peaks present or peaks missing in comparison to the corresponding absorption spectrum. In fact, an excitation spectrum can be considered as being the product of an absorption spectrum and a plot of the quantum yield as a function of the wavelength. A transition is observed in the excitation spectrum only if this level is efficient in populating the emitting level and thus in generating luminescence. If an energy level is absent in the excitation spectrum it means that this level is not efficient in

absorbing the excitation light and/or is not able in populating the emitting level. Another feature of an excitation spectrum is that, in addition to the energy levels of the emitting ion, also energy levels of the sensitizing ion or the antenna ligands are visible. The main application of an excitation spectrum is to determine the optimum excitation wavelength: the excitation wavelength for measuring a luminescence spectrum is set at the most intense peak or the maximum of the most intense band in the excitation spectrum. An excitation spectrum does also give access to higher energy levels of a lanthanide ion. Recording an excitation spectrum is the preferred method for determining these energy levels in powder samples or in very diluted crystals or solutions, for which measurement of the absorption spectrum is difficult or even impossible. Measurement of the excitation spectrum is also the preferred method for determination of the energy levels of a lanthanide ion in the vacuum ultraviolet (VUV) region [446,532-540]. The main disadvantage of an excitation spectrum is that it cannot be used for studies of intensities of f-f transitions. Whereas Judd-Ofelt intensity parameters Ω_λ can be derived from absorption spectra, this is not the case for an excitation spectrum. Whereas emission spectra reveal the presence of radiative transitions, excitation spectra can reveal the presence of non-radiative transitions between levels [541]. The presence or absence of levels in the excitation spectra can be used to establish whether decay occurs via a step-by-step process, or whether level-bypassing transitions occur.

Measurement of the excitation spectrum at different emission wavelengths allows detecting different europium(III) species in solution. If only one species is present, the different excitation spectra will look identical. If more than one species is present, differences in peak heights and integrated intensity ratios will be observed in the excitation spectra [297]. Excitation spectroscopy has often been used by Horrocks and coworkers for the study of the binding of the Eu^{3+} ion to specific sites in calcium-binding proteins and other metalloproteins [98,175,542-545]. The method consisted of excitation of the $^5\text{D}_0$ state by scanning a tunable

dye laser through the 578–580 nm spectral region, while monitoring the ${}^5D_0 \rightarrow {}^7F_2$ emission at 615 nm. Excitation spectroscopy was also used to study the kinetics of formation of europium(III) complexes and for the determination of complex stability constants [190,546-554]. Measurements of excitation spectra at 5 K of $\text{Eu}(\text{ClO}_4)_3$ dissolved in water revealed the presence of two peaks for the ${}^5D_0 \leftarrow {}^7F_0$ transition at 579.43 nm and 579.17 nm [555]. The transition at 579.43 nm was assigned to the eight-coordinate species $[\text{Eu}(\text{H}_2\text{O})_8]^{3+}$, while transition at 579.17 nm was assigned to the nine-coordinate complex $[\text{Eu}(\text{H}_2\text{O})_9]^{3+}$. The two complexes had also two different luminescence decay times: $123 \pm 9 \mu\text{s}$ for the eight-coordinate complex and $109 \pm 8 \mu\text{s}$ for the nine-coordinate complex. In D_2O , the luminescence decay times were much longer: $3.50 \pm 0.12 \text{ ms}$ for the eight-coordinate complex and $3.70 \pm 0.18 \text{ ms}$ for the nine-coordinate complex. The eight-coordinate complex forms the minor fraction and the nine-coordinate complex the major fraction. On the other hand, a study using $[\text{Eu}(\text{H}_2\text{O})_9][(\text{BrO}_3)_3]$, $[\text{Eu}(\text{H}_2\text{O})_9][(\text{C}_2\text{H}_5\text{SO}_4)_3]$ and $[\text{Eu}(\text{H}_2\text{O})_8]_2[(\text{V}_{10}\text{O}_{28})] \cdot 8\text{H}_2\text{O}$ as model compounds for nine- and eight-coordinate Eu^{3+} aquo species in solution concluded on the basis of a comparison of the ${}^5D_1 \leftarrow {}^7F_0$ laser excitation spectra and the ${}^5D_0 \rightarrow {}^7F_{1,2}$ emission spectra of the crystalline model crystal systems with those of 0.1 M aqueous solution of EuCl_3 that $[\text{Eu}(\text{H}_2\text{O})_8]^{3+}$ is the dominating europium(III) species in solution [556].

Excitation spectra have been used to systematically investigate vibronic transitions in the spectra of the Eu^{3+} ion [557]. A vibronic transition involves a simultaneous change in the electronic and vibrational states of the metal ion. Vibronic transitions in lanthanide spectroscopy have been reviewed by Hüfner [65] and by Blasse [558]. Vibronic transitions are very prominent in the spectra of centrosymmetric lanthanide complexes, because electric dipole transitions can be induced in these systems only by a vibronic coupling mechanism between the f electrons and *ungerade* vibrational modes [282,318,559,560]. However, also non-centrosymmetric lanthanide complexes can show vibronic transitions, but these are in

general less intense than the purely electronic transitions. Blasse and coworkers studied the variation of the electron-phonon coupling strength across the lanthanide series [498,499]. The electron-phonon coupling is strong in the beginning (Pr^{3+}) and at the end of the lanthanide series (Tm^{3+}), but small at the center (Eu^{3+} , Gd^{3+} , Tb^{3+}) [561-563]. Blasse compared the intensity of the vibronic transitions of the ${}^5\text{D}_0 \rightarrow {}^7\text{F}_2$ transition in the luminescence spectra with that of the ${}^5\text{D}_0 \rightarrow {}^7\text{F}_1$ magnetic dipole transition, and the intensity of the ${}^5\text{D}_2 \leftarrow {}^7\text{F}_0$ transition in the excitation (or absorption) spectra with that of the ${}^5\text{D}_1 \leftarrow {}^7\text{F}_0$ magnetic dipole transition [557]. He considered the excitation and the absorption spectra of europium(III) compounds to be more suitable for investigation of the vibronic transitions than the corresponding luminescence spectra, because the crystal field splitting of the ${}^7\text{F}_2$ level is often so large that the vibronic transitions of the ${}^5\text{D}_0 \rightarrow {}^7\text{F}_2$ transitions overlap with the electronic lines of ${}^5\text{D}_0 \rightarrow {}^7\text{F}_2$ transitions and other transitions, e.g. ${}^5\text{D}_0 \rightarrow {}^7\text{F}_3$. Moreover, the vibronic transitions are always less intense in the luminescence spectra (emission spectra) than in the excitation spectra. Depending on the host matrix, the vibronic intensities vary by about two orders of magnitude. Very intense vibronic transitions are observed for $\text{SrTiO}_3:\text{Eu}^{3+}$. The intensity of the vibronic transitions of the ${}^5\text{D}_2 \leftarrow {}^7\text{F}_0$ transition are ten times more intense as than that of the ${}^5\text{D}_1 \leftarrow {}^7\text{F}_0$ transition. In the case of $\text{SrTiO}_3:\text{Eu}^{3+}$, vibronic transitions accompany even the magnetic dipole transitions, although such vibronic transitions are forbidden by the selection rules [564]. The intensities of the vibronic transitions are very weak for $\text{CaSO}_4:\text{Eu}^{3+}$: the intensity of the vibronic transitions of the ${}^5\text{D}_2 \leftarrow {}^7\text{F}_0$ is about $1/10^{\text{th}}$ of that of the intensity of the ${}^5\text{D}_1 \leftarrow {}^7\text{F}_0$ transition [557]. Several authors describe vibronic transitions in excitation and emission spectra of europium(III) compounds with organic ligands [158,565-569].

6. Other spectroscopic techniques

Besides measurement of luminescence, excitation and optical absorption spectra, other techniques (optical, magnetic or magneto-optical) can also be used for determination of the position and assignment of the crystal-field energy levels inside the 4f shell of Eu^{3+} , and for probing the symmetry of the Eu^{3+} site: two-photon absorption (TPA), Zeeman spectroscopy and magnetic circular dichroism (MCD). Electron paramagnetic resonance (EPR) is not of interest for the study of Eu^{3+} , because EPR probes the splitting of the ground state and Eu^{3+} has a non-degenerate ground state.

6.1 Two-photon absorption (TPA)

Two-photon absorption (TPA) provides spectroscopic information which is complementary to that of the classical one-photon absorption spectroscopy. In a two-photon absorption process, two photons are absorbed simultaneously to excite an ion or molecule from the ground state to the excited state. The two photons can have the same energy, but their energies can also be different. For the measurement of TPA spectra, laser sources are required because TPA is a non-linear optical process that is several orders of magnitude weaker than (linear) absorption. TPA is an advantageous technique for 4f systems in centrosymmetric systems with a high symmetry (e.g. O_h), since the 4f-4f transitions are allowed by the two-photon transition mechanism. The electric dipole forbidden transitions (the zero-phonon lines) in a O_h symmetry can be detected in a two-photon spectrum. The two-photon spectrum is not blurred by vibronic structure, so that the transitions are sharp lines [570,571]. The one-photon transitions in a cubic host matrix are unpolarized, but the two-photon spectra show a polarization dependence which can be helpful to determine the symmetry labels. Since two-photon processes are in competition with one-photon processes, the non-stationary intermediate state of the two-photon process may not coincide with an

energy level to which a one-photon absorption can take place. Otherwise the one-photon absorption process will occur and not the two-photon absorption. This requirement restricts the use of two-photon absorption mainly to systems in the middle of the lanthanide series (Eu^{3+} , Gd^{3+} and Tb^{3+}), where a large energy gap exists between the ground ^{2S+1}L term and the first excited ^{2S+1}L term, although TPA spectra for other lanthanide ions have also been recorded. The conventional method to observe the TPA spectrum is to record a two-photon excitation spectrum. Studies of TPA spectra of Eu^{3+} are: $\text{LaF}_3:\text{Eu}^{3+}$ [572], $\text{CaF}_2:\text{Eu}^{3+}$ [573], $\text{KYF}_4:\text{Eu}^{3+}$ [574], $\text{KLuF}_4:\text{Eu}^{3+}$ [574], $\text{Y}_3\text{Al}_5\text{O}_{12}:\text{Eu}^{3+}$ [575], $\text{LaOCl}:\text{Eu}^{3+}$ [576], $\text{Cs}_2\text{NaEuCl}_6$ [570] and $\text{Cs}_2\text{NaYF}_6:\text{Eu}^{3+}$ [570,577,578]. The two-photon absorption process leads to luminescence at a longer wavelength than the absorbed light and thus to anti-Stokes emission. The two-photon absorption takes place via a real energy level ($^5\text{D}_0$) or via a virtual excited state. In the case of a virtual excited state, the Eu^{3+} ion can be excited with a near-infrared light source. It should be mentioned that two-photon excited luminescence of europium(III) compounds is a very active research field at the moment, but for biological studies rather than theoretical studies [27,33,85,579-586]. Europium(III) complexes are very often used for *in vitro* and *in vivo* studies of cells, but ultraviolet excitation light has a very limited penetration depth in tissues and it can also damage living cells. In addition, ultraviolet excitation can induce strong background fluorescence. This background fluorescence of the organic matrix can be eliminated by time-gated measurements, but two-photon excitation avoids the problems of background fluorescence, cell damage and excitation light absorption by tissues.

6.2 Zeeman spectroscopy

The *Zeeman effect* is the lifting of all the energy level degeneracies in the presence of a magnetic field. In the case of a rare-earth ion coordinated by ligands according to a defined geometry, the energy levels in question are the levels obtained after introduction of the

crystal-field perturbation on the free-ion levels. The total Hamiltonian introduced in equation (1) can be extended by a term describing the Zeeman effect:

$$H = H_{free\ ion} + H_{crystal\ field} + H_{Zeeman} \quad (11)$$

H_{Zeeman} is the *Zeeman Hamiltonian*. The wave functions are those which diagonalize the total Hamiltonian.

In uniaxial crystals, a distinction can be made between the parallel and the perpendicular Zeeman effect, depending on the orientation of the magnetic field with respect to the main crystal axis (*c*-axis). In the parallel Zeeman spectrum, twofold degenerate levels are split and the wave functions are diagonal in M . The magnitude of the splitting is linearly proportional to the strength of the magnetic field. When the light beam is along the main crystal axis (and thus parallel to the magnetic field), the transitions to the two Zeeman components are circularly polarized. If the light beam is perpendicular to the main crystal axis, the transitions are (π , σ) polarized. The Zeeman effect is especially useful to determine the quantum number M of crystal-field levels in systems with an odd number of electrons, since the splitting is proportional to M . The splitting of a level with $M = \pm 3/2$ will be three times as large as the splitting of a level with $M = \pm 1/2$. In the perpendicular Zeeman spectrum, the crystal field degeneracy is lifted, but the splitting is not linearly proportional to the strength of the magnetic field. Non-degenerate crystal field levels will be affected by the magnetic field too. The matrix elements are no longer diagonal in M . Zeeman spectra have been recorded by earlier workers in the field of lanthanide spectroscopy to study the energy level structure of Eu^{3+} ions in crystalline host matrices [587-589], but the technique has become less popular, especially after the development of the MCD technique (see section 6.3). Recent studies about the Zeeman effect in europium(III) compounds are very rare [590].

Although the Zeeman effect is in general measured in static magnetic fields, it is also possible to use pulsed magnetic fields as well, as illustrated in a study of the Zeeman splitting of crystal-field levels in the luminescence spectrum of $\text{YVO}_4:\text{Eu}^{3+}$ [591]. The photoluminescence intensity of Eu^{3+} doped nano-glass-ceramics decreases with increasing magnetic field strengths in strong pulsed magnetic fields (up to 40 Tesla) [592]. This decrease in luminescence intensity was explained by a cooperative effect of the Zeeman splitting, the change in site symmetry of the Eu^{3+} ions and the cross-relaxation effect between adjacent Eu^{3+} ions.

6.3 Magnetic circular dichroism (MCD)

Magnetic circular dichroism (MCD) finds its origin in the magnetically induced optical activity, due to the Zeeman effect. In an MCD spectrum, the differences in molar absorptivities for left (LCP) and right circularly polarized light (RCP), $\Delta\varepsilon = (\varepsilon_{LCP} - \varepsilon_{RCP})$, are measured as a function of frequency (or wavenumber) on samples placed in a longitudinal magnetic field (i.e. with the magnetic field lines parallel to the light beam) [593]. The majority of the MCD studies on trivalent rare-earth ions were devoted to the Eu^{3+} ion [195,212,492,513,593-606]. The non-degenerate ground state (7F_0) and the presence of excited states with a small total angular momentum J (e.g. 5D_1 and 5D_2) make the MCD spectrum of Eu^{3+} relatively easy to interpret in comparison with the MCD spectra of the other trivalent rare-earth ions. The MCD spectra of europium(III) compounds are dominated by signals which have the shape of the first derivative of a Gauss curve. These signals are the A terms. An A term can have a positive or negative sign. A positive A term has its positive lobe at the high wavenumber side of the spectrum. In this case the absorption of left circularly polarized light takes place at a higher energy (or wavenumber) than the absorption of right circularly polarized light. For a negative A term, the opposite is true. The sign of the A terms

in the MCD spectrum depends on the symmetry of the first coordination sphere around the Eu^{3+} ion (*vide infra*). The information extracted by MCD measurements is similar to the information obtained with a classical Zeeman spectroscopy experiment, where the splitting and mixing of energy levels in a magnetic field are studied (see section 6.2). However, MCD can also be measured in the case of broad absorption bands, whereas Zeeman spectra cannot. Typical MCD applications are the assignment of electronic transitions, measurement of the Zeeman splitting, investigation of magnetic and symmetry properties of electronic states, polarization studies and testing the reliability of crystal-field wave functions and intensity parameters. An MCD spectrum has a higher information content than the corresponding absorption spectrum, since in addition to the intensity, the MCD signal is characterized by a sign (positive or negative). MCD is an excellent method for detecting the presence of overlapping transitions in the absorption spectrum. The method is very sensitive to changes in the electronic structure, and therefore to changes in the physical structure.

Measurement of MCD spectra is rather similar to measurement of optical absorption spectra. The main differences are that the radiation incident on the sample must be circularly polarized and that the sample has to be placed in a longitudinal magnetic field (i.e. with the magnetic field lines parallel to the light beam). Most magnetic circular dichroism spectrometers are circular dichroism spectrometers extended with a magnet, although some instruments are especially designed for MCD measurements. To provide the magnetic field, either a permanent magnet, electromagnet or superconducting magnet can be used. The permanent magnet has the disadvantage that the magnetic field is rather weak and that the magnetic field cannot be switched off for CD measurements. An electromagnet is often the best choice, because it can produce a moderate magnetic field (ca. 10000 Gauss or 1 Tesla), it can be switched off and it is easy to use. A superconducting magnet can provide a strong magnetic field (typically 5 to 7 Tesla), but cooling with liquid helium is necessary. The light

beam from the light source is first linearly polarized and then circularly polarized by a Pockel's cell or photoelastic modulator. Most instruments have a single beam setup. Unfortunately, MCD measurements cannot be performed on all types of samples, since the circular polarization of the incident light beam should be altered only by sample absorption, resulting in the formation of elliptically polarized light. This means that MCD can be recorded only for optical isotropic samples or in an isotropic direction for anisotropic samples. There are no issues with solution samples. Cubic crystals and especially glasses have to be checked for absence of internal stress. Uniaxial crystals can be measured along the unique optic axis, but careful orientation of the sample is crucial. In principle, MCD spectra of biaxial crystals cannot be measured. It is difficult to record the MCD spectrum of powdered samples, due to strong light scattering.

The MCD signal for the ${}^5D_1 \leftarrow {}^7F_0$ magnetic dipole transition is a positive A term, regardless the symmetry of the Eu^{3+} site [606]. This transition can be used as a sign reference transition, in order to check the direction of the magnetic field (parallel or antiparallel to the light beam). Indeed, the signs of the MCD signals will change, if the direction of the magnetic field is reversed. The sign of the A term of the ${}^5D_2 \leftarrow {}^7F_0$ induced electric dipole transition depends on the site symmetry [606]. The sign of the A term is determined by the M level to which left circularly polarized light is absorbed and this is determined by the selection rule for induced electric dipole transitions. A negative A term occurs for D_{3h} symmetry and for a D_{2d} symmetry (Figure 17). On the other hand, a positive A term is expected for C_{4v} symmetry. MCD is also suitable for studying distortions which result in a symmetry lowering. A good example is the $D_{3h} \rightarrow D_3$ distortion. The tricapped trigonal prism TTP (C.N. = 9) is one of the most frequently observed coordination polyhedra for lanthanide systems, although not often in its full D_{3h} symmetry. When top and base of the TTP are twisted relative to each other over a distortion angle 2ϕ , the symmetry will be lowered to D_3 . D_3 molecules are optically active

(because the six fold inversion axis of the D_{3h} has been destroyed). Two enantiomorphous forms are possible, depending on the sign of the distortion angle 2ϕ . If $\phi = 30^\circ$, the symmetry will be D_{3d} . As mentioned above, one negative A term is expected for the induced electric dipole transition ${}^5D_2 \leftarrow {}^7F_0$ in a D_{3h} symmetry. In a D_3 symmetry two A terms will be observed for that transition (after correction for natural circular dichroism): a negative A term and a second A term which sign depends on the distortion angle 2ϕ . The $D_{3h} \rightarrow D_3$ distortion in $\text{Na}_3\text{Eu}(\text{ODA})_3 \cdot 2\text{NaClO}_4 \cdot 6\text{H}_2\text{O}$ (EuODA) has been studied by MCD spectroscopy [594].

The emission analogue of MCD is magnetic circularly polarized luminescence (MCPL), also called magnetic circularly polarized emission (MCPE) [607]. This technique has been used mainly to investigate europium(III) coordination compounds in solution [608-614].

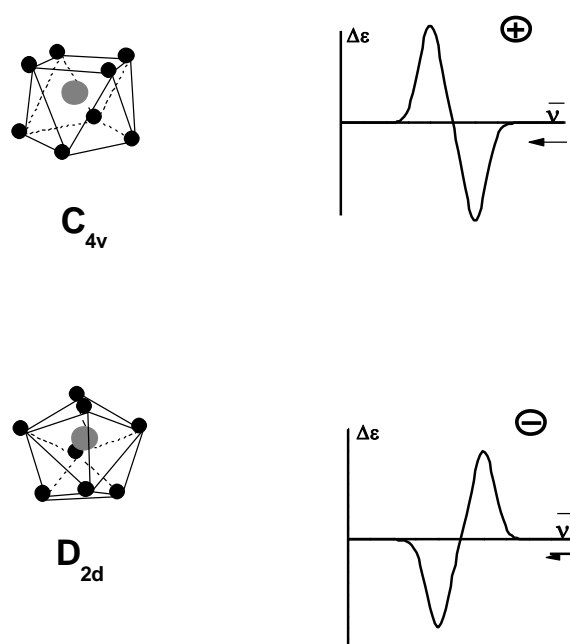


Figure 17. Sign of the A term in the MCD spectrum of the ${}^5D_2 \leftarrow {}^7F_0$ transition of Eu^{3+} in a C_{4v} symmetry (distorted square antiprism) and D_{2d} symmetry (dodecahedron).

7. Eu^{3+} as a spectroscopic probe

There are several reasons why the Eu^{3+} ion is so often used as a spectroscopic probe for the symmetry of the first coordination sphere of a trivalent lanthanide ion. First of all, the ground state (${}^7\text{F}_0$) and the most important emitting excited state (${}^5\text{D}_0$) are non-degenerate and are thus not split by the crystal-field effect. This greatly facilitates the interpretation of the experimental absorption and luminescence spectra. Secondly, the most important transitions in the luminescence spectra are from the ${}^5\text{D}_0$ excited state to ${}^7\text{F}_J$ levels with a low J value ($J = 0, 1, 2$). This also facilitates the interpretation of the spectra, because the number of possible crystal-field transitions is small. Thirdly, the wave functions of the ${}^7\text{F}_J$ levels and of the ${}^5\text{D}_0$, ${}^5\text{D}_1$ and ${}^5\text{D}_2$ excited states are well described within the intermediate coupling scheme and J is a good quantum number. J -mixing is limited so that there is only a small relaxation of the selection rules and an accurate theoretical description of the energy level structure of the $4f^6$ configuration of Eu^{3+} is possible. Fourthly, the different ${}^5\text{D}_0 \rightarrow {}^7\text{F}_J$ lines are well separated, so that there is virtually no overlap between the crystal-field levels belonging to different ${}^7\text{F}_J$ levels. Fifthly, europium(III) compounds often show an intense luminescence due to the large energy gap between the ${}^5\text{D}_0$ excited state and the highest level of the ${}^7\text{F}_J$ manifold (the ${}^7\text{F}_6$ level). It is also convenient that the luminescence is in the visible spectral region (red luminescence). Finally, the Eu^{3+} ion shows only a weak vibronic coupling and as a consequence the line widths of the crystal-field transitions are narrow, even at room temperature. The crystal-field fine structure is relatively easy to resolve, although spectral overlap may occur in case of weak crystal-field effects.

In principle, it is possible to determine the point group symmetry of the Eu^{3+} site by counting the number of crystal-field components that can be observed for the transitions ${}^5\text{D}_0 \rightarrow {}^7\text{F}_J$. This method is based on the selection rules for induced electric dipole and magnetic dipole transitions. The actual assignment of the point group symmetry can be made on the

basis of tables that list the number of expected crystal-field components for selected transitions for many different site symmetries (see Table 8 for an example [81]). Other authors have developed flow charts to aid the assignments of the point group symmetry [95,155].

Table 8. Number of crystal-field components for the ${}^5D_0 \rightarrow {}^7F_J$ ($J = 0-4$) transitions in the luminescence spectra of the Eu^{3+} ion in sites of different point group symmetry (adapted from ref. [81])

Point group	7F_0	7F_1	7F_2	7F_3	7F_4
C_1	1	3	5	7	9
C_s	1	3	5	7	9
C_2	1	3	5	7	9
C_{2v}	1	3	4	5	7
C_i	0	3	0	0	0
C_{2h}	0	3	0	0	0
D_2	0	3	3	6	6
D_{2h}	0	3	0	0	0
D_{2d}	0	2	2	3	3
D_3	0	2	2	4	4
C_3	1	2	3	5	6
C_{3v}	1	2	3	3	5
C_{3h}	0	2	1	3	4
C_{3i}	0	2	0	0	0
D_{3d}	0	2	0	0	0

D _{3h}	0	2	1	2	3
C ₄	1	2	2	3	5
C _{4h}	0	2	0	0	0
C _{4v}	1	2	2	2	4
D _{4h}	0	2	0	0	0
D _{4d}	0	2	0	1	2
S ₄	0	2	3	4	4
D ₄	0	2	1	3	3
C ₆	1	2	2	2	2
C _{6v}	1	2	2	2	2
D ₆	0	2	1	2	1
C _{6h}	0	2	0	0	0
D _{6h}	0	2	0	0	0
T	0	1	1	2	2
T _d	0	1	1	1	1
T _h	0	1	0	0	0
O	0	1	0	1	1
O _h	0	1	0	0	0
I _h	0	1	0	0	0

In practice, an unambiguous assignment of the point group symmetry on the basis of counting the number of observed crystal-field components in the luminescence or absorption spectra of europium(III) compounds is difficult, and often even impossible. A major difficulty is a small crystal-field splitting, leading to an overlap of peaks. In many cases, the overlapping peak can still be observed as a shoulder to a larger peak. Cooling the

europium(III) compound to liquid nitrogen temperature (77 K) or even lower temperatures will reduce the line widths and is beneficial for avoiding the spectral overlap. The spectral overlap results in a smaller number of lines than predicted by application of the selection rules for a given point symmetry group, and the compound has apparently a higher symmetry than the actual symmetry. As mentioned above, small crystal-field splittings are a direct consequence of a high coordination number: a large number of coordinating atoms distributed fairly evenly around the central metal ion tends to produce approximately a spherical field, with a low formal symmetry, but a small effective asymmetry [218]. Some point symmetry groups give the same number of crystal-field components for all the transitions in the luminescence or absorption spectrum. An example is the trio C_1 , C_s and C_2 . In such cases, information on the polarization of the transitions is required to assign a point symmetry group to the Eu^{3+} site. In Figure 18, the absorption spectra of europium(III) triacetate tetrahydrate (C_1 symmetry) at 4.2 K are shown [514]. The total lifting of the degeneracy of the energy levels is evident: $2J + 1$ lines for each ${}^5D_J \leftarrow {}^7F_0$ transition.

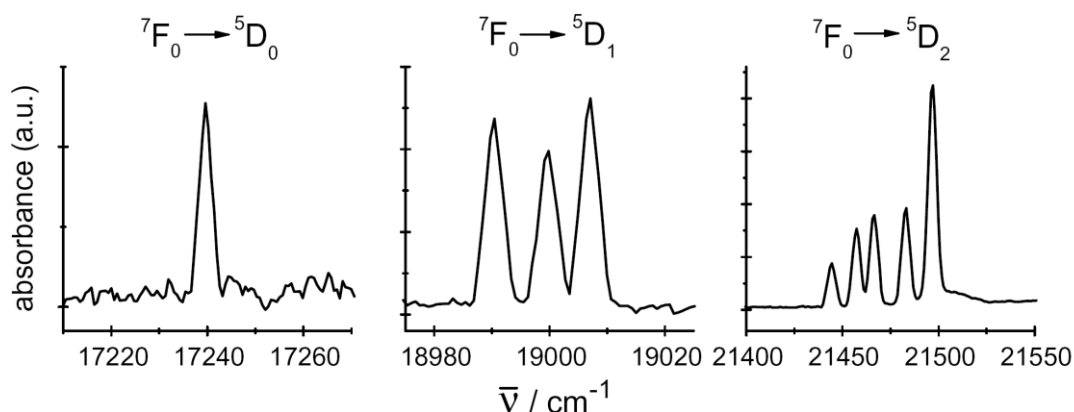


Figure 18. Absorption spectra of europium(III) triacetate tetrahydrate (C_1 symmetry) at 4.2 K. Reprinted with permission from reference [514]. Copyright 2008 Elsevier.

The overlap between the transitions originating from the 5D_1 excited state and those from the 5D_0 excited state complicate the interpretation of luminescence spectra. It has been discussed above how one can discriminate between the transitions from the different excited states. If a transition is weak, it is possible that it cannot be observed in the spectrum and fewer peaks are detected than predicted by the selection rules. On the other hand, spectra can show more lines than what is expected on the basis of the selection rules for a given point group. This is especially a problem for the interpretation of absorption spectra. These extra peaks are called *satellite lines*. One type of satellite lines are vibronic transitions, which occur both in absorption, excitation and luminescence spectra [557,615-617]. Another type is due to sites which are not optically equivalent. This is for instance the case for crystals in which the Eu^{3+} ion replaces a divalent cation. A typical example is CaF_2 . However, in such cases the Eu^{3+} is often reduced to the divalent state. However, the occupation of different sites can also occur if the Eu^{3+} ion replaces a trivalent ion. In the rare-earth garnet $A_3B_5O_{12}$ ($A = \text{Y, Lu, Gd}$ and $B = \text{Al, Ga}$), the Eu^{3+} ion enters preferentially in the A site with D_2 symmetry, but it can also take place in the B site with C_{3i} symmetry, especially when the doping concentration is high. The method of crystal preparation also has an influence on the distribution of the Eu^{3+} ions over the different sites. Crystal imperfections, such as interstitial ions, are another cause of satellite lines. Near-neighbor and next-near-neighbor interactions can also result in additional peaks [618,619]. It is evident that if impurities of other lanthanide ions are present in a europium(III)-doped crystal, these impurities will give rise to additional lines in the spectrum. This was a severe problem in the early days of rare-earth spectroscopy (before World War II), when rare-earth compounds were not readily available in sufficiently high purity. It is a good advice to have the possibility of impurities in mind if one finds in the absorption spectra unexpected lines in spectral regions where no transitions of Eu^{3+} are expected. In the luminescence spectra, these impurities do not show up, although one has to

be aware of the fact that even very low concentrations of some other rare-earth ions (e.g. Nd^{3+}) can efficiently quench the luminescence of Eu^{3+} .

The use of europium spectroscopy for site symmetry determination was important in times when single-crystal X-ray diffractometers were much less available and crystal-structure determination was much slower. The site symmetry of several europium(III) complexes have been determined by means of high resolution luminescence spectroscopy before the crystal structure of the compounds was known [286,620]. For instance, the luminescence spectrum of $[\text{Eu}(\text{terpy})_3](\text{ClO}_4)_3$ has been used to assign a D_3 symmetry to the $[\text{Eu}(\text{terpy})_3]^{3+}$ cation (Figure 19) [286]. The use of Eu^{3+} as spectroscopic probe is still useful if no crystals of a sufficient quality for single crystal X-ray diffraction are available. Europium luminescence spectroscopy is still of interest for symmetry determination of europium(III) complexes in solution, provided that a single complex with a well-defined structure is present in solution. Europium spectra have been used for probing the local structure of the Eu^{3+} ion in glasses [182,183,186,221,621-636]. It must be realized that many different sites are present in a glass matrix, often with a very wide variation in crystal-field parameters [182,623,624,627,636-638]. Site-selective spectroscopy can excite single sites, but it is difficult to get an overall picture of the glass structure. Eu^{3+} can be used to monitor the partial crystallization of glasses and the formation of glass ceramics [639-645].

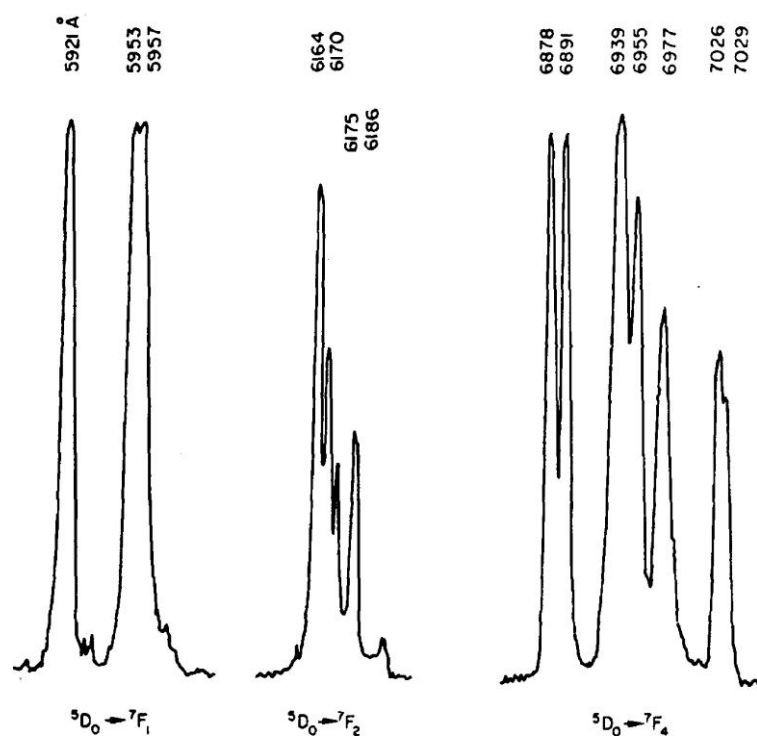


Figure 19. Luminescence spectrum of $[Eu(terpy)_3](ClO_4)_3$ at 180 K. The crystal-field fine structure can be explained by assuming a D_3 symmetry, with a slight perturbation to a lower symmetry. The slight perturbation is evident from the very small splitting of one of the lines of the ${}^5D_0 \rightarrow {}^7F_1$ transition. Reproduced with permission from reference [286]. Copyright 1969 Pergamon (Elsevier).

Recording high-resolution luminescence spectra of europium(III) compounds as a function of the temperature allows to detect small distortions in the crystal structure and phase transitions. A nice example of such a study is the luminescence study of $Eu(BrO_3)_3 \cdot 9H_2O$ by Bünzli and coworkers [152]. The luminescence spectra clearly demonstrate a symmetry lowering from D_{3h} to C_{3v} when cooling the sample from 295 K to 200 K. Upon lowering the temperature from 77 K to 4 K, transitions to several europium(III) sites appeared in the spectrum. Ions in the second coordination sphere of europium(III) distort the first coordination sphere and these small distortions can easily be visualized by high-resolution luminescence spectroscopy. The spectra of the solid compounds $M_3[Eu(DPA)_3]$, where $M =$

Li, Na, K, Rb, Cs, NH₄ and pyridinium, are good examples [646]. Divalent and trivalent counter ions give similar small changes in the spectra [647]. Other examples are spectra of tetrakis β-diketonate complexes [648], EDTA complexes [649] and triethylenetetraaminehexaacetate (TTHA) complexes [650]. Also different hydration states result in differences in the luminescence spectra [651]. One would not expect major changes in the luminescence spectra when the 2,2'-bipyridine (bipy) ligand is replaced by 4,4'-dimethyl-2,2'-bipyridine (dmbipy), yet the intensity ratio $I(^5D_0 \rightarrow ^7F_2)/I(^5D_0 \rightarrow ^7F_1)$ is quite different for the complexes $\text{Eu}(\text{bipy})_3\text{Cl}_3 \cdot 2\text{H}_2\text{O}$ and $\text{Eu}(\text{dmbipy})_3\text{Cl}_3 \cdot 2\text{H}_2\text{O}$ [652]. The luminescence spectra of europium(III) complexes of a series of aminopolycarboxylates show clear differences [159]. The same remark can be made for complexes of β-diketonates [275,653]. Recently, high-resolution luminescence spectroscopy was used to investigate how doping of Eu³⁺ ions into α-NaYF₄ and β-NaYF₄ distorts the local crystallographic symmetry of the host matrix [315]. Other recent studies on the use of the Eu³⁺ ion as a spectroscopic probe for small distortions of the local site symmetry have dealt with SrWO₄ [366], YBO₃ [654], and LaVO₄ [655]. Eu³⁺ luminescence spectroscopy has been used to probe the monoclinic, tetragonal and cubic phases of yttria-stabilized zirconia [656]. It can be clearly seen that the presence of an inversion center leads to very weak induced electric dipole transitions. By site selective excitation and application of the selection rules, sites with O_h and C_{3v} symmetry could be identified in ThO₂:Eu³⁺ crystals [657]. These two types of sites in ThO₂:Eu³⁺ have also been detected by time-resolved luminescence spectroscopy [658]. The luminescence spectra of Eu³⁺ have been used to monitor the devitrification process of a fluorozirconate glass to a glass ceramic [659]. By thermal treatment the glass starts to crystallize and this results in a sharpening of the transitions in the europium(III) luminescence and the appearance of crystal-field fine structure.

The intensity of the hypersensitive transition ${}^5D_0 \rightarrow {}^7F_2$ or the ratio R of the intensities of the ${}^5D_0 \rightarrow {}^7F_2$ and ${}^5D_0 \rightarrow {}^7F_1$ transitions, $I({}^5D_0 \rightarrow {}^7F_2)/I({}^5D_0 \rightarrow {}^7F_1)$ is often used as a measure for the asymmetry of the Eu^{3+} site. The reasoning is that, according to the Judd-Ofelt theory, the ${}^5D_0 \rightarrow {}^7F_2$ is strictly forbidden for a Eu^{3+} ion at a site with a center of symmetry (inversion center), so that the stronger the distortion of the site from a highly symmetric coordination polyhedron, the more intense the ${}^5D_0 \rightarrow {}^7F_2$ transition will become. It is true that the spectra of centrosymmetric systems often show a weak ${}^5D_0 \rightarrow {}^7F_2$ transition. For the centrosymmetric elpasolite $\text{Cs}_2\text{AgEuCl}_6$, the intensity of the ${}^5D_0 \rightarrow {}^7F_2$ transitions is about 25 times weaker than that of the ${}^5D_0 \rightarrow {}^7F_1$ transition at 77 K [318]. However, the statement that distortion leads in general to more intense ${}^5D_0 \rightarrow {}^7F_2$ transitions is not correct. First of all, the mere presence of a center of symmetry is not a sign of a high symmetry. Nobody would consider the triclinic point group C_i as a highly symmetric point group, yet a center of symmetry is present (in fact, the center of symmetry is the only symmetry element of the C_i group). Nobody would deny that the tetrahedron (T_d symmetry) is a highly symmetric coordination polyhedron, yet the tetrahedron has no center of symmetry. Secondly, a weak ${}^5D_0 \rightarrow {}^7F_2$ transition does not guarantee the presence of a center of symmetry and a Eu^{3+} ion at a site with an inversion center can give rise to a rather intense ${}^5D_0 \rightarrow {}^7F_2$ transition. As indicated in section 3.4, the ${}^5D_0 \rightarrow {}^7F_2$ transition is weak for europium(III) compounds with a square antiprism as the coordination polyhedron. An undistorted square antiprism has D_{4d} symmetry and no center of symmetry. Also europium(III) compounds in which the coordination polyhedron is a tricapped trigonal prism (D_{3h} symmetry) have a weak ${}^5D_0 \rightarrow {}^7F_2$ transition, although no center of symmetry is present. Examples of europium(III) compounds with a (slightly distorted) tricapped trigonal prism as the coordination polyhedron are $\text{Na}_3\text{Eu}(\text{ODA})_3 \cdot 2\text{NaClO}_4 \cdot 6\text{H}_2\text{O}$ (EuODA) [112], $[\text{Eu}(\text{H}_2\text{O})_9](\text{BrO}_3)_3$ [213], and $[\text{Eu}(\text{H}_2\text{O})_9](\text{EtOSO}_3)_3$ [215], all of which have a relatively weak ${}^5D_0 \rightarrow {}^7F_2$ transition.

Centrosymmetric europium(III) compounds with a relatively intense $^5D_0 \rightarrow ^7F_2$ transition are the elpasolites $Cs_2NaEuCl_6$ [205] and $Cs_2AgEuCl_6$ [318]. The intense $^5D_0 \rightarrow ^7F_2$ transition in the room temperature luminescence spectrum of this compound is due to strong vibronic interactions, i.e. a strong coupling between the electronic states of the Eu^{3+} ion and the vibrations of the host matrix. The vibronic transitions become less intense at low temperatures, so that cooling of the Cs_3EuCl_6 crystals results in a strong decrease in the intensity of the $^5D_0 \rightarrow ^7F_2$ transition. A better approach to judge whether a center of symmetry is present, is to consider the intensities of the $^5D_0 \rightarrow ^7F_2$ and the $^5D_0 \rightarrow ^7F_4$ transitions. If the intensities of these two transitions are very weak compared to the intensity of the $^5D_0 \rightarrow ^7F_1$ transition, it is very likely that a center of symmetry is present. The β -diketonate complex $[Eu(dbm)_3(H_2O)]$, (dbm = dibenzoylmethanate) is a good example to show that highly symmetric europium(III) complexes can have an intense $^5D_0 \rightarrow ^7F_2$ transition [158]. The EuO_7 cluster formed by the first coordination sphere has a capped distorted octahedron with C_{3v} symmetry. The water molecule caps the highly distorted octahedron formed by the dbm ligating atoms. The chelate rings and phenyl groups reduce the overall symmetry to C_3 . In fact, of the large number of reported structures of lanthanide β -diketonate complexes, the $[Ln(dbm)_3(H_2O)]$ are the only examples with the lanthanide ion at a site with a threefold or fourfold rotation axis. $SnO_2:Eu^{3+}$ is an example of a compound with at first sight a contradictory luminescence spectrum: the $^5D_0 \rightarrow ^7F_2$ transition is very weak (supposed to be a sign for a high symmetry), but the $^5D_0 \rightarrow ^7F_1$ transition is clearly split into three components (supposed to be a sign of a low symmetry) [283]. However, the crystal-field splitting in the luminescence spectrum is in perfect agreement with the D_{2h} symmetry of the Eu^{3+} site in $SnO_2:Eu^{3+}$. The weak $^5D_0 \rightarrow ^7F_2$ transition can be attributed to the presence of a center of symmetry, whereas the splitting of the 7F_1 level can be explained by the absence of a higher order symmetry axis (only C_2 axes are present). One has to be cautious when using the

symmetry of the Eu^{3+} site to predict the intensity of the ${}^5\text{D}_0 \rightarrow {}^7\text{F}_2$ transition in the luminescence spectrum. D_{4d} symmetry gives indeed always a low intensity for the ${}^5\text{D}_0 \rightarrow {}^7\text{F}_2$ transition, but in the case of D_3 symmetry the intensity of the ${}^5\text{D}_0 \rightarrow {}^7\text{F}_2$ transition depends on the geometry of the coordination polyhedron (distorted trigonal prism or distorted tricapped trigonal prism). The site symmetry of the borate $\text{GdAl}_3(\text{BO}_3)_4:\text{Eu}^{3+}$ and the oxydiacetate $\text{Na}_3\text{Eu}(\text{ODA})_3 \cdot 2\text{NaClO}_4 \cdot 6\text{H}_2\text{O}$ (EuODA) is in both cases D_3 and both compounds have only oxygen atoms in the first coordination sphere, but the ${}^5\text{D}_0 \rightarrow {}^7\text{F}_2$ transition is much more intense than the ${}^5\text{D}_0 \rightarrow {}^7\text{F}_1$ transition in $\text{GdAl}_3(\text{BO}_3)_4:\text{Eu}^{3+}$ compared to EuODA [660]. The difference is that the coordination polyhedron is a trigonal prism (coordination number = 6) in $\text{GdAl}_3(\text{BO}_3)_4:\text{Eu}^{3+}$ and a tricapped trigonal prism (coordination number = 9) in EuODA. Equatorial ligands have a negative effect on the intensity of the ${}^5\text{D}_0 \rightarrow {}^7\text{F}_2$ transition [660,661]. The ${}^5\text{D}_0 \rightarrow {}^7\text{F}_2$ transition is always weak for compounds with fluoride ligands, independent of the shape and symmetry of the coordination polyhedron. A typical feature of fluoride ligands is their low polarizability. The ${}^5\text{D}_0 \rightarrow {}^7\text{F}_2$ transition is very intense in the case of highly polarizable ligands, and especially in compounds with chelating rings, such as the β -diketonate complexes [662]. All these arguments show that the intensity ratio $R = I({}^5\text{D}_0 \rightarrow {}^7\text{F}_2)/I({}^5\text{D}_0 \rightarrow {}^7\text{F}_1)$ cannot be used as a measure of the asymmetry of the coordination environment. R is a function of different factors, not only the symmetry of the Eu^{3+} site, but also of the structure (shape) of the coordination polyhedron and the nature of the ligands. As mentioned in a recent review by Tanner, it is very difficult to define the degree of asymmetry [81]. How can one tell whether a given point group symmetry is more asymmetric than another one? One could count the number of symmetry elements of the point group. The most objective manner to quantify the degree of asymmetry is the *shape analysis*, which was first introduced by Kepert [663] and further developed by Raymond and coworkers for eight-coordinate rare earth complexes [664-666], but which could be extended to other coordination

numbers. The method is based on a comparison of all observed dihedral angles in a given structure with the corresponding ideal values. Dihedral angles along edges are defined as the angles between the normals to adjacent bounding faces of the polyhedron, where the vertices of that polyhedron are the ligand donor atoms around the metal. The first step is the calculation of all the dihedral angles of each pair of adjacent planes in the polyhedron. The second step is to find which superposition of the polyhedron on the targeted ideal polyhedron gives the smallest deviation for that idealized shape. Finally, the degree of distortion from an ideal polyhedron is evaluated by determining the “shape measure” S , which is the minimal mean deviation of dihedral angles along all edges. The idealized geometry that gives the smallest S value is the most suitable to describe the actual symmetry of the complex. Unfortunately, the shape analysis can be performed only if the coordinates of the atoms in the first coordination sphere are known. These can only be derived from single crystal data and not from luminescence or absorption spectra. A recent study on the use of shape analysis for the description of the coordination polyhedron of europium(III) complexes is the work of Hasegawa and coworkers on eight-coordinate asymmetric dodecahedral structures [667].

Europium luminescence has been used to monitor pressure-induced phase transitions. The structural changes occurring at the phase transitions are reflected in the crystal-field fine structure in the luminescence spectra [668-674]. Besides changes in the crystal-field splitting pattern, also changes in the intensity ratio $I(^5D_0 \rightarrow ^7F_2)/I(^5D_0 \rightarrow ^7F_1)$ can be monitored as a function of pressure [675,676]. Luminescence spectroscopy was used to study the reversible pressure-induced amorphous $\text{Eu}(\text{OH})_3$ [677]. It was observed that the pressure-induced amorphization was accompanied by a partial pressure-induced reduction of Eu^{3+} to Eu^{2+} . Compression of the EuZrF_7 crystalline phase at high pressures resulted in amorphization and the resulting luminescence spectrum was very similar to that of a fluorozirconate glass [678]. A combined X-ray diffraction and luminescence study of pressure-induced phase transitions

in $\text{Eu}_2(\text{MoO}_4)_3$ single crystals indicated that the amorphization starts by a disordering of the oxygen sublattice [679]. The study of the influence of pressure on the luminescence of europium-doped nanoparticles is a popular research topic [680-686]. Pressure changes have also an influence on the positions of the energy levels of the $4f^6$ electronic configuration of Eu^{3+} and on the position of the charge-transfer band [687-696]. The pressure-dependence of Eu^{3+} luminescence was used to measure the residual stresses in thermal barrier coatings, near the interfaces between different layers [697].

The use of the Eu^{3+} ion as a structural probe implies the assumption that the Eu^{3+} ions are well isolated in the host matrix and that no intermetallic $\text{Eu} \rightarrow \text{Eu}$ energy transfer occurs between neighboring Eu^{3+} centers. In general, the condition of site isolation is fulfilled in (dilute) solutions, but often not in highly doped solids [698-700]. This intermetallic $\text{Eu} \rightarrow \text{Eu}$ energy transfer limits the usefulness of the Eu^{3+} as structural probe because it makes the assignments of Eu^{3+} uncertain since in that case the emitting site is not necessarily the same as the excited site. The same issue has to be considered when studying polymetallic europium(III) complexes. For a long time, the intermetallic $\text{Eu} \rightarrow \text{Eu}$ energy transfer has been neglected during spectroscopic studies of the local symmetry of Eu^{3+} ions in such polymetallic assemblies, but this situation is changing [701,702].

One must avoid the pitfall of over-interpretation of europium(III) spectra. Luminescence and absorption spectra are very valuable for structural investigation of europium(III) compounds in solution, but the method has its shortcomings, as explained in the text above. Therefore, it is recommended to base the description of the structure of europium(III) complexes in solution on different experimental methods, which can give complementary pieces of information. As an example, the determination of the number of complexes in solution can be given. This can be done by counting the number of components for the ${}^5\text{D}_0 \leftarrow {}^7\text{F}_0$ transition in the luminescence or excitation spectra of the solution

containing europium(III) complexes. It has been mentioned that not all complexes will give an observable ${}^5D_0 \leftarrow {}^7F_0$ transition, because this transition will only be observed for complexes with a C_{nv} , C_n or C_s symmetry. In this case, also ${}^{89}\text{Y}$ NMR spectra could be considered [703,704]. The ${}^{89}\text{Y}$ nucleus is an interesting one for study by NMR, because this nucleus has nuclear spin $I = 1/2$, it has 100% natural abundance and the ${}^{89}\text{Y}$ chemical shifts span a range of more than 1300 ppm so that ${}^{89}\text{Y}$ NMR spectra are very sensitive to small changes in the ligand environment. Each yttrium(III) complex in solution is expected to give one single ${}^{89}\text{Y}$ resonance line, provided that it is a mononuclear complex or a polynuclear complex with only one type of chemical environment for Y^{3+} . Moreover, because of small differences in the ionic radius of Y^{3+} compared to that of Eu^{3+} , there is a good chance that yttrium(III) and europium(III) complexes are structurally very similar. Unfortunately, ${}^{89}\text{Y}$ has very long T_1 relaxation times, a low measuring frequency and a low receptivity. Therefore, high concentrations (sometimes concentration of more than 1 M are used) and long measurement times are required in classical excitation-acquisition experiments. To overcome the problems with the long T_1 relaxation times, relaxation agents (e.g. additions of small amounts of gadolinium salts) can be used to reduce the T_1 relaxation times [262]. The ${}^{89}\text{Y}$ NMR shifts can also be measured via the new 2D ${}^1\text{H}$, ${}^{89}\text{Y}$ and 2D ${}^{31}\text{P}$, ${}^{89}\text{Y}$ heteronuclear shift correlations through scalar coupling [705]. The ${}^{89}\text{Y}$ chemical shifts can be correlated to the coordination number, because the resonances shift upfield with increasing coordination number. Another technique that is very useful in combination with high-resolution luminescence spectroscopy of europium(III) compounds is extended X-ray absorption fine structure (EXAFS) spectroscopy [706-711]. This technique, which makes use of synchrotron radiation and which can be applied to different metal ions, provides information on the coordination number, the nature of the coordinating atoms and the interatomic distances. The advantage of EXAFS spectroscopy is that the element of interest can be selectively

investigated by exciting an electron from a well-defined core level. EXAFS reflects only the direct coordination of the excited atom, whereas all other compounds in the sample do not contribute to the spectral features of the signal. EXAFS provides information on metal complexes in solution revealing changes in the coordination sphere and especially about changes in stoichiometry. EXAFS data for europium(III) compounds are in general recorded at the Eu-L₃ edge. Whereas EXAFS can provide the coordination number and the nature of the coordination atoms, europium(III) luminescence spectra allow determination of the symmetry of the metal complex.

8. Nephelauxetic effect

The crystal-field perturbation does not only partly or fully lift the degeneracy of the $^{2S+1}L_J$ free-ion levels of the $4f^n$ configuration, but it also causes a shift of the barycenter of the $^{2S+1}L_J$ levels. The $4f-4f$ transitions experience a red-shift compared to the transitions in the free ion, i.e. to the ion in the gas phase. Jørgensen called this shift the "*nephelauxetic effect*" and attributed it to a covalent contribution to the bonding between the lanthanide ion and the ligands [64,712]. "Nephelauxetic" means "cloud expanding" and this name suggest that the size of the electron cloud around the lanthanide ion increases by transferring electron density to bonding molecular orbitals. An increase of the cloud size results in a decrease of the strength of the interelectronic repulsion. This is reflected by a diminution of the values of the Racah parameters (or Slater integrals) in the complex compared to the values for the free ion. However, Newman suggested that these changes of the Slater integrals cannot be due to covalency effects, but rather to dielectric effects caused by the local polarizability within the crystalline host matrix [713]. These dielectric effects also imply that the crystal-field parameters contribute to the description of the nephelauxetic effect. Caro and coworkers investigated systematically the nephelauxetic effect in lanthanide systems, with a focus on

non-degenerate levels, because here no crystal-field splitting occurs: ${}^2P_{1/2}$ of Nd^{3+} ($4f^3$), ${}^6P_{7/2}$ of Gd^{3+} ($4f^7$) and 5D_0 of Eu^{3+} ($4f^6$) [714,715]. They analyzed the effects of variation of the B_q^k crystal-field parameters on the energy gap between the 7F_0 and 5D_0 levels [716]. Changes in the values of the B_0^4 and B_0^6 parameters have no significant effect on the energy gap between the 7F_0 and 5D_0 level, but the B_0^2 parameter has. However, the strongest effect was observed for the B_2^2 parameter, which is non-zero only in the crystal-field potentials of orthorhombic and lower symmetries. The larger energy difference between the 7F_0 and 5D_0 levels caused by the B_q^2 parameters is mainly due to a strong lowering of the position of the 7F_0 level; the position of the 5D_0 level hardly changes on an absolute energy scale. Since the 7F_0 ground state is set at 0 cm^{-1} , a lowering of the position of the 7F_0 level with respect to the 5D_0 level results in a blue shift of the ${}^5D_0 \leftarrow {}^7F_0$ transition in the absorption spectrum. The authors correlate the fact that the B_2^2 parameter has the strongest influence on the ${}^5D_0 - {}^7F_0$ splitting with the shift of the ${}^5D_0 \leftarrow {}^7F_0$ transition to high energies in glasses, since the local symmetry of the Eu^{3+} ion in glasses is low and the B_2^2 parameter is non-zero only in low symmetries. The size of the correction of the nephelauxetic shift for the effect of J -mixing depends on the covalency of the metal-ligand bonds. Tanner and coworkers pointed to the fact that small shifts in the position of the ${}^5D_0 \rightarrow {}^7F_0$ level due to the nephelauxetic effect are often masked by crystal-field effects (J -mixing) [717]. They showed that J -mixing results in a lowering of the 7F_0 level. It is difficult to determine reliable electron-repulsion parameters (Slater parameters F^k) and spin-orbit coupling parameters ζ_{4f} for Eu^{3+} systems, due to the limited experimental information on different ${}^{2S+1}L_J$ levels. Especially the possibility to observe only a limited number of ${}^{2S+1}L$ terms (7F , 5D and 5L) is a major issue. Zolin and coworkers evaluated the contribution of J -mixing (due to strong crystal-field effects) to the shift of the ${}^5D_0 \leftarrow {}^7F_0$ transition in europium(III) complexes with EDTA and nitrilotriacetate ligands [718].

The energy of the 5D_0 level calculated for the Eu^{3+} in the gas phase is 17374 cm^{-1} [106]. In principle, this should be the highest possible wavenumber for the $^5D_0 \rightarrow ^7F_0$ transition in the luminescence spectrum and the $^5D_0 \leftarrow ^7F_0$ transition in the absorption spectrum, since the expansion of the electron cloud and the resulting decrease of the electronic repulsion will lead to a *red-shift* of this transition (shift to lower wavenumbers or longer wavelengths). Values reported for the position of the 5D_0 level in the hydrated europium(III) ion $[\text{Eu}(\text{H}_2\text{O})_9]^{3+}$ are 17277 cm^{-1} [719], 17276 cm^{-1} [720] and 17280 cm^{-1} [721]. Whereas the wavenumber of the $^5D_0 \rightarrow ^7F_0$ transition for most of the europium(III) complexes in solution is lying in the narrow range between 17225 and 17280 cm^{-1} [721], a much larger variation is observed for Eu^{3+} in crystalline host matrices. For instance, the $^5D_0 \rightarrow ^7F_0$ transition in $\text{Y}_2\text{O}_2\text{S}:\text{Eu}^{3+}$ is at 17151 cm^{-1} [49], whereas it is at 17336 cm^{-1} in $\text{Y}_6\text{WO}_{12}:\text{Eu}^{3+}$ [200]. In one of the geometrical isomers of tris(dipivaloylmethanato)(2,9-1,10-phenanthroline)europium(III), the 5D_0 level is at 17305 cm^{-1} [187]. In $\text{Mg}_3\text{FBO}_3:\text{Eu}^{3+}$, the $^5D_0 \rightarrow ^7F_0$ transition is at 567.7 nm , which corresponds to 17615 cm^{-1} [292]. The high energy of the 5D_0 level in $\text{Mg}_3\text{FBO}_3:\text{Eu}^{3+}$ seems to be contradictory, since it is higher than the value for Eu^{3+} in the gas phase (17374 cm^{-1}).

Amberger and coworkers observed very high values for the wavenumbers for the $^5D_0 \rightarrow ^7F_0$ transition in europium(III) compounds [722]. For instance, the $^5D_0 \rightarrow ^7F_0$ transition is located at 17522 cm^{-1} in $[\text{Eu}(\text{N}(\text{SiMe}_3)_2)_3]$ and 17618 cm^{-1} in $[\text{Eu}(\eta^5\text{-Cp})_3(\text{CNC}_6\text{H}_{11})]$ (where Cp = cyclopentadienyl). One could get the impression that these compounds show an anti-nephelauxetic behavior, but the Slater parameter F^2 in these compounds is smaller than those of $[\text{Eu}(\text{H}_2\text{O})_9]^{3+}$. However, crystal-field calculations on these compounds also show very large negative values for the B_0^2 crystal-field parameter. This large values lead to a stabilization of the 7F_0 level with respect to the 5D_0 level, resulting in a large energy difference between the 5D_0 and 7F_0 levels.

By studying the ${}^5D_0 \leftarrow {}^7F_0$ transition in the excitation spectra of 36 europium(III) complexes, Albin and Horrocks derived an empirical relationship between the wavenumber $\tilde{\nu}$ of this transition (in cm^{-1}) and the formal charge p on the ligands [723]:

$$\tilde{\nu} = -0.76p^2 + 2.29p + 17273 \quad (12)$$

The authors concluded that the observed nephelauxetic effect was not due to the covalency of the Eu-ligand bond, but rather to a decrease of the effective nuclear charge of Eu^{3+} upon binding to negatively charged ligands. The relationship more or less holds for ligands in which most of the donor atoms are negatively charged, but there are many violations of this relationship for complexes with neutral ligands. Later, it was suggested that the observed wavenumber shifts are better correlated to the sum of the partial charges on the ligand atoms than to the total formal charge [554], but also deviations from this correlation were found [721]. Moreover it is very difficult to determine accurate values of these partial charges. Frey and Horrocks ordered the atoms in the first coordination sphere of a Eu^{3+} ion according to their ability to produce a nephelauxetic effect with Eu^{3+} : $\text{Cl}^- > \text{OT} > \text{O} > \text{O}\beta > \text{ON} > \text{NT} > \text{OH} > \text{OE} > \text{OW}$, where OT = charged carboxylate oxygen, O = amide carbonyl oxygen, $\text{O}\beta$ = β -diketonate oxygen, ON = nitrate oxygen, NT = amine nitrogen, OH = hydroxyl oxygen, OE = ether oxygen, OW = water oxygen [721]. This trend is largely opposite to what is expected on the basis of the electronegativity of the ions or atoms: $\text{Cl}^- < \text{O}^- < \text{N} < \text{O}$. On the other hand, this trend follows the tendency of the ions or atoms to form a covalent bond with the Eu^{3+} ion, i.e. the tendency of the ions or atoms to share their electrons with Eu^{3+} . The nephelauxetic effect also depends on the coordination number: an increase in coordination numbers leads to a decrease in nephelauxetic shift.

Choppin and Wang investigated in detail the influence of the coordination number on the nephelauxetic effect and correlated the shift of the wavenumber of the ${}^5D_0 \leftarrow {}^7F_0$ transition with the number of donor atoms bound to the Eu^{3+} ion [720]. The wavenumber of the transition decreases as the coordination number increases. A linear regression analysis gave the equation:

$$CN_L = 0.237\Delta\tilde{\nu} + 0.628 \quad (13)$$

where CN_L is the maximum ligand coordination number and $\Delta\tilde{\nu}$ is the shift relative to the position of the ${}^5D_0 \leftarrow {}^7F_0$ transition in $[\text{Eu}(\text{H}_2\text{O})_9]^{3+}$ (17276 cm^{-1}). CN_L can be considered as the number of donor atoms coordinated to the Eu^{3+} ion, other than O atoms of H_2O . For instance, $CN_L = 0$ for $[\text{Eu}(\text{H}_2\text{O})_9]^{3+}$, $CN_L = 6$ for $[\text{Eu}(\text{EDTA})(\text{H}_2\text{O})_3]^-$, $CN_L = 8$ for $[\text{Eu}(\text{DOTA})(\text{H}_2\text{O})]^-$ and $CN_L = 9$ for $[\text{Eu}(\text{DPA})_3]^{3+}$. The correlation coefficient was 0.97. In all of the europium(III) complexes investigated, replacement of the coordination water molecules by a ligand caused a shift of the ${}^5D_0 \leftarrow {}^7F_0$ transition to lower energies (lower wavenumbers). By using equation 13 and by determining the number of coordinated water molecules (hydration number, section 10.2), it is possible to determine the total coordination number of europium(III) complexes in aqueous solution. Equation 13 also holds for Eu^{3+} ions solvated by DMSO molecules. In that case, the shifts $\Delta\tilde{\nu}$ are relative to the position of the ${}^5D_0 \leftarrow {}^7F_0$ transition of $[\text{Eu}(\text{DMSO})_x]^{3+}$ ($\tilde{\nu} = 17265 \text{ cm}^{-1}$). This shows that equation 13 is not solvent-dependent.

Malta and coworkers emphasize the importance of covalence in the mechanism of red-shifts observed for the ${}^5D_0 \rightarrow {}^7F_0$ transition of Eu^{3+} [724,725]. They proposed a new scale of covalency (*ordinal covalency scale*) and introduced the quantity of *overlap polarizability* (α_{OP}^*) to describe the degree of covalency of the chemical bond. There is an inverse linear

relationship between the *total polarizability* (sum of the α_{OP}^* values for all the coordinating atoms) and the wavenumber of the ${}^5D_0 \rightarrow {}^7F_0$ transition [726]. Malta also investigated the nephelauxetic effect of the ${}^5D_0 \rightarrow {}^7F_0$ transition as a function of the strength of the ligand field interaction [727]. There is some correlation between the red-shift of the ${}^5D_0 \rightarrow {}^7F_0$ transition and the ligand field strength parameter, but this correlation is less good than that observed for the total polarizability.

9. Judd-Ofelt parametrization of europium(III) spectra

9.1. Determination of Judd-Ofelt intensity parameters

The intensities of the transitions in the absorption spectra of europium(III) compounds can be expressed in terms of the *dipole strength* D . The dipole strength of a transition can be extracted from the absorption spectrum, using the formula:

$$D = \frac{1}{108.9 \times C \times d \times X_A(T)} \int \frac{A(\tilde{\nu})}{\tilde{\nu}} d\tilde{\nu}, \quad (14)$$

where C is the concentration of the europium ion (mol L^{-1}), d is the optical path length (cm), A is the *absorbance* and $\tilde{\nu}$ is the wavenumber (cm^{-1}). $X_A(T)$ is the fractional thermal population at temperature T (T in Kelvin) of level A from which the absorption process starts (7F_0 or 7F_1 in the case of Eu^{3+}). $X_A(T)$ is about 0.65 at room temperature, but the actual value has to be calculated using the energy difference between the 7F_0 and 7F_1 states, and the formula of the Boltzmann distribution. The dipole strength is expressed in D^2 (Debye²). The dipole strength of a magnetic dipole transition can be calculated by using only the 4f free-ion wave functions. However, for the calculation of the dipole strengths of the induced electric

dipole transitions, parameterization is necessary. In the framework of the Judd-Ofelt theory, the dipole strengths are described by three phenomenological parameters Ω_λ ($\lambda = 2, 4, 6$) [125,126,728]:

$$D = \frac{10^{36}}{2J+1} \frac{(n^2+2)^2}{9n} e^2 \sum_{\lambda=2,4,6} \Omega_\lambda \left| \langle J \| U^{(\lambda)} \| J' \rangle \right|^2. \quad (15)$$

The factor 10^{36} converts D^2 units into esu cm. The elementary charge e is 4.803×10^{-10} esu.

The degeneracy of the ground state is equal to $2J+1$ (i.e. 1 for Eu^{3+}). The $\langle J \| U^{(\lambda)} \| J' \rangle$ terms are the reduced matrix elements. The squared reduced matrix elements $\left| \langle J \| U^{(\lambda)} \| J' \rangle \right|^2$ are often abbreviated to $U^{(\lambda)}$. Tabulated reduced matrix elements for absorption and emission spectra can be found in the literature [719,729]. The term $\frac{(n^2+2)^2}{9n}$ corrects for the effect of the dielectric medium. The dipole strength of an induced electric dipole transition is proportional to the square of the matrix element in the dipole operator and therefore also to the square of the electric field at the lanthanide site. However, the lanthanide ions are in general not ions in a gas phase, but they are embedded in a dielectric medium. The lanthanide ion embedded in a dielectric medium not only feels the radiation field of the incident light, but also the field generated by the dipoles in the medium outside a spherical surface. The total field consisting of the electric field E of the incident light (electric field in the vacuum) plus the electric field of the dipoles is called the *effective field* E_{eff} , i.e. the field effective in inducing the electric dipole transition. The square of the matrix element in the electric dipole operator has to be multiplied by a factor $(E_{\text{eff}}/E)^2$. In a first approximation $(E_{\text{eff}}/E)^2 = (n^2+2)^2/9$, where n is the refractive index of the dielectric medium. The factor $(n^2+2)^2/9$ is the *Lorentz local field correction* and accounts for dipole-dipole corrections. For an absorption process, the

transition probability has to be divided by the energy (or photon) flux. The photon flux of a light beam does not alter when the light beam enters from a vacuum into the dielectric medium. The flux in vacuum is $(c/4\pi)E_0^2$ and that in the dielectric medium is $(v/4\pi)n^2E_0^2$, where c is the speed of light in vacuum, v is the speed of light in the medium and $v = c/n$. Therefore, an additional factor $1/n$ has to be included, so that this leads to the correction factor $\frac{(n^2+2)^2}{9n}$ in equation (15).

The dipole strength D is related to the often used *oscillator strength* f (dimensionless) by the following formula:

$$D = \frac{2.124 \times 10^6 f}{\tilde{\nu}} \quad (16)$$

In general, the Ω_λ parameters are determined via a least-squares fit, by minimizing the sum of the squares of the differences between experimental and calculated dipole strengths [94]. For europium(III) compounds, often an alternative approach is used, where advantage is taken of the fact that $U^{(2)}$ is the only non-zero squared reduced matrix element for the ${}^5D_2 \leftarrow {}^7F_0$ transition and that $U^{(4)}$ and $U^{(6)}$ are the only non-zero squared reduced matrix elements for the ${}^5D_4 \leftarrow {}^7F_0$ and ${}^5L_6 \leftarrow {}^7F_0$ transitions, respectively. The actual values are: $U^{(2)} = 0.0008$ for ${}^5D_2 \leftarrow {}^7F_0$, $U^{(4)} = 0.0011$, $U^{(6)} = 0.0155$ for ${}^5L_6 \leftarrow {}^7F_0$ [719]. The fact that so many squared reduced matrix elements are zero for Eu^{3+} is caused by the selection rules of the Judd-Ofelt theory [94]. Only transitions for which $\Delta J = 2, 4$ and 6 are allowed by the induced electric dipole mechanism if luminescence starts from a level for which $J = 0$ (i.e. 7F_0 or 5D_0). The ${}^5D_2 \leftarrow {}^7F_0$ and ${}^5D_4 \leftarrow {}^7F_0$ transitions do not overlap with the ${}^5D_2 \leftarrow {}^7F_1$ and ${}^5D_4 \leftarrow {}^7F_1$ transitions, respectively. The ${}^5L_6 \leftarrow {}^7F_0$ transition overlaps partially with the ${}^5L_6 \leftarrow {}^7F_1$ transition, but the

difference in intensity between the two transitions is so large, that the contribution of the ${}^5L_6 \leftarrow {}^7F_1$ transition to the total dipole strength can be neglected. Of course, by cooling the sample to 77 K, only transitions starting from the 7F_0 level are observed, since the 7F_1 level is not populated at this low temperature. As a consequence the Ω_2 parameter can be determined from the dipole strength of the ${}^5D_2 \leftarrow {}^7F_0$ transition, the Ω_4 parameter from the dipole strength of the ${}^5D_4 \leftarrow {}^7F_0$ transition, and the Ω_6 parameter from the dipole strength of the ${}^5L_6 \leftarrow {}^7F_0$ transition. The Ω_λ parameters for the $\text{Eu}^{3+}_{\text{aq}}$ ion are: $\Omega_2 = 1.62 \times 10^{-20} \text{ cm}^2$, $\Omega_4 = 5.65 \times 10^{-20} \text{ cm}^2$, $\Omega_6 = 5.02 \times 10^{-20} \text{ cm}^2$, while the parameter set for the $[\text{Eu}(\text{DPA})_3]^{3-}$ complex is: $\Omega_2 = 10.5 \times 10^{-20} \text{ cm}^2$, $\Omega_4 = 5.31 \times 10^{-20} \text{ cm}^2$, $\Omega_6 = 8.32 \times 10^{-20} \text{ cm}^2$ [156].

The Ω_λ parameters can also be determined from the luminescence spectra, by expressing the emission intensities in terms of the integrated areas under the emission bands in the luminescence spectrum. It is experimentally difficult to measure the absolute emission intensities. In the special case of the Eu^{3+} ion, it is possible to replace the absolute measurement by a relative one, if one considers the intensity of the ${}^5D_0 \rightarrow {}^7F_1$ magnetic dipole transition as a reference for transitions originating from the 5D_0 excited state. The intensity of the ${}^5D_0 \rightarrow {}^7F_1$ transition can be calculated exactly: $D_{\text{MD}} = 9.6 \times 10^{-42} \text{ esu}^2 \text{ cm}^2 = 9.6 \times 10^{-6} \text{ Debye}^2$ [157]. Most of the squared reduced matrix elements for transitions starting from the 5D_0 level are zero [719], except those for the ${}^5D_0 \rightarrow {}^7F_2$ transition ($U^{(2)} = 0.0032$), the ${}^5D_0 \rightarrow {}^7F_4$ transition ($U^{(4)} = 0.032$) and the ${}^5D_0 \rightarrow {}^7F_6$ transition ($U^{(6)} = 0.0002$). The experimental Ω_λ parameters can be calculated from the ratio of the integrated intensity of the ${}^5D_0 \rightarrow {}^7F_\lambda$ ($\lambda = 2, 4, 6$) transitions, $\int I_\lambda(\tilde{\nu}) d\tilde{\nu}$, to the integrated intensity of the ${}^5D_0 \rightarrow {}^7F_1$ transition, $\int I_1(\tilde{\nu}) d\tilde{\nu}$, by using the following equation [730]:

$$\Omega_\lambda = \frac{D_{\text{MD}} \tilde{\nu}_1^3}{e^2 \tilde{\nu}_\lambda^3 |\langle \Psi J | U^{(\lambda)} | \Psi J' \rangle|^2} \frac{9n^3}{n(n^2 + 2)^2} \frac{\int I_\lambda(\tilde{\nu}) d\tilde{\nu}}{\int I_1(\tilde{\nu}) d\tilde{\nu}}$$

(17)

Here, $\tilde{\nu}_1$ is the average wave number of the ${}^5D_0 \rightarrow {}^7F_1$ transition (in cm^{-1}), $\tilde{\nu}_\lambda$ is the average wave number of the ${}^5D_0 \rightarrow {}^7F_\lambda$ transition (in cm^{-1}). This average wave number $\tilde{\nu}_\lambda$ can be calculated by integration:

$$\tilde{\nu}_\lambda = \frac{\int \tilde{\nu} I(\tilde{\nu}) d\tilde{\nu}}{\int I(\tilde{\nu}) d\tilde{\nu}} \quad (18)$$

It should be noted that often only the Ω_2 and Ω_4 intensity parameters can be derived from the luminescence spectra, because the ${}^5D_0 \rightarrow {}^7F_6$ transition cannot be measured. Without knowledge of the dipole strength the ${}^5D_0 \rightarrow {}^7F_6$ transition, the Ω_6 parameter cannot be determined. The experimental Ω_λ parameters are often compared with those calculated by the computational Sparkle model [363,731-734].

9.2. Use of Judd-Ofelt parameters for calculation of photophysical quantities

The Judd-Ofelt parameters can be used to calculate the *radiative transition probabilities* $A(\Psi J, \Psi' J')$ of all the excited states [157]:

$$A(\Psi J, \Psi' J') = \frac{64\pi^4 \tilde{\nu}^3}{3h(2J+1)} \left[\frac{n(n^2+2)^2}{9} D_{ED} + n^3 D_{MD} \right]. \quad (19)$$

In this equation, $\tilde{\nu}$ is the average wave number of the transition (in cm^{-1}), h is the Planck constant (6.63×10^{-27} erg·s), $2J+1$ is the degeneracy of the initial state (1 for 5D_0). Note that the correction factor for an electric dipole transition in a dielectric medium is different for

emission spectra compared to absorption spectra, where the factor is $\frac{(n^2+2)^2}{9n}$. The reason is that for emission spectra, the transition probability has to be divided by the energy density instead of the energy (or photon flux). This means a division by n^2 rather than n . Moreover, the emission probability is proportional to the density of photon states, i.e. to the cube of the photon momentum, so that the correction factor has to be multiplied by n^3 . The combined effects of these two modifications give a correction factor of $\frac{n(n^2+2)^2}{9}$. For magnetic dipole transitions, the transition is induced by the magnetic field components of the incident light, so that no Lorentz local field correction has to be considered. Therefore the correction factor is only n^3 for MD transitions in emission spectra. For each transition, an $A(\Psi J, \Psi' J')$ value can be calculated. $D_{MD} = 9.6 \times 10^{-6}$ Debye² for the ${}^5D_0 \rightarrow {}^7F_1$ transition ($J = 0, J' = 1$), whereas $D_{MD} = 0$ for all other transitions. D_{ED} is given by the equation:

$$D_{ED} = e^2 \sum_{\lambda=2,4,6} \Omega_{\lambda} |\langle \Psi J || U^{(\lambda)} || \Psi J' \rangle|^2 \quad (20)$$

The elementary charge e is 4.803×10^{-10} esu. In the case of Eu^{3+} , there is no actual summation since the intensity of each ${}^5D_0 \rightarrow {}^7F_{\lambda}$ ($\lambda = 2, 4, 6$) induced electric dipole transition is determined only by a single Ω_{λ} intensity parameter. In this model, $A(\Psi J, \Psi' J') = 0$ for the ${}^5D_0 \rightarrow {}^7F_J$ ($J = 0, 3, 5$) transitions, because D_{ED} and D_{MD} are zero for these transitions.

The $A(\Psi J, \Psi' J')$ values can be used to calculate the radiative branching ratio $\beta_R(\Psi J, \Psi' J')$ from level J to level J' :

$$\beta_R(\Psi J, \Psi' J') = \frac{A(\Psi J, \Psi' J')}{\sum_{\Psi' J'} A(\Psi J, \Psi' J')}$$

(21)

Equation 21 is less useful if the Ω_λ parameters have been extracted from the luminescence spectra, because in that case the relative intensities of the transitions (i.e. the branching ratios) are known and have been used as experimental input for the calculation of the Ω_λ parameters. However, if the Ω_λ parameters have been derived from the absorption spectrum, equation 21 can be used to predict the relative intensities of the transitions in the luminescence spectrum. A very useful application of the Ω_λ parameters is the calculation of the radiative lifetime τ_{rad} of the excited level J , via the calculated radiative transition probabilities (see section 10.1).

9.3. Hypersensitivity

Hypersensitive transitions are one of the most intriguing phenomena in lanthanide spectroscopy. The intensities of most induced electric dipole transitions of lanthanide ions are not much affected by the local environment of the lanthanide ion, and the intensities vary by a factor of not more than two or three. However, a few transitions are very sensitive to the environment of the lanthanide ion. These transitions are called “*hypersensitive transitions*” [263]. Hypersensitive transitions are usually more intense for a complexed lanthanide ion than for the fully hydrated lanthanide ion in water, and the intensity can be enhanced in some cases by a factor of 100 or even more. For example, the intensity of the ${}^5\text{D}_0 \rightarrow {}^7\text{F}_2$ transition of the anionic europium(III) carbonate complex $[\text{Eu}(\text{CO}_3)_4]^{5-}$ is about 100 times more intense than the intensity of this transition for the hydrated Eu^{3+} ion in water [267]. Examples of hypersensitive transitions that are less intense than in aqueous solution are rare. As indicated in section 3.4, hypersensitive transitions obey the selection rules $|\Delta S| = 0$, $|\Delta L| \leq 2$ and $|\Delta J| \leq 2$ [94]. Although these selection rules are the same as those of pure electric quadrupole transition, calculations have revealed that the intensities of hypersensitive transitions are several orders of magnitude larger than those predicted for quadrupole transitions. Jørgensen

and Judd therefore called these transitions *pseudo-quadrupole transitions*, but this term is not often used [263].

Much attention has been paid in the literature to the explanation of the phenomenon of hypersensitivity, but there is still no commonly accepted theory [83,94,127,735]. It is safe to conclude that different factors contribute to the intensity of hypersensitive transitions, and that it is not possible to correlate hypersensitivity with just one experimental parameter, such as the symmetry of the Eu^{3+} site or the polarizability of the ligands. Judd noticed that hypersensitive transitions are associated with large values of the squared reduced matrix element $U^{(2)}$ [125]. Hypersensitivity is described by the Ω_2 parameter, if the $U^{(4)}$ and $U^{(6)}$ squared reduced matrix elements for the hypersensitive transition are small. This is the case for the Eu^{3+} ion. The intensities of the hypersensitive transition ${}^5\text{D}_0 \rightarrow {}^7\text{F}_2$ in the luminescence spectrum and the hypersensitive transition ${}^5\text{D}_2 \leftarrow {}^7\text{F}_0$ in the absorption spectrum are well described by the Ω_2 parameter. The greater sensitivity of Eu^{3+} to the ligand environment in comparison with Nd^{3+} can be understood from the values of the squared reduced matrix elements [736]. The hypersensitive transition ${}^5\text{D}_2 \leftarrow {}^7\text{F}_0$ of Eu^{3+} is proportional to the Ω_2 parameter, whereas the hypersensitive transition ${}^4\text{G}_{5/2}, {}^2\text{G}_{7/2} \leftarrow {}^4\text{I}_{9/2}$ of Nd^{3+} is proportional to all three Ω_λ parameters. Due to the zero value of the squared reduced matrix elements $U^{(4)}$ and $U^{(6)}$ for the ${}^5\text{D}_2 \leftarrow {}^7\text{F}_0$ transition of Eu^{3+} , it is sufficient to double the dipole strength of the Eu^{3+} transition to double the Ω_2 parameter, whereas an increase by a factor five in dipole strength is needed to double the Ω_2 parameter of Nd^{3+} . It should be noticed that two Eu^{3+} systems with the same value for the Ω_2 parameter do not necessarily show the same intensity for the hypersensitive transitions, because also the value of the refractive index n has to be taken into account via the Lorentz local field correction (see equation 15): the higher the refractive index, the more intense the transitions become [737].

As long as the Ω_2 parameter is treated as an adjustable parameter, the Judd-Ofelt theory gives a good agreement between calculated and experimental dipole strengths for hypersensitive transitions. However, the original Judd-Ofelt theory cannot give a theoretical explanation for hypersensitivity [127]. Later, Judd developed a theoretical model that relates hypersensitivity to symmetry [738]. According to Judd, hypersensitivity could only be observed for some point groups: C_s , C_1 , C_2 , C_3 , C_4 , C_6 , C_{2v} , C_{3v} , C_{4v} and C_{6v} . In these point groups, there is a non-vanishing A_{1q} crystal-field parameter and only this linear crystal-field parameter can change the Ω_2 parameter. Although some examples seemed to support this theory, many exceptions were soon found and it became evident that alternative explanations were required.

Jørgensen and Judd suggested that inhomogeneities in the dielectric surrounding the lanthanide ion could enhance the intensity of a hypersensitive transition [263]. According to this theoretical model, the electric field induces oscillating dipole moments in the ligands, which become secondary sources of radiation. Since the ligands are close to the central lanthanide ion, they produce an electric field that is very different to the plane wave that the lanthanide ions would feel in the absence of the dipoles in the medium. Since the dimensions of a lanthanide ion are much smaller than the wavelength of visible or ultraviolet radiation, there is only little spatial variation of the electric field in the neighborhood of the lanthanide ion, if only a homogeneous dielectric is considered. In an *inhomogeneous dielectric* with the asymmetric distribution of oscillating dipoles, the electric field possesses a strong quadrupole component. These quadrupole components are then assumed to induce f-f transitions according to an electric quadrupole transition mechanism. This theory has been criticized by several authors [127]. In a later paper, Judd showed that the model of the inhomogeneous dielectric is formally identical with the dynamic coupling model of Mason and coworkers

(*vide infra*) [661]. Both models give alternative descriptions for the same physical phenomenon.

A *covalency model of hypersensitivity* was developed by Henrie, Fellows and Choppin [83]. The basic idea for that model came from the observation of charge-transfer transitions in lanthanide complexes. The energies and intensities of these charge-transfer transitions are very sensitive to the type of ligand and to the lanthanide ion [518,739]. Henrie *et al.* argued that sensitivity to the ligand environment is intrinsically built in a model for hypersensitivity, if the hypersensitive transitions gain some charge transfer character. The authors modified the Judd-Ofelt theory by including charge-transfer states as perturbing states to be mixed with the $4f^n$ configuration, in addition to the perturbing configurations $4f^{n-1}5d^1$ and $4f^{n-1}5g^1$. They considered charge transfer states which arise from one-electron transfers from the ligand orbitals to the 4f orbitals of the lanthanide ion. The covalency model describing the mixing of charge transfer states into the $4f^n$ configurations provides a theoretical basis for the correlation of the intensity of hypersensitive transitions with the ligand pK_a . The hypersensitive transition ${}^5D_2 \leftarrow {}^7F_0$ of Eu^{3+} is more sensitive to the environment than any other transition of a trivalent lanthanide ion. This is due to the relatively low energy of the charge-transfer transition, combined with the relatively high value of the energy of the hypersensitive transition. The intensity is inversely proportional to the square of the energy difference between the hypersensitive transition and the charge transfer transition [83]. Blasse derived a correlation between the intensity of the hypersensitive transition ${}^5D_0 \rightarrow {}^7F_2$ and the charge-transfer energy: the lower the energy of the lowest charge transfer band, the more intense is the hypersensitive transition [522].

The hypersensitive transitions are not well described by the original Judd-Ofelt theory, since this theory cannot take all the metal-ligand interactions into account. In the classical Judd-Ofelt theory, the lanthanide ion is perturbed by the ligands. The ligands produce a static

potential of odd parity around the lanthanide ion. In this way, 4f states of mixed parity are produced. Transitions between these states can be induced directly by the electric dipole component of the light. Eventually, the ligands can be isotropically polarized by the lanthanide ion. However, it is assumed that the ligands are not influenced by the radiation field of the incident light. Therefore, the Judd-Ofelt theory is also called a *static coupling model*. The perturbing wave functions are localized on the central metal ion. In order to give a more accurate description for the intensity of hypersensitive transition, Mason developed a new theoretical model: the *dynamic coupling model (ligand polarization model)* [740-743]. In this model, dipoles are induced by the charge distribution caused by the f-f transition. Thus, the f electrons polarize the ligands. The ligand wave functions are perturbed by the lanthanide ion. The dynamic coupling mechanism gives a contribution to the Ω_2 parameter if the expansion of the odd part of the crystal field potential contains the terms A_{3q} . These terms are present if the point group contains no center of symmetry. In this case the induced dipoles can combine to a non-vanishing dipole moment. This dipole moment can interact with the radiation field. The point groups in question are C_s , C_n , C_{nv} , C_{3h} , D_n , D_{3h} , D_{2d} , S_4 , T and T_d . Kuroda *et al.* demonstrated that the intensity of the hypersensitive ${}^5D_2 \leftarrow {}^7F_0$ transition of Eu^{3+} in different systems with D_3 symmetry, can be described only adequately if anisotropic ligand polarization is considered [660,744]. They ignored *J*-mixing. The dynamic coupling model predicts the sequence $\Gamma > \text{Br}^- > \text{Cl}^- > \text{H}_2\text{O} > \text{F}^-$ for the intensity of hypersensitive transitions. The sequence is identical to the ligand polarizability order.

Judd has tried in collaboration with Carnall to find general relationships between the Ω_2 parameter and the polarizability α of the ligands [661,745]. The model calculations show that a large value of the Ω_2 parameter can be expected for systems with a triangle as coordination polyhedron (and also for a trigonal bipyramid), but a small value for systems with a tricapped trigonal prism as coordination polyhedron. However, no general expressions

could be derived for other coordination environments, because of the difficulty to describe the various ligand environments parametrically [745]. The prediction of highly intense hypersensitive transitions for europium(III) compounds with a trigonal bipyramid as coordination polyhedron is supported by experimental data. The trigonal bipyramid is not found for europium(III) coordination compounds (because a coordination number of 5 is too low for saturation of the coordination sphere), but the coordination polyhedron of the pentakis(nitrato) europate(III) complex $[\text{Eu}(\text{NO}_3)_5]^{2-}$ can be described as a trigonal bipyramid, by considering that each nitrate ion occupies a corner of a trigonal bipyramid. Since the nitrate ions are bidentate, the coordination number of the $[\text{Eu}(\text{NO}_3)_5]^{2-}$ complex is 10. Interestingly, the luminescence spectrum of $(\text{Ph}_3\text{EtP})_2[\text{Eu}(\text{NO}_3)_5]$ shows indeed a very intense ${}^5\text{D}_0 \rightarrow {}^7\text{F}_2$ transition [746]. Kuroda *et al.* give an explanation on the basis of geometric factor why the hypersensitive transitions of Eu^{3+} are more intense if the coordination polyhedron is a trigonal prism than when it is a tricapped trigonal prism [660].

10. Dynamics of excited states

10.1 Decay processes and lifetimes

After population of an excited state by radiative absorption or via energy transfer, three main processes are active in the relaxation (depopulation) of the excited state: (1) radiative decay, (2) non-radiative decay wherein the excitation energy is converted into vibrational quanta of the surroundings, and (3) non-radiative transfer of energy between like and unlike ions [747]. The lifetime of an excited state τ is a combination of all probabilities for radiative and non-radiative decay. The lifetime of levels which show a strong luminescence can be determined from the observed luminescence decay. The rates of decay by multiphonon relaxation are not directly observable. Their presence and relative importance is determined by comparison of the observed excited state lifetime with the total radiative lifetime, and the

differences are attributed to the occurrence of non-radiative transitions [748]. The radiative lifetime of an excited state can be determined by calculating the total spontaneous emission probability, via the Judd-Ofelt theory or via direct calculation (*vide infra*). The probabilities for non-radiative transitions within a crystal-field multiplet are usually much faster than radiative decay probabilities [541]. The transient behavior thus consists of rapid thermalization of the ion population among the crystal-field levels, followed by decay to the ground state. The transitions within a crystal-field multiplet are quite fast (rate constants $> 10^{10} \text{ s}^{-1}$) [65]. The smaller the energy gap to the next-lower J level, the shorter is the lifetime due to more important non-radiative decay [541]. The non-radiative decay between J multiplets is attributed to phonon emission arising from interactions of the orbital moment of the ions with the fluctuating crystal field caused by lattice vibrations. Often simultaneous emission of several phonons is required to conserve energy in a purely non-radiative transition. Studies on the non-radiative decay of rare-earth ions in LaCl_3 , LaBr_3 , LaF_3 , $\text{Y}_3\text{Ga}_5\text{O}_{12}$, Y_2O_3 and other matrices have illustrated that multiphonon relaxations involving the emission of as many as five phonons can effectively compete with radiative transitions for decay [749,750]. For energy gaps smaller than 1600 cm^{-1} , non-radiative decay becomes so important that luminescence is in general not detected from the upper J level, even not for matrices with low vibrational energies.

The *lifetime* τ is the time after which the population of an excited state has decayed to $1/e$ or 36.8 % of the initial population. Two methods can be used to measure luminescence lifetimes: time-domain and frequency-domain methods [751]. In the time-domain method, the sample is excited with a pulse of light. The width of the pulse is made as short as possible and should be ideally shorter than the lifetime of the excited state. For lifetime measurements on europium(III) compounds, typically a microsecond flash lamp is used. The time-dependent intensity is measured following the excitation pulse:

$$I(t) = I(0)\exp\left(\frac{-t}{\tau}\right) \quad (22)$$

$I(t)$ is the intensity at time t , $I(0)$ is the intensity at time $t = 0$, and τ is the lifetime. The intensity measurement is usually done by *Time Correlated Single Photon Counting* (TCSPC). For ions with a long lifetime such as the Eu^{3+} ion, the part of the measured decay closest to the excitation pulse is excluded from the analysis (“tail fitting”). In the case of single-exponential decay, the lifetime τ can be calculated from the slope of a plot of $\ln I(t)$ versus t . In case that the decay curve is not a single exponential, a numerical fitting procedure can be used. In the measurement of the decay time by the frequency-domain or phase-modulation method, the sample is excited with intensity-modulated light, typically a sine-wave modulation at a high frequency (the reciprocal frequency has to be comparable with the reciprocal of the decay time) [751]. When the luminescent sample is excited in this manner, the emission is forced to respond at the same modulation frequency. The lifetime of the luminophore causes the emission to be delayed in time relative to the excitation. The delay is measured as a phase shift, which can be used to calculate the decay time. Although frequency-domain measurements are often used in fluorescence spectroscopy of organic molecules, only few studies have been devoted to frequency-domain measurements on europium(III) compounds [752-756].

To avoid the necessity of unraveling multi-exponential time dependencies, it is recommended to excite the Eu^{3+} ion directly in the level of interest, whenever possible [757]. The lifetime of excited states from which luminescence is not readily detectable, can be determined by selective excitation of the ions into these levels and then monitoring the

transient luminescence from a lower level [758]. For the simple case where a level 2 decays directly to a luminescence level 1, the luminescence exhibits a maximum at time t_{max} :

$$t_{max} = \frac{\ln(\tau_2/\tau_1)}{\frac{1}{\tau_1} - \frac{1}{\tau_2}} \quad (23)$$

The excitation pulse is assumed to be much shorter than τ_1 and τ_2 . By measuring t_{max} and τ_1 , the lifetime τ_2 can be determined.

Weber made a detailed study of the relaxation processes for the excited states of the Eu^{3+} ion in LaF_3 [305]. $\text{LaF}_3:\text{Eu}^{3+}$ is an interesting model system, because luminescence can be observed from four excited states: $^5\text{D}_0$, $^5\text{D}_1$, $^5\text{D}_2$ and $^5\text{D}_3$. The excited state lifetimes were measured as a function of temperature between 77 K and 700 K, and for Eu^{3+} concentrations between 0.05 and 5 at.%. The excited states exhibit different relaxation properties, due to the level-dependent effects of competing radiative and non-radiative processes. Upon excitation in levels above the $^5\text{D}_3$ level, there is a very fast decay to the $^5\text{D}_3$ level and the $^5\text{D}_3$ level exhibits a simple mono-exponential decay without a rise time. For the decay of the $^5\text{D}_2$ state which was originally unpopulated, a growth in the luminescence intensity to a maximum at t_{max} is observed, followed by an exponential decay. For the progressively lower levels, the initial rate of intensity growth is smaller and t_{max} is shifted to longer times. From the observation that the $^5\text{D}_0/^5\text{D}_1$ luminescence intensity ratio is larger for excitation at 390 nm than for direct excitation in the $^5\text{D}_1$ state, it was concluded that level-bypassing transitions such as $^5\text{D}_2 \rightarrow ^5\text{D}_0$ are active, since a step-by-step decay via the $^5\text{D}_1$ level would result in two equal ratios. A good agreement was found between total calculated lifetimes and the observed lifetimes of the $^5\text{D}_0$ level, but the deviations for the $^5\text{D}_1$ and $^5\text{D}_2$ levels were larger (for a 0.07

% doped sample at 77 K). This indicates that non-radiative processes are not important for 5D_0 , but that they are non-negligible for 5D_1 and 5D_2 . Decay of the 5D_0 level by multiphonon emission in a fluoride matrix is improbable due to the large energy gap between the 5D_0 and 7F_6 levels (about 12000 cm^{-1}). Too many phonons are required to conserve energy. It was observed that an increase in temperature or Eu^{3+} concentration resulted in an increase in luminescence intensity from the lower 5D_J levels. Thus, the decay to lower 5D_J levels becomes increasingly important compared to spontaneous emission to the 7F_J levels. It was also observed that the lifetimes of the 5D_0 and 5D_1 do not depend on the Eu^{3+} concentration (except for very high concentrations), but that the 5D_2 and 5D_3 lifetimes show a strong concentration dependence. This is an indication that energy transfer between different Eu^{3+} ions occurs. For instance, the excitation energy can be transferred from an excited Eu^{3+} ion A to a non-excited Eu^{3+} ion B by pair transitions. For instance, the 5D_2 level of Eu^{3+} ion A can non-radiatively relax to the 7F level via the ${}^5D_2 \rightarrow {}^7F_4$ transition, and the transferred excitation energy is used to excite Eu^{3+} ion to the 5D_1 level via the ${}^5D_1 \leftarrow {}^7F_1$ transition. In a similar way, the 5D_3 level can relax via the pair transitions ${}^5D_3 \rightarrow {}^7F_4$ and ${}^5D_2 \leftarrow {}^7F_{0,1}$ at low temperatures (77 K). Quenching via pair transitions is also called *cross-relaxation*. At higher temperatures, the 5D_3 level can also relax via the pair transitions ${}^5D_3 \rightarrow {}^7F_5$ and ${}^5D_2 \leftarrow {}^7F_2$. The observed lifetimes of the 5D_1 and 5D_0 states are concentration-independent, because the necessary pair transitions are restricted by the selection rules. For $\text{Y}_2\text{O}_3:\text{Eu}^{3+}$, the observed lifetime of the 5D_0 level does not show a variation with the Eu^{3+} concentration, but the observed lifetimes of the 5D_0 and 5D_1 states become much shorter in heavily doped samples [749]. The observed luminescence lifetime of 5D_0 is temperature-independent, since multiphonon relaxation is not important for this level, as mentioned above. On the other hand, the observed lifetime of the 5D_1 state is strongly temperature-dependent, due to multiphonon relaxation. It must be noticed that ${}^5D_1 \rightarrow {}^5D_0$ relaxation is a second order effect and can only arise by admixing of 5D_2 into

5D_1 and 5D_0 states. A study of the temperature-dependence of the observed lifetime of the 5D_3 level in $YAlO_3$ indicated that not only the high-energy phonons have an influence on the multiphonon relaxation, but that lower-energy phonons contribute as well [758]. In $KY_3F_{10}:Eu^{3+}$, the lifetime of the 5D_0 state is temperature-independent, while that of the 5D_1 shows a strong temperature dependence [313,759]. The concentration quenching of the 5D_2 state is more pronounced in $Cs_2NaYF_6:Eu^{3+}$ than in $Cs_2NaYCl_6:Eu^{3+}$ [204]. In this matrix, ion-ion interactions have an influence on the lifetime of the 5D_0 state only for doping concentrations higher than 1 % [313]. The observed lifetimes of the 5D_0 excited state of Eu^{3+} are in the milliseconds range [148]. For simple inorganic host systems, the values range from 0.25 ms in YVO_4 [522] to 14.6 ms in $BaF_2:Eu^{3+}$ [590]. An unusually long observed lifetime for the 5D_0 excited state of 10.29 ms at 12 K has been reported for the microporous silicate $K_7[Eu_3Si_{12}O_{32}] \cdot xH_2O$ [760]. Low-lying charge-transfer states can have a dramatic influence on the observed lifetime of the 5D_0 state [526]. The observed lifetimes for the isostructural compounds $LiGdF_4:Eu^{3+}$ and $GdNbO_4:Eu^{3+}$ are 7.3 ms and 0.65 ms, respectively. The charge-transfer state is at a much higher energy for the fluoride host than for the niobate host. The following lifetimes have been measured at room temperature for a $Y_2O_2S:Eu^{3+}$ sample doped with 500 ppm of Eu^{3+} : 0.440 ms for 5D_0 , 0.165 ms for 5D_1 , 0.140 ms for 5D_2 and 0.145 ms for 5D_3 [761]. The lifetime of $Eu(ClO_4)_3$ dissolved in water shows hardly any variation as a function of the concentrations of Eu^{3+} and ClO_4^- : the values are ranging between 102 and 110 μs [257].

The rate of relaxation of an excited state J is governed by the combination of the probabilities for radiative (A) and non-radiative processes (W). The observed luminescence lifetime τ_{obs} of an excited state J is given by:

$$\frac{1}{\tau_{obs}} = \sum_{J'} A(\Psi_J, \Psi_{J'}) + \sum_{J'} W(\Psi_J, \Psi_{J'}) \quad (24)$$

where the summations are for transitions terminating on all final states J' . The radiative probability A includes both purely electronic and phonon-assisted (vibronic) transitions. The non-radiative probability W includes relaxation by multiphonon emission and effective energy transfer rates arising from ion-ion interactions. The radiative lifetime τ_{rad} of an excited level J is the luminescence lifetimes in the absence of non-radiative processes:

$$\frac{1}{\tau_{rad}} = \sum_{\Psi_{J'}} A(\Psi_J, \Psi_{J'}) \quad (25)$$

It can also be considered as the reciprocal of the first-order rate constant for the radiative process ($\tau_{rad} = k_r^{-1}$). τ_{rad} is sometimes called the *natural lifetime*, but this term is not recommended by the IUPAC. The radiative lifetime is not a constant for a given lanthanide ion. First, different radiative lifetimes can be defined for a lanthanide ion, one for each emitting level. In the case of Eu^{3+} most of the reported radiative lifetimes are those of the ${}^5\text{D}_0$ level, but it is also possible to define radiative lifetimes for the higher excited levels, e.g. ${}^5\text{D}_1$ and ${}^5\text{D}_2$. Secondly, the radiative lifetime also depends on the refractive index of the medium (see equation 19). Therefore, the radiative lifetime can be tuned by variation of ligands, solvents or composition of the inorganic host. The assumption that the radiative lifetime becomes equal to the observed luminescence lifetime at cryogenic temperatures (77 K or lower) is unlikely to be valid [89]. There is no evidence that no non-radiative processes occur under these experimental conditions.

In general, τ_{rad} is determined using equation (19) in section 9.2, in combination with equation (25). In the case of Eu^{3+} , the Judd-Ofelt intensity parameters Ω_λ are not needed to calculate τ_{rad} , if a corrected luminescence spectrum is known [157]. The corrected spectrum should represent the relative spectral photon flow versus wavelength. Such a corrected spectrum can be obtained with a spectrofluorimeter operating in photon counting mode after correction for the wavelength dependence of the detection sensitivity. If one assumes that the dipole strength of the ${}^5\text{D}_0 \rightarrow {}^7\text{F}_1$ magnetic dipole transition is a constant, the radiative lifetime τ_{rad} can be calculated using the following formula:

$$\frac{1}{\tau_{rad}} = A_{MD,0} n^3 \left(\frac{I_{tot}}{I_{MD}} \right) \quad (26)$$

Here n is the refractive index of the medium, $A_{MD,0}$ is the spontaneous emission probability for the ${}^5\text{D}_0 \rightarrow {}^7\text{F}_1$ magnetic dipole transition *in vacuo* and I_{tot}/I_{MD} is the ratio of the total integrated area of the corrected Eu^{3+} emission spectrum to the area of the ${}^5\text{D}_0 \rightarrow {}^7\text{F}_1$ band. $A_{MD,0}$ is 14.65 s^{-1} [157]. To correctly apply equation (26), all the transitions of the ${}^5\text{D}_0$ excited state to the ${}^7\text{F}_J$ ($J = 0-6$) levels have to be considered. If the transitions to the ${}^7\text{F}_5$ and ${}^7\text{F}_6$ levels are not included in the integration, an error of a few % will be made. One should not neglect the influence of the refractive index. The radiative lifetime of a complex in aqueous solution ($n = 1.33$) is about 30% longer than in the solid state ($n \approx 1.55$) [71]. For instance for the europium(III) tris dipicolinate complex $\text{Cs}_3[\text{Eu}(\text{dpa})_3]$, $\tau_{rad} = 4.1 \text{ ms}$ in aqueous solution, and $\tau_{rad} = 2.6 \text{ ms}$ in the solid state [762].

The *quantum yield* Φ is the ratio of the number of emitted photons to the number of absorbed photons. The *intrinsic quantum yield* Φ_{Ln}^{Ln} is the quantum yield observed for direct

excitation in the 4f levels of the lanthanide ion. The *overall quantum yield* Φ_{Ln}^L is determined after excitation into the absorbing bands of the ligands. The relationship between Φ_{Ln}^{Ln} and Φ_{Ln}^L is:

$$\Phi_{Ln}^L = \eta_{sens} \Phi_{Ln}^{Ln} = \eta_{sens} \frac{\tau_{obs}}{\tau_{rad}} \quad (27)$$

η_{sens} is the sensitization efficiency. There exists an inverse relationship between Φ_{Ln}^L and τ_{rad} : the shorter τ_{rad} , the larger will be Φ_{Ln}^L [763]. Thus, the shorter the radiative lifetime, the more emissive the europium(III) complex will be in a given coordination environment and medium. One way of shortening τ_{rad} is by placing the europium(III) complex in the vicinity of metallic surfaces or in contact with metallic nanoparticles [764-767]. Most often silver is used. On the other hand, silver nanoparticles distributed within a europium(III)-doped glass does not have an influence on the observed luminescence lifetime of the 5D_0 state [768]. Another way of reducing τ_{rad} is by perturbing the 4f levels by strong *J*-mixing, by strong vibrational coupling or by mixing of charge-transfer states into the 4f levels. $\Phi_{Ln}^L \leq \Phi_{Ln}^{Ln}$ so that the quantum yield cannot be increased by the process of sensitized luminescence. Since the luminescence intensity is the product of the absorption coefficient at the excitation wavelength and the quantum yield, a stronger light absorption by the chromophore (antenna) will lead to a more intense luminescence. The absorption coefficients of the chromophores can be more than three orders of magnitude larger than those of the f-f transitions of the lanthanide ion.

If the radiative lifetime is known, Φ_{Ln}^{Ln} can be calculated from the observed luminescence lifetime:

$$\Phi_{Ln}^{Ln} = \frac{\tau_{obs}}{\tau_{rad}} \quad (28)$$

On the other hand, knowledge of τ_{obs} and τ_{rad} allows determination of the probabilities for non-radiative relaxations. The overall quantum yield Φ_{Ln}^L can be experimentally measured via an absolute method using an integrating sphere [762], but most researchers prefer a relative method. In the relative method, the quantum yield of the unknown is compared with that of a reference sample (standard compound):

$$\Phi_X = \left(\frac{A_R}{A_X} \right) \left(\frac{E_X}{E_R} \right) \left(\frac{n_X}{n_R} \right)^2 \Phi_R \quad (29)$$

where Φ is the luminescence quantum yield, A is the absorbance at the excitation wavenumber, E is the area under the corrected emission curve (expressed in number of photons), and n is the refractive index of the solvents used. The subscripts R and X refer to the reference and the unknown, respectively. The ideal absorbance values for luminescence measurements lie between 0.04 and 0.05. When the absorbance is above 0.05, the emission intensity can no longer be assumed proportional to the concentration of the analyte (no linear relationship between the emission intensity and the concentration). Only when the sample and the reference have the same absorbance at the excitation wavelength, and absorbance up to 0.5 can be tolerated [769]. When the absorbance is too low, the impurities from the medium may become important with respect to the amount of analyte. Moreover, at low concentrations the dissociation of the complex in solution can be a problem, especially when the formation constants are not very high. It is advisable to use the same excitation wavelength for measuring the luminescence of the standard and the unknown. One should not choose the

excitation wavelength on the edge of an excitation band, because upon excitation on the edge, a slight change in wavelength will induce a large change in the amount of light absorbed.

When the same solvent is used for both the reference and the unknown, the factor $(n_X/n_R)^2$ will be equal to unity. For integration of the emission spectra, the spectra have to be expressed as a function of the wavenumber (cm^{-1}) and not as a function of the wavelength. Of course, the luminescence quantum yield has to be determined by using corrected emission spectra.

Finding a suitable reference (standard) is often a serious problem. The reference compound has to emit in the same spectral region as the lanthanide ion of interest. Most of the fluorescence standards are organic compounds that show broad-band emission, whereas the lanthanide ions exhibit line-like emission. For determination of the luminescence quantum yield of europium(III) complexes, cresyl violet ($\Phi = 54\%$ in methanol) or rhodamine 101 ($\Phi = 100\%$ in ethanol) can be used as standards [770]. Bünzli and coworkers proposed the use of the europium(III) tris(dipicolinate) complexes as secondary standards for luminescence quantum yield determination [762,769].

For solid samples, standard phosphors can be used [771,772]. A commercial phosphor that can be used as standard for luminescence quantum yields is $\text{Y}_2\text{O}_3:\text{Eu}^{3+}$ (3 %) (YOX-U719 Philips, $\Phi = 99\%$) [773]. The relevant expression is:

$$\Phi_X = \left(\frac{1 - R_R}{1 - R_X} \right) \left(\frac{\phi_X}{\phi_R} \right) \Phi_R, \quad (30)$$

where R is the amount of reflected excitation radiation and ϕ is the integrated photon flux (photons s^{-1}). It is also possible to determine the absolute quantum yield measurement of the heat dissipation by non-radiative deactivation. Gudmundsen and coworkers determined the absolute quantum efficiency of the europium(III) 2-thenoyltrifluoroacetate complex

[Eu(tta)₃] in acetone by a calorimetric method [774]. By this technique the temperature rise of the samples due to non-radiative deactivation is measured. The quantum efficiency in acetone at 25 °C was determined as 0.56±0.08. Only the ⁵D₀ → ⁷F₂ transition was considered, because the authors argue that this transition accounts for more than 95 % of the total emission of the complex. Yang *et al.* measured the non-radiative deactivation of europium(III) complexes by a photoacoustic method [775].

It is possible to separate the luminescence spectra of different europium(III) complexes present in solution by means of *time-gated spectroscopy*. Time-gated measurements are performed by using a pulsed excitation source (pulsed laser or a microsecond flash lamp). The recording of the luminescence decay curve is started after a selected delay time. If the time delay between the laser pulse and the start of recording the luminescence decay curve is short, the emission of both the slowly and fast decaying species is observed. By gradually increasing the delay time, the emission of the slowly decaying species becomes more prominent. Finally, the emission of the fast decaying species is eliminated and only the emission of the slowly decaying species remains. Time-gated spectroscopy is also useful to measure europium(III) spectra in biological samples, because the technique allows exclusion of the background fluorescence of the biological material [776-782]. Time-resolved detection of europium(III) forms the basis of several biomedical analyses and bioanalytical assays [33,93,783-786]. In section 3.8, it is described how time-gated spectroscopy of europium(III) samples can be used to discriminate between transitions starting from the ⁵D₀ excited state and those starting from the ⁵D₁ state.

Monitoring of the luminescence lifetime as a function of temperature has been used to detect phase transitions in europium(III)-containing liquid crystals [787]. Bünzli and coworkers measured the luminescence intensity and the excited state lifetime of a solvated Eu(NO₃)₃ complex of a 1,7-diaza-18-crown ether with mesogenic pendant arms as a function

of the temperature, with the aim to detect phase transitions [788,789]. The integrated intensities of the ${}^5D_0 \rightarrow {}^7F_2$ transition I_{obs} and the observed lifetime τ_{obs} of the 5D_0 state decrease with increasing temperatures due to more efficient non-radiative relaxation of the excited state at higher temperatures. The $\ln(\tau_{\text{obs}}/\tau_{295\text{K}})$ versus $1/T$ and $\ln(I_{\text{obs}}/I_{295\text{K}})$ versus $1/T$ curves showed upon heating a sigmoidal shape, with a marked variation at the melting point. Therefore, the luminescence measurements allowed to accurately detect the transition of the crystalline state to the hexagonal columnar phase during the first heating process. The corresponding $\ln(I_{\text{obs}}/I_{295\text{K}})$ versus $1/T$ cooling curve was quite monotonic, whereas the $\ln(\tau_{\text{obs}}/\tau_{295\text{K}})$ versus $1/T$ cooling curve closely followed the variation observed during heating. Yang *et al.* were able to detect the transition from a smectic A mesophase to the isotropic liquid by measuring the luminescence lifetimes as a function of temperature for a liquid-crystalline Lewis-base adducts of a non-mesomorphic salicylaldimine Schiff's base ligand to tris(2-thenoyltrifluoroacetato)europium(III) or tris(benzoyltrifluoroacetate) europium(III) complexes [790]. These studies showed that the monitoring of the luminescence lifetimes is superior compared to monitoring of the luminescence intensity as a function of the temperature.

Monitoring of the luminescence lifetime of the 5D_0 level as a function of pressure has been used to detected pressure-induced phase transitions, and it is a useful method in cases where the phase transition is not accompanied by a change in the crystal-field fine structure of the luminescence spectrum. Moreover, changes in the fine structure in the luminescence spectra reflect small changes in the first coordination sphere of the Eu^{3+} , whereas changes in luminescence lifetime depend on the entire crystal lattice symmetry. The pressure dependence of the luminescence lifetime of 5D_0 in $\text{YVO}_4:\text{Eu}^{3+}$ was measured up to 11 GPa [791]. Two different lifetime-pressure relationships were observed: one up to 6.2 GPa and one from 6.2 GPa up to 11 GPa. An abrupt decrease of the luminescence lifetime by a factor of about 1/3 at

6.2 GPa suggested the presence of pressure-induced phase change, from a zircon-type to a scheelite-type of structure. The luminescence lifetime increased with pressure in both crystalline phases and the change in lifetime per unit change in pressure are the same in both phases. The differences in lifetime are attributed to differences in interatomic distances. A study of the luminescence lifetime of $\text{La}_2\text{O}_2\text{S}:\text{Eu}^{3+}$ and $\text{Y}_2\text{O}_2\text{S}:\text{Eu}^{3+}$ as a function of pressure indicated that no significant new radiationless paths appear at high pressure [792]. In fluorophosphate glasses, the luminescence lifetime of the $^5\text{D}_0$ level decreases as a function of pressure [793]. The shortening of lifetime with increasing pressure as explained by the gradual increase in energy transfer processes, between the Eu^{3+} ions and pressure-induced defect centres. Similar decreases in luminescence lifetimes with increasing pressures have been observed for other types of europium-doped glasses [794,795].

10.2 Determination of hydration numbers

A useful application of measurement of the lifetime of the $^5\text{D}_0$ level of Eu^{3+} is the determination of the number of water molecules coordinated to the Eu^{3+} ion (number of water molecules in the first coordination sphere). This number is also known as the *hydration number* q . Knowledge of the hydration number is of important for the development of efficient MRI contrast agents, because only water molecules coordinated to the paramagnetic metal center are efficiently relaxed. MRI contrast agents contain a Gd^{3+} ion as the active center. However, the coordination chemistry of europium(III) is very similar to that of gadolinium(III), so that it can be assumed that the hydration numbers of these two ions are identical. The hydration number gives also information on the composition of europium(III) complexes in aqueous solutions. The method for the determination of the number of coordination water molecules is based on observations that the OH oscillators (vibrations) of coordinated H_2O molecules can efficiently non-radiatively depopulate the $^5\text{D}_0$ excited state of

Eu^{3+} , whereas the OD oscillators of coordinated D_2O molecules are much less efficient for non-radiative relaxation of the $^5\text{D}_0$ level [796-801]. The increase in the observed lifetime of the $^5\text{D}_0$ state of Eu^{3+} in heavy water compared to the lifetime in water was first reported by Kropp and Windsor [797,799]. These authors observed an increase in lifetime by a factor of 19.7 by deuteration. They also found that the increase is less pronounced in the case of EDTA complexes in water than in the case of the fully hydrated Eu^{3+} ion [799]. Later studies by Gallagher reported an even stronger increase in the observed luminescence lifetime: the observed lifetime of the $^5\text{D}_0$ state of the hydrated Eu^{3+} ion (0.4 M EuCl_3 solution) is 0.12 ms in H_2O and 3.9 ms in D_2O [802]. Replacement of H atoms in complexes by D atoms is a method to increase the luminescence quantum yield of europium(III) complexes [803-807]. There is an inverse relationship between the efficiency of vibrational quenching of the emissive excited state of the lanthanide ion and the energy gap between the emissive level and the next lower level (*energy gap law*) [808,809]. The smaller the harmonic number of vibrational quanta that is required to match the energy gap between the lowest emitting level and the next lower level of the lanthanide ion, the more effective the vibronic quenching will be. The energy of the fundamental OH vibration is 3450 cm^{-1} and that of the OD vibration is 2500 cm^{-1} . The energy gap between the $^5\text{D}_0$ emitting level and the highest level of the ^7F ground term ($^7\text{F}_6$) is about 12300 cm^{-1} . Therefore, the $^5\text{D}_0$ excited state is non-radiatively deactivated by energy transfer to the 3rd or 4th overtone of the OH vibration. If the O-H oscillator is replaced by an O-D oscillator, the energy of the $^5\text{D}_0$ level must be transferred to the 5th overtone of the OD vibration, and this process is much less efficient than transfer to the 3rd or 4th overtone [808].

Horrocks and Sudnick derived an empirical formula by measuring the luminescence decay rates of a series of crystalline europium(III) complexes, separately synthesized in H_2O and D_2O , and for which the number of coordinated water molecules was known from single

crystal X-ray diffraction studies [98,810]. The linear plot of the differences of the reciprocals of the observed lifetimes in ms^{-1} (exponential decay rate constants), measured for the complexes with coordinated H_2O and D_2O molecules, is given by the formula (*Horrocks–Sudnick formula*):

$$q = 1.05 \left[\frac{1}{\tau_{\text{H}_2\text{O}}} - \frac{1}{\tau_{\text{D}_2\text{O}}} \right] \quad (31)$$

The estimated error on the resulting q value was ± 0.5 water molecules. The Horrocks–Sudnick equation has proven to be very useful for the determination of the q values of europium(III) complexes in solution, but sometimes inconsistencies were found. The equation frequently yields non-integer q values and these are most often greater than the expected integer value. In other cases, the q values were different from those determined via other experimental methods. Several reasons have been given for these issues [811]. A first reason is that a given europium(III) complex can form different hydrated forms in solution. If the exchange of water molecules is fast compared to the decay of the ${}^5\text{D}_0$ state, the calculated q values will be a concentration-averaged value for the different europium(III) complexes in solution. A second reason is that not only water molecules but also other ligands containing X-H oscillators can shorten the observed lifetime of the ${}^5\text{D}_0$ state of Eu^{3+} . O-H oscillators in alcohols and N-H oscillators in amines with the O or N atom directly coordinated to the Eu^{3+} ion can significantly shorten the lifetime of the ${}^5\text{D}_0$ excited states. N-H oscillators of amide groups with the carboxylate oxygen atom coordinated to the Eu^{3+} ion can shorten the lifetime of the ${}^5\text{D}_0$ state to a small extent. A third reason for non-integral and larger than expected q values is that water molecules in the second coordination sphere can also to some degree shorten the lifetime of the ${}^5\text{D}_0$ excited state. To take into account the effect of X-H oscillators and water molecules in the second coordination sphere, Supkowski and Horrocks modified

the original Horrock–Sudnick equation. The general form of the *Supkowski–Horrocks formula* is:

$$q = 1.11 \left[\frac{1}{\tau_{\text{H}_2\text{O}}} - \frac{1}{\tau_{\text{D}_2\text{O}}} - \alpha - \beta n_{\text{OH}} - \gamma n_{\text{NH}} - \delta n_{\text{C=ONH}} \right] \quad (32)$$

where α describes the quenching of the $^5\text{D}_0$ excited state of Eu^{3+} by water molecules in the second coordination sphere, n_{OH} is the number of alcoholic O-H oscillators in the first coordination sphere of Eu^{3+} , n_{NH} is the number of amine N-H oscillators in the first coordination sphere of Eu^{3+} and $n_{\text{C=ONH}}$ is the number of amide N-H oscillators in which the amide carboxylic oxygen is coordinated to the Eu^{3+} ion. The respective contributions of these X-H oscillators to the deexcitation of the $^5\text{D}_0$ state are: $\beta = 0.45 \text{ ms}^{-1}$, $\gamma = 0.99 \text{ ms}^{-1}$ and $\delta = 0.075 \text{ ms}^{-1}$. One should notice that in the abstract of the Supkowski-Horrocks paper equation (32) is wrongly written as $q = 1.11[\tau_{\text{H}_2\text{O}}^{-1} - \tau_{\text{D}_2\text{O}}^{-1} - 0.31 + 0.45n_{\text{OH}} + 0.99n_{\text{NH}} + 0.075n_{\text{C=ONH}}]$, with plus signs for the OH, NH and C=ONH correction terms. This might cause confusion. Supkowski and Horrocks composed a simplified form of equation (32) by considering the literature lifetime value of 25 europium(III) complexes in solution:

$$q = 1.11 \left[\frac{1}{\tau_{\text{H}_2\text{O}}} - \frac{1}{\tau_{\text{D}_2\text{O}}} - 0.31 \right] \quad (33)$$

The estimated error on the resulting q value for this modified equation is ± 0.1 water molecules. The calculated q values can be correctly applied to europium(III) complexes that exist in one single form in solution. If X-H oscillators other than O-H are explicitly taken into account, equation 33 becomes:

$$q = 1.11 \left[\frac{1}{\tau_{\text{H}_2\text{O}}} - \frac{1}{\tau_{\text{D}_2\text{O}}} - 0.31 - 0.45n_{\text{OH}} - 0.99n_{\text{NH}} - 0.075n_{\text{C=ONH}} \right] \quad (34)$$

It is important to wait for a sufficiently long time before measuring the lifetimes in D₂O so that H/D exchange can take place between the X-H oscillators and D₂O.

Besides the equations for the q values presented above, several other equations have been proposed. For instance, Parker and coworkers proposed the following formula for the q value of europium(III) complexes of cyclen derivatives [812]:

$$q = 1.20 \left[\frac{1}{\tau_{\text{H}_2\text{O}}} - \frac{1}{\tau_{\text{D}_2\text{O}}} - 0.25 \right] \quad (35)$$

This formula is only reliable for low hydration numbers. The factor -0.25 corrects for contributions from outer sphere water molecules. Barthelemy and Choppin developed a formula that can be used to determine the q value, using only the lifetime of the ⁵D₀ state in water [813]:

$$q = 1.05 \times \frac{1}{\tau_{\text{H}_2\text{O}}} - 0.70 \quad (36)$$

The authors claim that this equation gives q values with the same experimental uncertainty as the values determined using the Horrocks-Sudnick formula (equation 31) [82].

Crystalline Na₃[Eu(ODA)₃]·2NaClO₄·6H₂O has been used as a model compound for the investigation of the effect of water molecules in the second coordination sphere on the non-radiative deactivation of the ⁵D₀ excited state [814]. In this compound, europium(III) is coordinated by three oxydiacetate molecules and there are no water molecules in the first coordination sphere. Water molecules are present only in the second coordination sphere.

Many authors have made use of the methods based on lifetime measurements for determination of the hydration number of Eu^{3+} ions. Typical studies are found in references [815-822]. A very nice study of the use of lifetime measurements for the determination of the hydration numbers is the work by May and coworkers on the hydration of the Eu^{3+} in binary mixtures of water and the ionic liquid 1-butyl-3-methylimidazolium chloride $[\text{C}_4\text{mim}]\text{Cl}$ [823]. With increasing water contents, the following four Eu^{3+} species were detected at 338 K: $[\text{EuCl}_x]_{3-x}$, $[\text{EuCl}_y(\text{H}_2\text{O})_{3-4}]_{3-y}$, $[\text{EuCl}_z(\text{H}_2\text{O})_6]_{3-z}$, and $[\text{Eu}(\text{H}_2\text{O})_{8,9}]^{3+}$ (where $x > y > z$). An interesting observation was that very little coordination of water molecules to the Eu^{3+} ion occurs at water-to- $[\text{C}_4\text{mim}]\text{Cl}$ molar ratios smaller than 1. This suggests that each mole of $[\text{C}_4\text{mim}]\text{Cl}$ can efficiently sequester 1 mole of water molecules, making them inaccessible for coordination to the Eu^{3+} ion. Above the water-to- $[\text{C}_4\text{mim}]\text{Cl}$ molar ratio of 1:1, the number of coordinated water molecules increased rapidly to 8 and then asymptotically approaches a value of about 9. The same research group has investigated the binding of water molecules to Eu^{3+} for $\text{Eu}(\text{Tf}_2\text{N})_3$ dissolved in the ionic liquid 1-butyl-1-methylpyrrolidinium bis(trifluoromethylsulfonyl)imide $[\text{bmpyr}][\text{Tf}_2\text{N}]$ [824]. In contrast to EuCl_3 in $[\text{C}_4\text{mim}]\text{Cl}$, $\text{Eu}(\text{Tf}_2\text{N})_3$ quantitatively binds added water molecules in $[\text{bmpyr}][\text{Tf}_2\text{N}]$. The weakly coordinating Tf_2N^- anion cannot compete with water for coordination to the Eu^{3+} ion, even not in the presence of just traces of water. It should be noted that in the case of these studies of hydration of Eu^{3+} ions in ionic liquids, the classic Horrocks-Sudnick formula (equation 31) has been used and not the modified Supkowski-Horrocks formula (equation 32), because the latter formula includes contributions to quenching from 'bulk' water outside the primary coordination sphere and is not appropriate for hydrated ionic liquids.

An alternative method for the determination of the hydration number of a lanthanide ion is by measuring the lanthanide-induced shift in the ^{17}O NMR spectrum of water [825-827]. Mainly the Dy^{3+} ion is used for these studies. The results by the luminescence method with

Eu³⁺ and the ¹⁷O NMR method should be comparable, provided that no change in the hydration number occurs across the lanthanide series between Eu³⁺ and Dy³⁺.

Luminescence lifetime measurements of [Eu(EDTA)]⁻ can be used to determine the mole fraction of H₂O in D₂O, with an accuracy of ±0.02 [828]:

$$\chi = \frac{0.37}{\tau} - 0.152 \quad (37)$$

Where χ is the mole fraction of H₂O in D₂O, and τ is the lifetime of the ⁵D₀ excited state (in ms).

11. Concluding remarks

Europium(III) compounds find widespread applications in lamp phosphors, luminescent markers and in biomedical analyses. In this sense, europium is not a unique lanthanide, since also terbium is used for the same applications. The spectroscopic properties of other lanthanide ions are valorized in technological applications, e.g. lasers. The Nd:YAG laser is a good example of such an application. However, the Eu³⁺ ion is truly unique as a spectroscopic probe, thanks to its very special electronic configuration. The ground state (⁷F₀) and the most important emitting excited state (⁵D₀) are non-degenerate and thus not split by crystal-field effects. The most important transitions in the luminescence spectra are from the ⁵D₀ excited state to the ⁷F_J levels with low *J* values (*J* = 0, 1, 2) and thus with a limited number of crystal-field levels. The same can be said for the absorption spectra, where the transitions are from the ⁷F₀ ground state to ⁵D_J levels (*J* = 0, 1, 2). The free-ion levels do not overlap and their wave functions can be described well within the Russell-Saunders coupling scheme. *J*-mixing is limited, so that there are not many violations of the selection rules. The Eu³⁺ ion shows only weak vibronic transitions if the Eu³⁺ ion is not at a centrosymmetric site. It is also convenient

that the luminescence is in the visible spectral region (red emission). All these factors make the interpretation of europium(III) spectra much easier compared to that of spectra of other lanthanide(III) ions. By applying the rules of group theory, it is possible to predict the number of crystal-field transitions that can be expected for the absorption and emission spectra of europium(III) compounds. By counting the number of observed crystal-field transitions, the point group symmetry of the Eu^{3+} site can be derived. The transition between the $^5\text{D}_0$ and $^7\text{F}_0$ state give information on the number of non-equivalent Eu^{3+} sites or on the number of europium(III) complexes that are present in solution. The hypersensitive transitions reflect even very small distortions in the coordination sphere. The Eu^{3+} ion is a probe for the local symmetry of the lanthanide ion. Therefore, high-resolution spectroscopic studies complement X-ray crystallographic studies on single crystals. Not only the fine structure in the spectra (fingerprinting), but also the observed lifetime of the $^5\text{D}_0$ excited states contains valuable information. The best example is the determination of the hydration number of the Eu^{3+} in solution or in hydrated crystals by the Horrocks-Sudnick or a similar formula.

This review paper tried to give a realistic overview of the information content that is available in the luminescence, excitation and absorption spectra of europium(III) compounds. The different transitions have been discussed in a systematic way. Europium(III) compounds with special spectroscopic properties have been highlighted. It has been discussed how the Judd-Ofelt theory can be applied to europium(III) spectra and how the intensity parameters are derived. Luminescence lifetimes give insight into the efficiency of conversion of the excitation energy into light. The reader is advised to find a good balance between extracting the correct information from europium(III) spectra and avoiding the pitfall of over-interpretation of the spectra. The Eu^{3+} ion as a spectroscopic probe does not stand on its own. Measurement of spectra of europium(III) compounds has to be complemented by the use of

other experimental techniques, which provide complementary information. Only in this way, a correct description of lanthanide-containing system can be achieved.

Acknowledgments

The author thank the KU Leuven for financial support (projects GOA/13/008 and IOF-KP RARE³).

References

- [1] S. Petoud, S. M. Cohen, J.-C. G. Bünzli, and K. N. Raymond, *J. Am. Chem. Soc.*, 125 (2003) 13324-13325.
- [2] S. Lis, *J. Alloys Compd.*, 341 (2002) 45-50.
- [3] K. Lunstroot, K. Driesen, P. Nockemann, L. Viau, P. H. Mutin, A. Vioux, and K. Binnemans, *Phys. Chem. Chem. Phys.*, 12 (2010) 1879-1885.
- [4] P. Lenaerts, K. Driesen, R. Van Deun, and K. Binnemans, *Chem. Mater.*, 17 (2005) 2148-2154.
- [5] L. R. Matthews and E. T. Knobbe, *Chem. Mater.*, 5 (1993) 1697-1700.
- [6] W. Strek, J. Sokolnicki, J. Legendziewicz, K. Maruszewski, R. Reisfeld, and T. Pavich, *Opt. Mater.*, 13 (1999) 41-48.
- [7] K. Binnemans, P. Lenaerts, K. Driesen, and C. Görller-Walrand, *J. Mater. Chem.*, 14 (2004) 191-195.
- [8] P. Lenaerts, A. Storms, J. Mullens, J. D'Haen, C. Görller-Walrand, K. Binnemans, and K. Driesen, *Chem. Mater.*, 17 (2005) 5194-5201.
- [9] P. Lenaerts, E. Ryckebosch, K. Driesen, R. Van Deun, P. Nockemann, C. Görller-Walrand, and K. Binnemans, *J. Lumin.*, 114 (2005) 77-84.
- [10] A. C. Franville, D. Zambon, R. Mahiou, and Y. Troin, *Chem. Mater.*, 12 (2000) 428-435.
- [11] H. R. Li, J. Lin, H. J. Zhang, L. S. Fu, Q. G. Meng, and S. B. Wang, *Chem. Mater.*, 14 (2002) 3651-3655.
- [12] K. Lunstroot, K. Driesen, P. Nockemann, C. Görller-Walrand, K. Binnemans, S. Bellayer, J. Le Bideau, and A. Vioux, *Chem. Mater.*, 18 (2006) 5711-5715.
- [13] K. Lunstroot, K. Driesen, P. Nockemann, K. Van Hecke, L. Van Meervelt, C. Görller-Walrand, K. Binnemans, S. Bellayer, L. Viau, J. Le Bideau, and A. Vioux, *Dalton Trans.*, (2009) 298-306.
- [14] K. Binnemans and C. Görller-Walrand, *Chem. Rev.*, 102 (2002) 2303-2345.
- [15] K. Binnemans and D. Moors, *J. Mater. Chem.*, 12 (2002) 3374-3376.
- [16] K. Driesen, C. Vaes, T. Cardinaels, K. Goossens, C. Görller-Walrand, and K. Binnemans, *J. Phys. Chem. B*, 113 (2009) 10575-10579.
- [17] M. Bredol, U. Kynast, and C. Ronda, *Adv. Mater.*, 3 (1991) 361-367.
- [18] U. Kynast and V. Weiler, *Adv. Mater.*, 6 (1994) 937-941.

- [19] D. Sendor and U. Kynast, *Adv. Mater.*, 14 (2002) 1570-1574.
- [20] D. Sendor, P. Junk, and U. Kynast, *Sol. St. Phen.*, 90-91 (2003) 521-526.
- [21] Y. J. Cui, Y. F. Yue, G. D. Qian, and B. L. Chen, *Chem. Rev.*, 112 (2012) 1126-1162.
- [22] J. Rocha, L. D. Carlos, F. A. A. Paz, and D. Ananias, *Chem. Soc. Rev.*, 40 (2011) 926-940.
- [23] K. Binnemans, *Chem. Rev.*, 109 (2009) 4283-4374.
- [24] L. D. Carlos, R. A. S. Ferreira, V. D. Bermudez, and S. J. L. Ribeiro, *Adv. Mater.*, 21 (2009) 509-534.
- [25] J. Feng and H. J. Zhang, *Chem. Soc. Rev.*, 42 (2013) 387-410.
- [26] B. Yan, *RSC Adv.*, 2 (2012) 9304-9324.
- [27] S. V. Eliseeva and J.-C. G. Bünzli, *Chem. Soc. Rev.*, 39 (2010) 189-227.
- [28] M. Elbanowski and B. Makowska, *J. Photochem. Photobiol. A*, 99 (1996) 85-92.
- [29] E. J. New, D. Parker, D. G. Smith, and J. W. Walton, *Curr. Opin. Chem. Biol.*, 14 (2010) 238-246.
- [30] D. Parker, *Aust. J. Chem.*, 64 (2011) 239-243.
- [31] J.-C. G. Bünzli, S. Comby, A. S. Chauvin, and C. D. B. Vandevyver, *J. Rare Earths*, 25 (2007) 257-274.
- [32] J.-C. G. Bünzli and S. V. Eliseeva, *J. Rare Earths*, 28 (2010) 824-842.
- [33] J.-C. G. Bünzli, *Chem. Rev.*, 110 (2010) 2729-2755.
- [34] C. R. Ronda, T. Justel, and H. Nikol, *J. Alloys Compd.*, 275 (1998) 669-676.
- [35] T. Justel, H. Nikol, and C. Ronda, *Angew. Chem. Int. Ed.*, 37 (1998) 3085-3103.
- [36] N. C. Chang, *J. Appl. Phys.*, 34 (1963) 3500-3504.
- [37] L. Ozawa and M. Itoh, *Chem. Rev.*, 103 (2003) 3835-3855.
- [38] A. Abdelkader and M. M. Elkholy, *J. Mater. Sci.*, 27 (1992) 2887-2895.
- [39] E. Zych, M. Wojtowicz, A. Dobrowolska, and L. Kepinski, *Opt. Mater.*, 31 (2009) 1764-1767.
- [40] E. Zych and J. Trojan-Piegza, *J. Lumin.*, 122 (2007) 335-338.
- [41] Y. A. Barbanel, V. V. Kolin, and V. P. Kotlin, *Sov. Radiochem.*, 33 (1991) 130-133.

- [42] E. A. Seregina, A. A. Seregin, and G. V. Tikhonov, *High Energ. Chem.*, 36 (2002) 223-228.
- [43] F. F. Chen, Z. Q. Bian, and C. H. Huang, *J. Rare Earths*, 27 (2009) 345-355.
- [44] N. P. Kuz'mina and S. V. Eliseeva, *Russ. J. Inorg. Chem.*, 51 (2006) 73-88.
- [45] I. Sage and G. Bourhill, *J. Mater. Chem.*, 11 (2001) 231-245.
- [46] C. R. Hurt, N. Mcavoy, S. Bjorklun, and N. Filipescu, *Nature*, 212 (1966) 179-180.
- [47] X. F. Chen, C. Y. Duan, X. H. Zhu, X. Z. You, S. S. S. Raj, H. K. Fun, and J. Wu, *Mater. Chem. Phys.*, 72 (2001) 11-15.
- [48] M. Elbanowski, B. Makowska, K. Staninski, and M. Kaczmarek, *J. Photochem. Photobiol. A*, 130 (2000) 75-81.
- [49] O. J. Sovers and T. Yoshioka, *J. Chem. Phys.*, 49 (1968) 4945-4954.
- [50] A. K. Levine and F. C. Palilla, *Appl. Phys. Lett.*, 5 (1964) 118-120.
- [51] A. K. Levine and F. C. Palilla, *Trans. N. Y. Acad. Sci.*, 27 (1965) 517-529.
- [52] J. F. Suyver and A. Meijerink, *Chemisch2Weekblad*, 98-4 (2002) 12-13.
- [53] E. Demarcay, *Compt. Rend.*, 130 (1900) 1469-1472.
- [54] W. Prandtl, *Ber. Dtsch. Chem. Ges. B*, 53B (1920) 1726-1728.
- [55] W. Prandtl, *Z. Anorg. Chem.*, 116 (1921) 96-101.
- [56] G. Urbain, *C. R. Hebd. Acad. Sci.*, 142 (1906) 205-207.
- [57] G. Urbain, *C. R. Hebd. Acad. Sci.*, 142 (1906) 1518-1520.
- [58] G. Urbain and H. Lacombe, *C. R. Hebd. Acad. Sci.*, 138 (1904) 627-629.
- [59] K. Binnemans and C. Görller-Walrand, *Chem. Phys. Lett.*, 235 (1995) 163-174.
- [60] G. Urbain, *Ann. Chim. Phys.*, 18 (1909) 289-226.
- [61] B. G. Wybourne, *Spectroscopic Properties of Rare Earths*, Interscience, New York, 1965.
- [62] G. H. Dieke, *Spectra and Energy Levels of Rare Earth Ions in Crystals*, Interscience, New York, 1968.
- [63] J. L. Prather, *Atomic Energy Levels in Crystals*; National Bureau of Standards Monograph, Vol. 19., U. S. Government Printing Office, Washington DC, 1961.
- [64] R. Reisfeld and C. K. Jorgensen, *Lasers and Excited States of Rare Earths*, Springer, Berlin, 1977.

- [65] S. Hübner, *Optical Spectra of Transparent Rare Earth Compounds*, Academic Press, New York, 1978.
- [66] G. K. Liu and B. Jacquier, *Spectroscopic Properties of Rare Earths in Optical Materials*, Springer, Berlin, 2005.
- [67] B. R. Judd, *Operator Techniques in Atomic Spectroscopy*, Princeton University Press, Princeton, 1998.
- [68] S. Hübner, in: S. P. Sinha (Ed.), *Systematics and Properties of the Lanthanides*, Vol. Vol. 109. Reidel, Dordrecht, 1983, pp. 313-388.
- [69] W. T. Carnall, in: K. A. Gschneidner jr. and L. Eyring (Eds.), Vol. 3. Elsevier, Amsterdam, 1979, pp. 171-208.
- [70] W. T. Carnall, J. V. Beitz, H. Crosswhite, K. Rajnak, and J. B. Mann, in: S. P. Sinha (Ed.), *Systematics and Properties of the Lanthanides*, Vol. Vol. 109. Reidel, Dordrecht, 1983, pp. 389-450.
- [71] J.-C. G. Bünzli, A. S. Chauvin, H. K. Kim, E. Deiters, and S. V. Eliseeva, *Coord. Chem. Rev.*, 254 (2010) 2623-2633.
- [72] S. V. Eliseeva, G. Aubock, F. van Mourik, A. Cannizzo, B. Song, E. Deiters, A. S. Chauvin, M. Chergui, and J.-C. G. Bünzli, *J. Phys. Chem. B*, 114 (2010) 2932-2937.
- [73] J.-C. G. Bünzli and S. V. Eliseeva, in: P. Hänninen and H. Härmä (Eds.), *Lanthanide Luminescence: Photophysical, Analytical and Biological Aspects*, Vol. Vol. 7. Springer, Berlin, 2010, pp. 1-45.
- [74] S. V. Eliseeva and J.-C. G. Bünzli, *New J. Chem.*, 35 (2011) 1165-1176.
- [75] J.-C. G. Bünzli and S. V. Eliseeva, in: J. Reedijk and K. R. Poeppelmeier (Eds.), *Comprehensive Inorganic Chemistry II, Volume 8: Coordination and Organometallic Chemistry*, Elsevier, Amsterdam, 2013, pp. 339-398.
- [76] J.-C. G. Bünzli and C. Piguet, *Chem. Soc. Rev.*, 34 (2005) 1048-1077.
- [77] J.-C. G. Bünzli, *Acc. Chem. Res.*, 39 (2006) 53-61.
- [78] S. Comby and J.-C. Bünzli, *Lanthanide near-infrared luminescence in molecular probes and devices*, Elsevier, 2007, pp. 217-470.
- [79] J.-C. G. Bünzli, *Chem. Lett.*, 38 (2009) 104-109.
- [80] J.-C. G. Bünzli, in: G. R. Choppin and J.-C. G. Bünzli (Eds.), *Lanthanide Probes in Life, Chemical and Earth Sciences: Theory and Practice*, Elsevier, Amsterdam, 1989, pp. 219-294.
- [81] P. A. Tanner, *Chem. Soc. Rev.*, 42 (2013) 5090-5101.
- [82] G. R. Choppin and D. R. Peterman, *Coord. Chem. Rev.*, 174 (1998) 283-299.

- [83] D. E. Henrie, R. L. Fellows, and G. R. Choppin, *Coord. Chem. Rev.*, 18 (1976) 199-224.
- [84] A. D'Aleo, F. Pointillart, L. Ouahab, C. Andraud, and O. Maury, *Coord. Chem. Rev.*, 256 (2012) 1604-1620.
- [85] Y. Ma and Y. Wang, *Coord. Chem. Rev.*, 254 (2010) 972-990.
- [86] L. Armelao, S. Quici, F. Barigelletti, G. Accorsi, G. Bottaro, M. Cavazzini, and E. Tondello, *Coord. Chem. Rev.*, 254 (2010) 487-505.
- [87] G. F. De Sa, O. L. Malta, C. D. Donega, A. M. Simas, R. L. Longo, P. A. Santa-Cruz, and E. F. da Silva, *Coord. Chem. Rev.*, 196 (2000) 165-195.
- [88] G. Vicentini, L. B. Zinner, J. Zukerman-Schpector, and K. Zinner, *Coord. Chem. Rev.*, 196 (2000) 353-382.
- [89] N. Sabbatini, M. Guardigli, and J. M. Lehn, *Coord. Chem. Rev.*, 123 (1993) 201-228.
- [90] F. S. Richardson, *Chem. Rev.*, 82 (1982) 541-552.
- [91] P. R. Selvin, *Annu. Rev. Biophys. Biomol. Struct.*, 31 (2002) 275-302.
- [92] I. Hemmilä and V. Laitala, *J. Fluoresc.*, 15 (2005) 529-542.
- [93] E. G. Moore, A. P. S. Samuel, and K. N. Raymond, *Acc. Chem. Res.*, 42 (2009) 542-552.
- [94] C. Görller-Walrand and K. Binnemans, in: K. A. Gschneidner jr. and L. Eyring (Eds.), *Handbook on the Physics and Chemistry of Rare Earths*, Vol. 25. Elsevier, 1998, pp. 101-264.
- [95] C. Görller-Walrand and K. Binnemans, in: K. A. Gschneidner jr. and L. Eyring (Eds.), *Handbook on the Physics and Chemistry of Rare Earths*, Vol. 23. Elsevier, Amsterdam, 1996, pp. 121-283.
- [96] D. Parker, R. S. Dickins, H. Puschmann, C. Crossland, and J. A. K. Howard, *Chem. Rev.*, 102 (2002) 1977-2010.
- [97] D. Parker, *Coord. Chem. Rev.*, 205 (2000) 109-130.
- [98] W. D. Horrocks and D. R. Sudnick, *Acc. Chem. Res.*, 14 (1981) 384-392.
- [99] J. I. Bruce, M. P. Lowe, and D. Parker, in: A. E. Merbach and E. Toth (Eds.), *The Chemistry of Contrast Agents in Medical Magnetic Resonance Imaging*, Wiley, Chichester, 2001, pp. 437-460.
- [100] M. C. Heffern, L. M. Matosziuk, and T. J. Meade, *Chem. Rev.*, 114 (2014) 4496-4539.
- [101] A. J. Freeman and R. E. Watson, *Phys. Rev.*, 127 (1962) 2058-2075.

- [102] W. C. Martin, R. Zalubas, and L. Hagan, Atomic Energy Levels - The Rare-Earth Elements; Nat. Stand. Ref. Data Ser., NSRDS-NBS 60, National Bureau of Standards, Gaithersburg, MD, 1978.
- [103] C. W. Nielson and G. F. Koster, Spectroscopic Coefficients for the p^n , d^n , and f^n Configurations, MIT Press, Cambridge, MA, 1963.
- [104] G. Racah, Phys. Rev., 76 (1949) 1352-1365.
- [105] J.-C. G. Bünzli, Inorg. Chim. Acta, 139 (1987) 219-222.
- [106] G. S. Ofelt, J. Chem. Phys., 38 (1963) 2171-2180.
- [107] M. T. Berry, M. F. Reid, and F. S. Richardson, J. Chem. Phys., 84 (1986) 2917-2925.
- [108] A. S. Souza and M. A. C. dos Santos, Chem. Phys. Lett., 521 (2012) 138-141.
- [109] H. M. Crosswhite and H. Crosswhite, J. Opt. Soc. Am. B, 1 (1984) 246-254.
- [110] Reid, M. F. Electronic Structure and Transition Intensities in Rare-Earth Materials. <http://www2.phys.canterbury.ac.nz/~mfr24/electronicstructure/00electronic.pdf> . 2013.
- [111] W. T. Carnall, G. L. Goodman, K. Rajnak, and R. S. Rana, J. Chem. Phys., 90 (1989) 3443-3457.
- [112] M. T. Berry, C. Schwieters, and F. S. Richardson, Chem. Phys., 122 (1988) 105-124.
- [113] K. Rajnak and B. G. Wybourne, Phys. Rev., 132 (1963) 280-290.
- [114] B. R. Judd, Phys. Rev., 141 (1966) 4-14.
- [115] C. Görller-Walrand, E. Huygen, K. Binnemans, and L. Fluyt, J. Phys. Condens. Matter., 6 (1994) 7797-7812.
- [116] B. R. Judd and H. Crosswhite, J. Opt. Soc. Am. B, 1 (1984) 255-260.
- [117] K. Binnemans, Bull. Soc. Chim. Belg., 105 (1996) 793-798.
- [118] C. Görller-Walrand, K. Binnemans, and L. Fluyt, J. Phys. Condens. Matter., 5 (1993) 8359-8374.
- [119] C. Rudowicz, M. Chua, and M. F. Reid, Physica B, 291 (2000) 327-338.
- [120] C. Rudowicz and J. Qin, J. Lumin., 110 (2004) 39-64.
- [121] C. Rudowicz and P. Gnutek, Physica B, 405 (2010) 113-132.
- [122] C. Rudowicz, P. Gnutek, and M. Karbowski, Opt. Mater., 33 (2011) 1557-1561.
- [123] C. K. Duan and P. A. Tanner, J. Phys. Chem. A, 114 (2010) 6055-6062.

- [124] H. Gobrecht, *Annalen der Physik* 5. Folge, 28 (1937) 673-700.
- [125] B. R. Judd, *Phys. Rev.*, 127 (1962) 750-761.
- [126] G. S. Ofelt, *J. Chem. Phys.*, 37 (1962) 511-520.
- [127] R. D. Peacock, *Struct. Bond.*, 22 (1975) 83-122.
- [128] B. M. Walsh, *Advances in Spectroscopy for Lasers and Sensing*, 231 (2006) 403-433.
- [129] M. P. Hehlen, M. G. Brik, and K. W. Kramer, *J. Lumin.*, 136 (2013) 221-239.
- [130] C. Görrler-Walrand, L. Fluyt, A. Ceulemans, and W. T. Carnall, *J. Chem. Phys.*, 95 (1991) 3099-3106.
- [131] B. Edlén, *J. Opt. Soc. Am.*, 43 (1953) 339-344.
- [132] T. Kushida and M. Tanaka, *Physical Review B*, 65 (2002).
- [133] L. Smentek and A. Kedzioriski, *J. Alloys Compd.*, 488 (2009) 586-590.
- [134] L. Smentek, *Phys. Rep.*, 297 (1998) 156-237.
- [135] L. Smentek, B. G. Wybourne, and B. A. Hess, *J. Alloys Compd.*, 323 (2001) 645-648.
- [136] L. Smentek, *Mol. Phys.*, 101 (2003) 893-897.
- [137] B. G. Wybourne, L. Smentek, and A. Kedzioriski, *Collect. Czech. Chem. Commun.*, 70 (2005) 905-922.
- [138] B. G. Wybourne and A. Kedzioriski, *J. Alloys Compd.*, 451 (2008) 18-34.
- [139] W. C. Nieuwpoort and G. Blasse, *Solid State Commun.*, 4 (1966) 227-229.
- [140] G. Nishimura and T. Kushida, *J. Phys. Soc. Jpn.*, 60 (1991) 683-694.
- [141] L. Smentek and B. A. Hess, *Mol. Phys.*, 92 (1997) 835-845.
- [142] A. S. Souza, Y. A. R. Oliveira, and M. A. C. dos Santos, *Opt. Mater.*, 35 (2013) 1633-1635.
- [143] P. Porcher and P. Caro, *J. Lumin.*, 21 (1980) 207-216.
- [144] M. Tanaka, G. Nishimura, and T. Kushida, *Phys. Rev. B*, 49 (1994) 16917-16925.
- [145] M. Tanaka and T. Kushida, *Phys. Rev. B*, 52 (1995) 4171-4178.
- [146] O. L. Malta, *Mol. Phys.*, 42 (1981) 65-72.
- [147] O. L. Malta, W. M. Azevedo, E. A. Gouveia, and G. F. de Sa, *J. Lumin.*, 26 (1982) 337-343.

- [148] X. Y. Chen and G. K. Liu, *J. Solid State Chem.*, 178 (2005) 419-428.
- [149] J. Hölsä and P. Porcher, *J. Chem. Phys.*, 76 (1982) 2790-2797.
- [150] B. R. Judd, *J. Phys. C: Solid State Phys.*, 13 (1980) 2695-2701.
- [151] K. H. Hellwege, P. Hill, and S. Huefner, *Solid State Commun.*, 5 (1967) 687-689.
- [152] E. Moret, F. Nicolo, J.-C. G. Bünzli, and G. Chapuis, *J. Less-Common Met.*, 171 (1991) 273-300.
- [153] V. Lavin, U. R. Rodriguez-Mendoza, I. R. Martin, and V. D. Rodriguez, *J. Non-Cryst. Solids*, 319 (2003) 200-216.
- [154] R. Reisfeld, R. A. Velapoldi, L. Boehm, and M. Ish-Shalom, *J. Phys. Chem.*, 75 (1971) 3980-3983.
- [155] K. Binnemans and C. Görller-Walrand, *J. Rare Earths*, 14 (1996) 173-180.
- [156] K. Binnemans, K. Van Herck, and C. Görller-Walrand, *Chem. Phys. Lett.*, 266 (1997) 297-302.
- [157] M. H. V. Werts, R. T. F. Jukes, and J. W. Verhoeven, *Phys. Chem. Chem. Phys.*, 4 (2002) 1542-1548.
- [158] A. F. Kirby and F. S. Richardson, *J. Phys. Chem.*, 87 (1983) 2544-2556.
- [159] C. C. Bryden and C. N. Reilley, *Anal. Chem.*, 54 (1982) 610-615.
- [160] G. Blasse, *Chem. Phys. Lett.*, 33 (1975) 616-618.
- [161] M. Karbowiak and S. Hubert, *J. Alloys Compd.*, 302 (2000) 87-93.
- [162] R. El Ouenzerfi, N. Kbir-Ariguib, M. Trabelsi-Ayedi, and B. Piriou, *J. Lumin.*, 85 (1999) 71-77.
- [163] P. Porcher, D. R. Svoronos, M. Leskelä, and J. Hölsä, *J. Solid State Chem.*, 46 (1983) 101-111.
- [164] J. Hölsä and P. Porcher, *J. Less-Common Met.*, 112 (1985) 121-125.
- [165] B. Piriou, Y. F. Chen, and S. Vilminot, *Eur. J. Solid State Inorg. Chem.*, 32 (1995) 469-481.
- [166] B. Piriou, Y. F. Chen, and S. Vilminot, *Eur. J. Solid State Inorg. Chem.*, 35 (1998) 341-355.
- [167] B. Piriou, M. Richard-Plouet, J. Parmentier, F. Ferey, and S. Vilminot, *J. Alloys Compd.*, 262 (1997) 450-453.
- [168] O. K. Moune, P. Porcher, and P. Caro, *J. Solid State Chem.*, 50 (1983) 41-50.
- [169] E. Antic-Fidancev, J. Hölsä, and M. Lastusaari, *J. Alloys Compd.*, 341 (2002) 82-86.

- [170] H. D. Xie, L. Xu, L. Qin, Y. L. Huang, D. L. Wei, S. I. Kim, and H. J. Seo, *Mater. Lett.*, 115 (2014) 18-20.
- [171] A. O. Wright, M. D. Seltzer, J. B. Gruber, and B. H. T. Chai, *J. Appl. Phys.*, 78 (1995) 2456-2467.
- [172] G. Blasse and A. Bril, *J. Chem. Phys.*, 46 (1967) 2579-2582.
- [173] C. C. L. Pereira, S. Dias, I. Coutinho, J. P. Leal, L. C. Branco, and C. A. T. Laia, *Inorg. Chem.*, 52 (2013) 3755-3764.
- [174] O. Deutschbein and R. Tomaschek, *Ann. Phys. (Berlin, Ger.)*, 29 (1937) 311-323.
- [175] W. D. Horrocks and D. R. Sudnick, *Science*, 206 (1979) 1194-1196.
- [176] J.-C. G. Bünzli and G. O. Pradervand, *J. Chem. Phys.*, 85 (1986) 2489-2497.
- [177] J.-C. G. Bünzli, D. Plancherel, and G. O. Pradervand, *J. Phys. Chem.*, 93 (1989) 980-984.
- [178] Y. R. Shen, C. M. Li, V. C. Costa, and K. L. Bray, *Phys. Rev. B*, 68 (2003) 014101.
- [179] S. N. Zhang, J. H. Huang, Y. J. Chen, X. H. Gong, Y. F. Lin, Z. D. Luo, and Y. D. Huang, *Opt. Mater. Express*, 3 (2013) 868-874.
- [180] F. Durville, G. Boulon, R. Reisfeld, H. Mack, and C. K. Jorgensen, *Chem. Phys. Lett.*, 102 (1983) 393-398.
- [181] J. A. Capobianco, T. F. Belliveau, G. Lord, D. J. Simkin, J. Tait, and P. J. Hayward, *Phys. Rev. B*, 34 (1986) 4204-4212.
- [182] P. Babu, K. H. Jang, E. S. Kim, R. Vijaya, C. K. Jayasankar, V. Lavin, and H. J. Seo, *J. Non-Cryst. Solids*, 357 (2011) 2139-2147.
- [183] V. Lavin, V. D. Rodriguez, I. R. Martin, and U. R. Rodriguez-Mendoza, *J. Lumin.*, 72-4 (1997) 437-438.
- [184] G. Boulon, M. Bouderbala, and J. Seriot, *J. Less-Common Met.*, 112 (1985) 41-66.
- [185] G. Boulon, *Mater. Chem. Phys.*, 16 (1987) 301-347.
- [186] R. Balda, J. Fernandez, J. L. Adam, and M. A. Arriandiaga, *Phys. Rev. B*, 54 (1996) 12076-12086.
- [187] R. C. Holz and L. C. Thompson, *Inorg. Chem.*, 32 (1993) 5251-5256.
- [188] M. Albin, R. R. Whittle, and W. D. Horrocks, *Inorg. Chem.*, 24 (1985) 4591-4594.
- [189] P. J. Breen and W. D. Horrocks, *Inorg. Chem.*, 22 (1983) 536-540.
- [190] M. Albin, G. K. Farber, and W. D. Horrocks, *Inorg. Chem.*, 23 (1984) 1648-1651.
- [191] C. L. Maupin, K. C. Smith, and J. P. Riehl, *J. Alloys Compd.*, 249 (1997) 181-184.

- [192] H. Kusama, O. J. Sovers, and T. Yoshioka, *Jpn. J. Appl. Phys.*, 15 (1976) 2349-2358.
- [193] R. L. Ahlefeldt, A. Smith, and M. J. Sellars, *Phys. Rev. B*, 80 (2009) 205106.
- [194] J. P. D. Martin, M. J. Sellars, P. Tuthill, N. B. Manson, G. Pryde, and T. Dyke, *J. Lumin.*, 78 (1998) 19-24.
- [195] R. W. Schwartz, *Mol. Phys.*, 30 (1975) 81-95.
- [196] O. A. Serra and L. C. Thompson, *Inorg. Chem.*, 15 (1976) 504-507.
- [197] J. Hölsä and M. Leskelä, *Mol. Phys.*, 54 (1985) 657-667.
- [198] J. Hölsä, K. Jyrkas, and M. Leskelä, *J. Less-Common Met.*, 126 (1986) 215-220.
- [199] E. Antic-Fidancev, K. Serhan, M. Taibi, M. Lemaitre-Blaise, P. Porcher, J. Aride, and A. Boukhari, *J. Phys. Condens. Matter.*, 6 (1994) 6857-6864.
- [200] O. Beaury, M. Faucher, and P. Caro, *Mater. Res. Bull.*, 13 (1978) 175-185.
- [201] B. Piriou, D. Fahmi, J. D'Expert-Ghys, A. Taitai, and J. L. Lacout, *J. Lumin.*, 39 (1987) 97-103.
- [202] E. Antic-Fidancev, *J. Alloys Compd.*, 300 (2000) 2-10.
- [203] Y. G. Galyametdinov, W. Haase, L. Malykhina, A. Prosvirin, I. Bikchantaev, A. Rakhmatullin, and K. Binnemans, *Chem. Eur. J.*, 7 (2001) 99-105.
- [204] P. A. Tanner, Y. L. Liu, N. M. Edelstein, K. M. Murdoch, and N. M. Khaidukov, *J. Phys. Condens. Matter.*, 9 (1997) 7817-7836.
- [205] P. A. Tanner and Y. L. Liu, *J. Alloys Compd.*, 204 (1994) 93-100.
- [206] D. L. Gao, H. R. Zheng, X. Y. Zhang, Z. X. Fu, Z. L. Zhang, Y. Tian, and M. Cui, *Appl. Phys. Lett.*, 98 (2011) 011907.
- [207] J. Hölsä and E. Kestilä, *J. Chem. Soc. , Faraday Trans.*, 91 (1995) 1503-1509.
- [208] C. Görller-Walrand, I. Hendrickx, L. Fluyt, M. P. Gos, J. D'Olieslager, and G. Blasse, *J. Chem. Phys.*, 96 (1992) 5650-5658.
- [209] C. Görller-Walrand, I. Hendrickx, L. Fluyt, P. Porcher, O. K. Moune-Minn, and G. Blasse, *J. Lumin.*, 42 (1989) 349-356.
- [210] B. R. Judd, *Proc. Roy. Soc. London Ser. A*, 241 (1957) 122-131.
- [211] A. F. Kirby and F. S. Richardson, *J. Phys. Chem.*, 87 (1983) 2557-2563.
- [212] C. Görller-Walrand, P. Verhoeven, J. D'Olieslager, L. Fluyt, and K. Binnemans, *J. Chem. Phys.*, 100 (1994) 815-823.

- [213] K. Binnemans and C. Görller-Walrand, *J. Phys. Condens. Matter.*, 8 (1996) 1267-1279.
- [214] K. H. Hellwege and H. G. Kahle, *Z. Phys.*, 129 (1951) 85-103.
- [215] T. Ohoka and Y. Kato, *Bull. Chem. Soc. Jpn.*, 56 (1983) 1289-1300.
- [216] E. V. Sayre and S. Freed, *J. Chem. Phys.*, 24 (1956) 1213-1219.
- [217] L. G. Deshazer and G. H. Dieke, *J. Chem. Phys.*, 38 (1963) 2190-2199.
- [218] D. A. Durham and F. A. Hart, *J. Inorg. Nucl. Chem.*, 31 (1969) 145-157.
- [219] K. Binnemans and C. Görller-Walrand, *Chem. Phys. Lett.*, 245 (1995) 75-78.
- [220] M. F. O. Bezerra, M. A. C. dos Santos, A. Monteil, and S. Chaussedent, *Opt. Mater.*, 30 (2008) 1013-1016.
- [221] M. J. Weber, J. A. Paisner, S. S. Sussman, W. M. Yen, L. A. Riseberg, and C. Brecher, *J. Lumin.*, 12 (1976) 729-735.
- [222] C. Cascales, R. Balda, J. Fernandez, M. A. Arriandiaga, and J. M. Fdez-Navarro, *J. Non-Cryst. Solids*, 352 (2006) 2448-2451.
- [223] C. Cascales, R. Balda, J. Fernandez, M. A. Arriandiaga, and J. M. Fdez-Navarro, *Opt. Mater.*, 31 (2009) 1092-1095.
- [224] G. Blasse, A. Bril, and W. C. Nieuwpoort, *J. Phys. Chem. Solids*, 27 (1966) 1587-1592.
- [225] G. Blasse, *Chem. Phys. Lett.*, 20 (1973) 573-574.
- [226] F. J. Avella, O. J. Sovers, and C. S. Wiggins, *J. Electrochem. Soc.*, 114 (1967) 613-616.
- [227] W. Y. Li, L. X. Ning, and P. A. Tanner, *J. Phys. Chem. A*, 116 (2012) 7337-7344.
- [228] P. A. Tanner and Z. F. Pan, *Inorg. Chem.*, 48 (2009) 11142-11146.
- [229] F. Fujishiro, T. Arakawa, and T. Hashimoto, *Mater. Lett.*, 65 (2011) 1819-1821.
- [230] D. K. Patel, B. Rajeswari, V. Sudarsan, R. K. Vatsa, R. M. Kadam, and S. K. Kulshreshtha, *Dalton Trans.*, 41 (2012) 12023-12030.
- [231] S. Basu, D. K. Patel, J. Nuwad, V. Sudarsan, S. N. Jha, D. Bhattacharyya, R. K. Vatsa, and S. K. Kulshreshtha, *Chem. Phys. Lett.*, 561 (2013) 82-86.
- [232] S. M. Melo, L. M. C. Jatahy, E. E. Castellano, and C. O. P. Santos, *Inorganica Chimica Acta-F-Block Elements Articles and Letters*, 109 (1985) 163-166.
- [233] S. Hubert, P. Thouvenot, and N. Edelstein, *Phys. Rev. B*, 48 (1993) 5751-5760.
- [234] S. Hubert and P. Thouvenot, *J. Alloys Compd.*, 180 (1992) 193-200.

- [235] K. Lunstroot, L. Baeten, P. Nockemann, J. Martens, P. Verlooy, X. P. Ye, C. Görrler-Walrand, K. Binnemans, and K. Driesen, *J. Phys. Chem. C*, 113 (2009) 13532-13538.
- [236] T. Grzyb and S. Lis, *J. Rare Earths*, 27 (2009) 588-592.
- [237] X. T. Zhang, T. Hayakawa, and M. Nogami, *Int. J. Appl. Ceram. Technol.*, 8 (2011) 741-751.
- [238] C. Y. Cao, H. K. Yang, J. W. Chung, B. K. Moon, B. C. Choi, J. H. Jeong, and K. H. Kim, *Mater. Res. Bull.*, 46 (2011) 1553-1559.
- [239] V. Sudarsan, F. C. J. M. van Veggel, R. A. Herring, and M. Raudsepp, *J. Mater. Chem.*, 15 (2005) 1332-1342.
- [240] S. Janssens, G. Williams, D. Clarke, and M. Sharp, *Physica Status Solidi B*, 248 (2011) 439-443.
- [241] S. Janssens, G. V. M. Williams, and D. Clarke, *J. Appl. Phys.*, 109 (2011).
- [242] D. S. Zhang, T. T. Yan, H. R. Li, and L. Y. Shi, *Microporous Mesoporous Mater.*, 141 (2011) 110-118.
- [243] C. Lorbeer, J. Cybinska, and A. V. Mudring, *Cryst. Growth Des.*, 11 (2011) 1040-1048.
- [244] Q. Ju, Y. S. Liu, D. T. Tu, H. M. Zhu, R. F. Li, and X. Y. Chen, *Chem. Eur. J.*, 17 (2011) 8549-8554.
- [245] C. Lorbeer, J. Cybinska, and A. V. Mudring, *Chem. Commun.*, 46 (2010) 571-573.
- [246] M. Karbowski, A. Mech, A. Bednarkiewicz, and W. Streck, *J. Alloys Compd.*, 380 (2004) 321-326.
- [247] M. Karbowski, A. Mech, L. Kepinski, W. Mielcarek, and S. Hubert, *J. Alloys Compd.*, 400 (2005) 67-75.
- [248] S. Lepoutre, D. Boyer, and R. Mahiou, *J. Lumin.*, 128 (2008) 635-641.
- [249] R. T. Wegh, H. Donker, K. D. Oskam, and A. Meijerink, *Science*, 283 (1999) 663-666.
- [250] M. Karbowski, A. Mech, A. Bednarkiewicz, W. Streck, and L. Kepinski, *J. Phys. Chem. Solids*, 66 (2005) 1008-1019.
- [251] A. Mech, M. Karbowski, L. Kepinski, A. Bednarkiewicz, and W. Streck, *J. Alloys Compd.*, 380 (2004) 315-320.
- [252] D. Zakaria, M. T. Fournier, R. Mahiou, and J. C. Cousseins, *J. Alloys Compd.*, 188 (1992) 250-254.
- [253] A. Bednarkiewicz, A. Mech, M. Karbowski, and W. Streck, *J. Lumin.*, 114 (2005) 247-254.

- [254] F. Fujishiro, M. Murakami, T. Hashimoto, and M. Takahashi, *J. Ceram. Soc. Jpn.*, 118 (2010) 1217-1220.
- [255] F. Fujishiro, R. Sekimoto, and T. Hashimoto, *J. Lumin.*, 133 (2013) 217-221.
- [256] F. Fujishiro, R. Sekimoto, and T. Hashimoto, *Mater. Lett.*, 65 (2011) 2492-2494.
- [257] J.-C. G. Bünzli and J. R. Yersin, *Inorg. Chem.*, 18 (1979) 605-607.
- [258] K. Binnemans, L. Malykhina, V. S. Mironov, W. Haase, K. Driesen, R. Van Deun, L. Fluyt, C. Görller-Walrand, and Y. G. Galyametdinov, *ChemPhysChem*, 2 (2001) 680-683.
- [259] Y. G. Galyametdinov, W. Haase, B. Goderis, D. Moors, K. Driesen, R. Van Deun, and K. Binnemans, *J. Phys. Chem. B*, 111 (2007) 13881-13885.
- [260] K. Binnemans, R. Van Deun, C. Görller-Walrand, W. Haase, D. W. Bruce, L. Malykhina, and Y. G. Galyametdinov, *Mater. Sci. Eng. C*, 18 (2001) 247-254.
- [261] V. S. Mironov, Y. G. Galyametdinov, A. Ceulemans, and K. Binnemans, *J. Chem. Phys.*, 113 (2000) 10293-10303.
- [262] J. A. Peters, J. Huskens, and D. J. Raber, *Prog. Nucl. Magn. Reson. Spectrosc.*, 28 (1996) 283-350.
- [263] C. K. Jorgensen and B. R. Judd, *Mol. Phys.*, 8 (1964) 281-290.
- [264] N. C. Chang and J. B. Gruber, *J. Chem. Phys.*, 41 (1964) 3227-3234.
- [265] H. F. Brito, O. L. Malta, and J. F. S. Menezes, *J. Alloys Compd.*, 303 (2000) 336-339.
- [266] J.-C. G. Bünzli, E. Moret, V. Foiret, K. J. Schenk, M. Z. Wang, and L. P. Jin, *J. Alloys Compd.*, 207 (1994) 107-111.
- [267] S. P. Sinha, in: S. P. Sinha (Ed.), *Systematics and Properties of the Lanthanides*, Vol. Vol. 109. Reidel, Dordrecht, 1983, pp. 451-500.
- [268] R. Nagaishi, T. Kimura, and S. P. Sinha, *Mol. Phys.*, 101 (2003) 1007-1014.
- [269] S. P. Sinha, *Fresen Z. Anal. Chem.*, 313 (1982) 238-239.
- [270] R. Nagaishi, M. Arisaka, T. Kimura, and Y. Kitatsuji, *J. Alloys Compd.*, 431 (2007) 221-225.
- [271] L. C. Thompson and S. C. Kuo, *Inorg. Chim. Acta*, 149 (1988) 305-306.
- [272] G. Blasse, G. J. Dirksen, and F. Zonnevijlle, *J. Inorg. Nucl. Chem.*, 43 (1981) 2847-2853.
- [273] Z. L. Fu, X. Y. Cui, S. B. Cui, X. D. Qi, S. H. Zhou, S. Y. Zhang, and J. H. Jeong, *CrystEngComm*, 14 (2012) 3915-3922.

- [274] S. Fujihara and M. Oikawa, *J. Appl. Phys.*, 95 (2004) 8002-8006.
- [275] L. R. Melby, E. Abramson, J. C. Caris, and N. J. Rose, *J. Am. Chem. Soc.*, 86 (1964) 5117-5125.
- [276] E. Butter and W. Seifert, *Z. Anorg. Allg. Chem.*, 368 (1969) 133-143.
- [277] A. F. Kirby, D. Foster, and F. S. Richardson, *Chem. Phys. Lett.*, 95 (1983) 507-512.
- [278] V. F. Zolin, V. M. Markushev, N. S. Rukk, and V. I. Tsaryuk, *Koord. Khim.*, 10 (1984) 1485-1491.
- [279] J.-C. G. Bünzli, S. Petoud, and E. Moret, *Spectrosc. Lett.*, 32 (1999) 155-163.
- [280] W. Y. Li and P. A. Tanner, *Chem. Phys. Lett.*, 494 (2010) 50-53.
- [281] W. Y. Li and P. A. Tanner, *Inorg. Chem.*, 49 (2010) 6384-6386.
- [282] P. A. Tanner, W. Y. Li, and L. X. Ning, *Inorg. Chem.*, 51 (2012) 2997-3006.
- [283] C. G. Ma, M. G. Brik, V. Kiisk, T. Kangur, and I. Sildos, *J. Alloys Compd.*, 509 (2011) 3441-3451.
- [284] G. Blasse and J. Van Keulen, *Chem. Phys. Lett.*, 124 (1986) 534-537.
- [285] J. P. Morley, J. D. Saxe, and F. S. Richardson, *Mol. Phys.*, 47 (1982) 379-406.
- [286] D. A. Durham, G. H. Frost, and F. A. Hart, *J. Inorg. Nucl. Chem.*, 31 (1969) 833-838.
- [287] M. Hasunuma, K. Okada, and Y. Kato, *Bull. Chem. Soc. Jpn.*, 57 (1984) 3036-3042.
- [288] L. Ozawa and P. M. Jaffe, *J. Electrochem. Soc.*, 118 (1971) 1678-1679.
- [289] C. Apostolidis, J. Rebizant, O. Walter, B. Kanellakopulos, H. Reddmann, and H. D. Amberger, *Z. Anorg. Allg. Chem.*, 628 (2002) 2013-2025.
- [290] J. E. Lowther, *J. Phys. C: Solid State Phys.*, 7 (1974) 4393-4402.
- [291] E. Antic-Fidancev, M. Lemaitre-Blaise, P. Porcher, N. Mercier, and M. Leblanc, *J. Solid State Chem.*, 116 (1995) 286-289.
- [292] D. van der Voort and G. Blasse, *J. Phys. Chem. Solids*, 52 (1991) 1149-1154.
- [293] G. Blasse, *Inorg. Chim. Acta*, 142 (1988) 153-154.
- [294] R. A. S. Ferreira, S. S. Nobre, C. M. Granadeiro, H. I. S. Nogueira, L. D. Carlos, and O. L. Malta, *J. Lumin.*, 121 (2006) 561-567.
- [295] N. J. Rose and E. Abramson, *J. Chem. Phys.*, 42 (1965) 1849-1850.
- [296] L. C. Thompson and S. C. Kuo, *J. Less-Common Met.*, 148 (1989) 173-179.

- [297] M. Albin, W. D. Horrocks, and F. J. Liotta, *Chem. Phys. Lett.*, 85 (1982) 61-64.
- [298] K. Zhuravlev, V. Tsaryuk, V. Kudryashova, V. Zolin, Y. Yakovlev, and J. Legendziewicz, *Spectrochim. Acta A*, 72 (2009) 1020-1025.
- [299] M. Bettinelli, A. Speghini, F. Piccinelli, A. N. C. Neto, and O. L. Malta, *J. Lumin.*, 131 (2011) 1026-1028.
- [300] M. Bortoluzzi, G. Paolucci, S. Polizzi, L. Bellotto, F. Enrichi, S. Ciorba, and B. S. Richards, *Inorg. Chem. Commun.*, 14 (2011) 1762-1766.
- [301] M. Bortoluzzi, G. Paolucci, M. Gatto, S. Roppa, F. Enrichi, S. Ciorba, and B. S. Richards, *J. Lumin.*, 132 (2012) 2378-2384.
- [302] C. J. Holler, M. Mai, C. Feldmann, and K. Müller-Buschbaum, *Dalton Trans.*, 39 (2010) 461-468.
- [303] R. Skaudzius, A. Katelnikovas, D. Enseling, A. Kareiva, and T. Justel, *J. Lumin.*, 147 (2014) 290-294.
- [304] E. Moret, J.-C. G. Bünzli, and K. J. Schenk, *Inorg. Chim. Acta*, 178 (1990) 83-88.
- [305] M. J. Weber, in: H. M. Crosswhite and H. W. Moos (Eds.), *Optical Properties of Ions in Crystals*, Wiley Interscience, New York, 1967, p. 467.
- [306] T. A. Hopkins, J. P. Bolender, D. H. Metcalf, and F. S. Richardson, *Inorg. Chem.*, 35 (1996) 5347-5355.
- [307] P. Babu and C. K. Jayasankar, *Physica B*, 279 (2000) 262-281.
- [308] J. Hölsä and P. Porcher, *J. Chem. Phys.*, 75 (1981) 2108-2117.
- [309] L. Ozawa and P. M. Jaffe, *J. Electrochem. Soc.*, 118 (1971) 1678-1679.
- [310] B. Bihari, K. K. Sharma, and L. E. Erickson, *J. Phys. Condens. Matter.*, 2 (1990) 5703-5713.
- [311] P. Porcher and P. Caro, *J. Chem. Phys.*, 65 (1976) 89-94.
- [312] P. Porcher and P. Caro, *J. Chem. Phys.*, 68 (1978) 4176-4182.
- [313] P. Porcher and P. Caro, *J. Chem. Phys.*, 68 (1978) 4183-4187.
- [314] M. J. Weber, in: H. M. Crosswhite and H. W. Moos (Eds.), *Optical Properties of Ions in Crystals*, Wiley Interscience, New York, 1967, pp. 467-484.
- [315] D. T. Tu, Y. S. Liu, H. M. Zhu, R. F. Li, L. Q. Liu, and X. Y. Chen, *Angew. Chem. Int. Ed.*, 52 (2013) 1128-1133.
- [316] J. Hölsä and E. Kestilä, *J. Alloys Compd.*, 225 (1995) 89-94.
- [317] H. D. Amberger, *Spectrochim. Acta A*, 34 (1978) 627-631.

- [318] S. C. Kuo, L. C. Thompson, and H. D. Amberger, *J. Alloys Compd.*, 225 (1995) 60-62.
- [319] R. Reisfeld, E. Greenberg, R. N. Brown, M. G. Drexhage, and C. K. Jorgensen, *Chem. Phys. Lett.*, 95 (1983) 91-94.
- [320] J. L. Adam, V. Poncon, J. Lucas, and G. Boulon, *J. Non-Cryst. Solids*, 91 (1987) 191-202.
- [321] M. Dejneka, E. Snitzer, and R. E. Riman, *J. Lumin.*, 65 (1995) 227-245.
- [322] R. Reisfeld, *Struct. Bond.*, 22 (1975) 123-175.
- [323] R. T. Wegh, H. Donker, K. D. Oskam, and A. Meijerink, *J. Lumin.*, 82 (1999) 93-104.
- [324] P. Ptacek, H. Schafer, K. Kompe, and M. Haase, *Adv. Funct. Mater.*, 17 (2007) 3843-3848.
- [325] H. S. Kiliaan, J. F. A. K. Kotte, and G. Blasse, *Chem. Phys. Lett.*, 133 (1987) 425-428.
- [326] M. Karbowski, A. Mech, and W. Ryba-Romanowski, *J. Lumin.*, 114 (2005) 65-70.
- [327] T. Grzyb, M. Weclawiak, and S. Lis, *J. Alloys Compd.*, 539 (2012) 82-89.
- [328] C. H. Liang, Y. C. Chang, and Y. S. Chang, *Appl. Phys. Lett.*, 93 (2008) 211902.
- [329] P. A. Tanner, C. K. Duan, G. H. Jia, and B. M. Cheng, *J. Solid State Chem.*, 188 (2012) 105-108.
- [330] H. D. Amberger, *Z. Phys. Chem. Neue Fol.*, 109 (1978) 125-128.
- [331] J. P. Morley, T. R. Faulkner, and F. S. Richardson, *J. Chem. Phys.*, 77 (1982) 1710-1733.
- [332] L. L. Wang, X. J. Xue, H. Chen, D. Zhao, and W. P. Qin, *Chem. Phys. Lett.*, 485 (2010) 183-186.
- [333] R. D. Peacock, *Chem. Phys. Lett.*, 35 (1975) 420-422.
- [334] A. A. F. Lagerwey and G. Blasse, *Chem. Phys. Lett.*, 31 (1975) 27-28.
- [335] C. Brecher, *J. Chem. Phys.*, 61 (1974) 2297-2315.
- [336] C. Görller-Walrand, I. Hendrickx, L. Fluyt, J.-C. G. Bünzli, and E. Moret, *Chem. Phys. Lett.*, 170 (1990) 223-230.
- [337] J. Blanc and D. L. Ross, *J. Chem. Phys.*, 43 (1965) 1286-1289.
- [338] V. I. Srdanov, M. R. Robinson, M. H. Bartl, X. Bu, and G. C. Bazan, *Appl. Phys. Lett.*, 80 (2002) 3042-3044.

- [339] C. Y. Yang, V. Srdanov, M. R. Robinson, G. C. Bazan, and A. J. Heeger, *Adv. Mater.*, 14 (2002) 980-983.
- [340] Y. G. Galyametdinov, A. A. Knyazev, V. I. Dzhabarov, T. Cardinaels, K. Driesen, C. Görrler-Walrand, and K. Binnemans, *Adv. Mater.*, 20 (2008) 252-257.
- [341] S. C. J. Meskers, J. P. Riehl, and H. P. J. M. Dekkers, *Chem. Phys. Lett.*, 216 (1993) 241-246.
- [342] S. I. Weissman, *J. Chem. Phys.*, 10 (1942) 214-217.
- [343] G. A. Crosby, R. E. Whan, and J. J. Freeman, *J. Phys. Chem.*, 66 (1962) 2493-2499.
- [344] R. E. Whan and G. A. Crosby, *J. Mol. Spectrosc.*, 8 (1962) 315-327.
- [345] G. A. Crosby, R. M. Alire, and R. E. Whan, *J. Chem. Phys.*, 34 (1961) 743-748.
- [346] S. Sato and M. Wada, *Bull. Chem. Soc. Jpn.*, 43 (1970) 1955-1962.
- [347] M. Latva, H. Takalo, V. M. Mikkala, C. Matachescu, J. C. Rodriguez-Ubis, and J. Kankare, *J. Lumin.*, 75 (1997) 149-169.
- [348] A. V. Hayes and H. G. Drickamer, *J. Chem. Phys.*, 76 (1982) 114-125.
- [349] M. Kleinerman, *Journal of Chemical Physics*, 51 (1969) 2370-2381.
- [350] B. Yan, H. J. Zhang, S. B. Wang, and J. Z. Ni, *J. Photochem. Photobiol. A*, 116 (1998) 209-214.
- [351] A. Strasser and A. Vogler, *Inorg. Chim. Acta*, 357 (2004) 2345-2348.
- [352] S. Tobita, M. Arakawa, and I. Tanaka, *J. Phys. Chem.*, 88 (1984) 2697-2702.
- [353] M. L. Bhaumik and M. A. El-Sayed, *J. Chem. Phys.*, 42 (1965) 787-788.
- [354] S. Tobita, M. Arakawa, and I. Tanaka, *J. Phys. Chem.*, 89 (1985) 5649-5654.
- [355] H. Kunkely, V. Pawlowski, A. Strasser, and A. Vogler, *Inorg. Chem. Commun.*, 11 (2008) 415-417.
- [356] W. Strek and M. Wierzchaczewski, *Chem. Phys.*, 58 (1981) 185-193.
- [357] O. L. Malta, H. F. Brito, J. F. S. Menezes, F. R. G. E. Silva, S. Alves, F. S. Farias, and A. V. M. de Andrade, *J. Lumin.*, 75 (1997) 255-268.
- [358] J. D. L. Dutra, M. A. M. Filho, G. B. Rocha, R. O. Freire, A. M. Simas, and J. J. P. Stewart, *J. Chem. Theory Comput.*, 9 (2013) 3333-3341.
- [359] G. B. Rocha, R. O. Freire, N. B. da Costa, G. F. de Sa, and A. M. Simas, *Inorg. Chem.*, 43 (2004) 2346-2354.
- [360] V. Divya, R. O. Freire, and M. L. P. Reddy, *Dalton Trans.*, 40 (2011) 3257-3268.

- [361] E. R. dos Santos, R. O. Freire, N. B. da Costa, F. A. A. Paz, C. A. de Simone, S. A. Junior, A. A. S. Araujo, L. A. O. Nunes, M. E. de Mesquita, and M. O. Rodrigues, *J. Phys. Chem. A*, 114 (2010) 7928-7936.
- [362] R. O. Freire, F. R. G. E. Silva, M. O. Rodrigues, M. E. de Mesquita, and N. B. D. Junior, *J. Mol. Modeling*, 12 (2005) 16-23.
- [363] J. D. L. Dutra and R. O. Freire, *J. Photochem. Photobiol. A*, 256 (2013) 29-35.
- [364] A. V. M. de Andrade, N. B. da Costa, A. M. Simas, and G. F. de Sa, *Chem. Phys. Lett.*, 227 (1994) 349-353.
- [365] A. V. M. de Andrade, N. B. da Costa, A. M. Simas, and G. F. de Sa, *J. Alloys Compd.*, 225 (1995) 55-59.
- [366] G. H. Jia, C. F. Wang, and S. Q. Xu, *J. Phys. Chem. C*, 114 (2010) 17905-17913.
- [367] J. Huang, J. Loriers, and P. Porcher, *C. R. Acad. Sci. , Ser. II*, 294 (1982) 545-548.
- [368] G. Blasse and B. C. Grabmaier, *Luminescent Materials*, Springer, Berlin, 1994.
- [369] M. G. Nikolic, D. J. Jovanovic, and M. D. Dramicanin, *Appl. Opt.*, 52 (2013) 1716-1724.
- [370] D. J. Jovanovic, Z. Antic, R. M. Krsmanovic, M. Mitric, V. Dordevic, B. Bartova, and M. D. Dramicanin, *Opt. Mater.*, 35 (2013) 1797-1804.
- [371] G. Blasse and A. Bril, *J. Chem. Phys.*, 45 (1966) 2350-2355.
- [372] T. Yamase, H. Naruke, A. M. S. Wery, and M. Kaneko, *Chem. Lett.*, (1998) 1281-1282.
- [373] G. Blasse, G. J. Dirksen, and F. Zonnevillje, *Chem. Phys. Lett.*, 83 (1981) 449-451.
- [374] Q. H. Luo, R. C. Howell, M. Dankova, J. Bartis, C. W. Williams, W. D. Horrocks, V. G. Young, A. L. Rheingold, L. C. Francesconi, and M. R. Antonio, *Inorg. Chem.*, 40 (2001) 1894-1901.
- [375] T. Yamase, T. Kobayashi, M. Sugeta, and H. Naruke, *J. Phys. Chem. A*, 101 (1997) 5046-5053.
- [376] M. D. Ward, *Coord. Chem. Rev.*, 251 (2007) 1663-1677.
- [377] T. Arakawa and M. Akamine, *Sens. Actuators B*, 91 (2003) 252-255.
- [378] M. A. Kessler, *Anal. Chim. Acta*, 364 (1998) 125-129.
- [379] B. C. Barja, S. E. Bari, M. C. Marchi, F. L. Iglesias, and M. Bernardi, *Sens. Actuators B*, 158 (2011) 214-222.
- [380] J. Legendziewicz and M. Borzechowska, *J. Alloys Compd.*, 300 (2000) 353-359.

- [381] S. X. Yan, J. H. Zhang, X. Zhang, S. Z. Lu, X. G. Ren, Z. G. Nie, and X. J. Wang, *J. Phys. Chem. C*, 111 (2007) 13256-13260.
- [382] R. B. Pode and S. J. Dhoble, *Physica Status Solidi B*, 203 (1997) 571-577.
- [383] G. Boulon, B. Moine, J. C. Bourcet, and F. Gaumemahn, *Bull. Am. Phys. Soc.*, 24 (1979) 901.
- [384] J. C. Bourcet, B. Moine, G. Boulon, R. Reisfeld, and Y. Kalisky, *Chem. Phys. Lett.*, 61 (1979) 23-24.
- [385] T. S. Chan, C. C. Kang, R. S. Liu, L. Chen, X. N. Liu, J. J. Ding, J. Bao, and C. Gao, *J. Comb. Chem.*, 9 (2007) 343-346.
- [386] G. Chen, Y. Shi, B. Li, N. Zhang, Y. Chi, and K. Dou, *J. Mater. Sci. Lett.*, 14 (1995) 1707-1709.
- [387] L. Chen, Y. Jiang, Y. G. Yang, J. Huang, J. Y. Shi, and S. F. Chen, *J. Phys. D*, 42 (2009) Article Number: 215104.
- [388] T. Y. Choi, Y. H. Song, Y. Y. Luo, K. Senthil, and D. H. Yoon, *J. Ceram. Process. Res.*, 12 (2011) S282-S285.
- [389] N. Dhananjaya, H. Nagabhushana, B. M. Nagabhushana, S. C. Sharma, B. Rudraswamy, N. Suriyamurthy, C. Shivakumara, and R. P. S. Chakradhar, *Appl. Phys. B*, 107 (2012) 503-511.
- [390] W. D. Fragoso, C. D. Donega, and R. L. Longo, *J. Lumin.*, 105 (2003) 97-103.
- [391] L. L. Han, Y. H. Wang, J. Zhang, and Y. Z. Wang, *Mater. Chem. Phys.*, 139 (2013) 87-91.
- [392] J. H. Hong, Z. G. Zhang, C. J. Cong, and K. L. Zhang, *J. Non-Cryst. Solids*, 353 (2007) 2431-2435.
- [393] M. N. Huang, Y. Y. Ma, X. Y. Huang, S. Ye, and Q. Y. Zhang, *Spectrochim. Acta A*, 115 (2013) 767-771.
- [394] G. F. Ju, Y. H. Hu, L. Chen, X. J. Wang, Z. F. Mu, H. Y. Wu, and F. W. Kang, *J. Electrochem. Soc.*, 158 (2011) J294-J299.
- [395] J. Lin and Q. Su, *High Temp. Mater. Sci.*, 36 (1996) 117-125.
- [396] B. N. Mahalley, S. J. Dhoble, R. B. Pode, and G. Alexander, *Appl. Phys. A*, 70 (2000) 39-45.
- [397] S. Qiang, C. Barthou, J. P. Denis, F. Pelle, and B. Blanzat, *J. Lumin.*, 28 (1983) 1-11.
- [398] U. Rambabu, N. R. Munirathnam, S. Chatterjee, B. S. Reddy, and S. D. Han, *Ceram. Int.*, 39 (2013) 4801-4811.

- [399] A. M. Ramirez, M. G. Hernandez, J. Y. Avila, A. G. Murillo, F. C. Romo, E. de la Rosa, V. G. Febles, and J. R. Miranda, *J. Mater. Res.*, 28 (2013) 1365-1371.
- [400] S. J. Sang, S. C. Lu, X. R. Qu, X. X. Yang, and L. L. Zhang, *Acta Phys. Sin.*, 61 (2012) Article Number: 227801.
- [401] A. D. Sontakke, A. Tarafder, K. Biswas, and K. Annapurna, *Physica B*, 404 (2009) 3525-3529.
- [402] A. V. Strel'tsov, V. P. Dmitrienko, T. A. Akmaeva, S. V. Kudryavtsev, A. O. Dmitrienko, and K. A. Razumov, *Inorg. Mater.*, 45 (2009) 889-893.
- [403] J. Y. Sun, J. B. Xian, Z. G. Xia, and H. Y. Du, *J. Lumin.*, 130 (2010) 1818-1824.
- [404] S. Takeshita, T. Isobe, T. Sawayama, and S. Niikura, *J. Lumin.*, 129 (2009) 1067-1072.
- [405] M. Q. Wang, X. P. Fan, and G. H. Xiong, *J. Phys. Chem. Solids*, 56 (1995) 859-862.
- [406] Q. Wang, Z. P. Ci, Y. H. Wang, G. Zhu, Y. Wen, B. T. Liu, and M. D. Que, *Acta Phys. Sin.*, 61 (2012) Article Number: 217802.
- [407] Z. L. Wang, H. B. Liang, M. L. Gong, and Q. Su, *Opt. Mater.*, 29 (2007) 896-900.
- [408] X. T. Wei, Y. H. Chen, X. R. Cheng, M. Yin, and W. Xu, *Appl. Phys. B*, 99 (2010) 763-768.
- [409] A. Xie, X. M. Yuan, Y. Shi, F. X. Wang, and J. J. Wang, *J. Am. Ceram. Soc.*, 92 (2009) 2254-2258.
- [410] G. B. Xie, *Chin. Phys. Lett.*, 30 (2013) Article Number: 087802.
- [411] W. Xu, C. R. Li, B. J. Chen, and Z. Q. Feng, *Acta Phys. Sin.*, 59 (2010) 1328-1332.
- [412] Y. N. Xue, F. Xiao, and Q. Y. Zhang, *Spectrochim. Acta A*, 78 (2011) 607-611.
- [413] Z. N. Yang, J. Li, J. B. Qiu, Z. W. Yang, Z. G. Song, R. F. Wang, X. Yu, Y. Yang, and D. C. Zhou, *Spectrosc. Spec. Anal.*, 33 (2013) 19-22.
- [414] M. L. Zhao, G. S. Li, L. S. Yang, and L. P. Li, *Nanosci. Nanotechnol. Lett.*, 5 (2013) 143-146.
- [415] H. Zhou, X. Yu, S. S. Qian, R. Shi, T. Wang, Q. Tang, P. H. Yang, Y. Yang, and J. B. Qiu, *Mater. Res. Bull.*, 48 (2013) 2396-2398.
- [416] H. K. Zhu, Z. G. Xia, H. K. Liu, R. Y. Mi, and Z. Hui, *Mater. Res. Bull.*, 48 (2013) 3513-3517.
- [417] N. F. Zhu, Y. X. Li, and X. F. Yu, *Chin. Phys. Lett.*, 25 (2008) 703-706.
- [418] G. Blasse and A. Bril, *J. Chem. Phys.*, 47 (1967) 1920-1926.

- [419] S. Z. Toma, F. F. Mikus, and J. E. Mathers, *J. Electrochem. Soc.*, 114 (1967) 953-955.
- [420] R. Reisfeld and N. Liebllich, *J. Electrochem. Soc.*, 121 (1974) 1338-1340.
- [421] A. G. Mirochnik, P. A. Zhikhareva, T. V. Sedakova, and V. E. Karasev, *Russian J. Phys. Chem. A*, 81 (2007) 297-300.
- [422] J. D. Axe and P. F. Weller, *J. Chem. Phys.*, 40 (1964) 3066-3069.
- [423] R. Reisfeld and L. Boehm, *J. Solid State Chem.*, 4 (1972) 417-424.
- [424] I. M. Azzouz and L. C. Klein, *Opt. Mater.*, 35 (2012) 292-296.
- [425] M. A. K. Elfayoumi, M. Farouk, M. G. Brik, and M. M. Elokr, *J. Alloys Compd.*, 492 (2010) 712-716.
- [426] G. Tripathi, V. K. Rai, and S. B. Rai, *Appl. Phys. B*, 84 (2006) 459-464.
- [427] H. Lin, D. L. Yang, G. S. Liu, T. C. Ma, B. Zhai, Q. D. An, J. Y. Yu, X. J. Wang, X. R. Liu, and E. Y. B. Pun, *J. Lumin.*, 113 (2005) 121-128.
- [428] P. R. Biju, G. Jose, V. Thomas, V. P. N. Nampoori, and N. V. Unnikrishnan, *Opt. Mater.*, 24 (2004) 671-677.
- [429] J. J. Velazquez, V. D. Rodriguez, A. C. Yanes, J. del Castillo, and J. Mendez-Ramos, *Appl. Phys. B*, 108 (2012) 577-583.
- [430] G. Tripathi, V. K. Rai, and S. B. Rai, *Opt. Commun.*, 264 (2006) 116-122.
- [431] P. L. Li, Z. Xu, S. L. Zhao, F. J. Zhang, and Y. S. Wang, *Mater. Res. Bull.*, 47 (2012) 3825-3829.
- [432] D. Kang, H. S. Yoo, S. H. Jung, H. Kim, and D. Y. Jeon, *J. Phys. Chem. C*, 115 (2011) 24334-24340.
- [433] Z. X. Fu, H. R. Zheng, and B. R. Liu, *Spectrosc. Spec. Anal.*, 31 (2011) 2183-2186.
- [434] Q. X. Li, J. P. Huang, and D. H. Chen, *J. Alloys Compd.*, 509 (2011) 1007-1010.
- [435] Y. C. Fang, S. Y. Chu, P. C. Kao, Y. M. Chuang, and Z. L. Zeng, *J. Electrochem. Soc.*, 158 (2011) J1-J5.
- [436] H. Y. Lin, Y. C. Fang, and S. Y. Chu, *J. Am. Ceram. Soc.*, 93 (2010) 3850-3856.
- [437] S. Hachani, B. Moine, A. El-akrmi, and M. Ferid, *J. Lumin.*, 130 (2010) 1774-1783.
- [438] J. P. Huang, Q. X. Li, and D. H. Chen, *Mater. Sci. Eng. B*, 172 (2010) 108-113.
- [439] E. Y. Lee and Y. J. Kim, *Electrochem. Solid St.*, 13 (2010) J110-J113.
- [440] Q. Wei and D. H. Chen, *Optics and Laser Technology*, 41 (2009) 783-787.

- [441] H. L. Zhu, E. Zhu, H. Yang, D. Jin, D. Yang, D. S. Li, and K. H. Yao, *J. Nanosci. Nanotechnol.*, 8 (2008) 1427-1431.
- [442] L. Q. An, J. Zhang, M. Liu, S. Chen, and S. W. Wang, *Opt. Mater.*, 30 (2008) 957-960.
- [443] Y. H. Won, H. S. Jang, W. Bin Im, and D. Y. Jeon, *J. Electrochem. Soc.*, 155 (2008) J226-J229.
- [444] V. Naresh and S. Buddhudu, *J. Lumin.*, 137 (2013) 15-21.
- [445] U. Caldino, E. Alvarez, A. Speghini, and M. Bettinelli, *J. Lumin.*, 135 (2013) 216-220.
- [446] R. Lisiecki, *J. Lumin.*, 143 (2013) 293-297.
- [447] M. Back, M. Boffelli, A. Massari, R. Marin, F. Enrichi, and P. Riello, *J. Nanopart. Res.*, 15 (2013) 1753-1-14.
- [448] W. W. Holloway, R. Newman, and M. Kestigian, *Phys. Rev. Lett.*, 11 (1963) 458-460.
- [449] P. R. Matthes, C. J. Holler, M. Mai, J. Heck, S. J. Sedlmaier, S. Schmiechen, C. Feldmann, W. Schnick, and K. Müller-Buschbaum, *J. Mater. Chem.*, 22 (2012) 10179-10187.
- [450] M. O. Rodrigues, J. D. L. Dutra, L. A. O. Nunes, G. F. de Sa, W. M. de Azevedo, P. Silva, F. A. A. Paz, R. O. Freire, and S. A. Junior, *J. Phys. Chem. C*, 116 (2012) 19951-19957.
- [451] L. Spaulding and H. G. Brittain, *Inorg. Chem.*, 22 (1983) 3486-3488.
- [452] L. Spaulding and H. G. Brittain, *J. Lumin.*, 28 (1983) 385-394.
- [453] H. G. Brittain, *Inorg. Chem.*, 18 (1979) 1740-1745.
- [454] H. G. Brittain, *J. Inorg. Nucl. Chem.*, 41 (1979) 561-565.
- [455] H. G. Brittain, *J. Lumin.*, 21 (1979) 43-51.
- [456] H. G. Brittain, *Inorg. Chem.*, 17 (1978) 2762-2766.
- [457] H. G. Brittain, *Inorg. Chem.*, 17 (1978) 2762-2766.
- [458] H. G. Brittain and F. S. Richardson, *J. Chem. Soc. Faraday Trans. II*, 73 (1977) 545-550.
- [459] S. E. Plush and T. Gunnlaugsson, *Dalton Trans.*, (2008) 3801-3804.
- [460] S. Lis, M. Elbanowski, B. Makowska, and Z. Hnatejko, *J. Photochem. Photobiol. A*, 150 (2002) 233-247.
- [461] W. J. Dong and C. D. Flint, *J. Chem. Soc. , Faraday Trans.*, 88 (1992) 2661-2665.

- [462] W. J. Dong and C. D. Flint, *J. Chem. Soc. , Faraday Trans.*, 88 (1992) 3435-3439.
- [463] S. Dai, W. Xu, D. H. Metcalf, and L. M. Toth, *Chem. Phys. Lett.*, 262 (1996) 315-320.
- [464] L. G. Deshazer and A. Y. Cabezas, *Proc. IEEE*, 52 (1964) 1355.
- [465] L. S. Fu, H. J. Zhang, S. B. Wang, Q. G. Meng, K. Y. Yang, and J. Z. Ni, *Chin. J. Chem.*, 17 (1999) 132-136.
- [466] G. H. Jia and P. A. Tanner, *J. Alloys Compd.*, 471 (2009) 557-560.
- [467] Y. Okamoto, Y. Ueba, I. Nagata, and E. Banks, *Macromolecules*, 14 (1981) 807-809.
- [468] E. A. Seregina, A. A. Seregin, and G. V. Tikhonov, *J. Alloys Compd.*, 341 (2002) 283-287.
- [469] S. P. Tanner and A. R. Vargenas, *Inorg. Chem.*, 20 (1981) 4384-4386.
- [470] R. Reisfeld, N. Lieblich, L. Boehm, and B. Barnett, *J. Lumin.*, 12 (1976) 749-753.
- [471] S. A. Nikitina and A. V. Stepanov, *Sov. Radiochem.*, 26 (1984) 755-758.
- [472] S. J. Lyle and N. A. Zatar, *Talanta*, 33 (1986) 355-357.
- [473] H. L. Guo, Y. Z. Zhu, S. L. Qiu, J. A. Lercher, and H. J. Zhang, *Adv. Mater.*, 22 (2010) 4190-4192.
- [474] J. L. Kropp, *J. Chem. Phys.*, 46 (1967) 843-847.
- [475] W. H. Fonger and C. W. Struck, *J. Chem. Phys.*, 52 (1970) 6364-6372.
- [476] M. D. Regulacio, M. H. Pablico, J. A. Vasquez, P. N. Myers, S. Gentry, M. Prushan, S. W. Tam-Chang, and S. L. Stoll, *Inorg. Chem.*, 47 (2008) 1512-1523.
- [477] W. M. Faustino, O. L. Malta, E. E. S. Teotonio, H. F. Brito, A. M. Simas, and G. F. de Sa, *J. Phys. Chem. A*, 110 (2006) 2510-2516.
- [478] G. K. Liu, M. P. Jensen, and P. M. Almond, *J. Phys. Chem. A*, 110 (2006) 2081-2088.
- [479] T. Kobayashi, H. Naruke, and T. Yamase, *Chem. Lett.*, (1997) 907-908.
- [480] G. D. R. Napier, J. D. Neilson, and T. M. Shepherd, *Chem. Phys. Lett.*, 31 (1975) 328-330.
- [481] M. T. Berry, P. S. May, and H. Xu, *J. Phys. Chem.*, 100 (1996) 9216-9222.
- [482] Y. Z. An, G. E. Schramm, and M. T. Berry, *J. Lumin.*, 97 (2002) 7-12.
- [483] S. Petoud, J.-C. G. Bünzli, T. Glanzman, C. Piguet, Q. Xiang, and R. P. Thummel, *J. Lumin.*, 82 (1999) 69-79.

- [484] R. Longo, F. R. G. E. Silva, and O. L. Malta, *Chem. Phys. Lett.*, 328 (2000) 67-74.
- [485] P. Gawryszewska, O. L. Malta, R. L. Longo, F. R. G. Silva, S. Alves, K. Mierzwicki, Z. Latajka, M. Pietraszkiewicz, and J. Legendziewicz, *ChemPhysChem*, 5 (2004) 1577-1584.
- [486] W. M. Faustino, O. L. Malta, and G. F. de Sa, *J. Chem. Phys.*, 122 (2005) Article Number: 054109.
- [487] L. S. Villata, E. Wolcan, M. R. Feliz, and A. L. Capparelli, *J. Phys. Chem. A*, 103 (1999) 5661-5666.
- [488] T. D. Pasatoiu, A. M. Madalan, M. U. Kumke, C. Tiseanu, and M. Andruh, *Inorg. Chem.*, 49 (2010) 2310-2315.
- [489] K. H. Hellwege and H. G. Kahle, *Z. Phys.*, 129 (1951) 62-84.
- [490] C. Brecher, H. Samelson, R. Riley, and A. Lempicki, *J. Chem. Phys.*, 49 (1968) 3303-3311.
- [491] A. K. Banerjee, A. K. Mukhopadhyay, R. K. Mukherjee, and M. Chowdhury, *Chem. Phys. Lett.*, 67 (1979) 418-419.
- [492] K. Binnemans and C. Görller-Walrand, *J. Chem. Soc. , Faraday Trans.*, 92 (1996) 2487-2493.
- [493] K. Binnemans and C. Görller-Walrand, *J. Phys. Condens. Matter.*, 9 (1997) 1637-1648.
- [494] K. H. Hellwege, S. Huefner, and J. Pelzl, *Z. Phys.*, 203 (1967) 227-234.
- [495] J. Chrysochoos, *J. Chem. Phys.*, 60 (1974) 1110-1112.
- [496] R. D. Peacock, *J. Chem. Phys.*, 61 (1974) 2483.
- [497] A. Ellens, H. Andres, M. L. H. terHeerdt, R. T. Wegh, A. Meijerink, and G. Blasse, *J. Lumin.*, 66-7 (1995) 240-243.
- [498] A. Ellens, H. Andres, A. Meijerink, and G. Blasse, *Phys. Rev. B*, 55 (1997) 173-179.
- [499] A. Ellens, H. Andres, M. L. H. terHeerdt, R. T. Wegh, A. Meijerink, and G. Blasse, *Phys. Rev. B*, 55 (1997) 180-186.
- [500] J. A. Koningstein, *Phys. Rev. A*, 136 (1964) A717-A725.
- [501] J. A. Koningstein, *J. Chem. Phys.*, 42 (1965) 1423-1428.
- [502] N. Vijaya and C. K. Jayasankar, *J. Mol. Struct.*, 1036 (2013) 42-50.
- [503] K. Linganna and C. K. Jayasankar, *Spectrochim. Acta A*, 97 (2012) 788-797.
- [504] K. U. Kumar, S. S. Babu, C. S. Rao, and C. K. Jayasankar, *Opt. Commun.*, 284 (2011) 2909-2914.

- [505] C. S. Rao, K. U. Kumar, and C. K. Jayasankar, *Solid State Sci.*, 13 (2011) 1309-1314.
- [506] G. Geier and C. K. Jorgensen, *Chem. Phys. Lett.*, 9 (1971) 263-265.
- [507] N. Graepi, D. H. Powell, G. Laurency, L. Zekany, and A. E. Merbach, *Inorg. Chim. Acta*, 235 (1995) 311-326.
- [508] F. A. Dunand and A. E. Merbach, *Inorg. Chem. Commun.*, 4 (2001) 719-722.
- [509] M. Polasek, J. Kotek, P. Hermann, I. Cisarova, K. Binnemans, and I. Lukes, *Inorg. Chem.*, 48 (2009) 466-475.
- [510] F. Yerly, F. A. Dunand, E. Toth, A. Figueirinha, Z. Kovacs, A. D. Sherry, C. F. G. C. Geraldes, and A. E. Merbach, *Eur. J. Inorg. Chem.*, (2000) 1001-1006.
- [511] B. R. Judd, *Proc. Roy. Soc. London Ser. A*, 228 (1955) 120-128.
- [512] J. Halwani, J. D'Expert-Ghys, B. Piriou, and P. Caro, *Analisis*, 15 (1987) 299-305.
- [513] K. Binnemans and C. Görlner-Walrand, *J. Alloys Compd.*, 250 (1997) 326-331.
- [514] M. Karbowski and A. Mondry, *Chem. Phys.*, 354 (2008) 86-93.
- [515] P. Solarz and Z. Gajek, *J. Phys. Chem. C*, 114 (2010) 10937-10946.
- [516] J. D'Expert-Ghys, J. Halwani, and B. Piriou, *Inorg. Chim. Acta*, 139 (1987) 303-306.
- [517] J. L. Ryan and C. K. Jorgensen, *J. Phys. Chem.*, 70 (1966) 2845-&.
- [518] P. Dorenbos, *J. Phys. Condens. Matter.*, 15 (2003) 8417-8434.
- [519] P. Dorenbos, *J. Lumin.*, 111 (2005) 89-104.
- [520] P. Dorenbos, *ECS J. Solid State Sci. Technol.*, 2 (2013) R3001-R3011.
- [521] J. L. Ryan, *Inorg. Chem.*, 8 (1969) 2053-2058.
- [522] G. Blasse, *Struct. Bond.*, 26 (1976) 43-79.
- [523] G. Blasse, *J. Solid State Chem.*, 4 (1972) 52-54.
- [524] L. Li and S. Y. Zhang, *J. Phys. Chem. B*, 110 (2006) 21438-21443.
- [525] L. Li, S. H. Zhou, and S. Y. Zhang, *J. Phys. Chem. C*, 111 (2007) 3205-3210.
- [526] G. Blasse, *J. Phys. Chem. Solids*, 50 (1989) 99.
- [527] C. W. Struck and W. H. Fonger, *J. Lumin.*, 1-2 (1970) 456-469.
- [528] W. M. Faustino, O. L. Malta, and G. F. de Sa, *Chem. Phys. Lett.*, 429 (2006) 595-599.

- [529] G. Blasse, M. Buys, and N. Sabbatini, *Chem. Phys. Lett.*, 124 (1986) 538-542.
- [530] T. Grzyb, M. Weclawiak, J. Rozowska, and S. Lis, *J. Alloys Compd.*, 576 (2013) 345-349.
- [531] T. Grzyb, M. Weclawiak, T. Pedzinski, and S. Lis, *Opt. Mater.*, 35 (2013) 2226-2233.
- [532] R. T. Wegh, A. Meijerink, R. J. Lamminmaki, and J. Hölsä, *J. Lumin.*, 87-9 (2000) 1002-1004.
- [533] L. Y. Jia, Z. B. Shao, Q. Li, Y. W. Tian, and J. F. Han, *Optics and Laser Technology*, 54 (2013) 79-83.
- [534] F. Zhang and Y. H. Wang, *J. Electrochem. Soc.*, 156 (2009) J258-J262.
- [535] J. Legendziewicz, M. Guzik, and J. Cybinska, *Opt. Mater.*, 31 (2009) 567-574.
- [536] Y. H. Wang, X. Guo, T. Endo, Y. Murakami, and M. Ushirozawa, *J. Solid State Chem.*, 177 (2004) 2242-2248.
- [537] H. B. Liang, Y. Tao, Q. Su, and S. B. Wang, *J. Solid State Chem.*, 167 (2002) 435-440.
- [538] H. B. Liang, Q. Su, Y. Tao, T. D. Hu, and T. Liu, *J. Alloys Compd.*, 334 (2002) 293-298.
- [539] Y. H. Wang, K. Uheda, H. Takizawa, U. Mizumoto, and T. Endo, *J. Electrochem. Soc.*, 148 (2001) G430-G433.
- [540] C. H. Lu, W. T. Hsu, and B. M. Cheng, *J. Appl. Phys.*, 100 (2006) 063535.
- [541] M. J. Weber, *Phys. Rev.*, 157 (1967) 262-272.
- [542] W. D. Horrocks and J. M. Tingey, *Biochemistry*, 27 (1988) 413-419.
- [543] S. Jain, J. T. Welch, W. D. Horrocks, and S. J. Franklin, *Inorg. Chem.*, 42 (2003) 8098-8104.
- [544] C. W. Mcnemar and W. D. Horrocks, *Biochim. Biophys. Acta*, 1040 (1990) 229-236.
- [545] A. L. Feig, M. Panek, W. D. Horrocks, and O. C. Uhlenbeck, *Chem. Biol.*, 6 (1999) 801-810.
- [546] S. L. Wu, S. J. Franklin, K. N. Raymond, and W. D. Horrocks, *Inorg. Chem.*, 35 (1996) 162-167.
- [547] D. A. Voss, E. R. Farquhar, W. D. Horrocks, and J. R. Morrow, *Inorg. Chim. Acta*, 357 (2004) 859-863.
- [548] J. J. Lessmann and W. D. Horrocks, *Inorg. Chem.*, 39 (2000) 3114-3124.

- [549] M. Albin, A. C. Goldstone, A. S. Withers, and W. D. Horrocks, *Inorg. Chem.*, 22 (1983) 3182-3184.
- [550] M. Albin, B. M. Cader, and W. D. Horrocks, *Inorg. Chem.*, 23 (1984) 3045-3050.
- [551] S. L. Wu and W. D. Horrocks, *J. Chem. Soc. Dalton Trans.*, (1997) 1497-1502.
- [552] S. L. Wu and W. D. Horrocks, *Anal. Chem.*, 68 (1996) 394-401.
- [553] S. L. Wu and W. D. Horrocks, *Inorg. Chem.*, 34 (1995) 3724-3732.
- [554] S. T. Frey, C. A. Chang, J. F. Carvalho, A. Varadarajan, L. M. Schultze, K. L. Pounds, and W. D. Horrocks, *Inorg. Chem.*, 33 (1994) 2882-2889.
- [555] B. Marmodee, K. Jahn, F. Ariese, C. Gooijer, and M. U. Kumke, *J. Phys. Chem. A*, 114 (2010) 13050-13054.
- [556] L. Tilkens, K. Randall, J. Sun, M. T. Berry, P. S. May, and T. Yamase, *J. Phys. Chem. A*, 108 (2004) 6624-6628.
- [557] G. Blasse, *Inorg. Chim. Acta*, 167 (1990) 33-37.
- [558] G. Blasse, *Int. Rev. Phys. Chem.*, 11 (1992) 71-100.
- [559] S. Hubert and P. Thouvenot, *J. Lumin.*, 54 (1992) 103-111.
- [560] T. R. Faulkner and F. S. Richardson, *Mol. Phys.*, 35 (1978) 1141-1161.
- [561] A. Ellens, S. Schenker, A. Meijerink, and G. Blasse, *J. Lumin.*, 69 (1996) 1-15.
- [562] A. Ellens, S. Schenker, A. Meijerink, and G. Blasse, *J. Lumin.*, 72-4 (1997) 183-184.
- [563] A. Ellens, B. Salemink, and A. Meijerink, *J. Solid State Chem.*, 136 (1998) 206-209.
- [564] T. R. Faulkner and F. S. Richardson, *Mol. Phys.*, 38 (1979) 1165-1178.
- [565] V. Tsaryuk, V. Zolin, and J. Legendziewicz, *Spectrochim. Acta A*, 54 (1998) 2247-2254.
- [566] V. Tsaryuk, J. Legendziewicz, L. Puntus, V. Zolin, and J. Sokolnicki, *J. Alloys Compd.*, 300 (2000) 464-470.
- [567] V. Tsaryuk, V. Zolin, L. Puntus, V. Savchenko, J. Legendziewicz, J. Sokolnicki, and R. Szostak, *J. Alloys Compd.*, 300 (2000) 184-192.
- [568] M. T. Berry, A. F. Kirby, and F. S. Richardson, *Mol. Phys.*, 66 (1989) 723-746.
- [569] G. Oczko and P. Starynowicz, *J. Mol. Struct.*, 740 (2005) 237-248.
- [570] J. R. G. Thorne, M. Jones, C. S. Mccaw, K. M. Murdoch, R. G. Denning, and N. M. Khaidukov, *J. Phys. Condens. Matter.*, 11 (1999) 7851-7866.

- [571] R. G. Denning, *Eur. J. Solid State Inorg. Chem.*, 28 (1991) 33-45.
- [572] L. E. Kholodenkov, A. G. Makhanev, and A. A. Kaminskii, *Physica Status Solidi B*, 126 (1984) 659-667.
- [573] L. E. Kholodenkov and A. G. Makhanev, *Physica Status Solidi B*, 120 (1983) K5-K8.
- [574] N. M. Khaidukov, X. Zhang, and J. P. Jouart, *J. Lumin.*, 72-4 (1997) 213-214.
- [575] L. E. Kholodenkov and A. G. Makhanev, *Physica Status Solidi B*, 125 (1984) 365-374.
- [576] J. Holsa, *Chem. Phys. Lett.*, 112 (1984) 246-248.
- [577] L. X. Ning, S. D. Xia, and P. A. Tanner, *J. Phys. Condens. Matter.*, 14 (2002) 8677-8685.
- [578] L. X. Ning, D. Y. Wang, S. D. Xia, J. R. G. Thorne, and P. A. Tanner, *J. Phys. Condens. Matter.*, 14 (2002) 3833-3843.
- [579] X. Y. Fu, G. S. Shao, R. C. Han, Y. Ma, F. M. Xue, F. Yang, L. M. Fu, J. P. Zhang, and Y. Wang, *Acta Phys. -Chim. Sin.*, 28 (2012) 2480-2486.
- [580] M. Shi, H. Li, M. Pan, F. F. Su, L. L. Ma, P. G. Han, and H. Z. Wang, *Chin. Opt. Lett.*, 9 (2011).
- [581] W. S. Lo, W. M. Kwok, G. L. Law, C. T. Yeung, C. T. L. Chan, H. L. Yeung, H. K. Kong, C. H. Chen, M. B. Murphy, K. L. Wong, and W. T. Wong, *Inorg. Chem.*, 50 (2011) 5309-5311.
- [582] S. V. Eliseeva, G. Aubock, F. van Mourik, A. Cannizzo, B. Song, E. Deiters, A. S. Chauvin, M. Chergui, and J.-C. G. Bünzli, *J. Phys. Chem. B*, 114 (2010) 2932-2937.
- [583] R. Hao, M. Li, Y. Wang, J. Zhang, Y. Ma, L. Fu, X. Wen, Y. Wu, X. Ai, S. Zhang, and Y. Wei, *Adv. Funct. Mater.*, 17 (2007) 3663-3669.
- [584] A. D'Aleo, G. Pompidor, B. Elena, J. Vicat, P. L. Baldeck, L. Toupet, R. Kahn, C. Andraud, and O. Maury, *ChemPhysChem*, 8 (2007) 2125-2132.
- [585] L. O. Palsson, R. Pal, B. S. Murray, D. Parker, and A. Beeby, *Dalton Trans.*, (2007) 5726-5734.
- [586] C. Andraud and O. Maury, *Eur. J. Inorg. Chem.*, (2009) 4357-4371.
- [587] K. H. Hellwege, U. Johnsen, H. G. Kahle, and G. Schaack, *Z. Phys.*, 148 (1957) 112-127.
- [588] H. G. Kahle, *Z. Phys.*, 155 (1959) 145-156.
- [589] H. G. Kahle, *Z. Phys.*, 155 (1959) 157-169.
- [590] J. P. R. Wells and R. J. Reeves, *Phys. Rev. B*, 64 (2001) Article Number: 035102.

- [591] Y. Han, G. Du, J. Han, X. Kan, and L. Li, *J. Low Temp. Phys.*, 170 (2013) 430-435.
- [592] W. Jiang, J. P. Zhang, W. B. Chen, P. Chen, J. B. Han, B. B. Xu, S. H. Zheng, Q. B. Guo, X. F. Liu, and J. R. Qiu, *J. Appl. Phys.*, 116 (2014) Article Number 123103.
- [593] K. Binnemans and C. Görller-Walrand, *J. Rare Earths*, 16 (1998) 204-210.
- [594] L. Fluyt, P. Verhoeven, H. Lambaerts, K. Binnemans, and C. Görller-Walrand, *J. Alloys Compd.*, 207 (1994) 51-54.
- [595] U. V. Valiev, J. B. Gruber, D. J. Fu, V. O. Pelenovich, G. W. Burdick, and M. E. Malysheva, *J. Rare Earths*, 29 (2011) 776-782.
- [596] J. B. Gruber, U. V. Valiev, G. W. Burdick, S. A. Rakhimov, M. Pokhrel, and D. K. Sardar, *J. Lumin.*, 131 (2011) 1945-1952.
- [597] C. Görller-Walrand and L. Fluyt, in: K. A. Gschneidner jr., J.-C. G. Bünzli, and V. K. Pecharsky (Eds.), *Handbook on the Physics and Chemistry of Rare Earths*, Vol. 40, Elsevier, Amsterdam, 2010, pp. 1-107.
- [598] C. Görller-Walrand, P. Verhoeven, J. D'Olieslager, L. Fluyt, and K. Binnemans, *J. Chem. Phys.*, 101 (1994) 7189.
- [599] C. Görller-Walrand and K. Binnemans, *Bull. Soc. Chim. Belg.*, 106 (1997) 685-689.
- [600] C. Görller-Walrand and J. Godemont, *J. Chem. Phys.*, 66 (1977) 48-50.
- [601] C. Görller-Walrand and J. Godemont, *J. Chem. Phys.*, 67 (1977) 3655-3658.
- [602] C. Görller-Walrand, *Chem. Phys. Lett.*, 115 (1985) 333-334.
- [603] C. Görller-Walrand and P. Vandeveld, *Bull. Soc. Chim. Belg.*, 94 (1985) 873-882.
- [604] C. Görller-Walrand, M. Behets, P. Porcher, and I. Laursen, *J. Chem. Phys.*, 83 (1985) 4329-4337.
- [605] C. Görller-Walrand, L. Fluyt, and V. Dirckx, *Eur. J. Solid State Inorg. Chem.*, 28 (1991) 201-208.
- [606] C. Görller-Walrand and L. Fluyt-Adriaens, *J. Less-Common Met.*, 112 (1985) 175-191.
- [607] J. P. Riehl and F. S. Richardson, *J. Chem. Phys.*, 66 (1977) 1988-1998.
- [608] F. S. Richardson and H. G. Brittain, *J. Am. Chem. Soc.*, 103 (1981) 18-24.
- [609] D. R. Foster and F. S. Richardson, *Inorg. Chem.*, 22 (1983) 3996-4002.
- [610] D. R. Foster, F. S. Richardson, L. M. Vallarino, and D. Shillady, *Inorg. Chem.*, 22 (1983) 4002-4009.
- [611] E. M. Stephens, D. R. Foster, and F. S. Richardson, *J. Less-Common Met.*, 126 (1986) 389-394.

- [612] R. Schultheiss and G. Gliemann, *J. Lumin.*, 35 (1986) 261-266.
- [613] M. Morita, K. Sawabe, E. Nishimura, and K. Eguchi, *J. Lumin.*, 40-1 (1988) 889-890.
- [614] M. Morita, T. Ozawa, and T. Tsubomura, *J. Lumin.*, 53 (1992) 495-498.
- [615] G. Blasse, G. J. Dirksen, and J. P. M. Vanvliet, *Inorg. Chim. Acta*, 142 (1988) 165-168.
- [616] P. Caro, O. K. Moune, E. Antic-Fidancev, and M. Lemaitre-Blaise, *J. Less-Common Met.*, 112 (1985) 153-173.
- [617] P. Caro, *J. Less-Common Met.*, 126 (1986) 239-245.
- [618] G. A. Prinz, *Phys. Lett.*, 20 (1966) 323-324.
- [619] G. A. Prinz, *Phys. Rev.*, 152 (1966) 474-481.
- [620] A. Seminara and A. Musumeci, *Inorg. Chim. Acta*, 95 (1984) 291-307.
- [621] M. T. Harrison and R. G. Denning, *J. Lumin.*, 69 (1996) 265-285.
- [622] M. T. Harrison, R. G. Denning, and S. T. Davey, *J. Non-Cryst. Solids*, 184 (1995) 286-291.
- [623] P. Babu, K. H. Jang, H. J. Seo, and C. K. Jayasankar, *J. Appl. Phys.*, 99 (2006).
- [624] S. S. Babu, P. Babu, C. K. Jayasankar, W. Sievers, T. Troster, and G. Wortmann, *J. Lumin.*, 126 (2007) 109-120.
- [625] C. Brecher and L. A. Riseberg, *Phys. Rev. B*, 21 (1980) 2607-2618.
- [626] S. P. Feofilov, K. S. Hong, R. S. Meltzer, W. Jia, and H. Liu, *Phys. Rev. B*, 60 (1999) 9406-9409.
- [627] H. Inoue, K. Soga, and A. Makishima, *J. Non-Cryst. Solids*, 222 (1997) 212-220.
- [628] V. Lavin, P. Babu, C. K. Jayasankar, I. R. Martin, and V. D. Rodriguez, *J. Chem. Phys.*, 115 (2001) 10935-10944.
- [629] V. Lavin, I. R. Martin, U. R. Rodriguez-Mendoza, and V. D. Rodriguez, *J. Phys. Condens. Matter.*, 11 (1999) 8739-8747.
- [630] C. Mancuso, J. A. Capobianco, A. Speghini, and M. Bettinelli, *Philos. Mag. B*, 82 (2002) 587-596.
- [631] G. Nishimura and T. Kushida, *Phys. Rev. B*, 37 (1988) 9075-9078.
- [632] R. Rolli, G. Samoggia, M. Bettinelli, A. Speghini, and M. Wachtler, *J. Non-Cryst. Solids*, 288 (2001) 114-120.

- [633] R. Rolli, G. Samoggia, G. Ingletto, M. Bettinelli, and A. Speghini, *Mater. Res. Bull.*, 35 (2000) 1227-1234.
- [634] R. Rolli, P. Camagni, G. Samoggia, A. Speghini, M. Wachtler, and M. Bettinelli, *Spectrochim. Acta A*, 54 (1998) 2157-2162.
- [635] V. P. Tuyen, T. Hayakawa, M. Nogami, J. R. Duclere, and P. Thomas, *J. Solid State Chem.*, 183 (2010) 2714-2719.
- [636] V. Venkatramu, D. Navarro-Urrios, P. Babu, C. K. Jayasankar, and V. Lavin, *J. Non-Cryst. Solids*, 351 (2005) 929-935.
- [637] G. Cormier, J. A. Capobianco, and C. A. Morrison, *J. Chem. Soc. , Faraday Trans.*, 90 (1994) 755-762.
- [638] V. Venkatramu, P. Babu, and C. K. Jayasankar, *Spectrochim. Acta A*, 63 (2006) 276-281.
- [639] D. Saurel, V. K. Tikhomirov, V. V. Moshchalkov, C. Görrler-Walrand, and K. Driesen, *J. Lumin.*, 129 (2009) 1575-1577.
- [640] C. E. Secu, C. Bartha, S. Polosan, and M. Secu, *J. Lumin.*, 146 (2014) 539-543.
- [641] C. E. Secu, R. F. Negrea, and M. Secu, *Opt. Mater.*, 35 (2013) 2456-2460.
- [642] C. Bensalem, M. Mortier, D. Vivien, and M. Diaf, *Opt. Mater.*, 33 (2011) 791-798.
- [643] M. Secu, C. E. Secu, S. Polosan, G. Aldica, and C. Ghica, *J. Non-Cryst. Solids*, 355 (2009) 1869-1872.
- [644] K. Driesen, V. K. Tikhomirov, and C. Görrler-Walrand, *J. Appl. Phys.*, 102 (2007) 024312-1-7.
- [645] Y. L. Yu, F. Y. Weng, D. Q. Chen, P. Huang, and Y. S. Wang, *J. Appl. Phys.*, 107 (2010) 093504.
- [646] N. A. Stump, G. K. Schweitzer, L. L. Pesterfield, J. R. Peterson, and G. M. Murray, *Spectrosc. Lett.*, 25 (1992) 1421-1432.
- [647] N. A. Stump, G. K. Schweitzer, G. M. Murray, and J. R. Peterson, *J. Lumin.*, 60-61 (1994) 104-107.
- [648] G. M. Murray, L. L. Pesterfield, N. A. Stump, and G. K. Schweitzer, *Inorg. Chem.*, 28 (1989) 1994-1998.
- [649] L. L. Pesterfield, N. A. Stump, G. K. Schweitzer, and J. R. Peterson, *J. Alloys Compd.*, 180 (1992) 201-207.
- [650] L. L. Pesterfield, N. A. Coker, and N. A. Stump, *Spectrosc. Lett.*, 33 (2000) 585-594.
- [651] G. M. Murray, R. V. Sarrío, and J. R. Peterson, *Inorg. Chim. Acta*, 176 (1990) 233-240.

- [652] S. P. Sinha, *J. Inorg. Nucl. Chem.*, 28 (1966) 189-193.
- [653] H. Bauer, J. Blanc, and D. L. Ross, *J. Am. Chem. Soc.*, 86 (1964) 5125-5131.
- [654] G. H. Jia, P. A. Tanner, C. K. Duan, and J. D'Expert-Ghys, *J. Phys. Chem. C*, 114 (2010) 2769-2775.
- [655] C. J. Jia, L. D. Sun, L. P. You, X. C. Jiang, F. Luo, Y. C. Pang, and C. H. Yan, *J. Phys. Chem. B*, 109 (2005) 3284-3290.
- [656] Y. Hui, Y. Zhao, S. M. Zhao, L. J. Gu, X. Z. Fan, L. Zhu, B. L. Zou, Y. Wang, and X. Q. Cao, *J. Alloys Compd.*, 573 (2013) 177-181.
- [657] M. Yin, J. C. Krupa, E. Antic-Fidancev, and A. Lorriaux-Rubbens, *Phys. Rev. B*, 61 (2000) 8073-8080.
- [658] S. K. Gupta, M. K. Bhide, S. V. Godbole, and V. Natarajan, *J. Am. Ceram. Soc.*, 97 (2014) 3694-3701.
- [659] J. E. Munoz-Santiuste, U. R. Rodriguez-Mendoza, J. Gonzalez-Platas, and V. Lavin, *J. Chem. Phys.*, 130 (2009) Article Number: 154501.
- [660] R. Kuroda, S. F. Mason, and C. Rosini, *J. Chem. Soc. Faraday Trans. II*, 77 (1981) 2125-2140.
- [661] B. R. Judd, *J. Chem. Phys.*, 70 (1979) 4830-4833.
- [662] K. Binnemans, in: K. A. Gschneidner jr., J.-C. G. Bünzli, and V. K. Pecharsky (Eds.), *Handbook on the Physics and Chemistry of Rare Earths*, Vol. 35. Elsevier, Amsterdam, 2005, pp. 107-272.
- [663] D. L. Kepert, in: S. J. Lippard (Ed.), *Progress in Inorganic Chemistry*, Vol. 23. John Wiley & Sons, Inc., Hoboken, NJ, USA, 1977, pp. 1-65.
- [664] A. E. V. Gorden, J. D. Xu, K. N. Raymond, and P. Durbin, *Chem. Rev.*, 103 (2003) 4207-4282.
- [665] M. Seitz, A. G. Oliver, and K. N. Raymond, *J. Am. Chem. Soc.*, 129 (2007) 11153-11160.
- [666] J. Xu, D. G. Churchill, M. Botta, and K. N. Raymond, *Inorg. Chem.*, 43 (2004) 5492-5494.
- [667] K. Miyata, T. Nakagawa, R. Kawakami, Y. Kita, K. Sugimoto, T. Nakashima, T. Harada, T. Kawai, and Y. Hasegawa, *Chem. Eur. J.*, 17 (2011) 521-528.
- [668] X. G. Zhao, K. Wang, T. T. Yan, Y. Yan, B. Zou, J. H. Yu, and R. R. Xu, *Chin. J. Chem.*, 30 (2012) 2066-2072.
- [669] R. Marin, G. Sponchia, E. Zucchetta, P. Riello, F. Enrichi, G. De Portu, and A. Benedetti, *J. Am. Ceram. Soc.*, 96 (2013) 2628-2635.

- [670] G. Chen, R. G. Haire, J. R. Peterson, and M. M. Abraham, *J. Phys. Chem. Solids*, 55 (1994) 313-316.
- [671] G. Chen, N. A. Stump, R. G. Haire, and J. R. Peterson, *J. Alloys Compd.*, 181 (1992) 503-509.
- [672] G. Chen, J. Hölsä, and J. R. Peterson, *J. Phys. Chem. Solids*, 58 (1997) 2031-2037.
- [673] N. A. Stump, G. Chen, R. G. Haire, and J. R. Peterson, *Appl. Spectrosc.*, 47 (1993) 1951-1952.
- [674] M. Maczka, W. Paraguassu, A. G. Souza, P. T. C. Freire, J. Mendes, and J. Hanuza, *Phys. Rev. B*, 77 (2008) 094137-1-9.
- [675] C. L. Lin, Y. C. Li, X. D. Li, R. Li, J. F. Lin, and J. Liu, *J. Appl. Phys.*, 114 (2013) Article Number: 163521.
- [676] C. Gong, Q. J. Li, R. Liu, Y. Hou, J. X. Wang, X. T. Dong, B. Liu, X. Yang, Z. Yao, X. Tan, D. M. Li, J. Liu, Z. Q. Chen, B. Zou, T. Cui, and B. B. Liu, *Phys. Chem. Chem. Phys.*, 15 (2013) 19925-19931.
- [677] G. Chen, N. A. Stump, R. G. Haire, and J. R. Peterson, *Solid State Commun.*, 89 (1994) 1005-1008.
- [678] V. Lavin, T. Troster, U. R. Rodriguez-Mendoza, I. R. Martin, and V. D. Rodriguez, *High Pressure Res.*, 22 (2002) 111-114.
- [679] D. Machon, V. P. Dmitriev, V. V. Sinitsyn, and G. Lucazeau, *Phys. Rev. B*, 70 (2004) 094117-1-10.
- [680] C. C. Zhang, Z. M. Zhang, R. C. Dai, Z. P. Wang, and Z. J. Ding, *J. Nanosci. Nanotechnol.*, 11 (2011) 9887-9891.
- [681] R. C. Dai, Z. M. Zhang, C. C. Zhang, and Z. J. Ding, *J. Nanosci. Nanotechnol.*, 10 (2010) 7629-7633.
- [682] Q. G. Zeng, G. T. Yang, F. Chen, J. Y. Luo, Z. M. Zhang, C. W. Leung, Z. J. Ding, and Y. Q. Sheng, *High Pressure Res.*, 33 (2013) 734-744.
- [683] H. S. Yuan, K. Wang, S. R. Li, X. Tan, Q. Li, T. T. Yan, B. Y. Cheng, K. Yang, B. B. Liu, G. T. Zou, and B. Zou, *J. Phys. Chem. C*, 116 (2012) 24837-24844.
- [684] Q. G. Zeng, Z. J. Ding, B. F. Lei, Y. Q. Sheng, and Z. M. Zhang, *High Pressure Res.*, 32 (2012) 412-418.
- [685] Z. Zhao, Q. G. Zeng, Z. M. Zhang, and Z. J. Ding, *J. Lumin.*, 122 (2007) 862-865.
- [686] R. C. Dai, Z. P. Wang, Z. M. Zhang, and Z. J. Ding, *J. Rare Earths*, 28 (2010) 241-245.
- [687] Y. B. Chi, S. X. Liu, Q. P. Wang, and L. Z. Wang, *Physica B*, 245 (1998) 293-300.

- [688] X. G. Zhao, T. T. Yan, K. Wang, Y. Yan, B. Zou, J. H. Yu, and R. R. Xu, *Eur. J. Inorg. Chem.*, (2012) 2527-2532.
- [689] G. Chen, N. A. Stump, R. G. Haire, J. R. Peterson, and M. M. Abraham, *J. Phys. Chem. Solids*, 53 (1992) 1253-1257.
- [690] G. Chen, R. G. Haire, and J. R. Peterson, *J. Solid State Chem.*, 102 (1993) 126-131.
- [691] S. S. Liu, Y. B. Chi, and L. H. Wang, *J. Lumin.*, 40-1 (1988) 395-396.
- [692] C. X. Guo, B. Li, Y. F. He, and H. B. Cui, *J. Lumin.*, 48-9 (1991) 489-493.
- [693] Y. B. Chi, S. X. Liu, H. N. Li, X. Y. Zhao, and L. Z. Wang, *Acta Phys. Sin. Ov. Ed.*, 6 (1997) 429-439.
- [694] Q. P. Wang, L. J. Lun, D. Z. Zhang, Y. B. Chi, and L. Z. Wang, *J. Phys. Condens. Matter.*, 4 (1992) 6491-6500.
- [695] J. Zhang, H. Cui, P. F. Zhu, C. L. Ma, X. X. Wu, H. Y. Zhu, Y. Z. Ma, and Q. L. Cui, *J. Appl. Phys.*, 115 (2014) 023502.
- [696] A. Kuznetsov, A. Laisaar, and J. Kikas, *Phys. Scr.*, T157 (2013) 014016.
- [697] Y. Zhao, C. L. Ma, F. X. Huang, C. J. Wang, S. M. Zhao, Q. L. Cui, X. Q. Cao, and F. F. Li, *J. Appl. Phys.*, 114 (2013) 073502.
- [698] M. Laberge, D. J. Simkin, G. Boulon, and A. Monteil, *J. Lumin.*, 55 (1993) 159-166.
- [699] M. Laberge, D. J. Simkin, and B. Dunn, *Chem. Phys. Lett.*, 182 (1991) 159-164.
- [700] M. Buijs, A. Meyerink, and G. Blasse, *J. Lumin.*, 37 (1987) 9-20.
- [701] A. Nonat, M. Regueiro-Figueroa, D. Esteban-Gomez, A. de Blas, T. Rodriguez-Blas, C. Platas-Iglesias, and L. J. Charbonniere, *Chem. Eur. J.*, 18 (2012) 8163-8173.
- [702] A. Zaim, S. V. Eliseeva, L. Guenee, H. Nozary, S. Petoud, and C. Piguet, *Chem. Eur. J.*, 20 (2014) 12172-12182.
- [703] R. E. White and T. P. Hanusa, *Organometallics*, 25 (2006) 5621-5630.
- [704] W. J. Evans, J. H. Meadows, A. G. Kostka, and G. L. Closs, *Organometallics*, 4 (1985) 324-326.
- [705] M. W. Loble, M. Casimiro, D. T. Thielemann, P. Ona-Burgos, I. Fernandez, P. W. Roesky, and F. Breher, *Chem. Eur. J.*, 18 (2012) 5325-5334.
- [706] P. Nockemann, B. Thijs, K. Lunstroot, T. N. Parac-Vogt, C. Görlner-Walrand, K. Binnemans, K. Van Hecke, L. Van Meervelt, S. Nikitenko, J. Daniels, C. Hennig, and R. Van Deun, *Chem. Eur. J.*, 15 (2009) 1449-1461.
- [707] C. Gaillard, I. Billard, A. Chaumont, S. Mekki, A. Ouadi, M. A. Denecke, G. Moutiers, and G. Wipff, *Inorg. Chem.*, 44 (2005) 8355-8367.

- [708] T. Stumpf, H. Curtius, C. Walther, K. Dardenne, K. Ufer, and T. Fanghanel, *Environ. Sci. Technol.*, 41 (2007) 3186-3191.
- [709] J. Jing, B. P. Burton-Pye, L. C. Francesconi, and M. R. Antonio, *Inorg. Chem.*, 47 (2008) 6889-6899.
- [710] S. Stumpf, I. Billard, C. Gaillard, P. J. Panak, and K. Dardenne, *Radiochim. Acta*, 96 (2008) 1-10.
- [711] L. D. Carlos, R. A. S. Ferreira, V. D. Bermudez, C. Molina, L. A. Bueno, and S. J. L. Ribeiro, *Phys. Rev. B*, 60 (1999) 10042-10053.
- [712] C. Joergensen, *Progr. Inorg. Chem.*, 4 (1962) 73-124.
- [713] D. J. Newman, *J. Phys. Chem. Solids*, 34 (1973) 541-545.
- [714] P. Caro, O. Beaury, and E. Antic, *J. Phys.*, 37 (1976) 671-676.
- [715] E. Antic-Fidancev, M. Lemaitre-Blaise, and P. Caro, *New J. Chem.*, 11 (1987) 467-472.
- [716] O. K. Moune and P. Caro, *J. Less-Common Met.*, 148 (1989) 181-186.
- [717] P. A. Tanner, Y. Y. Yeung, and L. X. Ning, *J. Phys. Chem. A*, 117 (2013) 2771-2781.
- [718] N. V. Bredenfel'd, M. I. Gaiduk, and V. F. Zolin, *Zh. Fiz. Khim.*, 45 (1971) 676-677.
- [719] W. T. Carnall, P. R. Fields, and K. Rajnak, *J. Chem. Phys.*, 49 (1968) 4450-4455.
- [720] G. R. Choppin and Z. M. Wang, *Inorg. Chem.*, 36 (1997) 249-252.
- [721] S. T. Frey and W. D. Horrocks, *Inorg. Chim. Acta*, 229 (1995) 383-390.
- [722] H. D. Amberger, H. Reddmann, and C. Hagen, *Inorg. Chim. Acta*, 358 (2005) 3745-3752.
- [723] M. Albin and W. D. Horrocks, *Inorg. Chem.*, 24 (1985) 895-900.
- [724] O. L. Malta, H. J. Batista, and L. D. Carlos, *Chem. Phys.*, 282 (2002) 21-30.
- [725] R. Q. Albuquerque and O. L. Malta, *Physics of Laser Crystals*, 126 (2003) 163-170.
- [726] A. P. Souza, S. Alves, and O. L. Malta, *Opt. Mater.*, 33 (2011) 402-407.
- [727] L. D. Carlos, O. L. Malta, and R. Q. Albuquerque, *Chem. Phys. Lett.*, 415 (2005) 238-242.
- [728] C. Gorller-Walrand and K. Binnemans, in: K. A. Gschneidner jr. and L. Eyring (Eds.), *Handbook on the Physics and Chemistry of Rare Earths*, Vol. 25. Elsevier, 1998, pp. 101-264.

- [729] Carnall, W. T., Crosswhite, H., and Crosswhite, H. M. Energy Level Structure and Transition Probabilities of the Trivalent Lanthanides in LaF₃, Technical Report ANL-78-XX-95, Argonne National Laboratory, Chemistry Division, Argonne, IL (USA). 1978.
- [730] L. Dacanin, S. R. Lukic, D. M. Petrovic, M. Nikolic, and M. D. Dramicanin, *Physica B*, 406 (2011) 2319-2322.
- [731] S. Shuvaev, V. Utochnikova, L. Marciniak, A. Freidzon, I. Sinev, R. Van Deun, R. O. Freire, Y. Zubavichus, W. Grunert, and N. Kuzmina, *Dalton Trans.*, 43 (2014) 3121-3136.
- [732] R. O. Freire, M. E. Mesquita, M. A. C. dos Santos, and N. B. da Costa, *Chem. Phys. Lett.*, 442 (2007) 488-491.
- [733] J. G. Santos, J. D. L. Dutra, S. A. Junior, R. O. Freire, and N. B. da Costa, *J. Phys. Chem. A*, 116 (2012) 4318-4322.
- [734] A. S. Borges, J. D. L. Dutra, R. O. Freire, R. T. Moura, J. G. Da Silva, O. L. Malta, M. H. Araujo, and H. F. Brito, *Inorg. Chem.*, 51 (2012) 12867-12878.
- [735] S. N. Misra and S. O. Sommerer, *Appl. Spectrosc. Rev.*, 26 (1991) 151-202.
- [736] R. D. Peacock, *Mol. Phys.*, 33 (1977) 1239-1246.
- [737] F. Auzel, *J. Alloys Compd.*, 380 (2004) 9-14.
- [738] B. R. Judd, *J. Chem. Phys.*, 44 (1966) 839-840.
- [739] P. Dorenbos, *J. Alloys Compd.*, 488 (2009) 568-573.
- [740] S. F. Mason, R. D. Peacock, and B. Stewart, *Chem. Phys. Lett.*, 29 (1974) 149-153.
- [741] S. F. Mason, R. D. Peacock, and B. Stewart, *Mol. Phys.*, 30 (1975) 1829-1841.
- [742] S. F. Mason, *J. Indian Chem. Soc.*, 63 (1986) 73-79.
- [743] S. F. Mason and B. Stewart, *Mol. Phys.*, 55 (1985) 611-620.
- [744] R. Kuroda, S. F. Mason, and C. Rosini, *Chem. Phys. Lett.*, 70 (1980) 11-16.
- [745] B. R. Judd, *J. Solid State Chem.*, 178 (2005) 408-411.
- [746] J.-C. G. Bünzli, B. Klein, G. O. Pradervand, and P. Porcher, *Inorg. Chem.*, 22 (1983) 3763-3768.
- [747] L. A. Riseberg and M. J. Weber, in: E. Wolf (Ed.), *Progress in Optics XIV*, North-Holland, Amsterdam, 1976, pp. 91-159.
- [748] M. J. Weber, *Phys. Rev.*, 157 (1967) 262-&.
- [749] M. J. Weber, *Phys. Rev.*, 171 (1968) 283-291.

- [750] L. A. Riseberg and H. W. Moos, *Phys. Rev.*, 174 (1968) 429-438.
- [751] J. R. Lakowicz, *Principles of Fluorescence Spectroscopy*, Springer, New York, 2006.
- [752] E. J. He, H. R. Zheng, Z. L. Zhang, X. S. Zhang, L. M. Xu, Z. X. Fu, and Y. Lei, *J. Nanosci. Nanotechnol.*, 10 (2010) 1908-1912.
- [753] I. Hyppanen, T. Soukka, and J. Kankare, *J. Phys. Chem. A*, 114 (2010) 7856-7867.
- [754] J. Vuojola, I. Hyppanen, M. Nummela, J. Kankare, and T. Soukka, *J. Phys. Chem. B*, 115 (2011) 13685-13694.
- [755] H. Lam, G. Rao, J. Loureiro, and L. Tolosa, *Talanta*, 84 (2011) 65-70.
- [756] P. Herman, B. P. Maliwal, H. J. Lin, and J. R. Lakowicz, *J. Microsc. Oxford*, 203 (2001) 176-181.
- [757] M. J. Weber, *Phys. Rev.*, 156 (1967) 231-241.
- [758] M. J. Weber, *Phys. Rev. B*, 8 (1973) 54-64.
- [759] C. Andraud, J. P. Denis, B. Blanzat, and A. Vadrine, *Chem. Phys. Lett.*, 101 (1983) 357-360.
- [760] D. Ananias, M. Kostova, F. A. A. Paz, A. N. C. Neto, R. T. De Moura, O. L. Malta, L. D. Carlos, and J. Rocha, *J. Am. Chem. Soc.*, 131 (2009) 8620-8626.
- [761] O. J. Sovers, M. Ogawa, and T. Yoshioka, *J. Lumin.*, 18-9 (1979) 336-340.
- [762] A. Aebischer, F. Gumy, and J.-C. G. Bünzli, *Phys. Chem. Chem. Phys.*, 11 (2009) 1346-1353.
- [763] J. C. G. Bünzli, A. S. Chauvin, H. K. Kim, E. Deiters, and S. V. Eliseeva, *Coord. Chem. Rev.*, 254 (2010) 2623-2633.
- [764] O. L. Malta, P. A. Santacruz, G. F. de Sa, and F. Auzel, *J. Lumin.*, 33 (1985) 261-272.
- [765] O. L. Malta and M. A. C. dos Santos, *Chem. Phys. Lett.*, 174 (1990) 13-18.
- [766] Y. H. Wang, X. R. Zhou, T. Wang, and J. Zhou, *Mater. Lett.*, 62 (2008) 3582-3584.
- [767] G. F. de Sa, W. M. Deazevedo, and O. L. Malta, *J. Lumin.*, 40-1 (1988) 133-134.
- [768] O. L. Malta, P. A. Santacruz, G. F. de Sa, and F. Auzel, *Chem. Phys. Lett.*, 116 (1985) 396-399.
- [769] A. S. Chauvin, F. Gumy, D. Imbert, and J.-C. G. Bünzli, *Spectrosc. Lett.*, 37 (2004) 517-532.
- [770] D. F. Eaton, *Pure Appl. Chem.*, 60 (1988) 1107-1114.

- [771] A. Bril and A. W. D. Jagerveenis, *J. Electrochem. Soc.*, 123 (1976) 396-398.
- [772] A. Bril and A. W. D. Jagerveenis, *J. Res. Nat. Bur. Stand. Sect. A*, 80 (1976) 401-407.
- [773] O. L. Malta, H. F. Brito, J. F. S. Menezes, F. R. G. E. Silva, C. D. Donega, and S. Alves, *Chem. Phys. Lett.*, 282 (1998) 233-238.
- [774] R. A. Gudmundsen, O. J. Marsh, and E. Matovich, *J. Chem. Phys.*, 39 (1963) 272-274.
- [775] Y. T. Yang, J. J. Li, X. Liu, S. Y. Zhang, K. Driesen, P. Nockemann, and K. Binnemans, *ChemPhysChem*, 9 (2008) 600-606.
- [776] S. Pandya, J. H. Yu, and D. Parker, *Dalton Trans.*, (2006) 2757-2766.
- [777] B. Song, G. L. Wang, M. Q. Tan, and J. L. Yuan, *J. Am. Chem. Soc.*, 128 (2006) 13442-13450.
- [778] A. Thibon and V. C. Pierre, *Anal. Bioanal. Chem.*, 394 (2009) 107-120.
- [779] J. Wu, G. L. Wang, D. Y. Jin, J. L. Yuan, Y. F. Guan, and J. Piper, *Chem. Commun.*, (2008) 365-367.
- [780] A. R. Lippert, T. Gschneidtner, and C. J. Chang, *Chem. Commun.*, 46 (2010) 7510-7512.
- [781] J. W. Walton, A. Bourdolle, S. J. Butler, M. Soulie, M. Delbianco, B. K. McMahon, R. Pal, H. Puschmann, J. M. Zwier, L. Lamarque, O. Maury, C. Andraud, and D. Parker, *Chem. Commun.*, 49 (2013) 1600-1602.
- [782] B. K. McMahon, R. Pal, and D. Parker, *Chem. Commun.*, 49 (2013) 5363-5365.
- [783] A. K. Hagan and T. Zuchner, *Anal. Bioanal. Chem.*, 400 (2011) 2847-2864.
- [784] R. Pal, A. Beeby, and D. Parker, *J. Pharm. Biomed. Anal.*, 56 (2011) 352-358.
- [785] I. Hemmilä and V. M. Mikkala, *Crit. Rev. Clin. Lab. Sci.*, 38 (2001) 441-519.
- [786] I. Hemmilä, S. Dakubu, V. M. Mikkala, H. Siitari, and T. Lovgren, *Anal. Biochem.*, 137 (1984) 335-343.
- [787] K. Binnemans, *J. Mater. Chem.*, 19 (2009) 448-453.
- [788] S. Suarez, O. Mamula, D. Imbert, C. Piguet, and J.-C. G. Bünzli, *Chem. Commun.*, (2003) 1226-1227.
- [789] S. Suarez, D. Imbert, F. Gumy, C. Piguet, and J.-C. G. Bünzli, *Chem. Mater.*, 16 (2004) 3257-3266.
- [790] Y. T. Yang, K. Driesen, P. Nockemann, K. Van Hecke, L. Van Meervelt, and K. Binnemans, *Chem. Mater.*, 18 (2006) 3698-3704.

- [791] G. Chen, N. A. Stump, R. G. Haire, J. R. Peterson, and M. M. Abraham, *Solid State Commun.*, 84 (1992) 313-315.
- [792] G. Webster and H. G. Drickamer, *J. Chem. Phys.*, 72 (1980) 3740-3747.
- [793] C. Basavapoornima, L. Jyothi, V. Venkatramu, P. Babu, C. K. Jayasankar, T. Troster, W. Sievers, and G. Wortmann, *J. Alloys Compd.*, 509 (2011) 1172-1177.
- [794] C. K. Jayasankar, K. R. Setty, P. Babu, T. Troster, and W. B. Holzapfel, *Phys. Rev. B*, 69 (2004) 214108-1-7.
- [795] S. S. Babu, P. Babu, C. K. Jayasankar, T. Troster, W. Sievers, and G. Wortmann, *J. Phys. Condens. Matter.*, 18 (2006) 1927-1938.
- [796] J. Heber, *Phys. Kondens. Mater.*, 6 (1967) 381-402.
- [797] J. L. Kropp and M. W. Windsor, *J. Chem. Phys.*, 39 (1963) 2769-2770.
- [798] J. L. Kropp and M. W. Windsor, *J. Chem. Phys.*, 45 (1966) 761-762.
- [799] J. L. Kropp and M. W. Windsor, *J. Chem. Phys.*, 42 (1965) 1599-1608.
- [800] Y. Haas and G. Stein, *J. Phys. Chem.*, 75 (1971) 3677-3681.
- [801] J. J. Freeman, D. E. Lawson, and G. A. Crosby, *J. Mol. Spectrosc.*, 13 (1964) 399-&.
- [802] P. K. Gallagher, *J. Chem. Phys.*, 43 (1965) 1742-1744.
- [803] Y. Hasegawa, M. Yamamuro, Y. Wada, N. Kanehisa, Y. Kai, and S. Yanagida, *J. Phys. Chem. A*, 107 (2003) 1697-1702.
- [804] K. Nakamura, Y. Hasegawa, Y. Wada, and S. Yanagida, *Chem. Phys. Lett.*, 398 (2004) 500-504.
- [805] W. R. Browne and J. G. Vos, *Coord. Chem. Rev.*, 219 (2001) 761-787.
- [806] T. C. Schwendemann, P. S. May, M. T. Berry, Y. Q. Hou, and C. Y. Meyers, *J. Phys. Chem. A*, 102 (1998) 8690-8694.
- [807] J. L. Zhang, B. W. Chen, X. Luo, and K. Dua, *Polym. Sci. B*, 55 (2013) 158-163.
- [808] G. Stein and E. Wurzburg, *J. Chem. Phys.*, 62 (1975) 208-213.
- [809] A. Heller, *J. Am. Chem. Soc.*, 88 (1966) 2058-2059.
- [810] W. D. Horrocks and D. R. Sudnick, *J. Am. Chem. Soc.*, 101 (1979) 334-340.
- [811] R. M. Supkowski and W. D. Horrocks, *Inorg. Chim. Acta*, 340 (2002) 44-48.
- [812] A. Beeby, I. M. Clarkson, R. S. Dickins, S. Faulkner, D. Parker, L. Royle, A. S. de Sousa, J. A. G. Williams, and M. Woods, *J. Chem. Soc. Perkin Trans. 2*, (1999) 493-503.

- [813] P. P. Barthelemy and G. R. Choppin, *Inorg. Chem.*, 28 (1989) 3354-3357.
- [814] P. S. May and F. S. Richardson, *Chem. Phys. Lett.*, 179 (1991) 277-281.
- [815] S. Lis and G. R. Choppin, *J. Alloys Compd.*, 225 (1995) 257-260.
- [816] R. S. Dickins, S. Aime, A. S. Batsanov, A. Beeby, M. Botta, J. Bruce, J. A. K. Howard, C. S. Love, D. Parker, R. D. Peacock, and H. Puschmann, *J. Am. Chem. Soc.*, 124 (2002) 12697-12705.
- [817] R. S. Dickins, J. A. K. Howard, C. L. Maupin, J. M. Moloney, D. Parker, J. P. Riehl, G. Siligardi, and J. A. G. Williams, *Chem. Eur. J.*, 5 (1999) 1095-1105.
- [818] S. Aime, M. Botta, D. Parker, and J. A. G. Williams, *J. Chem. Soc. Dalton Trans.*, (1996) 17-23.
- [819] M. Elbanowski, Z. Hnatejko, Z. Stryla, and S. Lis, *J. Alloys Compd.*, 225 (1995) 515-519.
- [820] T. Kimura and Y. Kato, *J. Alloys Compd.*, 275 (1998) 806-810.
- [821] M. Li and P. R. Selvin, *J. Am. Chem. Soc.*, 117 (1995) 8132-8138.
- [822] T. Gunnlaugsson, A. J. Harte, J. P. Leonard, and M. Nieuwenhuyzen, *Supramol. Chem.*, 15 (2003) 505-519.
- [823] S. Samikkanu, K. Mellem, M. Berry, and P. S. May, *Inorg. Chem.*, 46 (2007) 7121-7128.
- [824] A. Brandner, T. Kitahara, N. Beare, C. K. Lin, M. T. Berry, and P. S. May, *Inorg. Chem.*, 50 (2011) 6509-6520.
- [825] K. Djanashvili and J. A. Peters, *Contrast Media Mol. I.*, 2 (2007) 67-71.
- [826] K. Djanashvili, C. Platas-Iglesias, and J. A. Peters, *Dalton Trans.*, (2008) 602-607.
- [827] M. C. Alpoim, A. M. Urbano, C. F. G. C. Geraldés, and J. A. Peters, *J. Chem. Soc. Dalton Trans.*, (1992) 463-467.
- [828] E. H. Cornwall and W. D. Horrocks, *Anal. Biochem.*, 175 (1988) 59-62.